



#### DISCLAIMER

This report was prepared as an account of work sponsored by an agency of the United States Government. Neither the United States Government nor any agency thereof, nor any of their employees, makes any warranty, expressed or implied, or assumes any legal liability or responsibility for the accuracy, completeness, or usefulness of any information, apparatus, product, or process disclosed, or represents that its use would not infringe privately owned rights. Reference herein to any specific commercial product, process, or service by trade name, trademark, manufacturer, or otherwise does not necessarily constitute or imply its endorsement, recommendation, or favoring by the United States Government or any agency thereof. The views and opinions of authors expressed herein do not necessarily state or reflect those of the United States Government.

This report has been reproduced directly from the best available copy.

Available to DOE and DOE contractors from the Office of Scientific and Technical Information, P.O. Box 62, Oak Ridge, TN 37831; prices available from (615) 576-8401.

Available to the public from the National Technical Information Service, U.S. Department of Commerce, 5285 Port Royal Rd., Springfield VA 22161

DOE/BC/14953-14  
Distribution Category UC-122

Increased Oil Production and Reserves From Improved Completion  
Techniques in the Bluebell Field, Uinta Basin, Utah

Annual Report for the Period  
October 1, 1994 to September 30, 1995

By  
M. L. Allison  
C. D. Morgan

May 1996

Work Performed Under Contract No. DE-FC22-92BC14953

Prepared for  
U.S. Department of Energy  
Assistant Secretary for Fossil Energy

Edith Allison, Project Manager  
Bartlesville Project Office  
P.O. Box 1398  
Bartlesville, OK 74005

Prepared by  
Utah Geological Survey  
2363 South Foothill Drive  
Salt Lake City, UT 84109



## CONTENTS

ABSTRACT .....	1
EXECUTIVE SUMMARY .....	3
ACKNOWLEDGEMENTS .....	5
1. INTRODUCTION	
<i>Craig D. Morgan</i> .....	6
1.1 Project Status and Purpose .....	6
1.2 Geology and Field Background .....	6
2. LOG ANALYSIS AND PETROPHYSICS	
<i>Richard Jarrard</i> .....	12
2.1 Introduction .....	12
2.2 Log Digitizing and Editing .....	13
2.3 Core Plugs .....	13
2.4 Lithology from Core Plugs .....	13
2.5 Lithology Determination from Logs .....	14
2.6 Comparison of Percent-Shale Logs to Cuttings .....	14
2.7 Core-Plug Porosity .....	16
2.8 Porosity Logs .....	16
2.9 Comparison of Core-Based and Log-Based Porosities .....	18
2.10 Controls on Permeability and Production .....	20
2.11 Formation Water Resistivity and Water Saturation .....	22
2.12 Log Analyses and Production .....	23
2.13 Conclusions .....	23
3. OUTCROP STUDY OF THE GREEN RIVER FORMATION, WILLOW CREEK CANYON	
<i>Ann Garner and Thomas H. Morris</i> .....	24
3.1 Introduction .....	24
3.2 Measured Section .....	25
3.3 Petrography .....	27
3.4 Clay Analysis .....	27
3.5 Porosity and Permeability .....	27
3.6 Conclusions .....	34
4. CORE ANALYSES OF THE LOWER GREEN RIVER AND WASATCH FORMATIONS	
<i>MaryBeth Wegner and Thomas H. Morris</i> .....	35
4.1 Introduction .....	35
4.2 Core Descriptions .....	35
4.3 Petrography .....	38
4.4 Clay Analyses .....	38
4.5 Porosity and Permeability .....	42
4.6 Fractures .....	42

4.7	Conclusions .....	45
5.	<b>FRACTURE ANALYSES</b>	
	<i>M. Lee Allison and Craig D. Morgan</i> .....	48
5.1	Introduction .....	48
5.2	Subsurface Fractures .....	48
5.3	Problems .....	51
5.4	Conclusions .....	51
6.	<b>FORMATION EVALUATION AND MAPPING</b>	
	<i>Craig D. Morgan and Carol N. Tripp</i> .....	52
6.1	Introduction .....	52
6.2	Formation Evaluation .....	52
6.3	Thickness and Structure Maps .....	52
6.4	Conclusions .....	55
7.	<b>NUMERICAL SIMULATION MODELING OF HYDROCARBON PRODUCTION FROM THE GREEN RIVER AND WASATCH FORMATIONS</b>	
	<i>Milind D. Deo and Rajesh J. Pawar</i> .....	60
7.1	Introduction .....	60
7.2	Most Promising Beds .....	61
7.3	Fractured Reservoir Simulations - Lumped Models .....	64
7.4	Fractured Reservoir Simulations - Comprehensive Models .....	70
7.5	Geostatistics .....	72
7.6	Conclusions .....	76
8.	<b>COMPLETION TECHNIQUES</b>	
	<i>Richard Curtice</i> .....	77
8.1	Introduction .....	77
8.2	Production and Well Data .....	77
8.3	Stimulation Fluid Treatment Data .....	79
	8.3.1 Acid Additives .....	80
	8.3.2 Diverters .....	85
	8.3.3 Fracture Gradient .....	88
8.4	Correlations .....	89
8.5	Drilling-Mud Loss .....	90
8.6	Conclusions and Recommendations .....	91
9.	<b>FACTORS AFFECTING THE FORMATION AND RATE OF CALCIUM CARBONATE SCALING</b>	
	<i>J. Wallace Gwynn</i> .....	93
9.1	Introduction .....	93
9.2	Scale Types .....	93
9.3	Basic Chemistry of Calcium Carbonate Scaling .....	93
9.4	Water Chemistry in the Vicinity of the Michelle Ute Well .....	94
9.5	Methods of Predicting Scale Formation .....	94
9.6	Quantity and Rate of Scale Production .....	99
	9.6.1 Quantity of Scale .....	99

9.6.2	Rate of Scale Production .....	99
9.7	Factors Affecting CaCO <sub>3</sub> Scale Formation .....	100
9.7.1	Effect of Water Chemistry on the Precipitation of CaCO <sub>3</sub> .....	100
9.7.2	Effect of pH on the Precipitation of CaCO <sub>3</sub> .....	101
9.7.3	Effect of CO <sub>2</sub> Content on the Precipitation of CaCO <sub>3</sub> .....	104
9.7.4	Effects of Pressure Drops and Turbulence on the Precipitation of CaCO <sub>3</sub> .....	104
9.7.5	Effects of Water Salinity on the Precipitation of CaCO <sub>3</sub> .....	106
9.7.6	Effects of Temperature Changes on the Precipitation of CaCO <sub>3</sub> .....	106
9.8	Effect of Mixing Wasatch and Green River Formation Waters .....	106
9.9	Possible Scale-Mitigating Actions (Excluding Inhibitors) .....	109
9.10	Conclusions .....	110
10.	TECHNOLOGY TRANSFER	
	<i>Roger L. Bon</i> .....	111
10.1	Information Exhibits .....	111
10.2	Oral and Poster Presentations .....	111
10.2.1	Geological Society of America, Annual Meeting, October 1994, Seattle, WA. ....	111
10.2.2	American Association of Petroleum Geologists Annual Meeting and Exhibition, March 1995, Houston, TX. ....	111
10.2.3	American Association of Petroleum Geologists Rocky Mountain Section Meeting, July 1995, Reno, NV. ....	111
10.2.4	Ninth Annual Spring Research Conference, Brigham Young University, March 1995, Provo, UT .....	112
10.2.5	Utah Geological Association Meeting, August 1995, Salt Lake City, UT .....	112
10.3	Petroleum News .....	112
11.	PROPOSED DEMONSTRATION	
	<i>Craig D. Morgan, DeForrest Smouse, and Lewis Wells</i> .....	113
11.1	Introduction .....	113
11.2	Michelle Ute Well .....	113
11.3	Malnar Pike Well .....	114
11.4	New Well .....	114
11.5	Benefits and Value .....	114
REFERENCES	.....	115

## ILLUSTRATIONS

Figure 1.1. The Uinta Basin with Bluebell, Altamont, and Cedar Rim fields shown .....	7
Figure 1.2. Bluebell field with study sites and Roosevelt Unit shown .....	8
Figure 1.3. Cross section from the Michelle Ute to Malnar Pike wells .....	10
Figure 2.1. Log-based and core-based porosities versus depth. ....	19
Figure 2.2. Crossplots of permeability versus porosity .....	21
Figure 3.1. Relative proportions of the various rock types identified in the outcrop. ....	26
Figure 3.2. Relative proportions of the main constituents in the arenite from the outcrop. ....	28
Figure 3.3. X-ray diffraction plot of arenite with chlorite, illite, and kaolinite. ....	29
Figure 3.4. X-ray diffraction of arenite with chlorite, illite, kaolinite, and some smectite. ....	30
Figure 3.5. Relative proportions of chlorite, illite, and kaolinite in outcrop samples. ....	31
Figure 3.6. Arenite porosity and permeability crossplot. ....	33
Figure 4.1. Index map of the Bluebell field. ....	36
Figure 4.2. Cross-section showing depth and formation of sampled core. ....	37
Figure 4.3. Breakdown of sandstone compositions from point-counted samples. ....	39
Figure 4.4. Breakdown of the percentage of different rock types present in cores. ....	39
Figure 4.5. Example of the X-ray diffraction pattern of a typical arenite in the subsurface. ....	41
Figure 4.6. Total number of feet described of each lithology, and the number of feet containing at least one fracture. ....	43
Figure 4.7. Percentage of each rock type that is fractured .....	44
Figure 4.8. Relative fracture density of clastic rocks. ....	46
Figure 4.9. Relative fracture density of carbonate rocks .....	47
Figure 5.1. Fracture orientations from well logs and oriented cores .....	49
Figure 5.2. Fracture orientation by depth .....	50
Figure 6.1. Structure contour map of the middle marker of the Green River Formation (upper Wasatch transition). ....	56
Figure 6.2. Structure contour map of the lower Wasatch transition. ....	57
Figure 6.3. Isopach map of the Wasatch Formation. ....	58
Figure 6.4. Isopach map of the lower Wasatch transition. ....	59
Figure 7.1. The oil saturation distribution around the Michelle Ute well .....	65
Figure 7.2. The pressure distribution around the Michelle Ute well .....	66
Figure 7.3. Comparison of the actual (field oil) to simulated (sim oil) oil production for the Michelle Ute well using the lumped, fractured model. ....	68
Figure 7.4. Comparison of the Actual (field oil) to simulated (sim oil) oil production for the Malnar Pike well using the lumped, fractured model. ....	69
Figure 7.5. Comparison of the field (field oil) to simulated (sim oil) oil production for the Michelle Ute well using the comprehensive, fractured model. ....	71

Figure 7.6. Comparison of the field (field gas) to simulated (sim gas) gas production for the Michelle Ute well using the comprehensive, fractured model. . . . .	71
Figure 7.7. Porosity distributions in two cross sections of a hypothetical four-section reservoir. . . . .	74
Figure 7.8. Oil saturation distributions in two cross sections of a hypothetical four-section reservoir. . . . .	75
Figure 8.1. Treatment volumes and resulting hydrocarbon production. . . . .	80
Figure 8.2. Frequency of additives used in treatments. . . . .	81
Figure 8.3. Friction pressure loss per 1,000 feet (305 m) of 2-7/8 inch (7 cm) diameter tubing for HCl, brine, and KCl water. . . . .	83
Figure 8.4. Friction pressure loss per 1,000 feet (305 m) of 2-7/8 inch (7 cm) diameter tubing for gelled acid, gelled KCl solution, and acid with friction reducer. . . . .	84
Figure 8.5. Number of times used and type of carrier fluid for each type of diverter . . . . .	86
Figure 8.6. Frequency of diverter action by quality of action. . . . .	88
Figure 8.7. Frequency of various fracture gradients. . . . .	89
Figure 8.8. Average decline curves by consecutive treatments. . . . .	90
Figure 9.1. Trilinear diagram showing the chemical composition of 44 waters in the general vicinity of the Michelle Ute well . . . . .	95
Figure 9.2. Trilinear diagram showing the chemical composition of 18 waters in the immediate vicinity of the Michelle Ute well. . . . .	96
Figure 9.3. Precipitation of calcite at equilibrium temperatures from the same water at three different pH values. . . . .	103
Figure 9.4. Precipitation of calcite at equilibrium temperatures from the same water but containing different amounts of CO <sub>2</sub> . . . . .	105
Figure 9.5. Precipitation of calcite at equilibrium temperatures from waters of the same chemical composition, but varying degrees of dilution or salinity. . . . .	107
Figure 9.6. Plot of initial BHT versus depth from the land surface in the Wasatch Formation. . . . .	107
Figure 9.7. Precipitation of calcite at equilibrium temperatures from the same water but at increasing initial BHT. . . . .	108
Figure 9.8. Precipitation of calcite at equilibrium temperatures from varying-ratio mixtures of average Wasatch Formation and average Green River Formation waters . . . . .	108

## TABLES

Table 2.1. The mud (cuttings) logs for 13 wells that were examined and compared to the shale-percentage plots. . . . .	15
Table 3.1. Depositional environments identified in the Willow Creek Canyon measured section . . . . .	25
Table 3.2. Listing of the permeability, porosity, clay content, and lithologic name of outcrop samples. . . . .	32
Table 4.1. Formation, depth, lithology, clay content, porosity, and permeability of core samples. . . . .	40
Table 5.1. Location and type of subsurface fracture data . . . . .	48
Table 6.1. Evaluation of beds in the Michelle Ute well. . . . .	53
Table 6.2. Evaluation of beds in the Malnar Pike well. . . . .	54
Table 7.1. Reservoir characteristics of all the perforated beds in the Michelle Ute well. . . . .	62
Table 7.2. Reservoir characteristics of all the perforated beds in the Malnar Pike well. . . . .	63
Table 7.3. Reservoir characteristics of the lumped, fractured reservoir model for the Michelle Ute well. . . . .	67
Table 7.4. Reservoir characteristics of the lumped, fractured reservoir model for the Malnar Pike well. . . . .	67
Table 7.5. Reservoir characteristics of the lumped, fractured 4-square mile area model in the Roosevelt Unit. . . . .	70
Table 9.1. Oil-well water chemistry of 44 waters in the general vicinity of the Michelle Ute well. . . . .	97
Table 9.2. Oil-well water chemistry of 18 similar waters in the immediate vicinity of the Michelle Ute well. . . . .	98
Table 9.3. Average water chemistry in the immediate vicinity of the Michelle Ute well. . . . .	99
Table 9.4. Pounds of calcite precipitated from 1,000 BW of varying chemical compositions . . . . .	101
Table 9.5. Effect of mixing Michelle Ute and Uinta River water on the precipitation of CaCO <sub>3</sub> . . . . .	101
Table 9.6. Changes in pH and bicarbonate values over time . . . . .	102
Table 9.7. Specific gravity and current mole-percent content of gases from wells in the vicinity of the Michelle Ute well. . . . .	104
Table 9.8. Comparison of average Wasatch and Green River Formation waters in the vicinity of the Michelle Ute well. . . . .	109

## ABSTRACT

The Bluebell field produces from the Tertiary lower Green River and Wasatch Formations of the Uinta Basin, Utah. The productive interval consists of thousands of feet of interbedded fractured clastic and carbonate beds deposited in a fluvial-dominated deltaic lacustrine environment. Wells in the Bluebell field are typically completed by perforating 40 or more beds over 1,000 to 3,000 vertical feet (300-900 m), then applying an acid-fracture stimulation treatment to the entire interval. This completion technique is believed to leave many potentially productive beds damaged and/or untreated, while allowing water-bearing and low-pressure (thief) zones to communicate with the wellbore. Geologic and engineering characterization has been used to define improved completion techniques.

Characterization of outcrop, core, and digital well logs show that, in the Green River and Wasatch Formations, intergranular permeability of 0.1 milliDarcy (mD) or more is present only when clay content is 4 percent or less and intergranular porosity is 6 percent or more. Total gamma-ray count, which is generally logged in most wells, is a poor indicator of clay content. Uranium content, which contributes to the total gamma-ray count, varies independently of clay content. Clay content is generally less in the Wasatch Formation than in the Green River Formation.

Examination of core from the Bluebell field shows that all potential reservoir rock types are moderately fractured, and that fracture density is not depth related. Two approximately orthogonal fracture sets are present at the surface but in the subsurface, fractures tend to be oriented northwest-southeast at shallow depths and west-east at deeper horizons. Most fractures in the Bluebell cores are 90 percent or more, calcite filled.

The study identified reservoir characteristics of beds that have the greatest long-term production potential. Various bed parameters including clay content, bed thickness, porosity, fluid saturation, oil volume, and drilling shows were evaluated and mapped. Volumetric calculations and numerical reservoir simulations were performed. The characterization of the reservoirs is more complete than previously performed. This evaluation will be used to: (1) select intervals to be stimulated in the demonstration wells, and (2) compare to the actual results from the demonstration wells for quantifying the reliability of the individual bed parameters and the overall comprehensive analysis.

Homogeneous and fracture (dual-porosity, dual-permeability) reservoir simulation models of the Michelle Ute and Malnar Pike demonstration wells were constructed. In the models the radius of influence of the well on the reservoir is about 400 feet (120 m) in the homogenous model and 1,000 feet (300 m) in the fracture model. Operators of the Bluebell and neighboring Altamont fields have occasionally seen evidence of interference in wells as far as a mile (1.6 km) apart, far greater than the simulation models indicate. Also, where two wells per section have been drilled the production history of the second well often indicates that the reservoir pressure has been reduced over a large area. We believe the larger area of influence is the result of a few (perhaps one to four) high-permeability (possibly intensely fractured) beds within the productive interval. The high permeability beds may be where most of the stimulation fluids go during recompletion attempts, leaving potentially productive beds untreated. Effective diversion during a stimulation treatment is an important part of improving completion techniques in the Bluebell field.

Data was gathered from the operators on 246 stimulation treatments from 67 wells within the Bluebell field. The database consists of 108 different parameters for each stimulation treatment. Analyses of the database revealed several ways to improve completion techniques in the Bluebell field. They are: (1) improve on the identification of productive and nonproductive beds, (2) improve diversion, (3) increase down-hole treating pressure by reducing friction, and (4) more consistent use of corrosion, iron, and scale inhibitors, and surfactants.

Composition of waters produced from wells in the Bluebell field was analyzed to determine the physical and chemical variables which cause and can be used to control scaling. Variations in six parameters: (1) basic water chemistry, (2) pH, (3) carbon dioxide (CO<sub>2</sub>) content, (4) pressure, (5) salinity, and (6) temperature, were tracked to determine their effects on the precipitation of calcium carbonate from produced oil-well waters. Waters with high percentages of both calcium and bicarbonate favor greater precipitation. Low pH (more acidic) waters precipitate less than high pH (more basic) waters. High CO<sub>2</sub>-content favors less precipitation than low CO<sub>2</sub>-content waters. Decreases in pressure and/or turbulence favor the precipitation of calcium carbonate. Reductions in salinity favor less precipitation, and increased temperatures, both initial and equilibrium, favor increased precipitation. The co-production of Green River Formation and Wasatch Formation waters increases the amount of calcium carbonate scale that is produced over that which is produced from Wasatch water alone.

The results of the characterization study will be demonstrated in three wells in the Bluebell field. In the Michelle Ute well several zones (about 500 feet [150 m] thick) consisting of numerous perforated beds, will be stimulated with a high-diversion, low-friction acid treatment. In the Malnar Pike well three or more beds will be horizontally drilled about 10 feet (3 m) beyond the well bore using a hydro-jet lance tool. The beds will be individually stimulated using a pinpoint injection tool. In both wells, reservoir conditions before and after the stimulation treatment will be documented with the use of pulsed neutron decay, dipole sonic, temperature, and spinner logs, and radioactive tracers in the treatment fluids. This will allow us to determine how well the treatment was dispersed, how many beds had fractures opened or induced by the treatment, which beds are producing and how much, and quantify the role of fractures in production of the reservoir.

The oil-producing beds identified in Michelle Ute and Malnar Pike wells will be correlated and mapped. These data will be used to help select a location for a new test well to be drilled in the field. Formation evaluation, selection of perforated intervals, and type of stimulation in the new well will be based on the experience gained from the Michelle Ute and Malnar Pike demonstrations.

## EXECUTIVE SUMMARY

The objective of the project is to increase oil production and reserves from improved completion techniques in the Uinta Basin, Utah. To accomplish this objective a two-year geologic and engineering characterization of the Bluebell field was conducted. The study evaluated surface and subsurface data, current completion techniques, and common production problems.

A 2,786-foot (849.2-m) stratigraphic section of the Green River Formation in the Willow Creek Canyon area of Carbon and Duchesne Counties, Utah, was previously examined and described in Allison (1995). Over 1,600 feet (488 m) of core from 10 different wells in the Bluebell field were described. Analyses of outcrop and core included thin section examination, grain point-count, x-ray diffraction, porosity, and permeability.

Two hundred forty geophysical well logs from 80 wells in and around the Bluebell field were digitized. The digital data was used for field-wide correlation, detailed porosity, clay content, and fluid saturation calculations.

Surface fracture orientations were previously mapped throughout the field and in the Green River Formation in other areas of the basin. Subsurface fracture analysis was done using bore-hole imaging logs and orientated core data.

Stratigraphic cross sections and interval thickness maps were constructed. Thickness, porosity, and fluid saturation were determined for all beds in the productive interval of the Michelle Ute and Malnar Pike demonstration wells that meet the minimum criteria, as determined by the study, for long-term production. These beds are being correlated in neighboring wells and thickness maps are being constructed. This analysis will be used in the reservoir simulation modeling and in selecting intervals for completion in the demonstration wells.

Fluid property, production, and fracture data; log-derived pay-zone thicknesses, porosities, and water saturations; as well as core-derived permeabilities and porosities were compiled. Single-well homogeneous and dual-porosity, dual-permeability, fractured-reservoir numerical simulation models were constructed for the Michelle Ute and Malnar Pike demonstration wells. Homogeneous and fractured simulation models were constructed covering a 4-square-mile area encompassing the demonstration wells in the Roosevelt Unit area and a 4-square-mile area in the western portion of Bluebell field. Each of the reservoir simulation models were subjected to internal analysis and the following reservoir properties were examined: (1) original-oil-in-place in each of the producing zones, (2) original reservoir pressure, (3) oil produced and oil remaining in each of the modeled layers, and (4) current reservoir pressure.

Presently, we are incorporating reservoir descriptions based on geostatistical models into the reservoir simulators. In contrast to the lumped-zone, fractured models presented in this report we are also completing layer-by-layer, fractured models.

Data was gathered from the operators on 246 stimulation treatments from 67 wells within the Bluebell field. The database consists of 108 different parameters for each stimulation treatment. This database was then analyzed by engineers of Halliburton Energy Service's Tech. Team in Denver, Colorado and Vernal, Utah. The analyses identified several ways to improve the method and types of fluids used in stimulation treatments in the Bluebell field. These recommendations will be used in treating the demonstration wells.

Composition of waters produced from wells in the Bluebell field was analyzed to determine the physical and chemical variables which cause and can be used to control scaling. The analyses included: (1) the types of scale that are found, (2) the basic chemistry of calcium carbonate scale formation, (3) the water chemistry that is found in the vicinity of the Michelle Ute well, (4) methods of predicting scale formation, (5) quantity and rate of scale production, (6) factors which affect the tendency for scale formation, (7) the effect of mixing Wasatch and Green River waters on scaling, and (8) potential scale-mitigating methods, beyond the use of scale inhibitors.

Three demonstrations are recommended to show how oil recovery can be improved from old and new wells in the Bluebell field: (1) recompleting the Michelle Ute well by stimulating individual pressure zones (each about 500 feet [150 m] thick) using a high-diversion, low-friction treatment, (2) recompleting the Malnar Pike well by horizontally drilling 10 feet (3 m) directionally into three or more key beds using an extended-reach hydro-jet lance tool, stimulating each bed separately with a pinpoint injection tool, and (3) selecting a location, drilling, evaluating, perforating, and stimulating a new well based on the knowledge gained from the characterization study and results of the first two demonstrations. Each demonstration is designed to allow detailed documentation of success or failure of each aspect of the characterization and stimulation techniques.

## **ACKNOWLEDGEMENTS**

This research is performed under the Class I Oil Program of the U. S. Department of Energy (DOE), Pittsburgh Energy Technology Center contract number DE-FC22-92BC14953. The Contracting Officer's Representative is Edith Allison, with the DOE Bartlesville Project Office. Additional funding was provided by the Utah Office of Energy and Resource Planning.

The following individuals and companies provided valuable advice and data: Dave Ponto with Dowell-Schlumberger, Denver, CO; Doug Howard consulting engineer, Roosevelt, UT; Coastal Oil and Gas Corporation (ANR), Denver, CO; Flying J Petroleum Incorporated, North Salt Lake, UT; and Pennzoil Exploration and Production Company, Houston, TX. Geotechnical assistance was provided by Kimberley Waite, Utah Geological Survey and Mike Hobart, University of Utah Department of Geology and Geophysics.

Thanks is given to Duane Wales, Gary Williams Energy for the gas analyses. Thanks is further given to Coastal Energy, Quinex Energy, Flying J, Pennzoil, and the Utah Division of Water Quality for furnishing the water analyses that have been used within this report.

This report or portions of it were reviewed by Rick Gdanski, Arne Hultquist, Matthew Hoffman, Wayne Pierce, and Mason Tomson.

# 1. INTRODUCTION

*Craig D. Morgan*  
Utah Geological Survey

## 1.1 Project Status and Purpose

The two-year characterization study of the Bluebell field, Duchesne and Uintah Counties, Utah, consisted of separate, yet related tasks. The characterization tasks were: (1) log analysis and petrophysics, (2) outcrop studies, (3) cuttings and core analysis, (4) subsurface mapping, (5) new logs and cores, (6) fracture analysis, (7) geologic characterization synthesis, (8) analysis of completion techniques, (9) reservoir analysis, (10) best completion technique identification, (11) best zones or areas identification, and (12) technology transfer.

The following report details the work, interpretation, and recommendations resulting from the second year of the characterization study. Not every task is detailed in a chapter. As an example, task 7 (geologic characterization synthesis); task 10 (best completion techniques identification); and task 11 (best zones or areas identification); represent the culmination of all the tasks into the final recommendations and proposed demonstration.

The characterization study resulted in a better understanding of the Tertiary Green River and Wasatch Formations reservoirs. The study yielded recommended methods for improved bed evaluation and completion techniques. The findings of the study have been, and will continue to be, made available to the public and industry, through an active technology transfer program.

A three-part demonstration will be conducted in 1995 through 1998. The demonstration program will show the effectiveness and help improve the formation evaluation techniques developed as part of the study. Also, the demonstration program will show the direct applications and benefits of the different completion techniques developed as part of the study.

A successful demonstration combined with an aggressive technology transfer program and implementation of the techniques by operators, will increase the oil recovered, and reduce premature abandonment of wells in the Bluebell field. The techniques to be demonstrated will be applicable to other fields in the Uinta Basin and other fluvial-dominated deltaic reservoirs nation-wide.

## 1.2 Geology and Field Background

The Bluebell field is the largest oil producing field in the Uinta Basin. Bluebell is one of three contiguous oil fields; Bluebell, Altamont, and Cedar Rim (figure 1.1). The basin is an asymmetrical syncline deepest in the north-central area near the basin boundary fault. The Bluebell field produces oil from the Eocene-Paleocene Green River and Wasatch Formations near the basin center.

The Bluebell field is 251 square miles (650 km<sup>2</sup>) in size and covers all or parts of Townships 1 North, 1 and 2 South, Ranges 1 East and 1 through 3 West, Uintah Base Meridian (figure 1.2). Over 133 million barrels of oil (MMBO [18,620,000 MT]) and 168 billion cubic feet (BCF [4.8 billion m<sup>3</sup>]) of associated gas have been produced

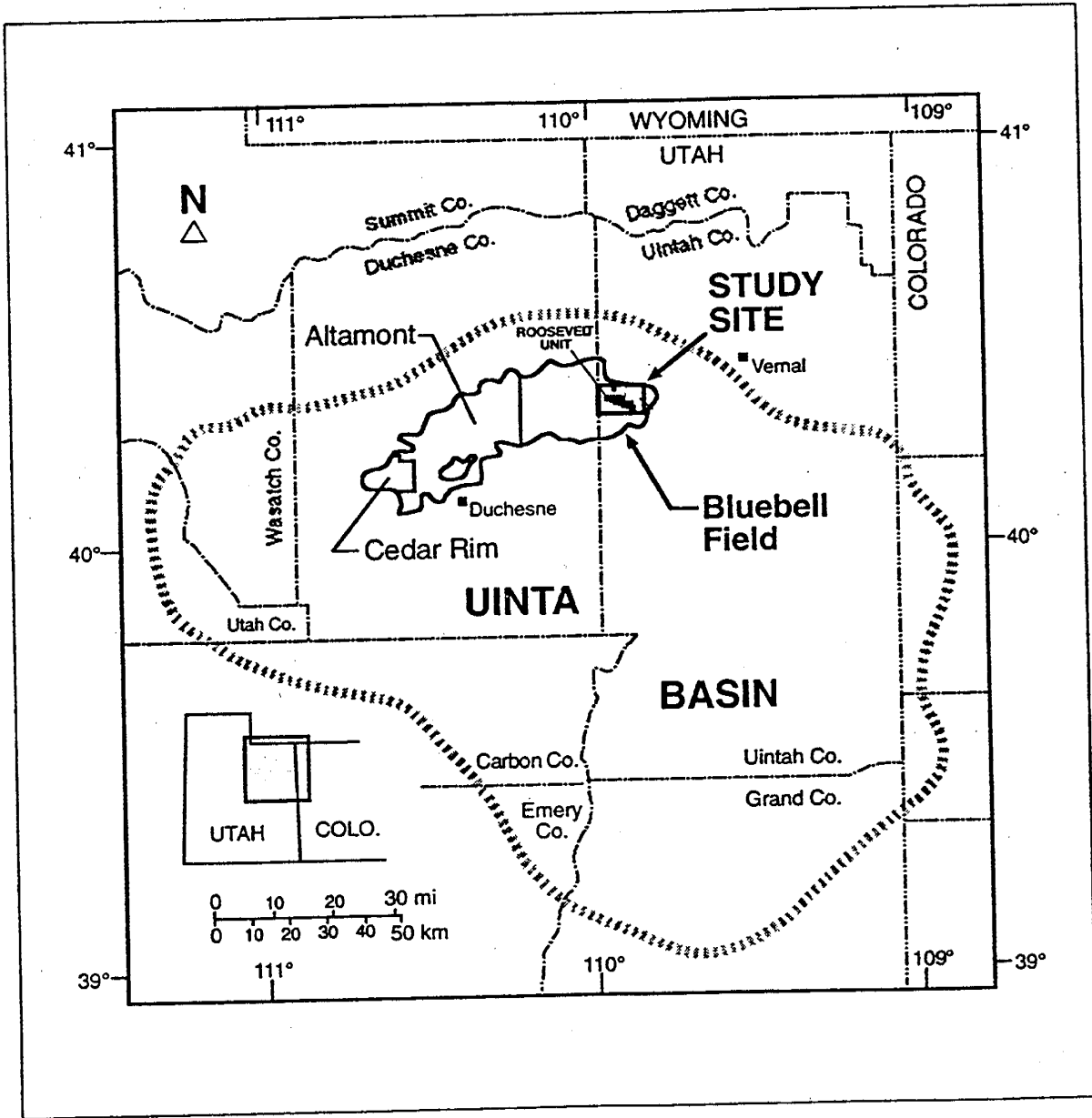


Figure 1.1 The Uinta Basin with Bluebell, Altamont, and Cedar Rim fields shown.

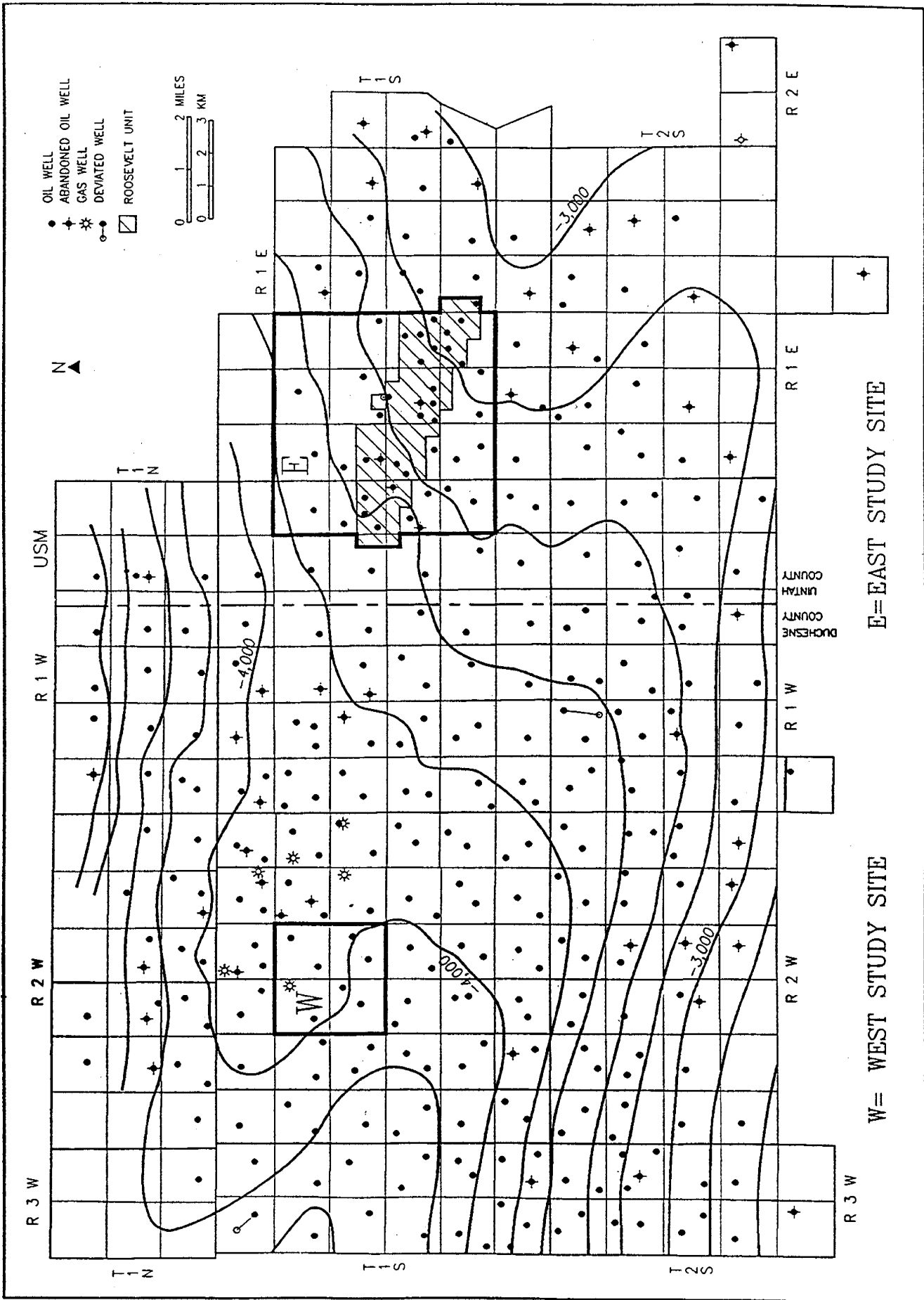


Figure 1.2 Bluebell field with study sites and Roosevelt Unit shown.

(September 30, 1995). The spacing is two wells per section, but much of the field is still produced at one well per section. The Roosevelt Unit within the Bluebell field operates under the unit agreement. Although some wells have produced over 3 MMBO (420,000 MT), most produce less than 0.5 MMBO (70,000 MT).

The Green River and Wasatch Formations were deposited in intertonguing relationship in and around ancestral Lake Flagstaff and Lake Uinta. Depositional cycles show rapid lake level fluctuations and changes in water chemistry (Fouch and Pitman, 1991, 1992; Fouch and others, 1992). The Green River and Wasatch Formations were deposited in alluvial-fluvial, marginal-lacustrine, and open-lacustrine environments. The depositional environments are described in detail by Fouch (1975, 1976, 1981), Ryder and others (1976), Pitman and others (1986), Pitman and others (1982), Bruhn and others (1983), Stokes (1986), Castle (1991), Fouch and Pitman (1991, 1992), Fouch and others (1990) and Franczyk and others (1992).

The production at Bluebell comes from three primary intervals: (1) lower Green River Formation/upper Wasatch transition, (2) Wasatch Formation, and (3) lower Wasatch transition (possible Flagstaff equivalent) (figure 1.3). The lower Green River/upper Wasatch transition is informally defined as from the middle marker to the top of the Wasatch (redbeds). The lower Green River/upper transition, upper transition/Wasatch, and Wasatch/lower transition contacts are transitional and intertonguing, as a result they are difficult to identify accurately.

The lower Wasatch transition (Flagstaff equivalent?), consists dominantly of carbonate with minor sandstone beds that were deposited in marginal to open-lacustrine environments. The lower Wasatch is productive throughout most of the field. In the east portion of the field, lower Wasatch is a primary productive interval, while in the west portion both the Wasatch sandstone and lower Wasatch carbonate are productive.

The Wasatch production is primarily from sandstone and siltstone beds deposited in alluvial to fluvial-deltaic environments. The source for the Wasatch redbeds (sandstone, siltstone, and red shale) in Bluebell field was the Uinta Mountains to the north. The Wasatch redbeds thin rapidly from north to south through the field, with the best sandstone development occurring in the west portion of the field.

The lower Green River/upper Wasatch transition production is from interbedded calcareous sandstone, limestone, marlstone, and ostracodal limestone, deposited in fluvial-deltaic and carbonate mud flat environments. Many of the lower Green River beds are laterally extensive and highly fractured.

Individual beds in the lower Green River and Wasatch producing interval are difficult to evaluate. Fracturing and complex formation water chemistries make conventional geophysical log analysis highly questionable. Economics have discouraged open hole and/or production testing of individual beds. Therefore, it is not clearly understood which beds in any particular well are potentially significant producers, limited producers, water producers, or thieves. As a result, the common practice is to perforate numerous beds over thousands of vertical feet and apply an acid-frac treatment, generally 20,000 gallons (75,700 l) of hydrochloric acid (HCL). The typical well in the Bluebell field has between 1,500 to 2,000 feet (457-610 m) of gross perforations. As a result, the treatment is being applied to both clastic and carbonate, fractured and unfractured beds, overpressured and normally pressured zones.

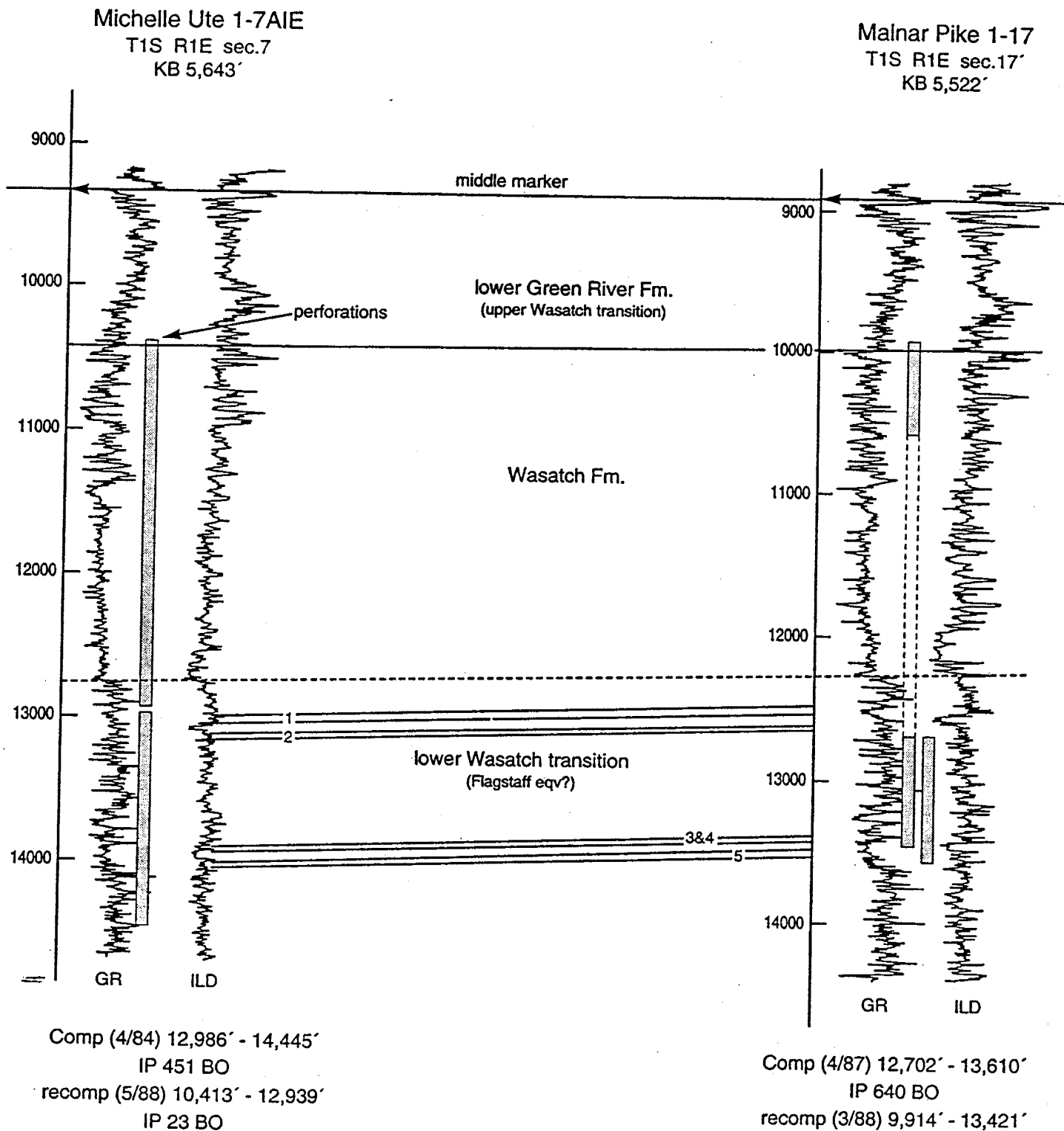


Figure 1.3 Cross section from the Michelle Ute to Mainar Pike wells using gamma ray (GR) and resistivity (ILD) curves. Datum is the middle marker of the Green River Formation. Correlated zones 1 through 5 are the beds originally recommended for recompletion by the operator before the project began.

Although much of the work was field-wide, the project is concentrated on two study sites. The east study-site is in the eastern portion of the Bluebell field (figure 1.2) and includes the Roosevelt unit. The area has lower Green River/upper Wasatch transition, Wasatch, and lower Wasatch transition zones. Some wells commingle lower Wasatch, Wasatch, and lower Green River/upper Wasatch production. This part of the field typically has the poorest producers, generally less than 200,000 BO (28,000 MT) per well and many, less than 100,000 BO (14,000 MT) per well.

The west study site is in the west-central portion of the field (figure 1.2). It includes some of the best producing wells with cumulative production of over 3 MMBO (420,000 MT) per well. Many of the wells were originally drilled and completed in the lower Green River/upper Wasatch transition. Oil production ranged from 93,000 to 436,000 BO (13,000 to 61,000 MT) from nine beds with a cumulative thickness of 20 to 90 feet (6.1-27.4 m). These wells were later deepened and completed in the Wasatch and lower Wasatch transition and produced greater than 1,000,000 BO (140,000 MT) per well. Geophysical logs, test and production data are more complete in the west study-site than the east study site.

## 2. LOG ANALYSIS AND PETROPHYSICS

*Richard Jarrard*  
University of Utah

### 2.1 Introduction

Quantitative log analysis is normally the primary method for identifying lithology, porosity, and water saturation of individual beds, and then selecting the best zones to perforate. However, in Bluebell field, quantitative log analysis is seldom undertaken, for several reasons: (1) poor hole conditions leading to poor-quality logs, (2) inability of standard logs to identify open fractures, and (3) inaccurate water resistivities leading to poor estimates of water saturation.

These problems may stem (in part) from: (1) the many vintages of logs, (2) the variety of log types, (3) the large numbers of operators (each working with only a few wells), and (4) the use of paper logs rather than digitized logs. If so, a more comprehensive, field-wide program of log analysis might offer insights that have eluded researchers studying individual wells. To test this idea, we digitized logs from about 80 wells and performed digital, interactive log analysis. Because 80 is only a fraction of the over 300 Bluebell wells, we confined our analyses to the best-quality logs. One product of the resulting database of digital logs was inter-well correlation for a large number of horizons (Morgan and Tripp, this volume). In this chapter the focus is on a different objective: log-based determination of lithology, porosity, and optimum conditions for production.

Digitized logs were used to produce percent-shale (percent-clay) plots for 80 wells, porosity plots for 49 wells, and water-saturation plots for four wells. The reliability of log-based estimation of these parameters was evaluated, using core plugs and cuttings for ground truth. The analyses showed: (1) log-based determination of percent-shale is relatively straightforward (although determination of the non-shale component is non-unique), (2) that clean-formation porosity is best determined using an average of neutron and density porosity, and (3) that uncertainties in fluid resistivity preclude accurate calculation of water saturation. The porosity estimates for *in-situ* reservoir rocks are substantially less than previous estimates of 5 to 20 percent; our log-based estimate is 4 to 8 percent, and our core-based estimate is 2 to 7 percent.

Based on core-plug analyses, it was determined that sufficient intergranular permeability for long-term producibility will be found only among rocks that are nearly shale-free and have porosities greater than 6 percent. Gamma-ray logs are only a moderately good indicator of shale-free rocks; spectral-gamma logs are substantially better. Neutron/density averaging can indicate zones with adequate porosity, but only if hole conditions do not excessively degrade log accuracy and if shaly zones are avoided. Of the many beds typically chosen for completion in a Bluebell field well, a large number appear to be promising based on overly optimistic porosity determinations, but will have only transient production. It is hoped that increased attention to these two factors: (1) shale-free beds, and (2) reliably determined high porosities, will significantly increase the average producibility of zones chosen for completion.

## 2.2 Log Digitizing and Editing

The efficiency of the log digitizing effort was increased by changing from digitizing tablet software, to a system which scans logs, displays the scanned image on the computer, and then lets the user control and correct an automatic computer-digitizing algorithm. This change resulted in the completion of all digitizing, on schedule, even though more wells and longer depth intervals were digitized than originally planned.

The selection of logs to digitize was based partly on a log-quality criterion, but many logs still needed editing, such as: (1) removal of depth or scaling errors, (2) elimination of logs with major depth shifts or calibration problems, (3) merging of different logging runs into a composite log, and (4) conversion of density-porosity and neutron-porosity logs to a common matrix assumption. Well errors requiring correction included: (1) inaccurate locations, (2) well name changes, and (3) inaccurate elevations. Editing of individual bad spots in all individual logs was not practical, but as described later, most washouts were removed and selected logs were edited.

## 2.3 Core Plugs

Logging results were to be compared to data from cuttings and to a few core-plug measurements of porosity and permeability. But, the use of cuttings was de-emphasized because of the huge variability in quality of cutting logs. Instead, analyses of core plugs were substantially increased; data correlated included porosity, permeability, and X-ray diffraction- (XRD-) based gross mineralogy on 196 samples. Core plugs and cuttings were used to provide ground truth for the log-based lithology and porosity analyses.

## 2.4 Lithology from Core Plugs

The XRD analyses of core plugs provided semi-quantitative estimates of mineral concentrations. Quartz was present in all samples and was the dominant component of nearly all samples. Feldspar was also present in nearly all samples, normally at a concentration much smaller than the quartz concentration. Clay minerals, calcite, and ankerite/dolomite were also common, with widely varying concentrations. The XRD finding of ankerite in many samples means that cuttings or log-based descriptions of dolomite should be dolomite or ankerite. The core-plug sampling intentionally over-represented cleaner formations because they have the greatest potential of being reservoir rocks

Although the XRD data are only semi-quantitative, they can be used to investigate the possible relationship, between clean-formation lithology and reservoir properties. For example, are limestone beds more porous and permeable than sandstone beds, perhaps because of secondary porosity? The preliminary examinations yielded little evidence that either porosity or permeability depend strongly on relative content of quartz, feldspar, calcite, or dolomite/ankerite.

## 2.5 Lithology Determination from Logs

Calculating lithology and porosity by log inversion, then conducting a shaly-sand hydrocarbon analysis were attempted. The relative proportions of quartz, dolomite, and limestone however, are poorly resolved by log inversion, causing the inversion to give unstable values. Because porosity is determined simultaneously in the inversion, the instability in the mineralogy solutions resulted in unstable porosity determinations as well.

The inversion problem is evident even in the simplest solutions, such as use of neutron and density logs to determine two mineral components plus porosity. Neutron/density crossplots of clean formations can suggest quartz+feldspar versus dolomite+ankerite dominance, but a crossplot is under-determined for deriving three to five mineral components. Such crossplots typically show 5 to 15 percent of the samples plotting above the quartz line and therefore causing inversions to give *negative* concentrations of limestone and dolomite. The XRD data of core samples shows this is caused in part, by feldspar and is not just noise.

For most purposes, relative proportions of quartz, dolomite, and limestone are of minor value; porosity determination is a notable exception, which will be discussed later. The key lithologic variable is shale content, which controls both intergranular permeability and fracturing. Therefore, gamma-ray logs were used to determine percent shale instead of multi-log inversion.

The percent-shale plots are based on converting the natural gamma-ray log to shale percentage, assuming a clean-sand line of 45 API units and a shale line of 120 API units. Linear interpolation of values between these extremes were used, rather than the curved Dresser relationships. Logs with obvious gamma-ray problems were not used.

Clay content can be accurately estimated from the computed gamma-ray (CGR) log (potassium [K] plus thorium [Th] contributions to total gamma radiation). Uranium, however, is not present primarily in clays and is therefore not correlated with CGR, K, or Th. Consequently, total gamma-ray count is a less reliable indicator of clay content than is CGR from spectral gamma-ray count. A potential complication in the use of either spectral or total gamma-ray logs for clay estimation is that an immature, clay-free sandstone or limestone can have the same gamma-ray response as a mature, clay-containing sandstone or limestone, although only the former has good intergranular permeability. This potential problem does not appear to be common, although some evidence was found that the clean-formation baseline is not identical for all of the best-producing beds.

## 2.6 Comparison of Percent-Shale Logs to Cuttings

The 80 shale-percentage plots cannot be directly compared to core plugs, because core plugging avoided shale-rich rocks. Also, these data cannot be compared to core descriptions, because coring is somewhat biased towards intervals thought to contain reservoir rocks. Instead, the plots were compared to continuous cuttings logs (table 2.1).

Table 2.1. The mud (cuttings) logs for 13 wells that were examined and compared to the shale-percentage plots.

Well Name and Number	Location (Section, Township, Range, Uinta Base Line)	Cuttings Depth in Feet
Ute Tribal 1	15, T. 1 N., R. 1 E.	80 - 9,635
Redcap JDC 30-4*	30, T. 1 S., R. 2 E.	5,000 - 13,545
Roosevelt Unit C-11*	18, T. 1 S., R. 1 E.	8,500 - 13,500
Ute Tribal 1-25A1E*	25, T. 1 S., R. 1 E.	7,500 - 10,100
Ute Tribal RU-18A1E	27, T. 1 S., R. 1 E.	5,000 - 10,182
Roosevelt Unit 9W*	28, T. 1 S., R. 1 E.	9,600 - 13,500
Horrocks 2-4A1*	4, R. 1 S., R. 1 W.	7,600 - 15,680
Perfect 10 1-10A1*	10, T. 1 S., R. 1 W.	5,300 - 14,800
Chasel 2-17A1*	17, T. 1 S., R. 1 W.	8,000 - 14,240
E.J. Asay 1	20, T. 1 S., R. 1 W.	7,000 - 16,025
Fred Bassett 22-1	22, T. 1 S., R. 1 W.	5,000 - 13,920
Bradley 23-1	23, T. 1 S., R. 1 W.	3,500 - 13,820
Mr. Boom Boom 2-19A1*	29, T. 1 S., R. 1 W.	5,000 - 14,500

\* indicates geophysical well logs were digitized

These wells include nearly all of the better quality cuttings logs archived at the Utah Geological Survey (UGS) Sample Library for wells from the eastern half of Bluebell field. A few logs were excluded because they covered only short depth intervals, were difficult to interpret, or were south of the Roosevelt Unit study area. Wells with digitized logs are indicated by an asterisk.

Cuttings logs from different wells are inconsistent in many respects, for many reasons. Some cuttings logs identify the depths of individual sandstone beds relatively precisely (although far below the resolution of percent-shale logs), whereas others simply indicate a zone hundreds of feet thick with "10 percent sand, 90 percent shale." The amount of carbonate detected varies between wells, from none at all to moderately abundant, although the actual amount of carbonate may be comparable among many of these wells for similar depth intervals.

Although the cuttings-based estimates of carbonate versus quartz are of quite variable reliability, they are broadly consistent with published sedimentary facies descriptions. The upper Wasatch transition, which includes both fluvial-deltaic and lacustrine sediments, appears from cuttings to be shale dominated, with common-to-rare thin sandstone and limestone beds. The Wasatch Formation, which is mostly red beds, shale, and siltstone, appears from cuttings to be the most sandstone-rich portion of the stratigraphic section studied, containing both shale-dominant and sandstone-dominant intervals and with erratic indications of limestone. The lower Wasatch transition, which is largely lacustrine, is shale dominated, with locally abundant sandstone or limestone (Allison, 1995).

The percent-shale logs shows a 500- to 1,500-foot (152.4- to 457.2-m) thick Wasatch Formation interval of consistently very low percent-shale, bracketed by broad zones with generally much higher shale content but with many thin clean zones. These features are confirmed by the cuttings-based patterns described above.

## 2.7 Core-Plug Porosity

Core data was obtained from 196 plugs from a wide range of depths (from above the middle marker (Ryder and others, 1976) to nearly the deepest section normally drilled). Of the 196 samples, 73 contained visible microfractures. Most of these microfractures are probably drilling-induced (or, more accurately, caused by the change from *in-situ* to laboratory pressures). Porosities of these microfractured plugs were, in general, slightly higher than those of unfractured samples, therefore, they were not compared to logs (including them would not have changed the conclusions).

Thin sections of core (Wegner and Morris, this volume) show that some core plugs contained detectable amounts of "dead oil". The core plug samples were not treated to remove this oil prior to porosity determination. The presence of oil in some samples would cause the measurements to slightly underestimate porosity. This bias is considered to be minor. For example, this bias would also cause grain densities to be underestimated, but a pattern of lower matrix densities among the lower-porosity samples was not detected.

The grain densities of the core plugs are generally lower than had been expected, averaging 2.66 grams per cubic centimeter (g/cc). Garner and Morris (this volume) found a similar pattern in outcrop samples (which have no dead oil). In contrast, porosities calculated from density logs normally assume a matrix value of 2.68 g/cc in Roosevelt Unit area and 2.71 g/cc in western Bluebell field. Core-based XRD analyses suggest that feldspar may account for the low observed matrix density.

## 2.8 Porosity Logs

Log-based porosity can be calculated from any of the four standard logs: (1) density, (2) neutron, (3) sonic, or (4) resistivity. In Bluebell field, industry practice is to calculate porosity either by simple averaging of neutron and density porosities or by converting sonic travel time to porosity. The former is preferred if hole conditions are good enough to permit satisfactory neutron and density logging. In unusually ragged holes, a sonic log is run instead to provide porosities.

Using the mineral end points established from XRD, the accuracy of various log-based methods of porosity determination in shale-free reservoir rocks was evaluated. None of the four standard logs gives even roughly accurate porosity determination when used alone. The accuracy of porosity calculation from density, neutron, and sonic logs is very dependent on the relative proportions of calcite, dolomite, and quartz. For all three logs, porosities are biased by several percent, depending on mineralogy. Porosity determination from resistivity is completely impractical for Bluebell logs, not only because of the frequent occurrence of hydrocarbons but predominantly (as we will discuss later) because of the poor estimates of water resistivity.

Neutron and sonic porosity bias is particularly large in shaly rocks. Clay-mineral presence causes neutron logs to greatly overestimate porosity, because bound water in shales is attributed to pores. Sonic porosities are also overestimated, because the matrix velocity of shale is much less than that of the shale-free components.

Bad hole conditions cause bias in density logs. Washed out intervals (particularly shale but often reservoir rocks too) result in unreliably low density readings and therefore overestimates of porosity. Furthermore, the density log is converted to porosity by assuming a single matrix density for the entire log, typically 2.68 g/cc or 2.71 g/cc depending on location within Bluebell field. The core-plug determinations of matrix density, however, showed a surprisingly low average value of 2.66; all previous density-based porosities therefore have been overestimated.

The results suggest the common practice in the Bluebell field of determining porosity from a sonic log, rather than from neutron/density, is a source of considerable error. We found that the reliability of sonic porosities is highly variable downhole. Not only does the sonic overestimate porosity substantially in shale, but also it introduces error among shale-free rocks: depending on lithology, it may underestimate porosity by up to 5.7 percent or overestimate porosity by up to 2.7 percent.

The best log-based porosity estimator for shale-free rocks in the Bluebell field is simply the average of density-porosity and neutron-porosity (both calculated assuming limestone matrix). The biases in both measurements are of opposite sign and approximately cancel (within about 1 porosity unit). This result confirms the adequacy of established practice of averaging density and neutron porosities, with a very important caution: density washouts and clay-bearing intervals must be excluded because porosities will be overestimated in such zones.

Washouts are commonly identified on density logs. All density values less than 2.45 g/cc were excluded; the vast majority of such data are unreliable. The original operator's choice of either sandstone matrix (matrix density 2.68 g/cc) or limestone matrix (matrix density 2.71 g/cc) was used, although slightly more accurate final porosities are achieved with limestone matrix.

Three main sources of error remain in neutron/density porosity plots: (1) depth shifts, (2) bed boundaries, and (3) washouts. Depth shifts of the gamma-ray log with respect to the porosity logs cause shaly beds on the latter to be identified as clean, causing an overestimate of porosity because of the bound-water influence. At bed boundaries, the gamma-ray log may give a clean-sand value and yet the neutron log may show some shale; porosities are overestimated. The criterion for identifying washouts (density less than 2.45 g/cc) still allows the edges of most washouts to be counted as reliable and used in porosity estimation. A more accurate approach is to hand edit every washout, but this is impractical for tens to hundreds of washouts per well. Residual washouts, like the other two errors, cause porosities to be overestimated.

The porosity logs for five wells were carefully edited in order to evaluate the net effect of the three sources of error. All data were deleted that *may* be unreliable due to any of the errors. Note that this editing is conservative: excluded data may not be bad but nearly all of the included data are reliable. Consequently, the actual amount of clean formation is certainly much greater than that shown by such edited porosity logs. Plots comparing the raw and edited logs show that the "raw" porosity logs, and by extension the rest of the 49 porosity logs, do have quite a few points that are too high,

but the overall pattern of most wells is unchanged. Anomalously high porosities at a few wells, however, probably result from excessive amounts of these errors.

Averaged porosities over depth intervals of about 1,000 feet (304.8 m) are plotted versus depth and compared on a single plot (figure 2.1), for the five wells with edited porosities. "Error bars" shown for depth and porosity are depth range and standard deviation, respectively.

## 2.9 Comparison of Core-Based and Log-Based Porosities

Published estimates of the porosity of reservoir rocks in the Wasatch and upper Wasatch transition are about 5 to 20 percent (Lucas and Drexler, 1975; Chidsey, 1993). Log analyses, in contrast, show that a majority of clean-formation porosities are 4 to 8 percent. Higher porosities are present infrequently. Log-based porosity estimation is easily biased upward by clay effects on either the sonic or neutron log or by washouts on the density log. Considerable effort was made to exclude biased data. As a result, the porosities are lower than might normally be determined from these logs.

The core and log porosities are dominated by reservoir rocks. Core and log porosities were determined for sandstone, limestone, and dolomite, but not shale. As previously mentioned, even slightly shaly rocks were excluded from log-based porosity estimation. Shaly rocks were not entirely excluded from the core-based analyses, but only a few samples have clay contents greater than the 10 percent threshold (based on XRD) at which log-based porosity analysis is definitely biased. Both core and log porosities exhibit somewhat non-normal distributions, with tails extending out to high porosity. This tail is more distinctive in the core data, so core porosities were averaged using the median rather than mean. The median core-based porosity is 1.0 percent (1.5 percent excluding samples with any detectable clay). This value is much lower than the published porosities of 5 to 20 percent; it is also significantly lower than the log-based estimates of 4 to 8 percent.

The two porosity determination techniques are not exactly comparable, because log porosities include both intergranular and fracture porosity, whereas the core-plug porosities are limited to intergranular porosity. Note that including microfractured core plugs would not have eliminated this difference, because many microfractures were not present *in situ*, and core plugs are incapable of sampling large-scale fractures that may provide the majority of the downhole fracture porosity. Fracture porosity is typically about 1 to 2 percent; adding this amount to the core-plug values gives a core-based estimate of 2 to 7 percent for most *in-situ* porosities. This core-based estimate is in reasonable agreement with our estimate of 4 to 8 percent based on logs.

Figure 2.1 shows plots of porosity versus depth for both core-based and log-based data. Neither dataset exhibits a simple compaction trend within the depths analyzed; other factors such as cementation, secondary porosity, and lithologic variations must dominate compaction-related, depth-dependent porosity decreases. Core and log data do indicate higher porosities at about 8,000 to 9,700 feet (2,438-2,957 m) than below that depth. Log data indicate a subtle porosity increase downhole between 10,000 and 13,000 feet (3,050-3,950 m). Too few clay-free core data are available below 11,200 feet (3,400 m) to resolve that change.

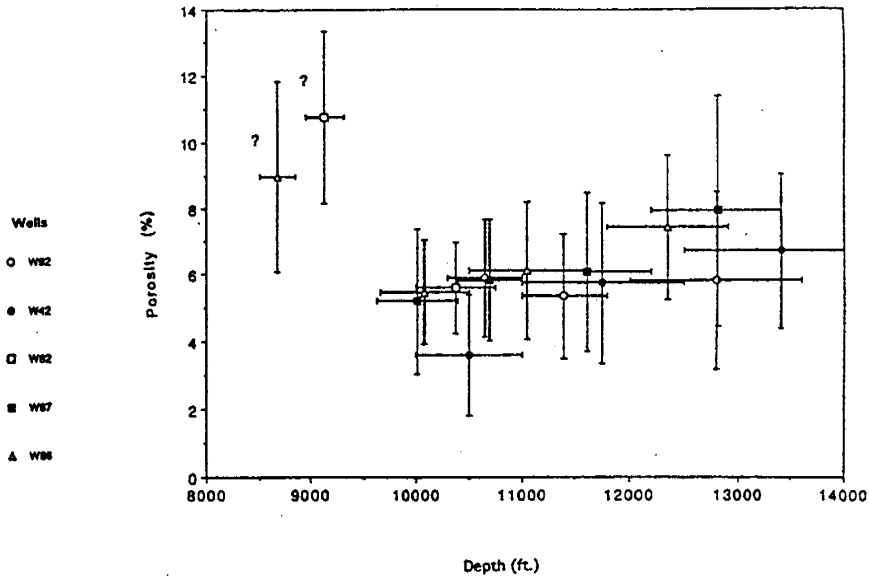


Figure 2.1A.

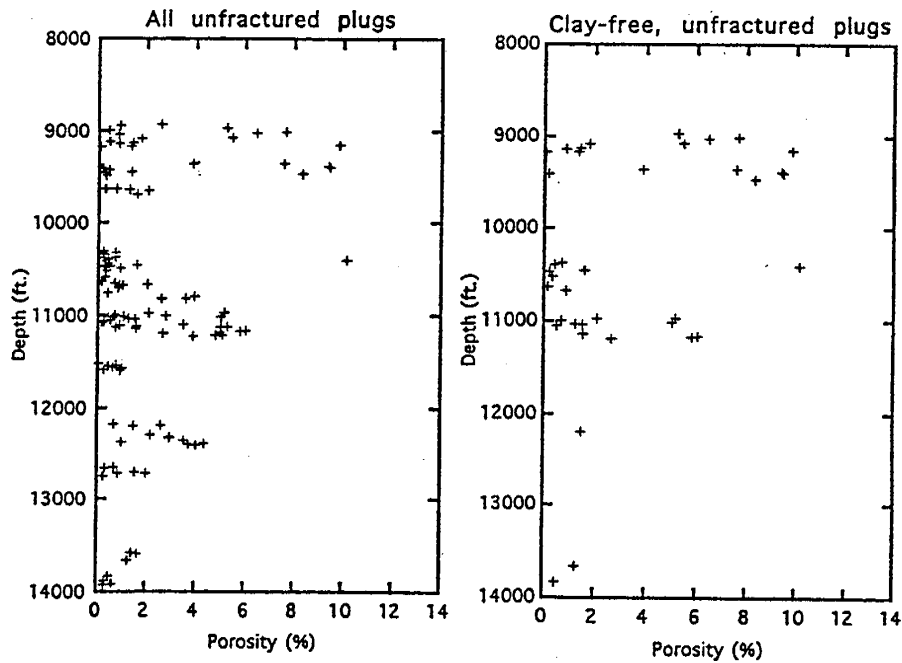


Figure 2.1B.

Figure 2.1. Log-based and core-based porosities versus depth. Note that these porosities are much lower than previous estimates of 5 to 20 percent for Bluebell porosities. 1A: log-based porosities for five wells (W92 is 2-22 Ute, section 22, T. 1 S., R. 1 E.; W42 is 1-18 Chasel, section 18, T. 1 S., R. 1 E.; W82 is RU 13, section 13, T. 1 S., R. 1 W.; W87 is RU C-11, section 18, T. 1 S., R. 1 W.; and W86 is RU 5, section 20 T. 1 S. R. 1 W.). 1B: core-based porosities for samples lacking visible fractures; 1C: log-based porosities for the two demonstration wells (W43 is 1-7 Michelle Ute, and W46 is 1-17 Malnar Pike).

## Log-based Porosities

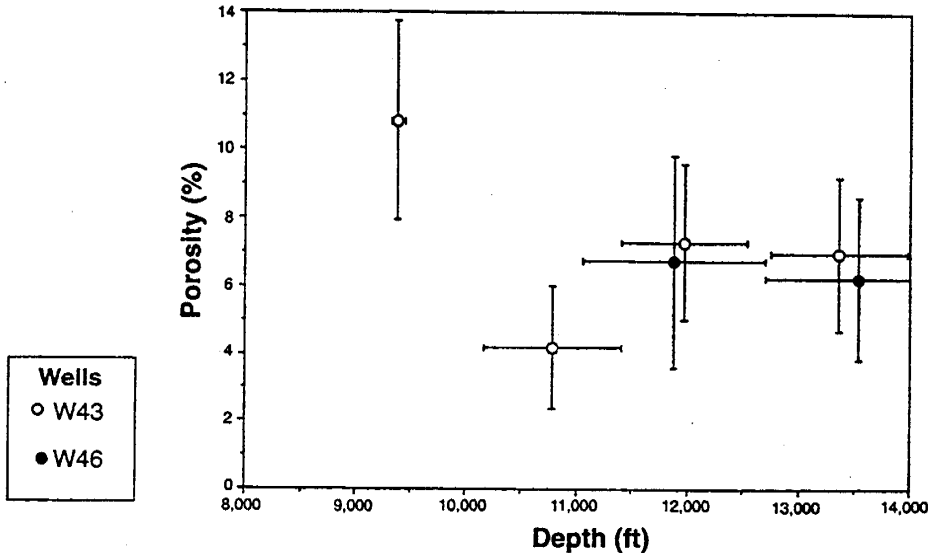


Figure 2.1C

### 2.10 Controls on Permeability and Production

Fractures are believed to be the dominant permeability mode for hydrocarbon production in the Uinta Basin. Fracture permeability can be several orders of magnitude higher than intergranular permeability, and fracture permeability is the reason that the second well in a section almost always produces less oil than the first well. Many log types give a qualitative indication of fracture intensity, but the approach normally used in Bluebell field development is more direct: operators perforate at the mud-gas kicks, interpreting them as indicative of both fracture permeability and hydrocarbon presence.

Unfortunately, some mud-gas kicks indicate beds that provide long-term production, whereas others result in only short-term production. Both may indicate fracture permeability plus hydrocarbon presence, but the difference is intergranular permeability. Hydrocarbon production requires porosity; and fracture porosity is only 1 to 2 percent, similar to our median core-plug intergranular porosity, but substantially less than many measured intergranular porosities. If intergranular permeability is small,

production rapidly wanes, whereas substantial intergranular permeability provides continuing hydrocarbon production. According to this scenario, it is important to identify beds that not only have mud-gas kicks but also have high intergranular permeability.

Core-plug analyses show that two factors control intergranular permeability: clay content and porosity. Examining only those samples that lack visible fractures, it was discovered that both porosity and permeability are highly dependent on clay content: porosity is somewhat lower, and permeability is much lower, in samples containing clay minerals than in clean samples (figure 2.2). Although XRD-based determination of clay content is only semi-quantitative, it appears that even 2 to 4 percent clay is sufficient

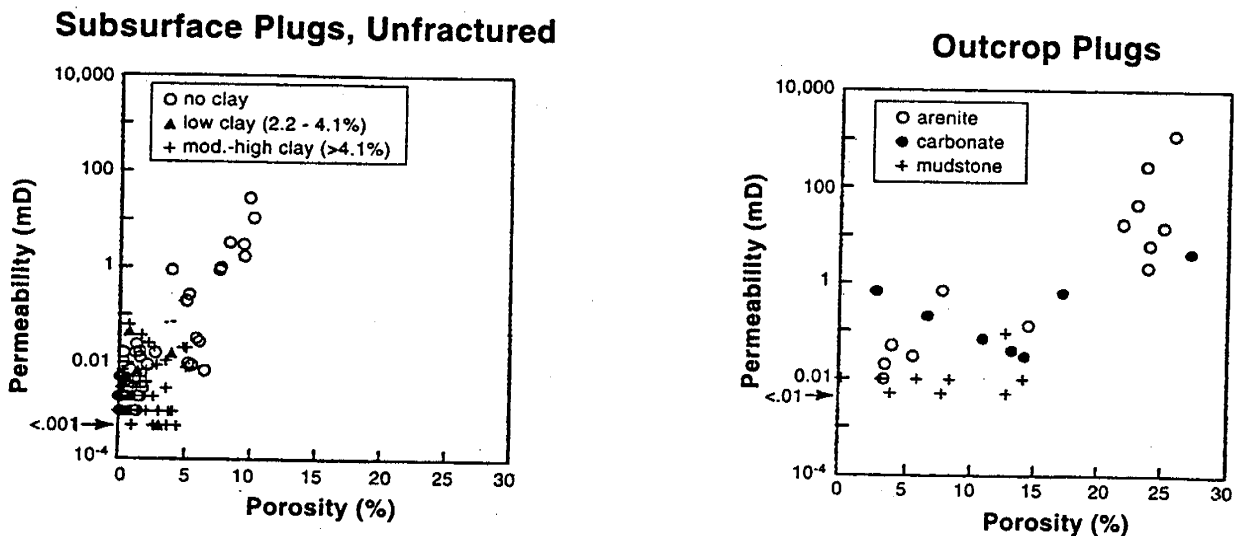


Figure 2.2. Crossplots of permeability versus porosity, for core plugs from both well cores and outcrops. Note that only clay-free rocks show a linear relationship between porosity and permeability.

to reduce intergranular permeability to values less than 0.1 mD. This extreme sensitivity of permeability to clay content suggests that the clays are secondary and reduce permeability by clogging pore throats.

The conclusion is that one needs to confine perforations to clean beds. This objective is an achievable tactic for improving production, because shale percentage is the easiest and most reliable mineral component to determine from logs.

Among clay-free core plugs, a linear relationship exists between porosity and the logarithm of permeability (figure 2.2). Such relationships are found in many other fields, although their slopes need to be locally determined. Based on this relationship, the

highest intergranular permeability, and therefore the best chance of long-term production, will be found in *porous, shale-free beds*.

## 2.11 Formation Water Resistivity and Water Saturation

As anticipated, estimations of water saturation are dubious. Consequently, water saturations ( $S_w$ ) were calculated for only four wells. Potential problems with water saturation calculations include: (1) intertool differences in depths of penetration, (2) intertool differences in detection of formation damage, (3) intertool differences in sensitivity to intergranular versus fracture porosity, and most important (4) highly variable formation-water resistivity ( $R_w$ ).

Formation-fluid resistivity was obtained in two ways: (1) from the UGS catalog of  $R_w$  measurements (Gwynn, 1995), and (2) estimates based on Pickett plots. Plots of  $R_w$  versus depth provided in the UGS catalog show variability of over an order of magnitude at a given depth, and no clear trend of changing  $R_w$  with depth. To examine the possibility that lumping all of Bluebell in those plots might obscure local patterns that are more consistent, depth and  $R_w$  were plotted on a map of the eastern portion of the field, and then divided into four geographic regions, plotting  $R_w$  versus depth separately for each region. Dispersion is higher in the south, and the dispersion in the greater Roosevelt Unit area is significantly smaller than in the field as a whole. The median  $R_w$  in the greater Roosevelt Unit area is 0.74 ohm•m at 68 degree Fahrenheit ( $^{\circ}\text{F}$  [ $20^{\circ}\text{C}$ ]), and no systematic variation is evident with depth, except for temperature-dependent variations. Assuming a thermal gradient in these wells of 81 $^{\circ}\text{F}/\text{mile}$  (28 $^{\circ}\text{C}/\text{km}$ ) (which is significantly higher than that implied by bottomhole temperatures because of drilling-induced hole cooling), this  $R_w$  corresponds to a downhole range of 0.24 to 0.195 ohm•m at 221.5 to 283.1 $^{\circ}\text{F}$  (105-139 $^{\circ}\text{C}$ ) at 10,000 to 13,000 feet (3,050-3,950 m) respectively.

Formation-fluid resistivity was estimated at four wells with Pickett plots as well: log/log plots of deep resistivity (ILD) versus porosity, on which one can pick  $R_w$  if some water-saturated ( $S_w=1.0$ ) zones are available. These plots were employed at all four wells with edited porosity data. Using the water-catalog-based  $R_w$  of 0.24 to 0.195 ohm•m for 10,000 to 13,000 feet (3,050-3,950 m) (221.5-283.1 $^{\circ}\text{F}$  [105-139 $^{\circ}\text{C}$ ]) gave extremely high water saturations, with 40 to 90 percent of the points having an apparent water saturation of more than 1.0.

The values of  $R_w$  estimated from the Pickett plots for the four wells were all lower than those predicted from water samples. Removing temperature-dependent effects by expressing the estimated value of  $R_w$  at 10,000 feet (3,050 m) (221.5 $^{\circ}\text{F}$  [105 $^{\circ}\text{C}$ ]), the values of  $R_w$  were 0.077, 0.175, 0.081, and 0.136 ohm•m for the four wells. These values were used to calculate water saturations for the clean zones with the most reliable porosities.

Unfortunately, these attempts to determine water saturations provided no improvements over standard industry practices in Bluebell field: look for mud-gas kicks, and confirm qualitatively that resistivity suggests *some* hydrocarbon presence rather than water-filled porosity.

## 2.12 Log Analyses and Production

Detailed comparison of the log results to production is precluded by two factors: (1) most wells penetrated a very large number of beds, so their production cannot be linked to the log properties of individual beds, and (2) log-based estimation of water saturation is very imprecise for these formations. However, the following two observations are: (1) the much higher production in western Bluebell than in eastern Bluebell can be associated with generally much higher proportions of clean reservoir rock; and (2) the Wasatch Formation is generally less productive than the transition zones immediately above and below it, in spite of its relatively high proportion of clean reservoir, because its porosities tend to be lower than in the bracketing zones.

## 2.13 Conclusions

Analyses of core plugs show that intergranular permeability will be found only among rocks that are nearly shale-free and have porosities greater than 6 percent. Even 2 to 4 percent clay content can significantly reduce permeability. The spectral-gamma is the most reliable log for determining clay content.

An average of the porosities calculated from the neutron and density readings is the most reliable log-based method to determine intergranular porosity. Porosity calculated from sonic traveltime is a source of considerable error.

Uncertainties in fluid resistivity preclude accurate calculations of water saturation; measurements and calculations of the water resistivity are highly variable. The median  $R_w$  in the Roosevelt Unit area is 0.74 ohm•meter at 68 °F (20 °C) and no systematic variation is evident with depth, except for temperature-dependent variations.

### 3. OUTCROP STUDY OF THE GREEN RIVER FORMATION, WILLOW CREEK CANYON

*Ann Garner and Thomas H. Morris*  
Brigham Young University

#### 3.1 Introduction

Approximately 2,790 feet (850 m) of the lower Green River Formation were measured and described in the Willow Creek Canyon area on the southwest flank of the Uinta Basin. Outcrop of the Green River Formation were studied to establish the general stratigraphic framework and broad facies belts of the Altamont and Bluebell field areas in order to better understand reservoir capacity and production potential. From this, we were to draw conclusions and make recommendations as to the specific lithologic units in the formation that should be targeted as potential prolific producers of hydrocarbons.

Five different steps were taken to complete this task. First, 2,790 feet (850 m) of outcrop of the lower Green River Formation (also known as the Green River and Wasatch transition zone) in the Willow Creek area were measured and described. Second, samples were taken, which represented the volumetric majority of lithology present in the outcrop, for use in various laboratory studies. Third, core plugs from the lithologic samples were analyzed for porosity, vertical and horizontal permeability, and grain density. Fourth, 33 thin sections were made from these samples and each thin section was petrographically classified. The sand-dominated clastic rocks (16 in all) were subjected to a 300 grain point-count analysis. Fifth, the remains of the initial samples were analyzed for clay content using x-ray diffraction as described by Moore and Reynolds (1989).

The outcrop study indicates that the rock type with the best reservoir characteristics is arenite. Arenite beds in the lower half of the measured section tend to have the best intergranular porosity and permeability. These arenite beds contain less swelling clays than arenite beds in the upper part of the section and are commonly interbedded with shale and mudstone which may serve as hydrocarbon source rocks. Comparison of outcrop data with limited data from subsurface cores of the lower Green River Formation shows: (1) more smectite is present in the outcrop than in the core and (2) arenite from the outcrop contain more feldspars and lithic fragments than arenite from core. Porosity and permeability data, along with petrography and clay analysis of outcrop samples suggest that the lower part of the Green River Formation has better reservoir rock than the upper part.

General facies "belts" in the Green River Formation have been described on a basin-wide scale (Fouch, 1975; Ryder and others, 1976). Remy (1991) and Smith (1986) have described in more detail the depositional environments of the Green River and Colton Formations, respectively. These formations were studied in the south-central and southwest part of the Uinta Basin, but neither of these studies nor the previously mentioned ones addressed the specific problem of reservoir potential. Morris and others (1991) described the lithofacies of the Colton Formation, and Morris and Richmond (1992) studied the reservoir quality and characteristics of the major clastic facies within that formation.

Although the measured section and the petrography of the thin sections made from outcrop samples will be discussed here, the actual documentation will not be included. Copies of those documents can be found in the annual report of this project for the period from September 30, 1993 to September 30, 1994 (Allison, 1995).

### 3.2 Measured Section

A complete stratigraphic section of the lower Green River Formation was measured along road outcrops of Highway 33 (191) on the south flank of the Roan Cliffs in Willow Creek Canyon, Utah. The section begins in the NW1/4SE1/4 section 23, T. 11 S., R. 8 W., Matts Summit 7-1/2 minute U.S. Geological Survey quadrangle and ends in the W1/2SE1/4 section 11, T. 7 S., R. 8 W., Jones Hole 7-1/2 minute quadrangle. This section rests stratigraphically above the red beds of the Colton Formation. The transition from Colton rocks to Green River rocks is gradual in the study area. Measurements were made using a Jacob's staff and the units were described according to Dott's (1964) and Dunham's (1962) classification schemes. The section consists of 2,789.2 feet (850.16 m) of 695 distinct lithologic units and 19 different rock types. The most abundant rock types were silty limy mudstone and limy mudstone which represent 25 percent and 13 percent of the total thickness, respectively (figure 3.1).

Several intertonguing facies of lacustrine rocks are represented in the outcrop demonstrating that the lake may have been shallow and that facies belts shifted rapidly over an extensive area with minimal change in water depth. Nevertheless, generalized depositional environments have been identified by Ryder and others (1976). The depositional environments identified in the measured section are shown in table 3.1.

Table 3.1. Depositional environments identified in the Willow Creek Canyon measured section. Measurements shown are from the base of the section up.

Distance Above the Base of the Measured Section	Depositional Environment
0 to 219 feet (67.0 m)	open lacustrine
219 to 285 feet (67.0-87.0 m)	deltaic
285 to 369 feet (87.0-112.5 m)	interdeltaic grading upward to open lacustrine
369 to 461 feet (112.5-140.5 m)	open lacustrine grading upward to marginal lacustrine, "carbonate marker" of Cashion (1967)
461 to 525 feet (140.5-160.0 m)	interdeltaic with occasional fluvial channels
525 to 1,498 feet (160.0-456.5 m)	interdeltaic to lake margin carbonate flat with occasional fluvial channels
1,498 to 1,903 feet (456.5-580.0 m)	fluvial-deltaic to interdeltaic
1,903 to 2,789 feet (580.0-850.0 m)	lake margin carbonate flat

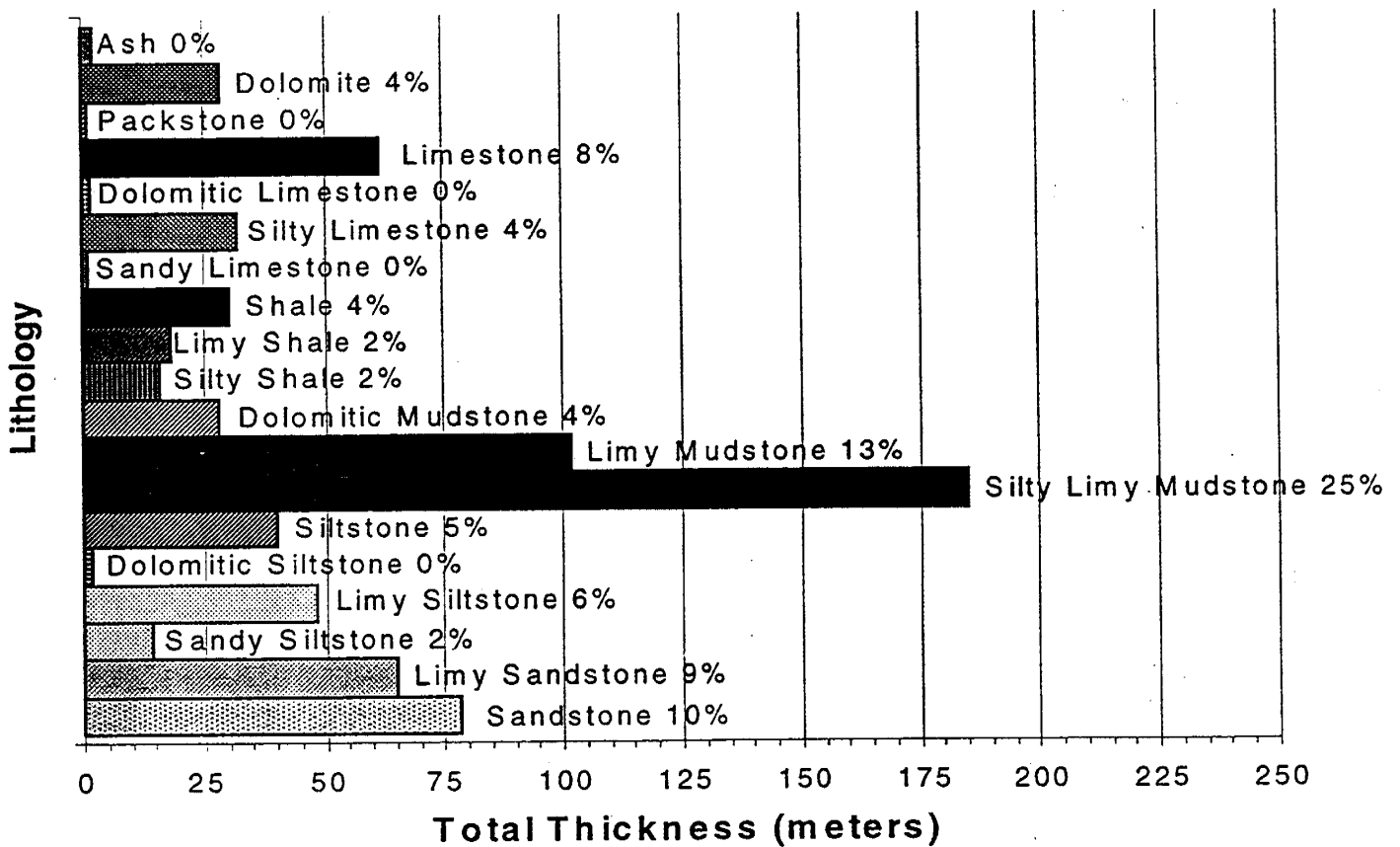


Figure 3.1. Relative proportions of the various rock types identified in the outcrop. The most abundant rock types are silty, limy mudstone and limy mudstone which represent 25 and 13 percent of the total thickness, respectively.

### 3.3 Petrography

Thirty-three thin sections were made from samples that represent the volumetric majority of measured section lithology. Each thin section was petrographically classified and all sand-dominated clastic rocks were subjected to a 300 grain point-count analysis. Thirteen of the 16 point-counted samples were classified as feldspathic arenite, and the other three were feldspathic wacke (figure 3.2). The classification scheme used for the clastic rocks was from Carozzi (1993), which was modified from Dott (1964). Carbonate rocks were classified according to Dunham (1962).

Other workers have found that the cores from the Altamont and Bluebell fields contain much less feldspar than the measured section samples and are thought to have been sourced from the Uinta Mountains to the north and the Sevier orogenic belt to the west. According to studies by Ryder and others (1976) and Fouch and others (1992), the sediment source of the outcrop was from feldspar-rich topographic highs to the south such as the San Rafael and the Uncompahgre uplifts.

### 3.4 Clay Analysis

Each of the samples that were petrographically analyzed were also examined for clay content. The procedure used was that described by Moore and Reynolds (1989); oriented clay samples on glass plates were analyzed by x-ray diffraction (XRD) using a Scintag XDS-2000  $\theta$ - $\theta$  X-ray powder diffractometer. To confirm the presence of swelling clays the samples were saturated with ethylene glycol, and were again analyzed by XRD. The clays identified by this method from outcrop samples are chlorite, illite, kaolinite, and varying mixtures of each of these with smectite resulting in mixed-layer clays (figures 3.3 and 3.4). These data suggest that the samples become slightly lower in smectite content with depth (figure 3.5). The presence of kaolinite in outcrop samples suggests that at least at the fringes of ancient Lake Uinta, the sediment was deposited in well-oxygenated and relatively fresh water (Hosterman and Dyni, 1972). Clay analysis of cores from the Bluebell field indicates that the same suite of clays is present but that there is typically less smectite and kaolinite. Variations in the overall clay content from the outcrop to the core are probably due to the initial differences in feldspar content and to subsequent diagenetic factors (different pressure and temperature regimes for example; Velde, 1992).

### 3.5 Porosity and Permeability

Core plugs were taken from every rock type that was petrographically analyzed. Permeabilities of the plugs were determined by using a pressure transducer in a Hassler sleeve. Permeabilities varied from less than 0.01 mD in mudstones to 1,241 mD in feldspathic arenite. Measured porosities varied in mudstone from 2 to 13 percent, and in arenite from 3 to 27.2 percent (table 3.2). Porosities from the lab were compared to point-counted porosities. In general there was good agreement; where there is some disagreement an explanation is given in the petrologic description. It appears that the arenite have much greater interparticle porosity. Crossplot porosity and permeability values of arenite are distinctly grouped into tight and open sandstone (figure 3.6). In the lower Green River Formation the tight sandstone are found in the

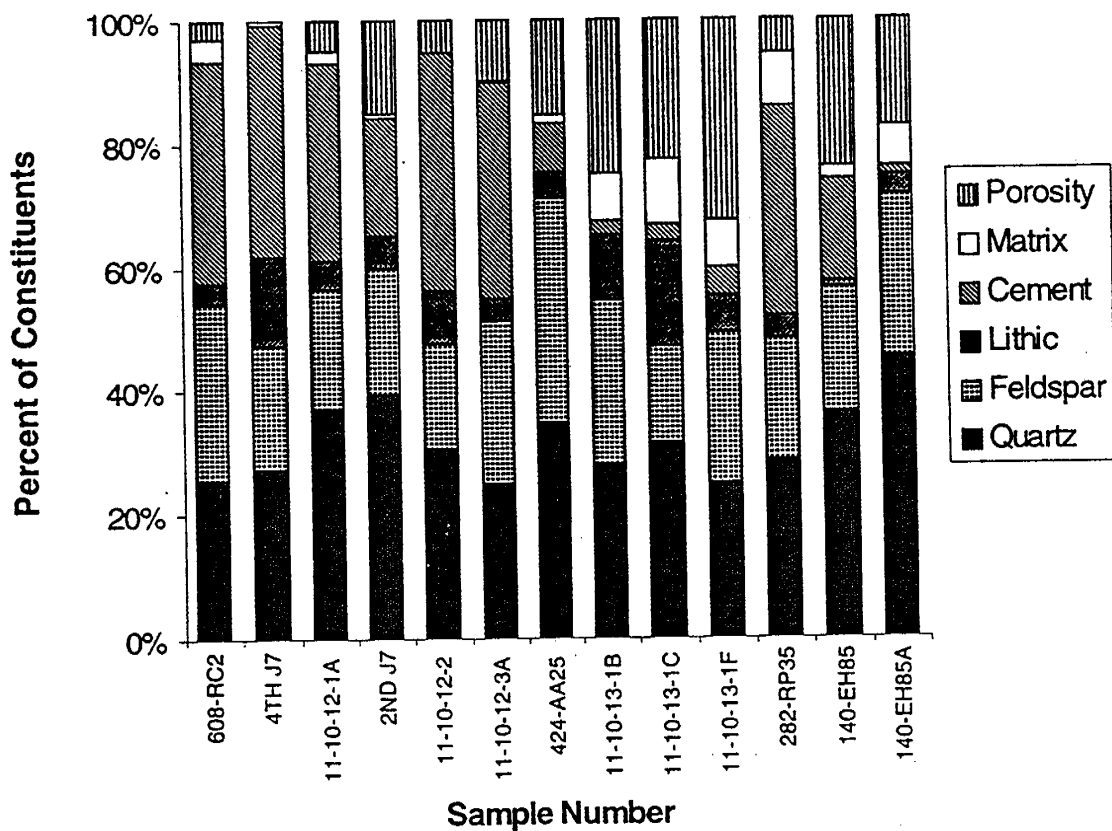


Figure 3.2. Relative proportions of the main constituents in the arenites from the outcrop. The left side of the graph corresponds with the top of the measured section, and the samples to the right are increasingly stratigraphically lower in the section. The amount of cement in the samples tends to decrease, while the amount of matrix and porosity fluctuates but tends to increase toward the base of the measured section.

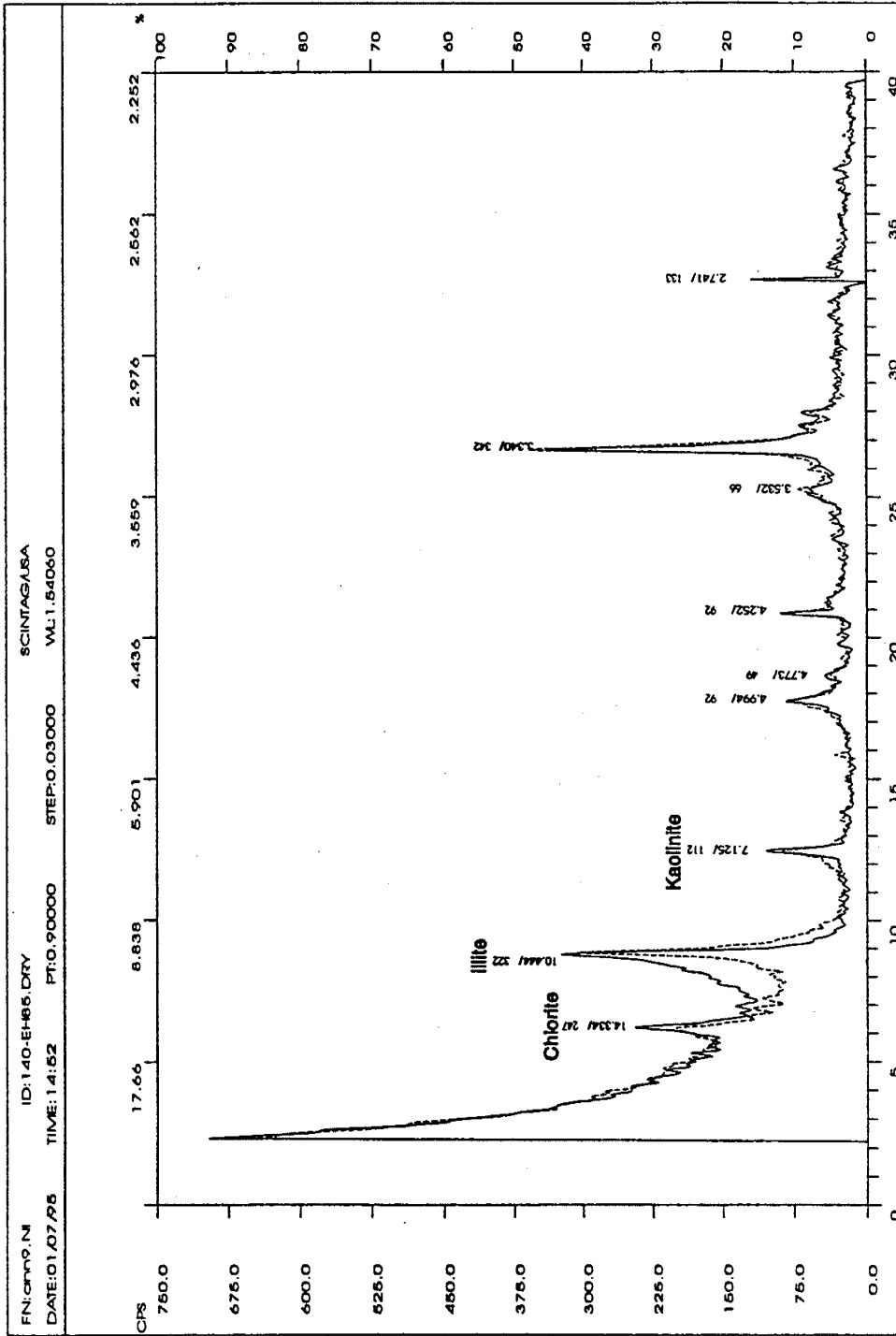


Figure 3.3. X-ray diffraction plot of an arenite with chlorite, illite, and kaolinite (the primary peaks of which have been labeled) and very little associated smectite. The dashed line identifies the XRD plot of the second analysis of the sample which was run after it had been saturated with ethylene glycol. The very slight shifting of the illite peak to the left in this second analysis indicates that there is a small amount of smectite associated with the illite, suggesting the presence of a mixed-layer swelling clay. Since the chlorite and kaolinite peaks do not shift at all, there is no smectite associated with either of those clays. The label "CPS" on the left-hand y-axis represents counts/second, the bottom x-axis is the degree of  $2\theta$  with  $\theta$  ranging from 1 to 20, and the top x-axis is "d" in Bragg's Law ( $2d\sin\theta = n\lambda$ ) where "d" is the spacing between clay layers in angstroms.

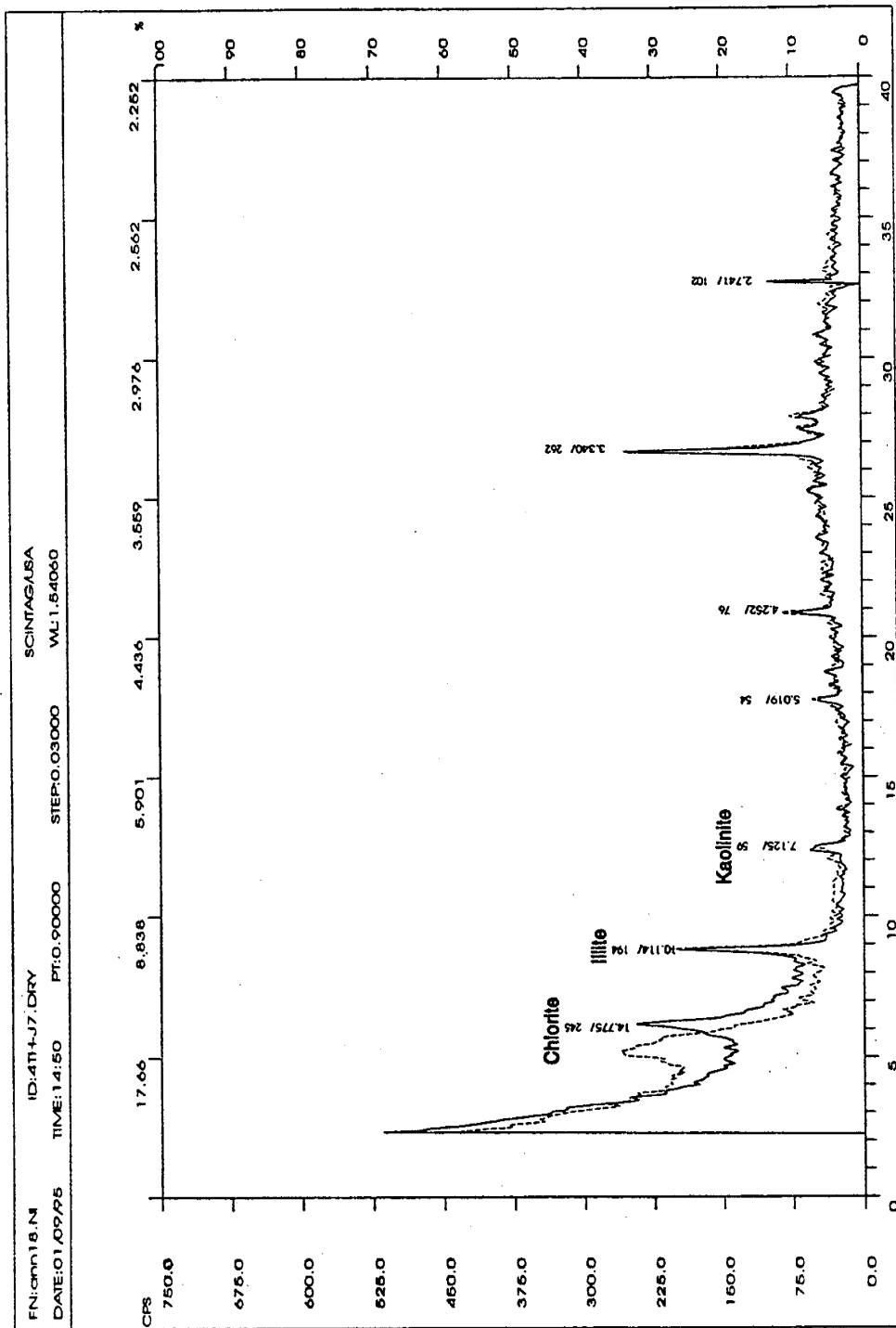


Figure 3.4. X-ray diffraction plot of an arenite with chlorite, illite, and kaolinite (the primary peaks of which have been labeled) and some smectite. The dashed line identifies the XRD plot of the second analysis of the sample which was run after it had been saturated with ethylene glycol. The significant shifting of the chlorite peak to the left in this second analysis indicates that there is a lot of smectite associated with the chlorite, implying the presence of a mixed-layer swelling clay. There is no smectite associated with the illite peak and very little with the kaolinite peak. The label "CPS" on the left-hand y-axis represents counts/second, the bottom x-axis is the degree of  $2\theta$  with  $\theta$  ranging from 1 to 20, and the top x-axis is "d" in Bragg's Law ( $2d\sin\theta = n\lambda$ ) where "d" is the spacing between clay layers in angstroms.

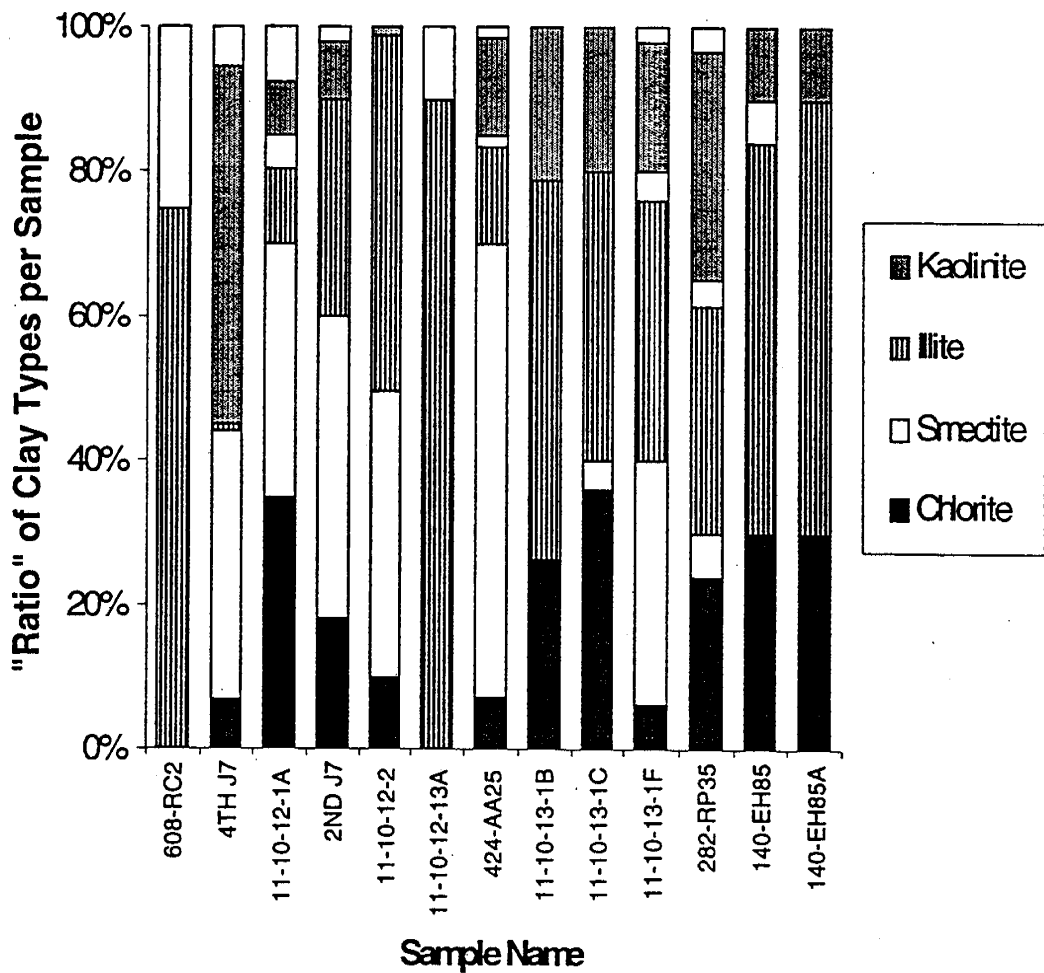


Figure 3.5. Relative proportions of chlorite, illite, and kaolinite in outcrop samples and their individual association with smectite. The left side of the graph corresponds with the top of the measured section and the samples increase in depth (down section) to the right. The amount of smectite associated with the other three clays tends to decrease with depth.

Table 3.2. Listing of the permeability, porosity, clay content, and lithologic name of outcrop samples.

SAMPLE NAME	Meters Above Base	Horiz. Perm (mD)	Vert. Perm (mD)	Porosity (%)	Clay Content	Comments	Lithology
5-DN5	6.3	0.07	0.05	10.90	Cs, Is, K, z	mostly K	Feldspathic wacke
7-DN7	7.8	0.66	0.02	2.70			Fossiliferous packstone
21-DN21	21.3				Cs, Is, K	moderate/equal	Fossiliferous wackestone
36-DN36	34.5				cS, Is, K, z	moderate/equal	Wackestone
37-DN37	35.7	4.40	0.53	27.20	Cs, Is, Ks	very little of any	Ostracodal packstone
43	48.2	<0.01	<0.01	7.70	Cs, Is, K	very little of any	Mudstone
47-DN47	59.6	<0.01	0.01	3.80	Cs, l	very little of any	Mudstone
102-EH47	103.9	93.+	<0.01	4.70	CS, Is	very little of any	Mudstone
113-EH58 (BAG)	129.2	0.01	0.01	3.10	cS, Is, Ks?	very little of any	Mudstone
113-EH58 (BLOCK)	129.2	0.01	0.01	5.80	Cs, Is, Ks?	very little of any	Mudstone
140-EH85	149.9	285.00	208.00	23.70	Cs, l, Ks, z	more illite	Feldspathic arenite
140-EH85A	149.9	46.00	19.00	23.00	Cs, Is, Ks, z	more illite	Feldspathic arenite
265-RP18	379.8	0.20	<0.01	6.60	Cs, Is, Ks, Z	moderate/equal	Feldspathic wacke
282-RP35	394.3	0.13	0.05	14.50	Cs, Is, z	moderate/equal	Feldspathic arenite
11-10-13-1c	528.0	2.20	0.53	23.90	Cs, Is, K, Z	scanty/equal	Subfeldspathic arenite
11-10-13-1b	534.0	6.50	2.00	24.00	Cs, Is, K, z	moderate/equal	Feldspathic arenite
11-10-13-1f	535.5	15.00	1.30	25.10	cS, Is, Ks, z	mostly cS, & Is	Feldspathic arenite
424-AA25	558.5	18.00	4.40	21.90	cS, Is, K	mostly cS	Feldspathic arenite
438-AA39	571.9				cS, Is	mostly cS	Mudstone
451-AA52	584.1	0.01	<0.01	8.30	cS, Is, Ks	very little of any	Peloidal quartz mudstone
479-CC4	614.8	<0.01	<0.01	12.80	cS, Is, z	very little of any	Peloidal mudstone
J3	650.7	0.04	0.03	13.20	Cs, Is, Ks, Z	mostly Cs & K	Feldspathic wacke
2nd J7	653.7	1241.00	1342.00	25.80	cS, Is, K, z	mostly cS & Is	Feldspathic arenite
11-10-12-2	653.7	0.02	0.02	3.40	cS, Is, K, Z	mostly cS & Is	Feldspathic arenite
11-10-12-13a A	653.7	0.01	0.01	3.30	Is	also brushite	Feldspathic arenite
11-10-12-13a B	653.7	0.05	NA	3.90	Is	also brushite	Feldspathic arenite
4th J7	654.2	3.4+	0.01	4.00	cS, l, Ks, z	mostly cS & Is	Feldspathic arenite
11-10-12-1A	654.2	0.03	0.02	5.50	CS, Is, z	mostly cS	Feldspathic arenite
IH10	693.0	0.63	0.88	17.20	cS, Is	very little of any	Fossiliferous packstone
GB2	740.2	0.03	0.02	14.20	Cs, Is, K, Z	mostly Cs & K	Quartz wacke w/ clay clasts
608-RC2	752.4	0.69	0.02	7.70	Is	also brushite	Feldspathic arenite
623-RC17	762.6	0.01	<0.01	0.20	cS	maybe some l	Mudstone
638-RC32 A	776.3	0.09	0.01	12.70	cS, Is	mostly cS	Mudstone
638-RC32 B	776.3	0.01	<0.01	14.10	cS, Is	mostly cS	Mudstone

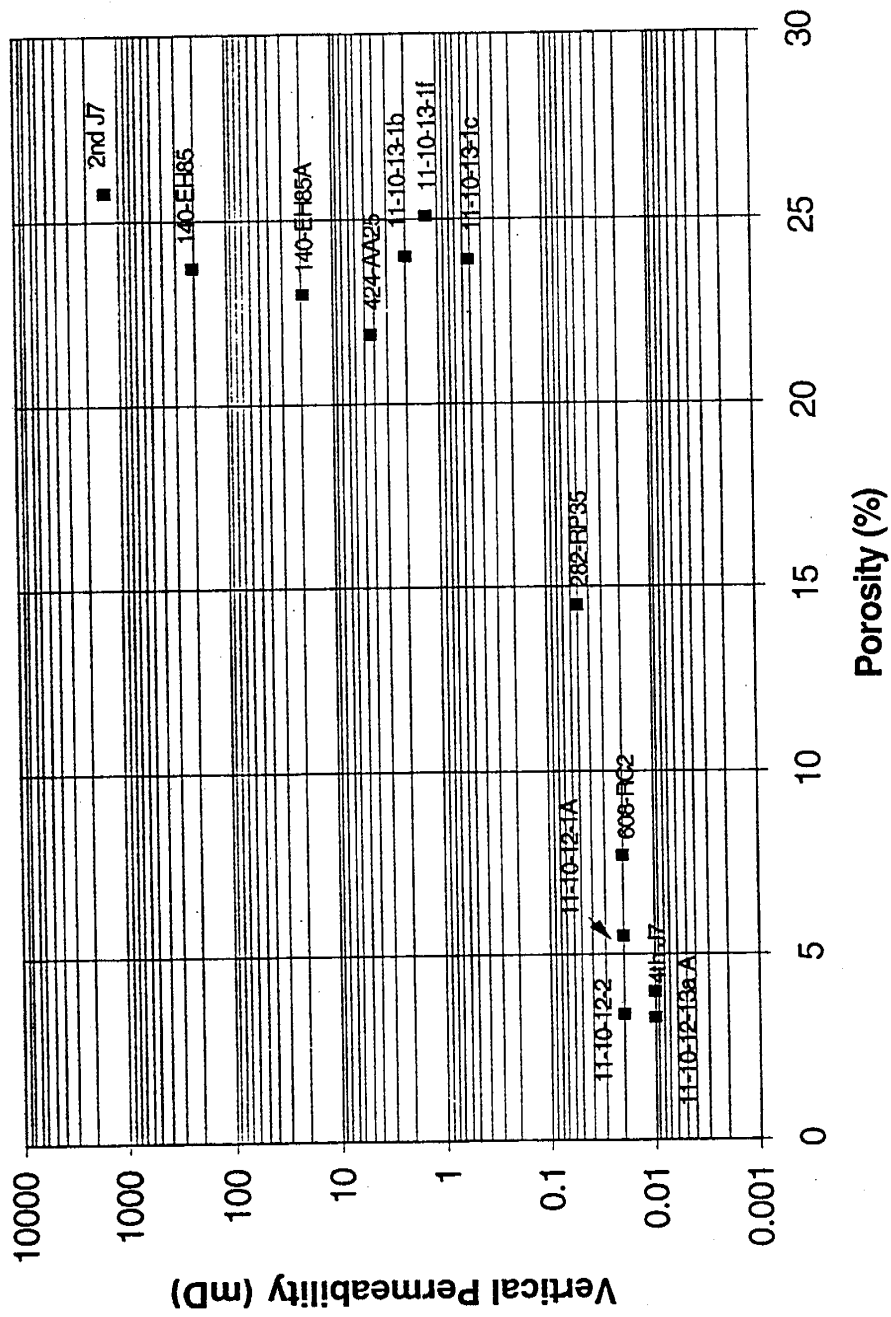


Figure 3.6. Crossplotted porosity and permeability values of arenites. The low porosity sandstone beds (lower left) are found in the upper part of the measured section and the relatively higher porosity sandstone beds (upper right) are found throughout the middle and lower part of the section.

upper part of the measured section, and the open sandstone extend throughout the middle and lower part. This grouping may be due either to secondary diagenesis that has reduced the interparticle porosity subsequent to uplift and exposure of the formation, or to initial compositional differences in sediments as they were deposited.

### 3.6 Conclusions

Arenite in outcrop tend to have the largest amount of intergranular porosity and highest permeability of rocks in the Green River Formation and therefore are potentially the best reservoir rock in the subsurface. The most porous arenite are found at the base of the lower Green River Formation which overlies the Colton Formation (Wasatch equivalent). These arenite beds extensively interbedded with shale and mudstone which likely served as hydrocarbon source rocks. Relatively abundant mixed-layer clays are present in the outcrop but the amount of swelling clays decreases toward the base of the section.

Comparison of outcrop and limited core data from the Bluebell field of the lower Green River Formation, show more smectite is present in the outcrop than in the cores. The arenite at the outcrop are typically feldspathic and those from the cores are subfeldspathic. The difference in mineral composition from outcrop to subsurface is most likely due to a mixing of provenances. The outcrop lithology is sourced predominately from feldspar-rich highlands to the south but the clastic sediments in the Bluebell field near the basin center most likely comes from the quartz-rich Uinta Mountains to the north, the Sevier orogenic belt to the west, as well as from the highlands to the south (Ryder and others, 1976). The smaller amount of feldspar in the cores may also be due to the difference in transportation distance with most of the feldspar being chemically and mechanically degraded before deposition at the basin center. The difference in kaolinite content between the outcrop and the core is probably due to gradational water chemistries from the margin of the basin to the center (Hosterman and Dyni, 1972).

The part of the lower Green River Formation described in the bottom half of the measured section would most likely produce hydrocarbons in the subsurface because: (1) this section is rich in arenite of relatively high porosity and permeability, (2) the arenite in the lower half of the outcrop are thicker than those in the upper half, and (3) less swelling clay is present in the arenite found in the lower half of the section.

## 4. CORE ANALYSES OF THE LOWER GREEN RIVER AND WASATCH FORMATIONS

*MaryBeth Wegner and Thomas H. Morris*  
Brigham Young University

### 4.1 Introduction

Cores from the Bluebell field were selected for study based on their proximity to the two main study areas in the field, as well as their availability for study and sampling. Ten cores consisting of 1,613 feet (489 m) of section from the lower Green River and Wasatch Formations were studied. The cores were described in terms of lithology, clay type, permeability, and fractures. Seventy-eight percent of the rocks studied are siliciclastic, while only 22 percent are carbonate. The beds with the most apparent potential to be hydrocarbon reservoirs are permeable arenite that overlie fractured mudstone. A variety of sandstone beds are found in the subsurface at Bluebell field, ranging from lithic wacke to quartz arenite. Clays, especially mixed-layer clays, are present in very small amounts.

Naturally occurring fractures are believed to be a significant factor in hydrocarbon production because intergranular porosity and permeability is very low in all rock types studied. Fractures in sandstone beds are commonly vertical to near-vertical to bedding, long (greater than 3.3 feet [1 m], length measured in the core although many fractures extend out of the plane of the sample), from 0.03 to 0.13 inches (0.5-3.0 mm) wide, and only partially calcite-filled. Fractures in mudstone beds have multiple orientations, but have a higher fracture density than is found in the sandstone beds. However, fractures in mudstone beds are very short (commonly less than 4 inches (10.2 cm)), generally less than 0.03 inches (0.5 mm) wide, and almost completely calcite-filled. Organic-rich mudstone intersected by fractures may be important hydrocarbon source beds and are often in contact with better quality reservoir sandstone beds.

Quartz arenite beds have slightly higher porosity and permeability, less swelling clay, and more large, open fractures, than most other rock types present. The most prospective beds may be arenite in contact with fractured mudstone as a hydrocarbon source rock.

### 4.2 Core Descriptions

Ten cores were selected for description from Bluebell field based on their availability, proximity to the study areas, and stratigraphic position (figures 4.1 and 4.2). Six of the cores are in or near the west study area (T. 1 S., R. 2 W.), three are in or near the east study area (T. 1 S., R. 1 E., and R. 1 W.), and one is between and south of the two study areas (T. 2 S., R. 1 W.). Samples encompass the Green River and Wasatch Formations, including the Flagstaff Member of the lower Green River Formation and the Green River-Wasatch transition zone (figure 4.2).

Cores were described in terms of lithology, color, grain size, sorting, porosity, hydrocarbon and bitumen staining, sedimentary structures, contacts, fossil content, bioturbation, cement, fractures, and any other notable characteristics.

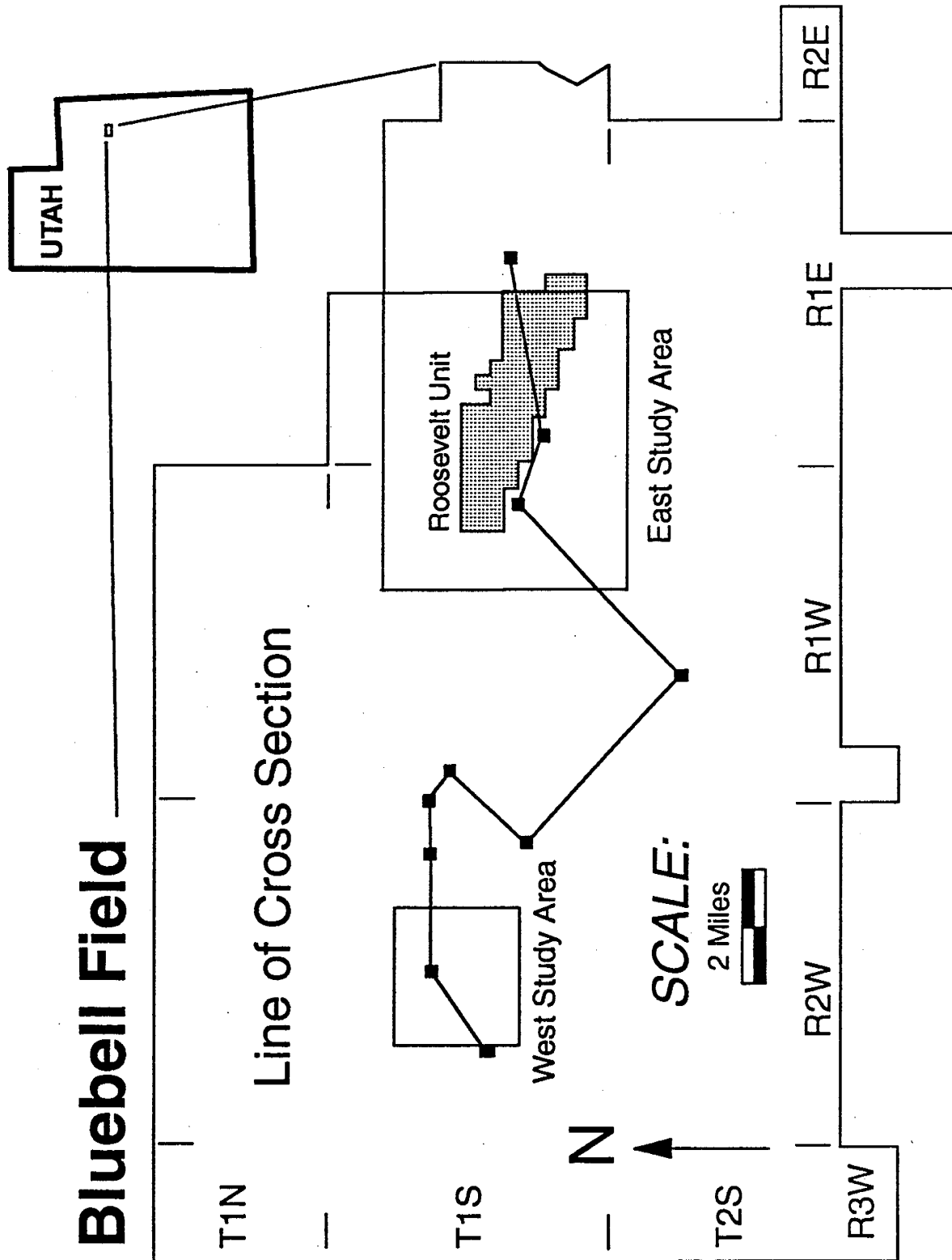


Figure 4.1. Index map of the Bluebell field. Core locations are depicted as squares. Line of cross section shown is displayed in figure 4.2.

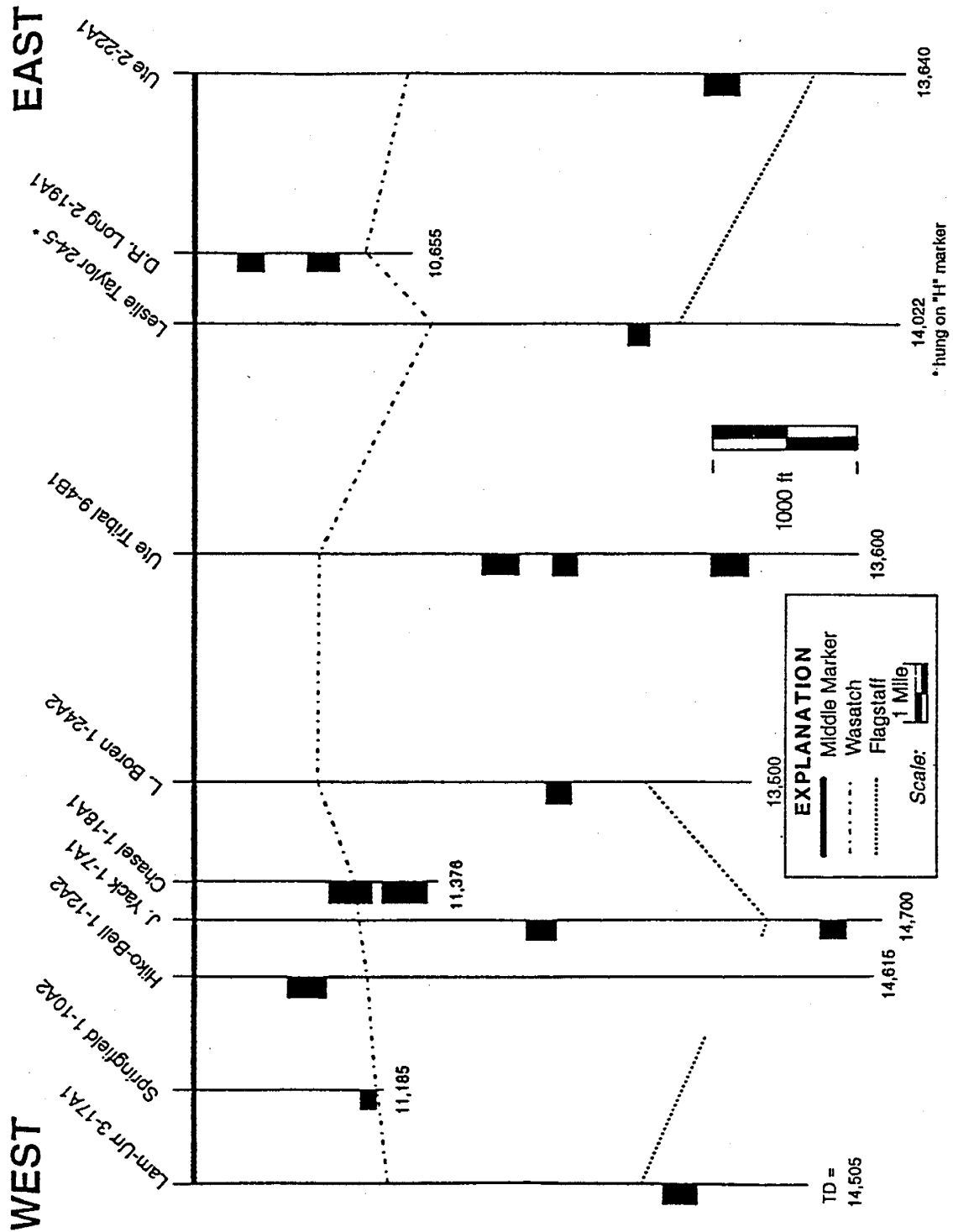


Figure 4.2. Cross section showing depth and formation of sampled core. Core indicated as black rectangles. For line of section, see figure 4.1.

Fractures were further described by orientation (vertical, horizontal, or haphazard), filling material, percent of the fracture filled, relative frequency, width, and length.

Rock types were named according to Dott's (1964) and Dunham's (1962) classification schemes. A total of 1,613 feet (489 m) were described (Appendix A).

### 4.3 Petrography

Petrographic analyses of samples from the cores were completed in order to determine the overall lithology and the specific composition of the sandstone beds. Seventy-two thin sections were made from samples that represented a majority of the rock types present in the core. All thin sections were described petrographically and 51 sand-dominated sections were subjected to a 300 grain point-count analysis (Appendix B). Dominant rock types in the core are sandstone of varying composition, and limy mudstone. Figure 4.3 indicates the abundance of various sandstone compositions. In general, feldspar and lithic fragments seem to be present in nearly equal amounts in most thin sections counted. These compositional data are similar to those of Fouch and others (1992). The most abundant lithology found in the subsurface were sandstone and mudstone, comprising 39 and 15 percent, respectively (figure 4.4).

In contrast, the most abundant lithology found in the outcrops were silty, limy mudstone, and limy mudstone, representing 25 and 13 percent of the total amount described, respectively (Garner and Morris, this volume). Of the sand-dominated clastic samples in the outcrop, 13 were feldspathic arenite and three were feldspathic wacke.

Of the total core described, 78 percent was siliclastic, while only 22 percent was carbonate. This is probably not an accurate reflection of the true ratio of siliclastic to carbonate rocks in the subsurface. Rather, it probably reflects operator bias to core siliclastic intervals since sandstone beds are considered the best reservoirs in the Bluebell field.

### 4.4 Clay Analyses

Clay analyses using an X-Ray Powder Diffractometer were completed on 35 samples from the cores in an effort to determine the types of swelling and movable clays present. Swelling and movable clay are believed to be a problem in plugging the near-wellbore environment. The samples included arenite, mudstone, shale, and different carbonate rock types. One dry analysis of each oriented sample was done to determine specific clay content. Following this initial run, all samples were saturated with ethylene glycol and analyzed again to confirm the presence or absence of swelling clays (table 4.1).

Figure 4.5 is an example of a typical arenite in the subsurface. Based on the semi-quantitative analyses, core samples show very low concentrations of smectitic mixed-layer clays throughout. Where they do exist, they are primarily illite-smectite or chlorite-smectite mixed layers, with only minor kaolinite-smectite mixed layers present. Nearly-pure illite dominates the core samples, but chlorite is also found, in smaller amounts, in many of the samples. Kaolinite is less prevalent.

n=53

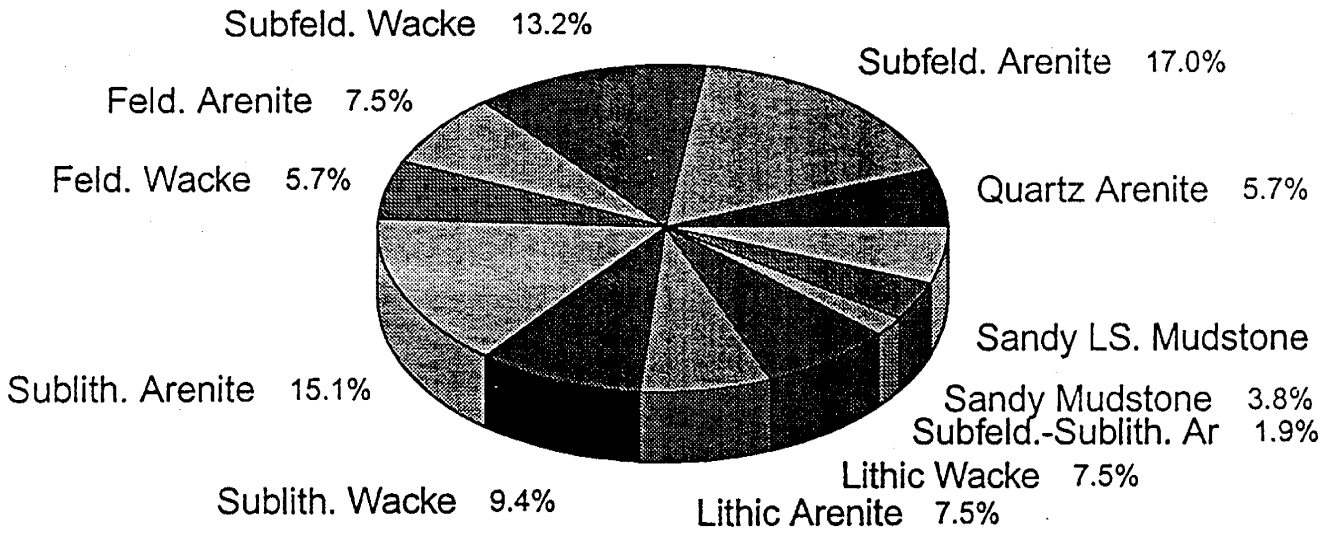


Figure 4.3. Percentage of different clastic rock compositions in 53 point-counted subsurface samples.

Total Feet Measured = 1612.98

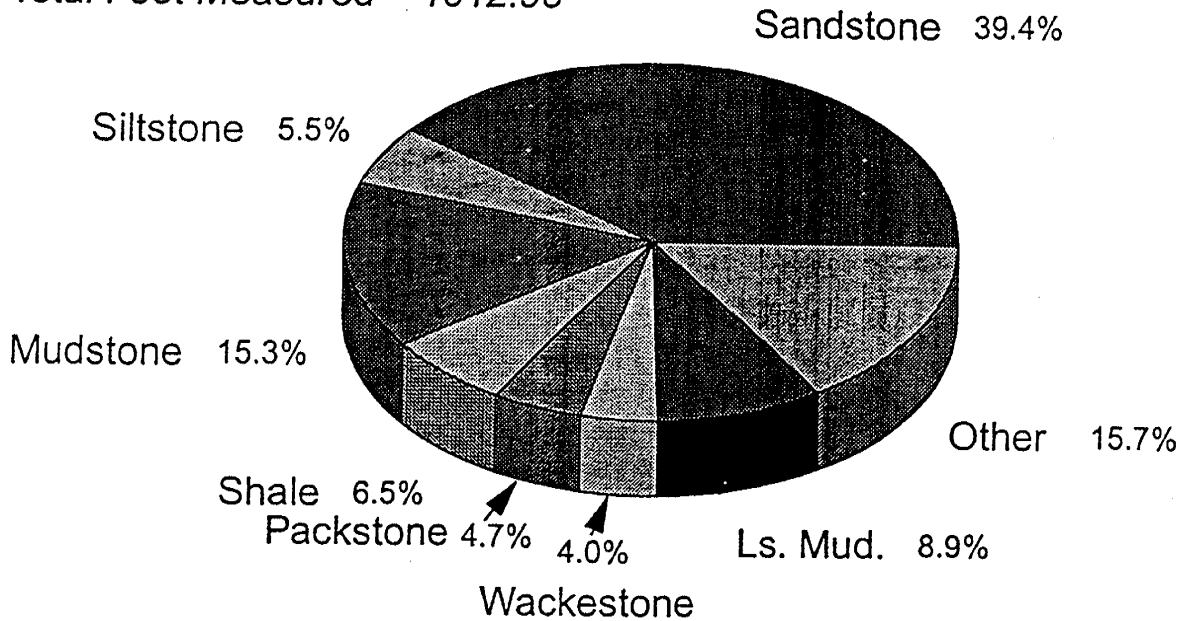


Figure 4.4. Percentage of different rock types present in 10 sampled cores.

Table 4.1. Formation, core number, sample depth, lithology, clay type(s), clay type(s), porosity, permeability, and depth of the porosity/permeability measurement. I (i) = illite, Cl (cl) = chlorite, K (k) = kaolinite, s = smectite (smectitic), Z (z) = zeolites. Lower case symbol indicates trace amounts present (e.g. sl = significant illite present, along with minor amounts of illite-smectite mixed-layer clay). All porosity and permeability data were obtained from Brian McPherson and Rich Jarrard from the University of Utah. NA = not available, h = horizontal, v = vertical.

Formation	Core	Depth (ft)	Lithology	Clay	Thickness (ft)	% Porosity	Perm. (mD)	Depth (ft) (P & P)
Flagstaff	P17	13,587	ls mudstone	sl, Cl	2.33	NA	NA	NA
Flagstaff	P17	13,590	ls mudstone	sl, Cl	2.00	2.82	0.461	13,590
Flagstaff	P17	13,603	wackestone	sl, k	1.33	0.29	0.001	13,603
Flagstaff	P17	13,609	ls mudstone	l, (k)	2.13	0.92	0.007	13,615
Flagstaff	P17	13,656	ss-illithic arenite	sl, Cl, k	6.54	1.27	0.024	13,660
Green River	CSM	11,121.5	ss-subfield. arenite	sl, scl	0.92	NA	NA	NA
Green River	CSM	11,128	wackestone	sl, cl	7.42	NA	NA	NA
Green River	CSM	11,146.5	ss-subfield. wacke	sl, cl	18.50	NA	NA	NA
Green River	CSM	11,157.5	ss-subfield. arenite	sl, cl, (k)	1.42	NA	NA	NA
Green River	CHIKO	10,482	mudstone	l	52.13	0.27 (h); 0.3 (v)	0.002 (h); 0.004 (v)	10,481
Green River	CHIKO	10,596	ls mudstone	l (cl, k, z)	0.83	NA	NA	NA
Green River	CHIKO	10,629.5	ss-subfield. wacke	l	3.83	NA	NA	NA
Wasatch	C17A1	12,252	ss-subfield. arenite	sl, Cl, k	4.38	NA	NA	NA
Wasatch	C17A1	12,264	ss-subfield. arenite	sl, Cl	6.17	NA	NA	NA
Wasatch	C17A1	12,303	ss-quartz arenite	sl, sCl, z?	5.08	NA	NA	NA
Flagstaff	C17A1	14,372	ss-illithic arenite	sl, K	3.50	NA	NA	NA
Flagstaff	C17A1	14,384	ss-sublith. arenite	sl, cl, K	2.33	NA	NA	NA
Wasatch	CCHAS	10,632	packstone	sl	7.00	0.15 (h)	0.001 (h)	10,632
Wasatch	CCHAS	10,795	int. ss(subl. w)-silt.	sl, Cl	60.00	3.95 (v)	0.001 (v); 0.002 (h)	10,795
Wasatch	CCHAS	11,010.5	ss-sublith. arenite	sl, sCl	5.58	5.04 (h)	0.2 (h)	11,010
Wasatch	CCHAS	11,203	ss-feld. wacke	sl	9.33	4.8 (h); 5.08 (h)	0.021 (h)	11,209
Wasatch	CBOR	12,159	ls mudstone	sl, cl	20.08	NA	NA	NA
Wasatch	CBOR	12,168.5	ss-sublith. arenite	sl, Cl, k	5.75	0.68 (h)	0.002 (h)	12,173
Wasatch	C94B1	11,023.5	mudstone	sl, Cl, k	61.00	0.88	0.001	11,030
Wasatch	C94B1	11,094	ls mudstone	sl, Cl, k	4.17	NA	NA	NA
Wasatch	C94B1	11,110.5	ss-illithic arenite	l, cl, k	5.00	1.57	0.005	11,111
Wasatch	C94B1	11,141	mudstone	sl, Cl, k	29.33	0.49	0.001	11,143
Wasatch	C94B1	12,671	mudstone	sl, Cl	9.67	NA	NA	NA
Green River	BVP19	9177	shale	sl	22.58	2.53 (h)	0.034 (h)	9191
Green River	BVP19	9638	mudstone	sl, cl, k	5.25	NA	NA	NA
Green River	BVP19	9648	ss-subfield. arenite	sl, k	1.00	3.06 (h); 2.04 (v)	0.002 (h); 0.001 (v)	9652
Wasatch	BVP22	12,289	ss-sublith. wacke	K, Z	10.00	2.17 (h)	0.026 (h)	12,290
Wasatch	BVP22	12,299	shale	l, K, Z	1.00	4.25 (h)	0.001 (h)	12,299
Wasatch	BVP22	12,307	packstone	Z, s	4.50	3.2 (h)	0 (h)	12,308
Wasatch	BVP22	12,365	ss-sublith. wacke	l, Cl, k	7.33	1.67 (h)	0.001 (h)	12,365

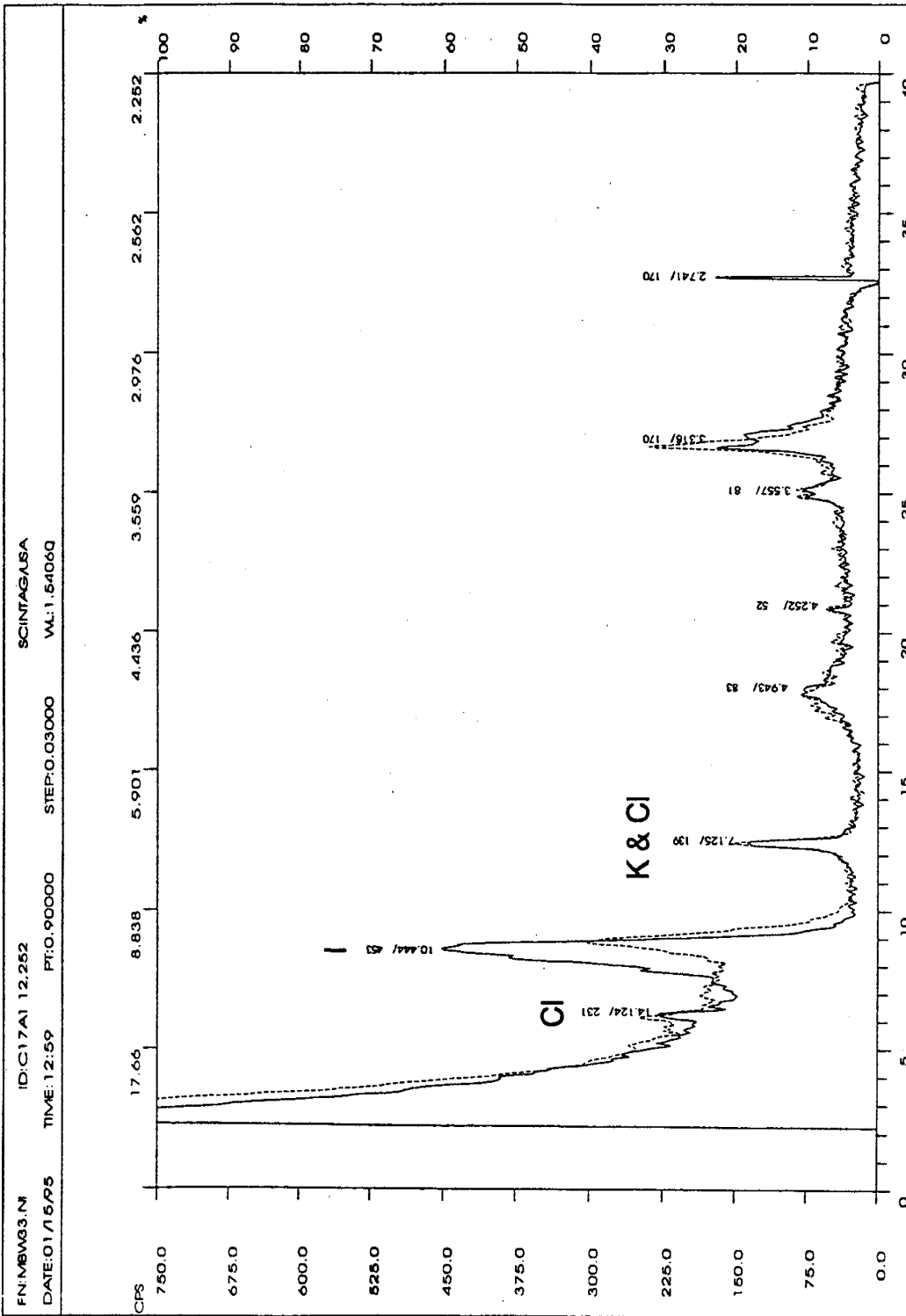


Figure 4.5. Example of the X-ray diffraction pattern of a typical arenite in the subsurface. This sample is a subfeldspathic arenite from core C17A1, taken at a depth of 12,252 feet (3,734 m). Solid line is the initial, dry run; dashed line is the glycol-saturated run. Note that the clay peaks line up on top of each other, suggesting very little swelling clay is present. Minor swelling clay is, however, associated with some of the illite. The top x-axis is the d-spacing, as determined by the Bragg Law ( $n\lambda = 2d\sin\theta$ ). The bottom x-axis is the refraction angle in degrees  $2\theta$ . CPS = count per second. I = illite, Cl = chlorite, K = kaolinite.

In the outcrop, clays are predominantly illite, chlorite, kaolinite, with varying amounts of illite-smectite, chlorite-smectite, and kaolinite-smectite mixed-layer clays (Garner and Morris, this volume). Kaolinite and mixed-layer clays are present in significantly higher concentrations in the outcrop samples than in the core. Further, smectite concentration decreases stratigraphically downward from the middle Green River to the Green River-Wasatch transition in the outcrop, while there is no such noticeable trend in the subsurface cores from this study.

Although there is reasonably low concentrations of swelling clays in the core samples, even low concentrations of any swelling clay present in the reservoir rock can seriously hinder permeability (Jarrard, this volume).

#### **4.5 Porosity and Permeability**

Porosity and permeability analyses were completed in order to determine which rock types have potential for storing hydrocarbons and for providing a path to the wellbore. Porosity and permeability data in the subsurface were obtained from Brian McPherson and Richard Jarrard from the University of Utah, Salt Lake City. Of the 219 samples tested, 85 percent have less than 4 percent porosity and less than 0.05 mD permeability. In general, porosity and permeability tend to be slightly higher in the arenite beds that contain significantly more quartz than lithic fragments and feldspar. Overall, most rock types sampled have very low intergranular porosity and permeability (figure 4.6).

The range of porosity and permeability in similar rock types differ significantly between the outcrop and the subsurface cores. Permeability in outcrop samples varies from less than 0.01 mD to 1,241 mD, and porosity varies from 2 to 27 percent (Garner and Morris, this volume). The higher porosity and permeability in outcrop samples may be attributed either to unloading, diagenesis, a difference in provenance, surface weathering effects, or a shallower burial history. The outcrops on the southwest margin of the Uinta Basin were sourced by igneous rocks in the south, resulting in more feldspathic rocks than those found in the central portion of the basin (Garner and Morris, this volume). The Uinta Mountains north of the basin are predominantly metasedimentary Precambrian rocks and were probably the dominant source for the central portion of the basin, although a southern source may have also contributed. Core from the Bluebell field in the north to central portion of the basin contain more quartz and less feldspar than the outcrop along the south margin of the basin. Most of the lithic fragments in the core samples are chert, suggestive of the metamorphic provenance to the north.

#### **4.6 Fractures**

Naturally occurring fractures are important in hydrocarbon production in the Uinta Basin. Therefore, fractures were described in an effort to determine which rock types have the most fracture permeability. Figure 4.7 shows the observed frequency of fractures in the cores of different rock types. The frequency was calculated by determining how much of the total footage of each rock type contained at least

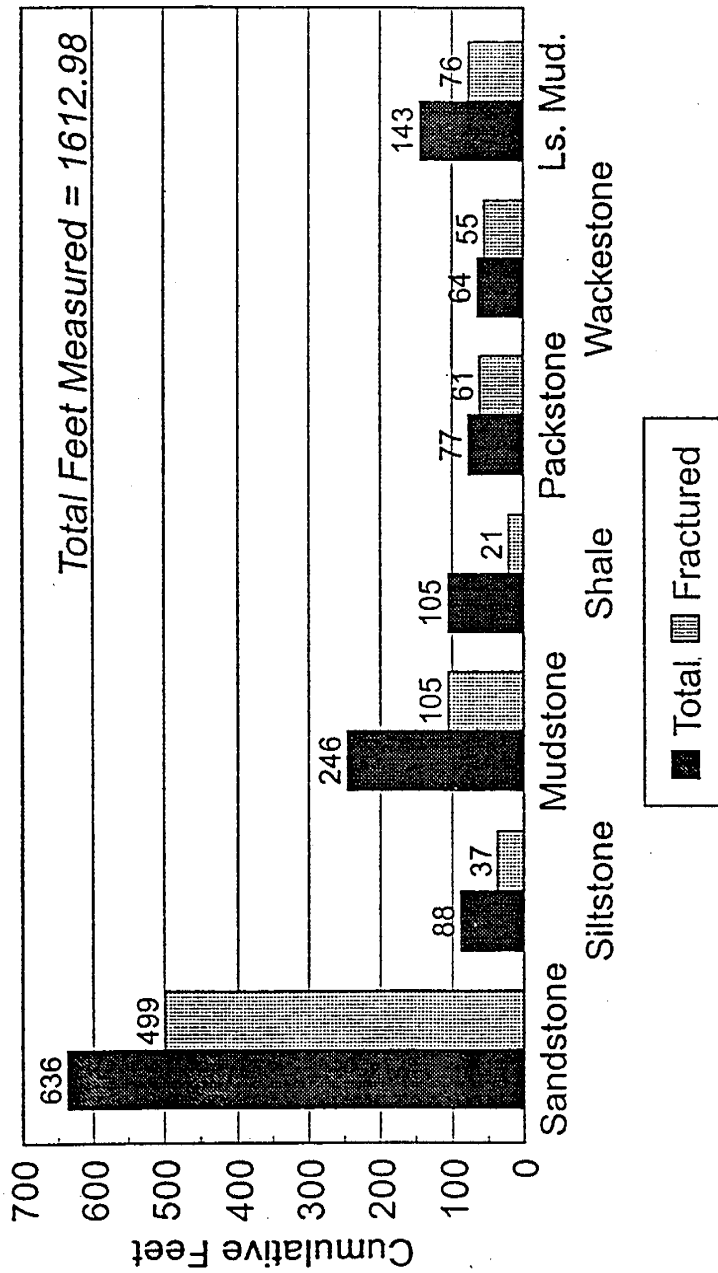


Figure 4.6. Total number of feet described of each lithology adjacent to the total number of feet containing at least one fracture.

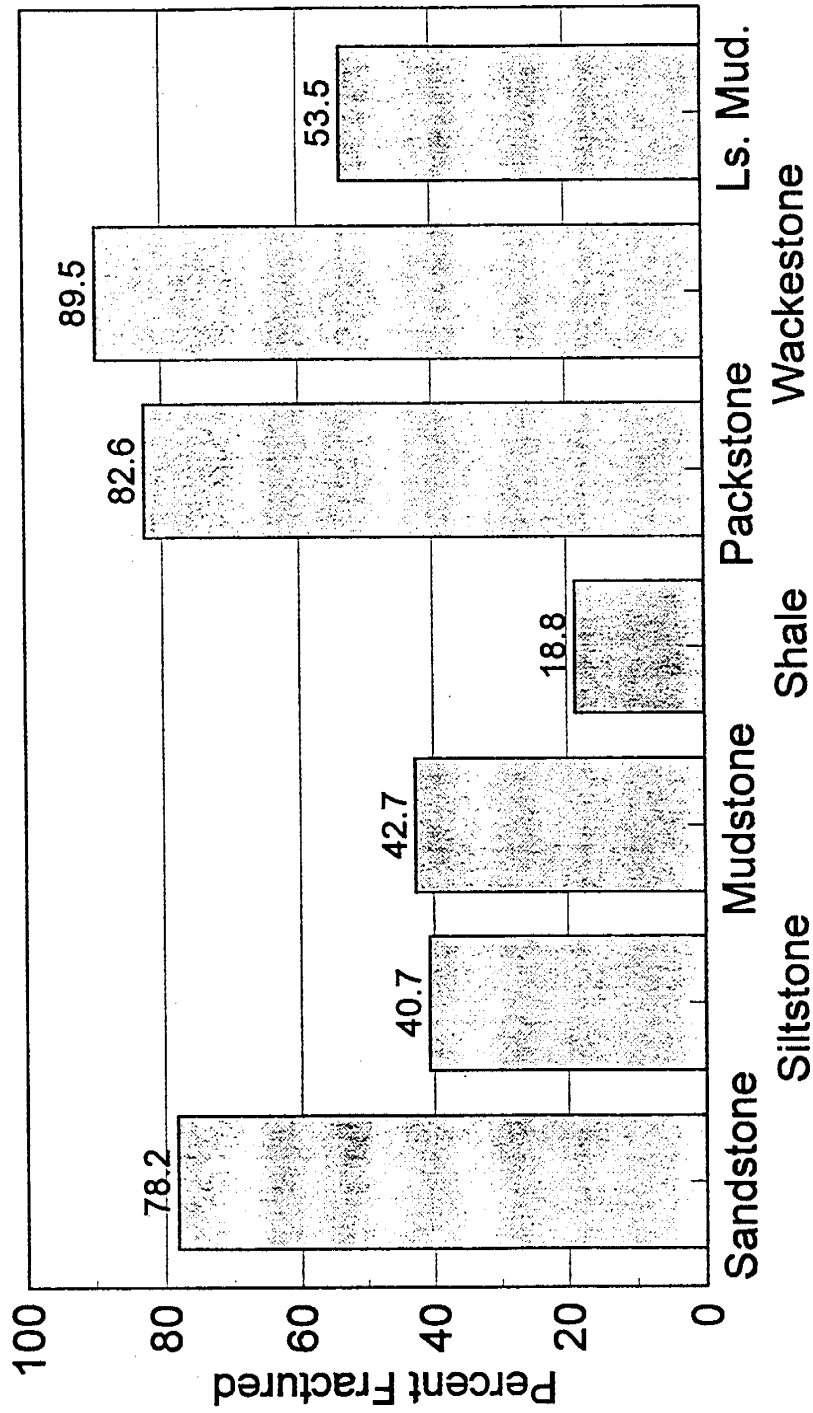


Figure 4.7. Percentage of each rock type that is fractured; obtained from figure 4.6.

one noticeable fracture. From this, a percentage of fracturing of each rock type was derived. Figure 4.8 shows that within the cores that were studied, 78 percent of sandstone beds and 42 percent of clastic mudstone beds are fractured.

Lucas and Drexler (1975) suggest that dense carbonate mudstone have the best potential to fracture. In contrast, Narr and Currie (1982) found that well-indurated sandstone beds are more likely to be fractured. Results of this study suggest that both conclusions are accurate for different reasons. Subsurface fracturing does relate to lithology. Fracture density, orientation, and filling vary with differing rock types (figures 4.8 and 4.9). Sandstone beds tend to have the lowest fracture density, but where present, the fractures are longer (greater than 3.3 feet [1 m], length measured in the core although many fractures extend out of the plane of the sample) and generally have more separation (from 0.03 to 0.13 inches [0.5-3.0 mm]), than most other rock types. Fractures in sandstone beds also tend to be vertical to near vertical, with interconnections rarely visible in coresamples. These results concur with Narr and Currie (1982), in that the most productive fractures seem to be found in well-indurated sandstone, and that a very high percentage of sandstone beds are fractured (figure 4.8).

Clastic and carbonate mudstone beds in the cores have high fracture densities. These fractures display numerous interconnections due to their multiple orientations. The fractures are primarily calcite-filled, have very narrow separation (less than 0.03 inch [0.5 mm]) and are short (generally less than 8 inches [10.2 cm] when length can be determined). These results support the observations of Lucas and Drexler (1975) because mudstone beds have the highest fracture density and a high percentage of mudstone beds are fractured (figure 4.8). Mudstone beds may be more important as hydrocarbon source rocks than reservoirs. When at least partially open, the high density fracturing provides good migration pathways to the higher quality reservoir clastic beds.

#### 4.7 Conclusions

Analyses of core from the Bluebell field indicates that the most promising hydrocarbon reservoirs are arenite with high quartz content, low concentrations of swelling clays, relatively high porosity and permeability, large, open fractures, and that overlie fractured mudstone.

A comparison of core with outcrop data show some differences between the two areas. The sandstone beds in outcrop tend to be more feldspathic. There is significantly more swelling clay present in outcrop compared to subsurface samples. These differences between outcrop and the cores from the lower Green River Formation suggest that the Willow Creek Canyon area on the southwest flank of the basin had a different clastic source than the center and north portions of the basin. The minor feldspar content of the core may be attributed to two factors: (1) either the feldspar percentage was continually being reduced by chemical and mechanical weathering during northward transport, or (2) the sources from both north and south mixed in the Bluebell field area, subsequently diluting the original feldspar concentration.

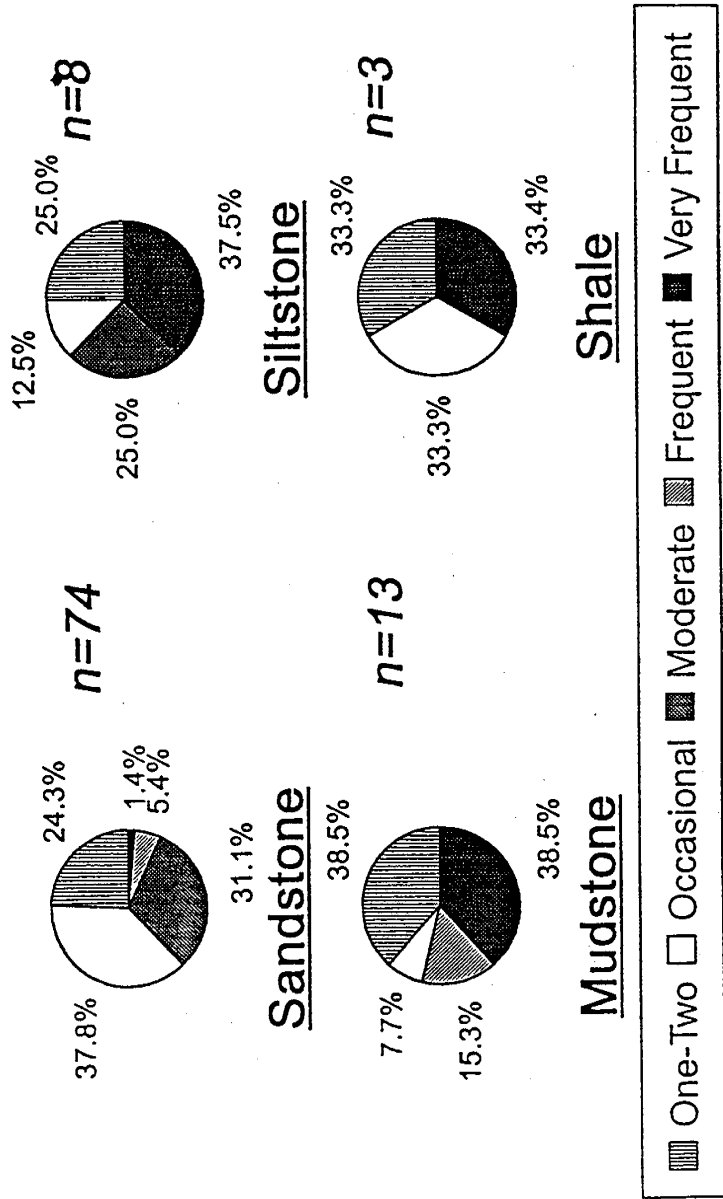


Figure 4.8. Relative fracture density of clastic rocks. N is the number of samples of each lithology used to determine percentages.

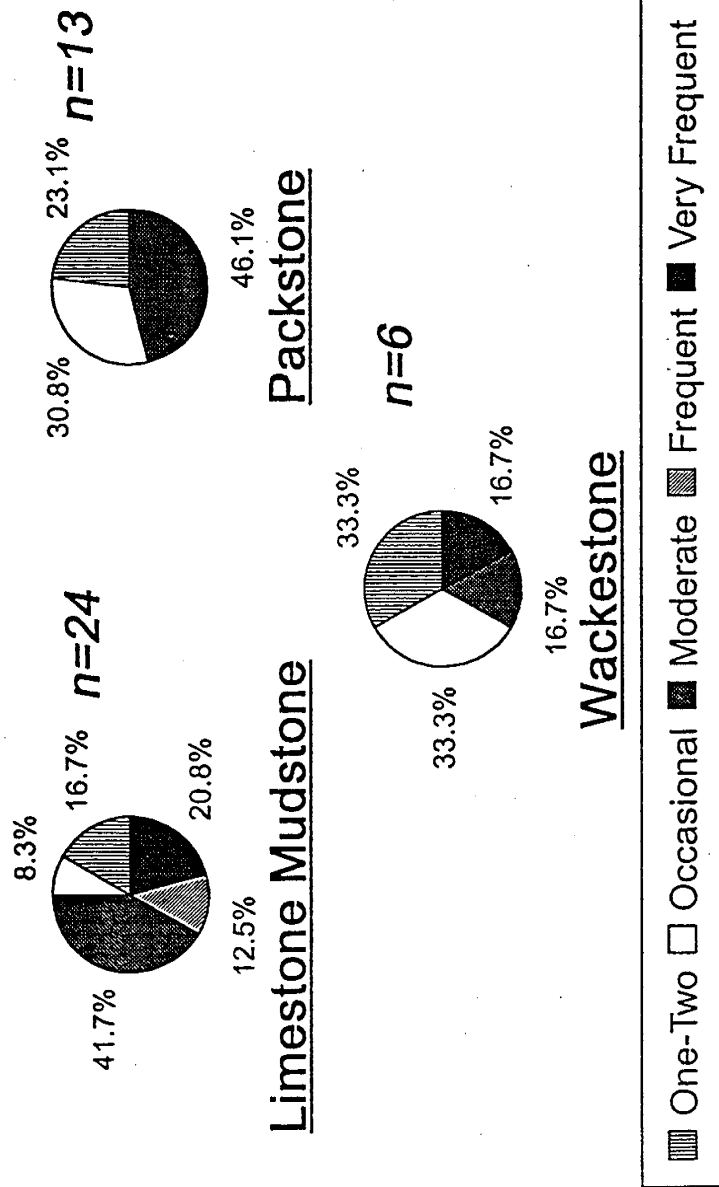


Figure 4.9. Relative fracture density of carbonate rocks. N is the number of samples of each lithology used to determine percentages.

## 5. FRACTURE ANALYSES

*M. Lee Allison and Craig D. Morgan*  
Utah Geological Survey

### 5.1 Introduction

Fracturing is believed to play a critical role in well producibility in the Bluebell field. Fracture data were gathered from the surface (first year of the project) and subsurface from the study area. Additional data were collected from previously published core and outcrop studies in the field (table 5.1).

Two sets of subsurface fractures are present across the field but appear to be vertically segregated from each other. The orthogonal fractures prevalent at the surface were not observed in the subsurface. East-west subsurface fractures are associated with the producing intervals of the most productive wells. Northwest-southeast fractures are present stratigraphically above the east-west set. All reservoir rock types have at least a moderate amount of fracturing in core samples. Limited core data indicates that fracture density is not depth dependent.

Gathering of subsurface fracture data was greatly hampered by the reduction in drilling activity in the Bluebell field. Only three wells were drilled and logged with borehole imaging tools during the two-year characterization study. The current amount of fracture data is not sufficient to quantify the role of fracturing in well producibility in the Bluebell field.

Table 5.1. Location and type of subsurface fracture data in the Bluebell field.

Operator	Well name	Location (UBM)	Data source	Number of points	Depth of data (In feet)
Pennzoil E&P	Lamb 2-16A2	sec.16 T1S R2W	FMI <sup>1</sup>	70	6,490-10,890
Pennzoil E&P	Ballard 2-15B1	sec.15 T2S R1W	FMI <sup>1</sup>	58	9,430-12,500
Pennzoil E&P	Cornaby 2-14A2	sec.14 T1S R2W	CBIL <sup>2</sup>	33	9,590-12,625
Pennzoil E&P	Johnson 1-27A2	sec.27 T1S R2W	Core <sup>3</sup>	50	11,448-13,500
Flying J	Ute 2-22A1E	sec.22 T1S R1E	Core <sup>4</sup>	22	12,288-12,408

<sup>1</sup> FMI: Schlumbergers Formation Micro-Imager report, 1994 (unpublished)

<sup>2</sup> CBIL: Western Atlas Circumferential Imaging Log report, 1994 (unpublished)

<sup>3</sup> Narr, W.N., 1977, Masters thesis Univ. of Toronto

<sup>4</sup> Christensen Diamond Products core report, 1982 (unpublished)

### 5.2 Subsurface Fractures

Two sets of subsurface fractures are present across the Bluebell field but appear to be vertically segregated from each other. The orthogonal (NW-SE and E-W) fracture set prevalent at the surface was not observed in the subsurface (figure 5.1). East-west subsurface fractures are associated with the producing intervals of the most productive wells. Northwest-southeast fractures are present above the E-W set. Some wells

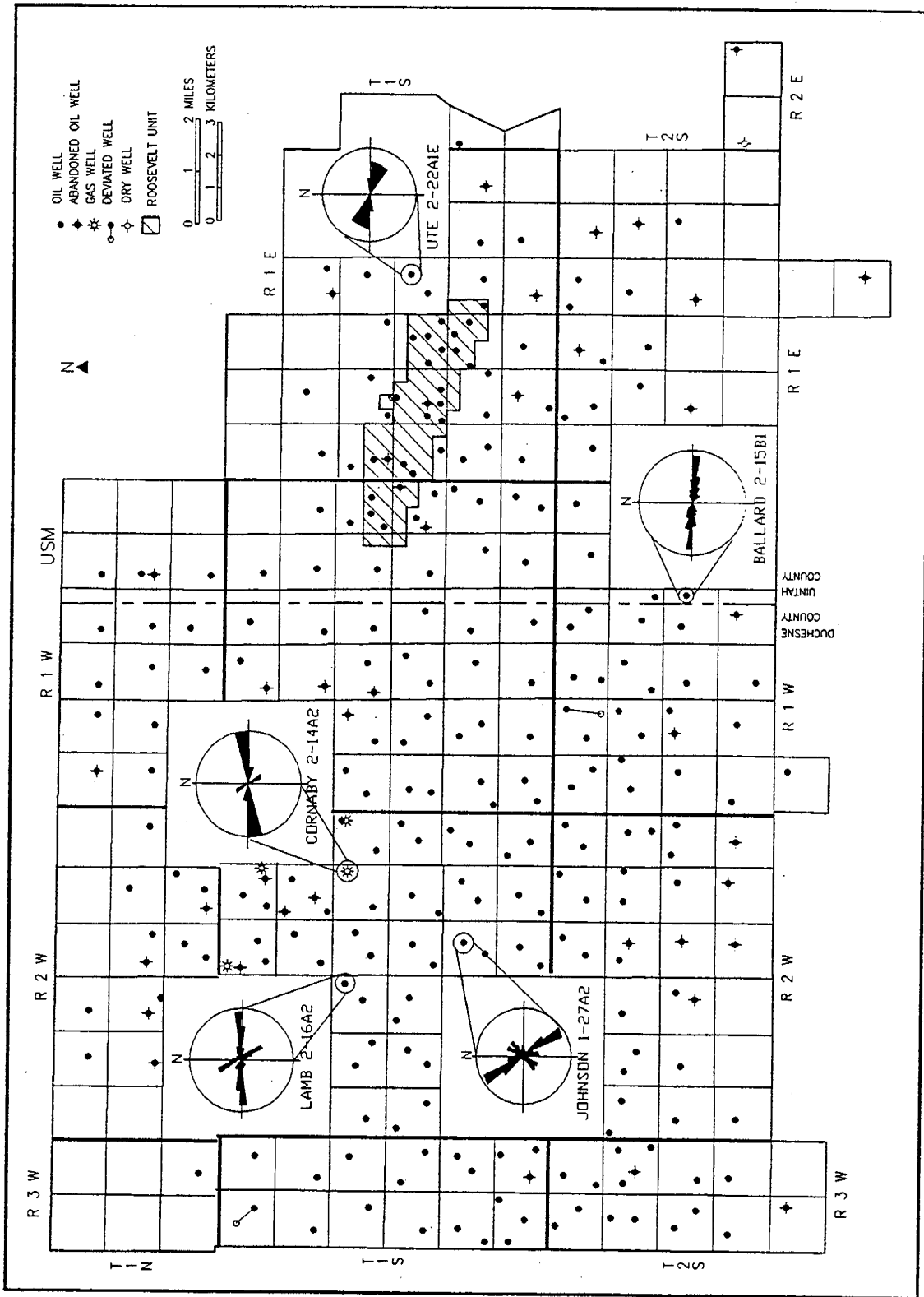


Figure 5.1. Fracture orientations from well logs and oriented cores in the Bluebell field. See table 5.1 for well and operator names.

bottom in rocks with the NW-SE set so it is not certain that the E-W set exists at depth everywhere in the field.

The transition from NW-SE to E-W oriented fractures is found at different depths in each well, in both absolute and stratigraphic terms (figure 5.2). It is shallowest (between -1,500 and -3,100 feet [-457 and -945 m], sea level elevation) in the Pennzoil Lamb 2-16A2 well which is the most westerly and northerly of the five wells with fracture data. In the Pennzoil Cornaby 2-14A2 well the transition is at approximately -4,600 feet (-1,400 m). Both wells have all of their perforations in horizons with E-W fractures. Both wells are in sections where cumulative production exceeded 2 MMBO (280,000 MT) per well. The transition from one fracture direction to the other is in the Green River Formation in both wells.

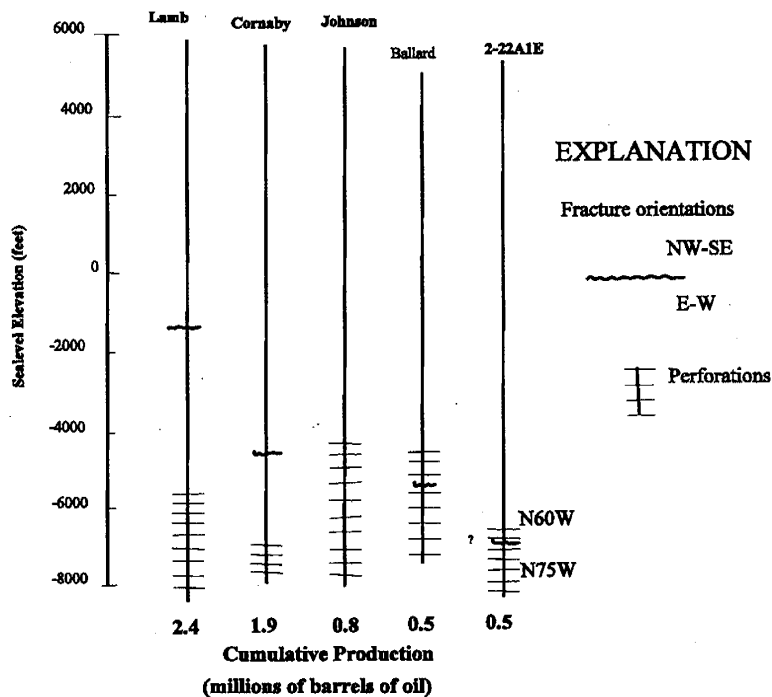


Figure 5.2. Fracture orientation by depth in the Bluebell field.

In the Pennzoil Johnson 1-27A2, only NW-SE oriented fractures are present. The E-W fractures may be present below total depth of the well, 13,617 feet (4,151 m) (-7,980 feet [2,432 m] sea level elevation). The well bottomed in the Wasatch Formation. Cumulative production of this long-time producer has been less than 500,000 BO (70,000 MT).

Flying J's Ute 2-22A1E well has a poorly defined transition at around -7,300 feet (-2,229 m) sea level elevation, in the Wasatch Formation. There is only 15 degrees of azimuthal variation between the orientation of the two "sets" of fractures. The majority of perforations are in the lower, more E-W oriented, fractured rocks. Cumulative production has been about 800,000 BO (112,000 MT) from this well.

Generally, the wells with the greatest number of perforations in horizons with E-W oriented fractures have the greatest cumulative oil production in the field. Wells with all or most of the perforations in rocks with NW-SE oriented fractures have significantly lower cumulative oil production. This may indicate that the E-W oriented fractures are a primary source of producible oil.

The Pennzoil Ballard 2-15B1 well has the majority of perforations in rocks with E-W oriented fractures. This well is new and has a limited production history, but if the E-W fractures are the primary oil conduits the Ballard well should ultimately be an excellent producer. However, the initial well in the same section has a cumulative oil production much less than the better wells in the field.

### **5.3 Problems**

Fewer imaging or dip logs were obtained from the field than anticipated due to the sharp decrease in the number of wells drilled during the project. As a result we have only five sets of subsurface data: three modern imaging logs and two oriented cores. In addition, the log processing by the service companies were summarized in working reports but comprehensive data lists were not generated. The borehole breakout interpretations provided by the service companies appear to be in error. Until and unless they can be corrected, we have no usable in-situ stress data.

### **5.4 Conclusions**

Well with E-W oriented fractures appear to be the most prolific oil producers. Directionally drilling north or south would intersect the maximum number of these fracture sets. East-west oriented fractures should be the primary drilling target. In general, wells should be deviated along N-S to NE-SW directions to enhance fracture production in the Bluebell field.

## **6. FORMATION EVALUATION AND MAPPING**

*Craig D. Morgan<sup>1</sup> and Carol N. Tripp<sup>2</sup>*  
Utah Geological Survey<sup>1</sup>  
Consulting Geologist<sup>2</sup>

### **6.1 Introduction**

Thickness and structure contour mapping of thick correlative intervals in the lower Green River and Wasatch Formations show a general north to south, up-dip thinning of mapped intervals. The mapped intervals identify gross depositional patterns of the primary productive intervals in the Green River and Wasatch Formations. Thickness mapping of individual beds which will identify more detailed depositional patterns is now underway.

Individual beds that met the minimum criteria for long-term production as determined by the characterization study, have been correlated and analyzed in the wells throughout the study area. The minimum standard for a bed is to be at least 6 feet (1.8 m) thick based on a gamma-ray count of 60 API units (45 API units in the Wasatch redbeds) and have an average porosity of 6 percent or more. Thickness, porosity, and oil saturation mapping of these individual beds will provide a geologic model for: (1) reservoir engineering characterization, (2) identification of key beds for recompletion in the demonstration wells, and (3) evaluation of the area's potential for future drilling.

### **6.2 Formation Evaluation**

To identify beds with the greatest hydrocarbon potential in the Michelle Ute and Malnar Pike wells (the proposed demonstration wells) all the beds were analyzed for critical parameters that were determined by the characterization study. Parameters of beds that meet a minimum standard were compiled (tables 6.1 and 6.2). The tables also include drilling shows and original-oil-in-place (OOIP) calculations.

The tables will be used to rank the individual beds prior to any recompletion work. Comparison of the demonstration results with the rankings from the table will quantify which parameters are the most reliable for formation evaluation.

### **6.3 Thickness and Structure Maps**

Field-wide structure contour maps and cross sections were constructed for numerous horizons using the digital well database. Good field-wide correlation was obtained for the middle marker (Ryder and others, 1976) and many of the horizons in the upper Wasatch transition zone. Field-wide correlation of the deeper lower Wasatch transition zone using the digital log database was less successful because the lower transition is less laterally continuous than the upper Wasatch transition zone.

Table 6.1. Evaluation of beds in the Michelle Ute well. Beds thickness is defined by gamma-ray count of 60 API units or less. Each bed has a thickness of 6 feet (1.8 m) or more, and porosity of 6 percent or more, within the 60 API unit bed definition.

Top of Bed feet	Thickness feet	Rt <sup>1</sup> ohm meter	X-Plot <sup>2</sup> Porosity	Sw <sup>3</sup> percent	OOIP MSTB <sup>4</sup>	Oil produced <sup>5</sup> MSTB	Oil Remaining MSTB	Mudlog Rating <sup>6</sup>
10,511	17	125	8	22	226	2	224	
10,702	12	125	9	20	184	1	183	
10,788	14	80	6	24	136	1	135	
10,842	26	200	9	14	429	2	427	
10,928	15	105	9	22	225	2	223	
11,774	6	7	15	47	102	1	101	
12,281	6	12	14	39	109			
12,291	11	10	8	74	49			
12,565	7	10	7	84	17			
12,784	8	15	9		20			
12,807	7	8	9	73	36			
12,838	12	20	7	60	72			
12,938	7	25	9		34			
13,006	8	15	9	54	71	7	64	
13,020	14	28	9	39	164	6	158	
13,219	7	18	10		233	4	229	
13,243	9		7					
13,281	13		6					
13,319	6	10	10	98	1	1	0	
13,407	7	12	16	33	160	8	152	
13,472	6	28	6	59	32			
13,501	8		8					
13,542	8	25	9		39	4	35	
13,676	9		10					
13,750	6		7					
13,762	14		10					
13,778	12		11					
13,850	14	35	9		115	5	110	
13,870	14		10					

Top of Bed feet	Thickness feet	Rt <sup>1</sup> ohm•meter	X-Plot <sup>2</sup> Porosity	Sw <sup>3</sup> percent	OOIP MSTB <sup>4</sup>	Oil produced <sup>5</sup> MSTB	Oil Remaining MSTB	Mudlog Rating <sup>6</sup>
13,888	7		11					
13,896	7	20	9	44	75	5	70	
13,924	6		7					
14,054	9		11					
14073	7	40	6	49	46	1	45	
14281	6	25	6	62	29	4	25	
14431	7	25	6	62	34	5	29	

<sup>1</sup>Rt = deep resistivity

<sup>2</sup>X-Plot = cross plot; porosity determined by averaging the calculated density and neutron porosity

<sup>3</sup>Sw = water saturation calculated using resistivity of the formation water (Rw) of 0.10

<sup>4</sup>OOIP MSTB = original-oil-in-place reported in thousands of stock-tank-barrels

<sup>5</sup>Oil produced = cumulative oil production as of December 31, 1994 (from Utah Division of Oil, Gas and Mining), not all perforated beds are shown as a result summation of the column is less than the total

<sup>6</sup>Mudlog Rating = rating of drill shows by DeForrest Smouse, the smaller the number the better the drill show

Table 6.2. Evaluation of beds in the Malnar Pike well. Beds thickness is defined by gamma-ray count of 60 API units or less. Each bed has a thickness of 6 feet (1.8 m) or more, and porosity of 6 percent or more, within the 60 API unit bed definition.

Top of Bed feet	Thickness feet	Rt <sup>1</sup> ohm•meter	X-Plot <sup>2</sup> Porosity	Sw <sup>3</sup> Percent	OOIP MSTB <sup>4</sup>	Oil Produced <sup>5</sup> MSTB	Oil Remaining MSTB	Mudlog Rating <sup>6</sup>
9,028	14	130	6	19	132			
9,583	8	60	8	21	98	1	97	2
9,950	10	50	7	26	101	1	100	1.7
10,101	13	85	10	14	218	1	217	1.5
10,290	23	140	7	16	263	1	262	1.6
12,163	11	32	9	28	139			1.8
12,700	8	25	9	31	97	0	97	1.7
12,804	6	40	10	23	89			
13,186	6	30	12	22	109	1	108	
13,238	12	20	10	32	159			
13,254	16	25	11	26	253			
13,334	11	45	10	21	169	1	168	5
13,366	8	15	11	34	113	1	112	3
13,414	7	150	6	18	59			1.6
13,434	6	15	14	27	119	0	119	1.7

Top of Bed feet	Thickness feet	Rt <sup>1</sup> ohm-meter	X-Plot <sup>2</sup> Porosity	Sw <sup>3</sup> Percent	OOIP MSTB <sup>4</sup>	Oil Produced <sup>5</sup> MSTB	Oil Remaining MSTB	Mudlog Rating <sup>6</sup>
13,485	7	80	9	18	88	1	87	1.8
13,570	11	18	9	37	99	1	98	1.8
14,270	6	60	10	18	96	6	90	1.8
14,346	16	45	7	29	155	6	149	1.7

<sup>1</sup>Rt = deep resistivity

<sup>2</sup>X-Plot = cross plot; porosity determined by averaging the calculated density and neutron porosity

<sup>3</sup>Sw = water saturation calculated using resistivity of the formation water (Rw) of 0.10

<sup>4</sup>OOIP MSTB = original-oil-in-place reported in thousands of stock-tank-barrels

<sup>5</sup>Oil produced = cumulative oil production as of December 31, 1994 (from Utah Division of Oil, Gas and Mining), not all perforated beds are shown as a result summation of the column is less than the total

<sup>6</sup>Mudlog Rating = rating of drill shows by DeForrest Smouse, the smaller the number the better the drill show

Within the Roosevelt Unit area, isopach and structure mapping of the upper Wasatch transition zone (lower Green River), Wasatch Formation, and lower Wasatch transition zone (Flagstaff equivalent?) is completed. The broad west to northwest plunging anticline that is mapped at the middle marker horizon of the Green River Formation (figure 6.1) is absent at the lower Wasatch horizon which dips north towards the basin axis (figure 6.2). The isopach map of the Wasatch shows north to south thinning (figure 6.3). The Wasatch is dominately a fluvial and alluvial deposit derived from the Uinta Uplift north of the mapped area. The isopach map of the lower Wasatch transition shows a number of north to south lobes. This pattern is believed to be caused by deposition of fluvial-dominated deltas into Lake Uinta. Isopach mapping of individual beds is underway and should more accurately define shoreline trends and deltaic buildups.

The qualifying beds in the Michelle Ute and Malnar Pike wells are being correlated and mapped throughout the Roosevelt Unit area. Qualifying beds identified in other wells but not occurring in the Michelle Ute and Malnar Pike wells, are being mapped and correlated throughout the area also. Structure and thickness mapping of the qualifying beds will be used to determine the areal extend of key beds in the demonstration wells and to help select a drill site for a new well.

## 6.4 Conclusions

Geophysical well log analysis using the strict criteria identified by this study, can identify beds believed to have hydrocarbon potential. The value of the criteria used can not be proven until the predicted results are compared to actual results in the demonstration wells. Comparison of the predicted results to actual results will be used to revise the criteria if necessary and improve the well log analysis techniques.

Thickness mapping can identify general depositional patterns and areas of possible deltaic buildups. Thickness of individual key beds should identify areas with good stratigraphic trapping potential.



R1W R1E

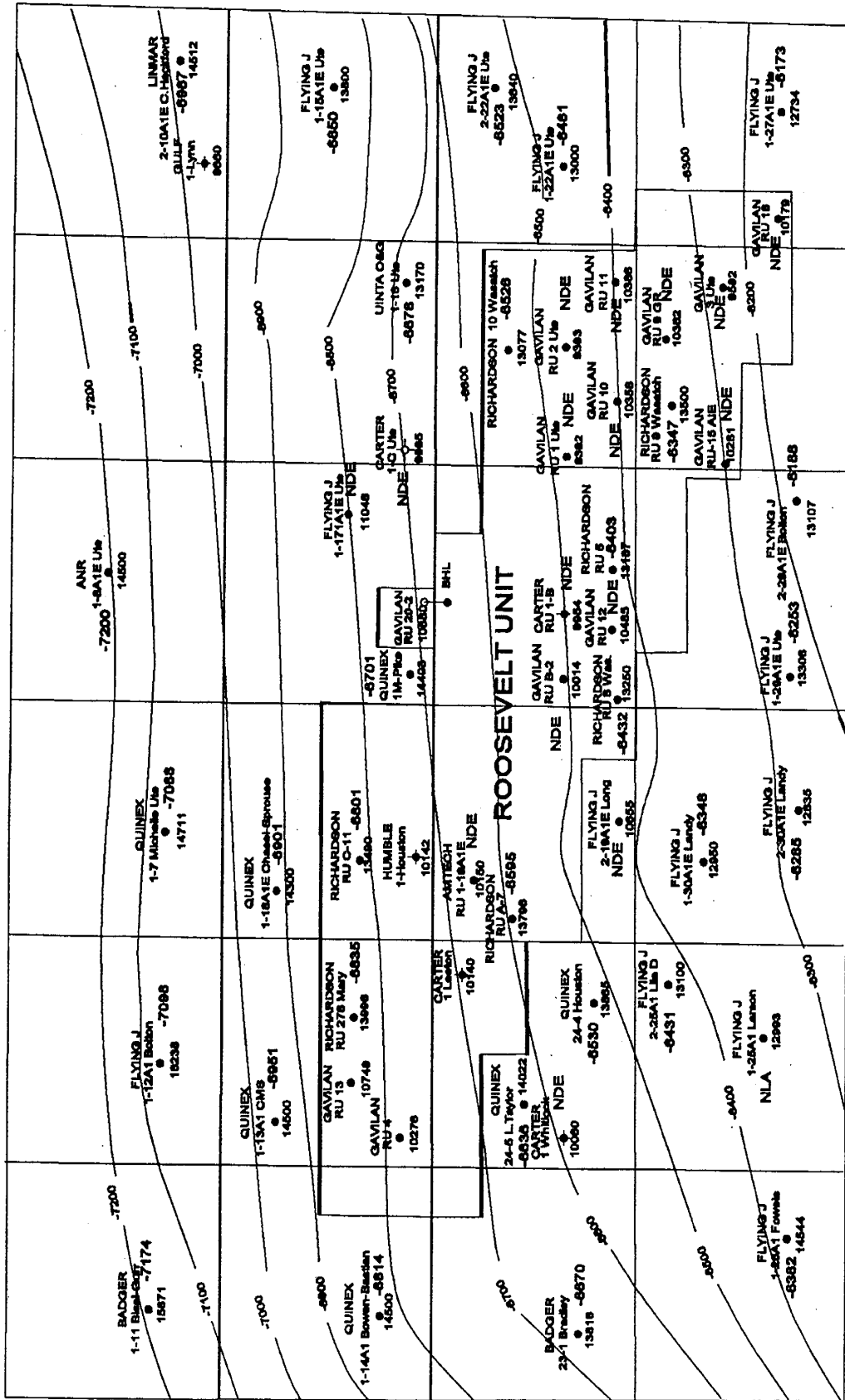


Figure 6.2 Structure contour map of the lower Wasatch transition. Contour interval is 100 feet.

R 1 W R 1 E

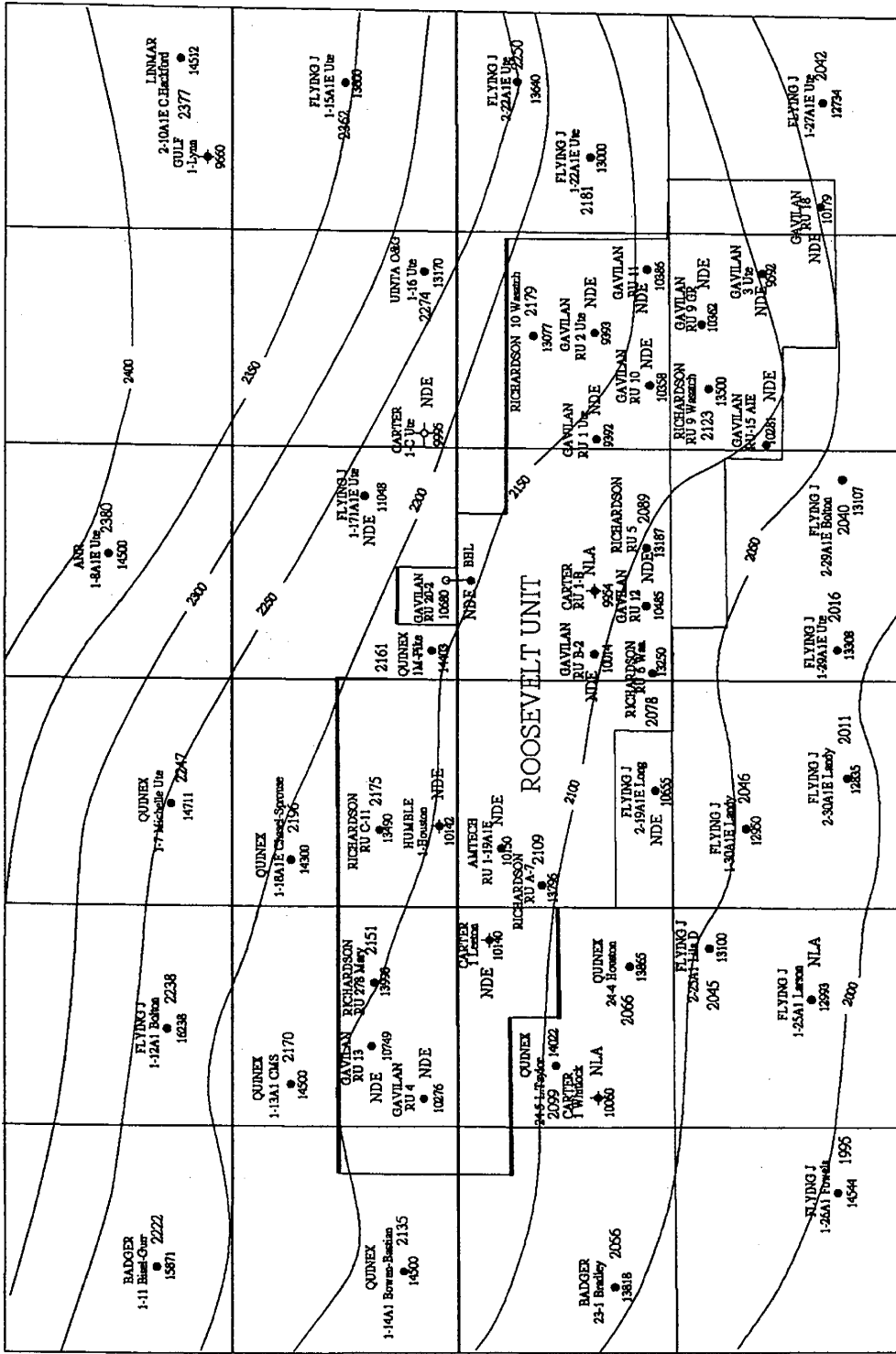


Figure 6.3 Isopach map of the Wasatch Formation. Contour interval is 50 feet.

R1W R1E

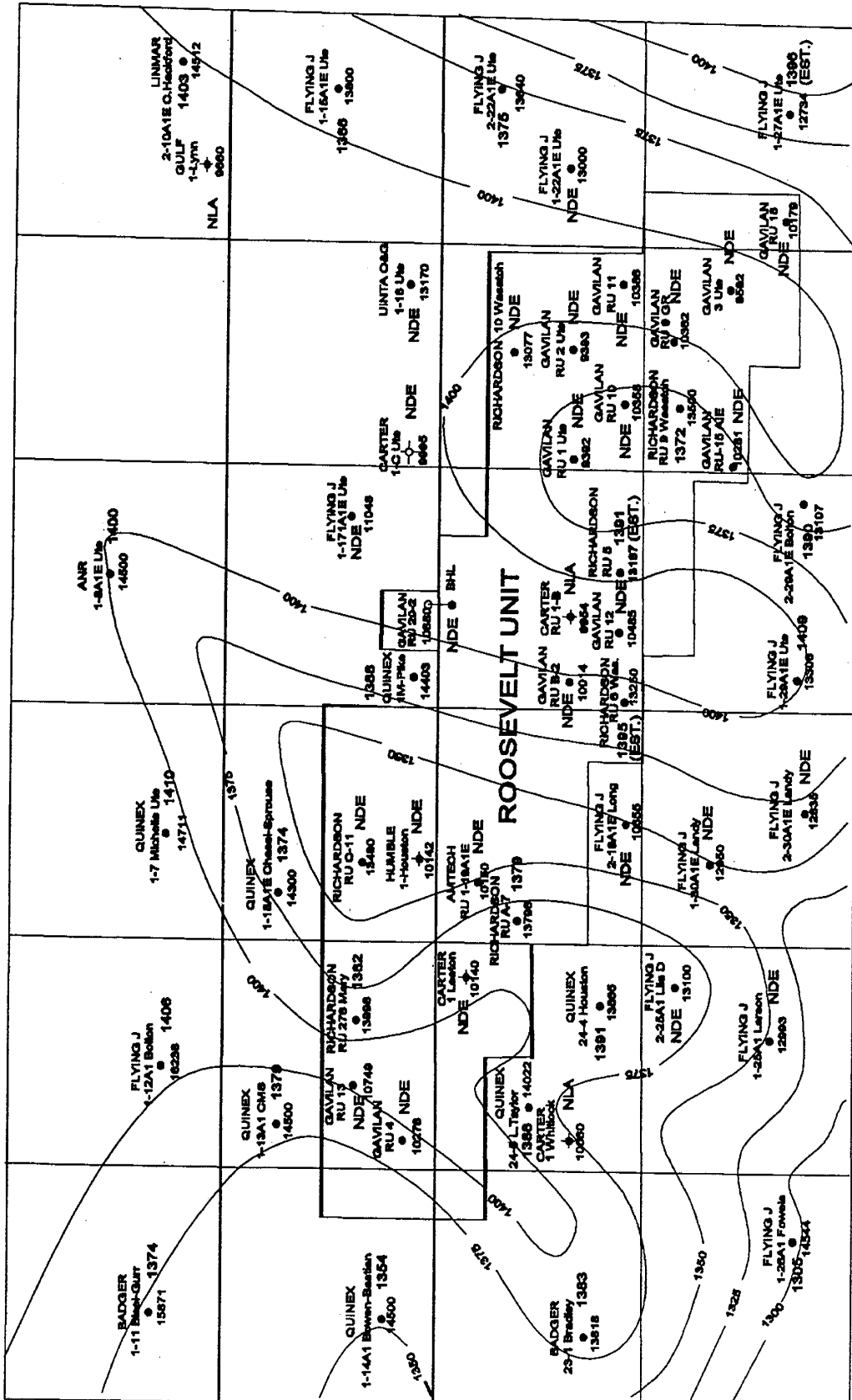


Figure 6.4 Isopach map of the lower Wasatch transition. Contour interval is 25 feet.

## **7. NUMERICAL SIMULATION MODELING OF HYDROCARBON PRODUCTION FROM THE GREEN RIVER AND WASATCH FORMATIONS**

*Milind D. Deo and Rajesh J. Pawar*  
University of Utah

### **7.1 Introduction**

The objective of the reservoir analysis was to compile all of the relevant reservoir data and integrate the data into a reservoir simulation model. The idea was to match the reservoir production history and to use the same models for predicting future reservoir performance. The first modeling effort was based on log-derived porosities and fluid saturations of all the perforated beds (open to the wellbore) in the proposed demonstration wells, Michelle Ute and Malnar Pike (tables 7.1 and 7.2). The geologic characterization resulted in specific criteria to identify beds with the best hydrocarbon potential. The beds in the Michelle Ute and Malnar Pike wells that meet the criteria were re-evaluated (tables 6.1 and 6.2). Modeling of these beds and similar beds in the surrounding wells, is currently underway.

The OOIP values in the perforated beds were estimated by using log-generated porosities and water saturations. The oil produced from the individual beds could be determined using reservoir simulation results. The OOIP and the oil produced from individual beds allowed calculation of the oil left behind in various beds and thus delineated the most promising beds in certain parts of the field. The reservoir simulations also helped identify beds with adequate reservoir pressure in order to sustain economic levels of production.

The reservoir fluid property data for the field was compiled and reported earlier (Allison, 1995). Additional data on core porosities and permeabilities and limited data on fractures became available this year, some of which was used in reservoir simulators. Even though dual-porosity, dual-permeability fractured reservoir models were used to study the reservoir performance, the available fracture information has not directly been integrated into the models. A geostatistical approach, described later, will be used to extrapolate the available fracture information.

The reservoir simulation models consisted of homogeneous and fractured single-well models and homogeneous and fractured regional models. The single well models were for the original demonstration wells; Michelle Ute and Malnar Pike. Two regional models were selected for analysis; a 4-square mile (10.4 km<sup>2</sup>) area in the eastern half of the field and a 4-square mile (10.4 km<sup>2</sup>) area in the western half of the field consisting of some of the largest producers in the field. All of the wells in this western regional model were owned and operated by Pennzoil Exploration and Production Company. The reservoir characteristics employed in all the models and the reservoir simulation results were presented in the earlier annual report (Allison, 1995). Since numerical difficulties were encountered in executing large-scale multi-layered fractured models, simulations using lumped fractured models were performed first. This limitation was later overcome and in this report, both the lumped and the detailed fractured models are presented.

The permeabilities both for the intergranular and the fracture systems which had to be employed to match the oil and gas production data in the two wells, were extremely low. Furthermore, the simulations revealed that the reservoir permeability continued to deteriorate as oil production continued. The simulations confirm two basic observations in the Bluebell field. The first is that there is a substantial amount of oil left behind in the field and the second is that some sort of permeability enhancement is essential for the economical production of this oil. The reservoir characterization data which has been gathered in this project, lends itself to integration and subsequent interpolation/extrapolation via geostatistical principles. Standard geostatistical techniques were modified and streamlined so that they could be applied to this project.

## 7.2 Most Promising Beds

The reservoir characteristics of the perforated beds in Michelle Ute and Malnar Pike wells are shown in tables 7.1 and 7.2. The geologic data (thickness, porosity, and oil saturation [which was calculated as one minus the reported water saturation]) were based on log analysis. A limited 40-acre (16.2 ha) areal extent was used in the single-well models. The OOIP reported for each of the beds was obtained by using the water saturation reported. The OOIP was about 1.75 million stock tank barrels (MMSTB) (245,000 MT) over a relatively small area of 40 acres (16.2 ha) for the Michelle Ute well. Incorporation of reported water saturations into reservoir simulators resulted in the production of much larger volumes of water than were actually produced in the field. Hence, oil saturations of 0.7 were used in the reservoir simulators. The log-interpreted saturation values are averages over the entire thickness of each bed. The bed thickness interpreted to be oil bearing may be a zone of oil-bearing layers interbedded with fine, shaly non-oil-bearing layers. These types of reservoir pay zones will be much harder to represent in reservoir simulators. In any case, both the methods yield substantial OOIP values within the limited 40-acre (16.2 ha) area. The OOIP numbers for the Malnar Pike well were even more substantial (5.2 MMSTB [728,000 MT]).

The oil produced from each of the individual beds using the homogeneous model is also shown in table 7.1 for Michelle Ute and in table 7.2 for Malnar Pike. It is clear from these data that most of the perforated beds still contain significant portions of the OOIP. In the production of oil from both the Michelle Ute and the Malnar Pike wells, different beds were opened (perforated) at different times. The Michelle Ute well thus has three sets of perforations, while the Malnar Pike well has two sets of perforations. In history matching the performance of these two wells, this perforation history was reproduced in the simulators. In both the Michelle Ute and the Malnar Pike wells, the first sets of perforations accounted for most of the oil produced. In the homogeneous models (tables 7.1 and 7.2), low absolute permeabilities were used to match the production data. It was necessary to use progressively lower permeabilities as new beds were perforated in both the wells indicating greater levels of formation damage in the newer beds. The layers with the first set of perforations in Michelle Ute had permeabilities of about 0.6 mD, while the second and the third sets had permeabilities of 0.1 and 0.07 mD

Table 7.1. Reservoir characteristics of all the perforated beds in the Michelle Ute well.

Bed	Depth in feet	Thickness in feet	Porosity	So <sup>1</sup>	OOIP (STB) Based on So	Oil Produced (STB) OOIP Based on So=0.7
1	10414	2	0.04	0.5	8540	259
2	10448	2	0.02	0	0	203
3	10470	12	0.02	0.29	14860	1123
4	10521	10	0.08	0.78	133224	1511
5	10603	1	0.03	0	0	124
6	10709	9	0.08	0.8	122976	1399
7	10795	6	0.09	0.76	87620	1037
8	10861	14	0.09	0.86	231349	2230
9	10938	11	0.09	0.78	164865	1759
10	11188	5	0.04	0.15	6405	708
11	11237	1	0.04	0.21	1793	144
12	11707	1	0.03	0	0	134
13	11777	6	0.15	0.53	101840	1293
14	11827	1	0.1	0.58	12383	213
15	11937	1	0.14	0.65	19429	234
16	11955	1	0.15	0.57	18254	235
17	12348	1	0.06	0.27	3459	189
18	12438	1	0.16	0.72	24595	232
19	12989	6	0.12	0.65	99918	6563
20	12997	2	0.05	0.25	5338	1316
21	13002	4	0.11	0.74	69516	4212
22	13010	8	0.09	0.46	70711	7317
23	13023	6	0.09	0.61	70327	5574
24	13096	4	0.05	0.22	9394	2595
25	13102	4	0.05	0	0	2592
26	13221	6	0.06	0.26	19984	4351
27	13320	4	0.06	0.02	1025	2913
28	13328	4	0.09	0.46	35356	3723
29	13347	2	0.05	0.25	5338	517
30	13358	1	0.05	0.16	1708	259
31	13363	2	0.05	0.12	2562	517
32	13409	6	0.16	0.67	137323	7754
33	13547	6	0.06	0.38	29207	4254
34	13652	2	0.05	0.16	3416	518
35	13804	4	0.04	0.21	7174	2172
36	13854	6	0.07	0.55	49319	4613
37	13873	2	0.05	0.31	6619	527
38	13899	6	0.09	0.56	64562	5409
39	13999	6	0.04	0.15	7686	3109
40	14008	4	0.04	0	0	2096
41	14067	2	0.07	0.11	3288	597
42	14077	4	0.06	0.51	26132	1091
43	14284	6	0.06	0.38	29207	4090
44	14435	7	0.06	0.38	34075	4679
45	14443	4	0.06	0.18	9223	2690
			Totals		1749996	99075

<sup>1</sup>So is the oil saturation defined as 1 - water saturation

Table 7.2. Reservoir characteristics of all the perforated beds in the Malnar Pike well.

Bed	Depth in feet	Thickness	Porosity	So <sup>1</sup>	OOIP(STB) Based on So	Oil Produced (STB) OOIP Based on So=0.7
1	9582	10	0.08	0.64	99639	574
2	9914	6	0.18	0.61	128207	646
3	9925	3	0.05	0.37	10801	130
4	9933	4	0.04	0	0	151
5	9940	3	0.07	0.51	20842	127
6	9950	16	0.07	0.45	98082	822
7	10054	18	0.03	0.61	64103	610
8	10074	4	0.2	0.72	112094	539
9	10081	3	0.1	0.55	32110	847
10	10101	12	0.1	0.8	186823	786
11	10289	24	0.07	0.8	261552	1066
12	12702	4	0.09	0.56	39233	358
13	12716	4	0.14	0.74	80645	449
14	12976	4	0.09	0.53	37131	349
15	13026	8	0.14	0.78	170008	716
16	13084	9	0.17	0.78	232244	869
17	13136	6	0.18	0.74	155530	664
18	13165	15	0.15	0.83	363428	1154
19	13186	4	0.17	0.8	105866	500
20	13200	6	0.32	0.86	321335	827
21	13224	8	0.09	0.74	103687	601
22	13276	4	0.14	0.65	70837	459
23	13336	10	0.14	0.76	207062	857
24	13370	8	0.16	0.7	174368	808
25	13402	10	0.12	0.68	158799	844
26	13415	8	0.07	0.51	55580	560
27	13434	4	0.08	0.45	28023	324
28	13486	8	0.08	0.63	78465	572
29	13500	6	0.16	0.7	130776	615
30	13516	10	0.14	0.72	196164	821
31	13570	14	0.12	0.65	212511	1016
32	13588	6	0.09	0.63	66205	498
33	13600	10	0.06	0.1	11676	610
34	13826	14	0.12	0.56	183086	8457
35	13854	6	0.06	0.55	38532	3003
36	13898	8	0.1	0.6	93411	5049
37	13956	2	0.1	0.65	25299	1444
38	13970	6	0.12	0.58	81268	4162
39	13986	10	0.06	0.6	70058	4540
40	14060	6	0.14	0.43	70292	4605
41	14082	6	0.18	0.65	136614	5068
42	14118	8	0.06	0.63	58849	3830
43	14140	6	0.06	0.43	30125	2984
44	14160	2	0.06	0.3	7006	1119
45	14168	4	0.07	0.51	27790	2239
46	14184	6	0.1	0.68	79400	3806
47	14230	4	0.14	0.65	70837	76286
48	14266	13	0.07	0.65	115110	6148
49	14350	10	0.1	0.5	97303	6042
			Totals		5198804	86484

<sup>1</sup>So is the oil saturation defined as 1 - water saturation

respectively. The layers with the first set of perforations in Malnar Pike had permeabilities of 0.34 mD and the second set had permeabilities of 0.016 mD. The low permeabilities employed in the history match indicate two significant aspects of the reservoir: (1) even though there is great deal of oil still in the reservoir, unless the permeabilities are enhanced by some means, it is not producible at economic rates, and (2) the new layers opened have lower permeabilities than initially opened beds.

The areal oil saturation distribution in the Michelle Ute well is shown in figure 7.1. It is clear from the figure that the oil saturations are affected only over a radius of about 400 feet (121.9 m) in these tight homogeneous models and even in the affected portion, the oil saturation remains fairly high. The pressure influence is also felt over a similar distance (figure 7.2). The pressure and saturation distributions around Malnar Pike are similar to those shown for Michelle Ute in figures 7.1 and 7.2.

Based on the analysis of single-well models of the Michelle Ute and Malnar Pike wells, the following beds are interpreted to have the largest amount of remaining potential for hydrocarbon production.

Michelle Ute: Beds 8, 32, 13, 19, 22, 4, 37, 23, 21, and 44.

Malnar Pike: Beds 18, 20, 31, 34, 11, 16, 23, 30, 24, and 25.

Because of thin interbedded shale in some beds, targeting individual beds for recompletion or treatment may be risky, particularly for thin beds. However, selected interval recompletion may prove to be beneficial for improving oil production from both the wells. In the Malnar Pike well particularly, the beds between 13,000 to 13,400 feet (3,962.4-4,084.3 m) contain over a million barrels of oil (140,000 MT). Bed number 18 in the Malnar Pike well, containing over 300,000 BO (42,000 MT) in place may be a bed which could be an individual target. In the Michelle Ute well, beds 21-23 contain about 250,000 BO (35,000 MT).

### **7.3 Fractured Reservoir Simulations - Lumped Models**

Single-well simulations were also performed using dual-porosity, dual-permeability fractured models. Numerical difficulties were encountered in performing simulations of models which represented each of the producing intervals in the Michelle Ute and Malnar Pike wells separately. Hence, multiple producing intervals were lumped into pseudo-layers and simulations were performed using these limited-layer systems. The pertinent reservoir characteristics of these fractured models are listed in tables 7.3 and 7.4. The oil production predicted by these models matched the field results reasonably well. The model and field oil production comparisons for the Michelle Ute and the Malnar Pike wells are shown in figures 7.3 and 7.4 respectively.

These fractured reservoir models for the Michelle Ute and the Malnar Pike wells revealed that the radius of influence is larger due to the presence of fractures. The radius of influence increased to about 1,000 feet (304.8 m) compared to about 400 feet (121.9 m) for the homogeneous models. Most wells in the field are spaced farther apart than 1,000 feet (304.8 m). The field experience however indicates that wells drilled subsequently in a section, in general, produce less oil than the initial wells. The fracture permeabilities used in the Michelle Ute model were about 0.2 mD and in the Malnar Pike model were of the order of 1.0 mD. The low fracture permeabilities used for history matching indicate that the fractures may not be completely open for fluid flow. Field experience with regard to the first and subsequent wells in individual sections indicates that there may be higher permeability beds in the reservoir responsible for initial high oil production. The near-wellbore formation damage makes these beds less

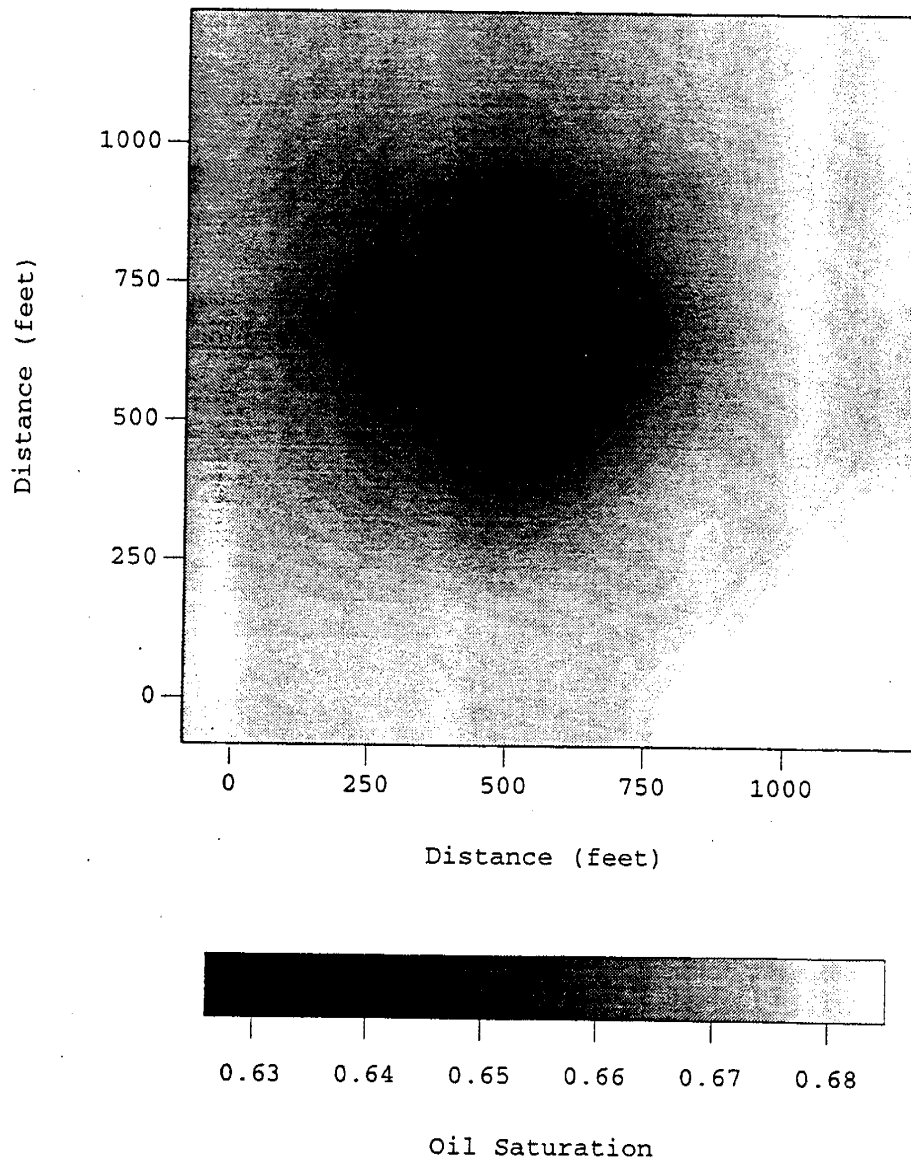


Figure 7.1. The oil saturation distribution around the Michelle Ute well (as of March, 1993).

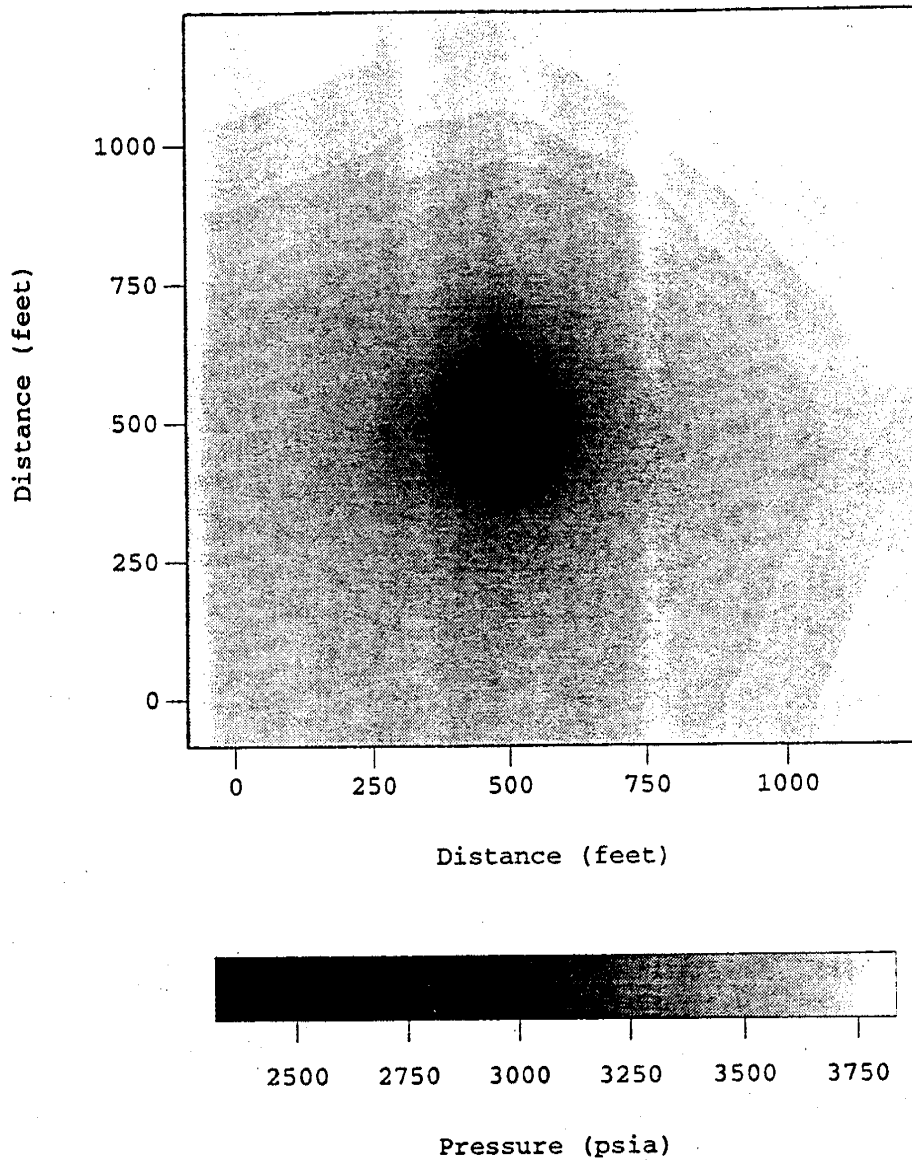


Figure 7.2. The pressure distribution around the Michelle Ute well (as of March, 1993).

Table 7.3. Reservoir characteristics of the lumped, fractured reservoir model for the Michelle Ute well.

Bed	Depth in feet	Thickness in feet	So <sup>1</sup>	OOIP(STB)	Oil Produced(STB)
1	11221	84	0.7	926004	43381
2	11946	2	0.7	43821	1727
3	12393	2	0.7	33250	1419
4	13105	40	0.7	496559	27300
5	13434	25	0.7	328641	17657
6	13830	30	0.7	259026	16111
7	14255	23	0.7	212572	12798

<sup>1</sup>So is the oil saturation defined as 1 - water saturation

Table 7.4. Reservoir characteristics of the lumped, fractured reservoir model for the Malnar Pike well.

Bed	Depth in feet	Thickness in feet	So <sup>1</sup>	OOIP(STB)	Oil Produced (STB)
1	9833	67	0.7	711644	4147.09
2	11567	56	0.7	579562	3621.63
3	13202	62	0.7	1403277	4350.39
4	13605	98	0.7	1501738	5172.9
5	13990	52	0.7	703639	37983
6	14250	45	0.7	528330	31038.7

<sup>1</sup>So is the oil saturation defined as 1 - water saturation

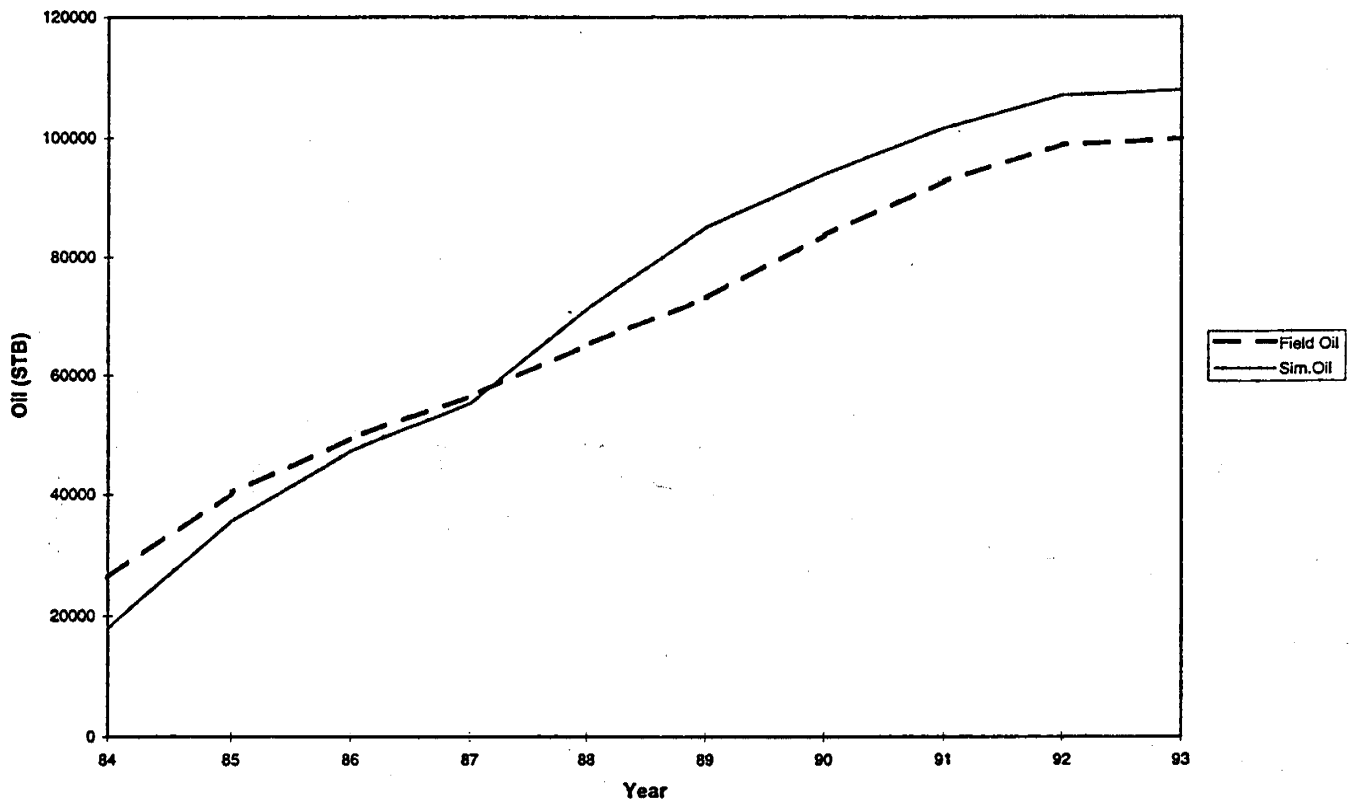


Figure 7.3. Comparison of the actual (field oil) to simulated (sim oil) oil production for the Michelle Ute well using the lumped, fractured model.

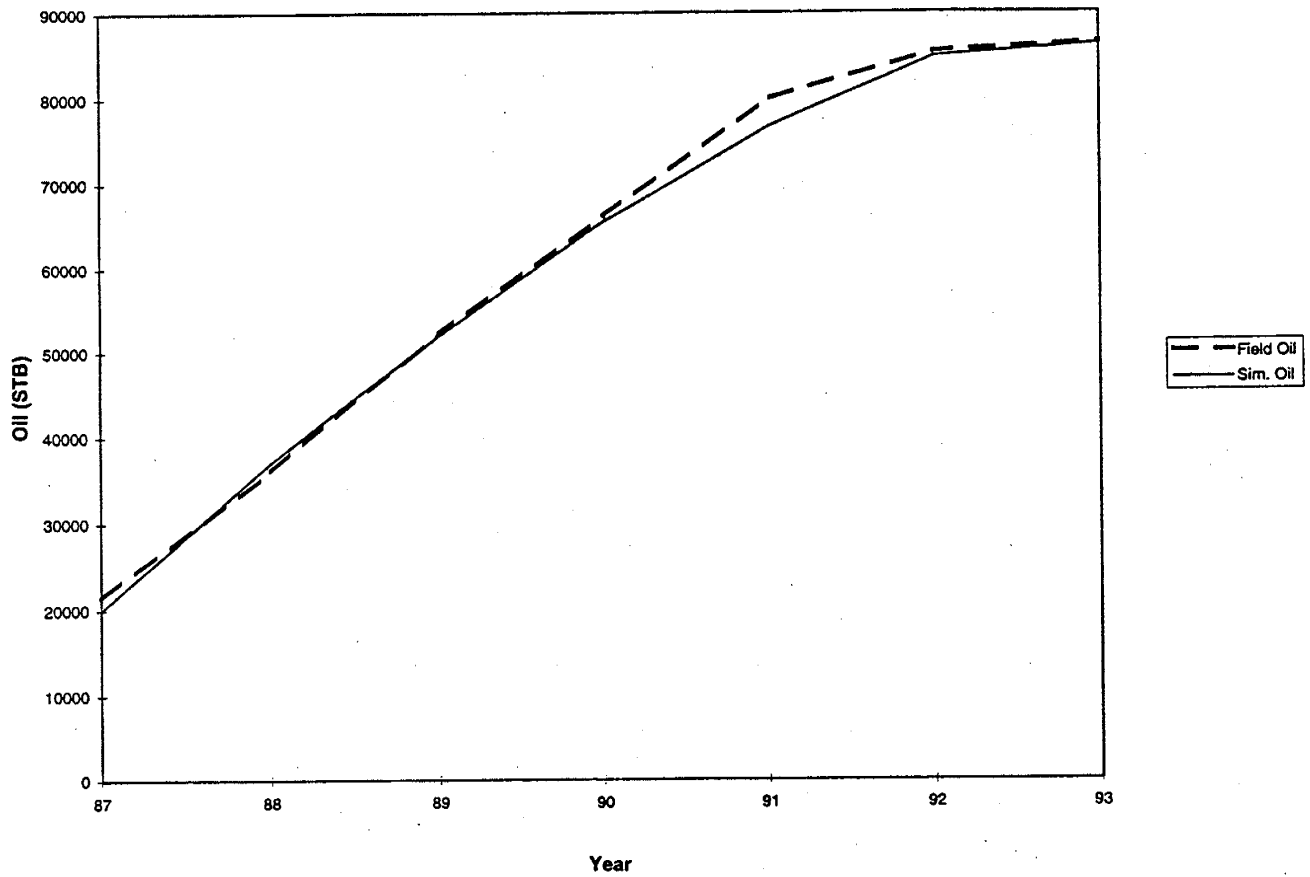


Figure 7.4. Comparison of the Actual (field oil) to simulated (sim oil) oil production for the Malnar Pike well using the lumped, fractured model.

productive over time. Individual bed testing would be required to verify this hypothesis. Thus, these models also indicate that there is a great deal of oil left in the reservoir and that in order to mobilize the oil, the fracture permeabilities would have to be increased through treatment.

Using reservoir characteristics of five correlated beds in the Roosevelt Unit area, a 4-square-mile (10.4 km<sup>2</sup>) area was modeled. The reservoir characteristics of the model shown in table 7.5 also reveal that each of the five beds contain significant quantities of oil. From an oil production perspective, all the beds have promise. The permeabilities of various blocks in the model for history matching range from about 0.05 to 0.3 mD. This oil will have to be produced through permeability improvement, at least in the near-wellbore region.

Table 7.5. Reservoir characteristics of the lumped, fractured 4-square mile area model in the Roosevelt Unit.

Bed	Depth in feet	Average Thickness in feet	Average Porosity	So <sup>1</sup>	OOIP (MSTB)	Oil Produced (MSTB)
1	13000	22	0.148	0.7	36966	192
2	13100	10	0.115	0.7	9876	71
3	13915	10	0.084	0.7	8254	63
4	13925	8	0.119	0.7	8169	60
5	14000	6	0.174	0.7	7485	63

<sup>1</sup>So is the oil saturation defined as 1 - water saturation

#### 7.4 Fractured Reservoir Simulations - Comprehensive Models

In the fractured reservoir model around the Michelle Ute well which accounted for all of the known layers, an 8 X 8 X 137 Cartesian grid was employed. The block dimensions in the x and the y directions were 165 feet (50.3 m) each, while the dimensions in the z direction varied according to the individual layer thicknesses. Of the 137 layers, 69 were oil bearing. The fractures were vertical, spaced at 165 feet (50.3 m) and extended only 500 feet (152.4 m) from the wellbore in all directions. The intergranular porosity varied in accordance with the porosity data for the individual layers, while the fracture porosity was constant at  $2 \times 10^{-6}$ . The initial reservoir pressure and water saturation also varied in accordance with the individual layer data. The initial gas-oil ratio (GOR) was constant at 800 standard cubic feet per stock tank barrel (scf/STB [160 m<sup>3</sup>/MT]) and thus the initial bubble point pressure was also constant at 3,900 pounds per square inch (psi [26,890 kPa]).

The fracture permeability was constant at 0.23 mD and the intergranular permeability varied from 0.005 to 0.09 mD. After four years of production (after the third set of perforations), the intergranular permeability was reduced to 8 percent of its original value (uniformly).

The simulation results of oil and gas production are compared to the field results in figures 7.5 and 7.6. The oil production is matched reasonably well, while the gas production is consistently underpredicted by the simulator. More work is being done to obtain better matches with the field data. The trends for Malnar Pike well are similar and more work is being done on that model as well.

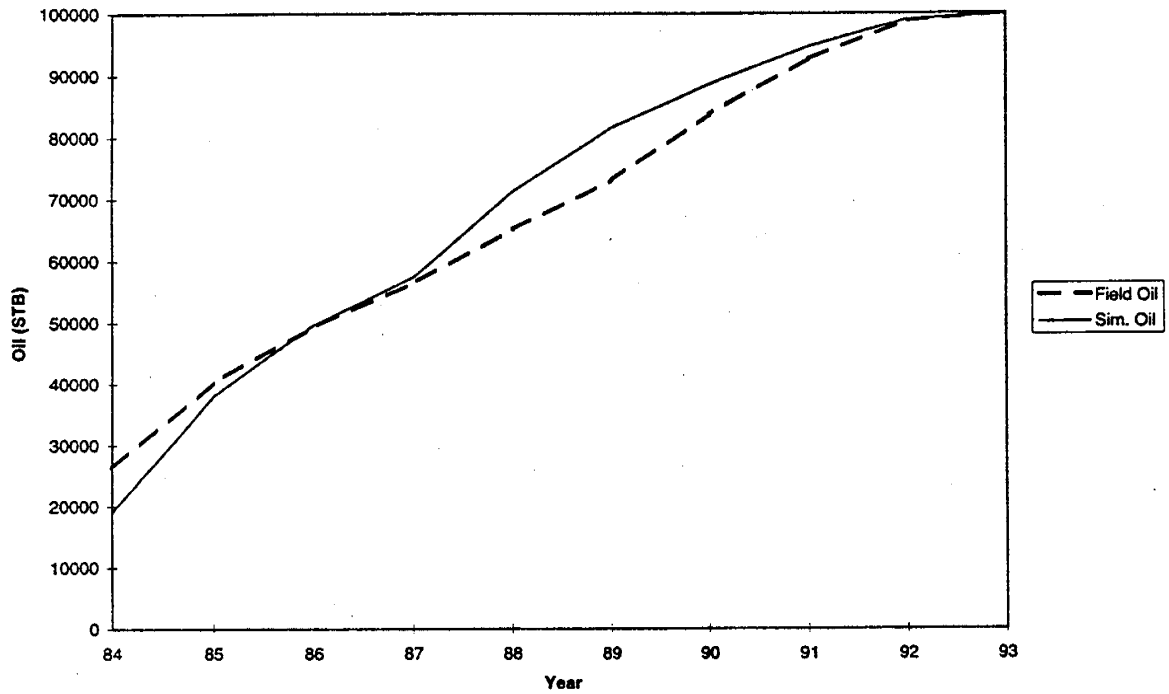


Figure 7.5. Comparison of the field (field oil) to simulated (sim oil) oil production for the Michelle Ute well using the comprehensive, fractured model.

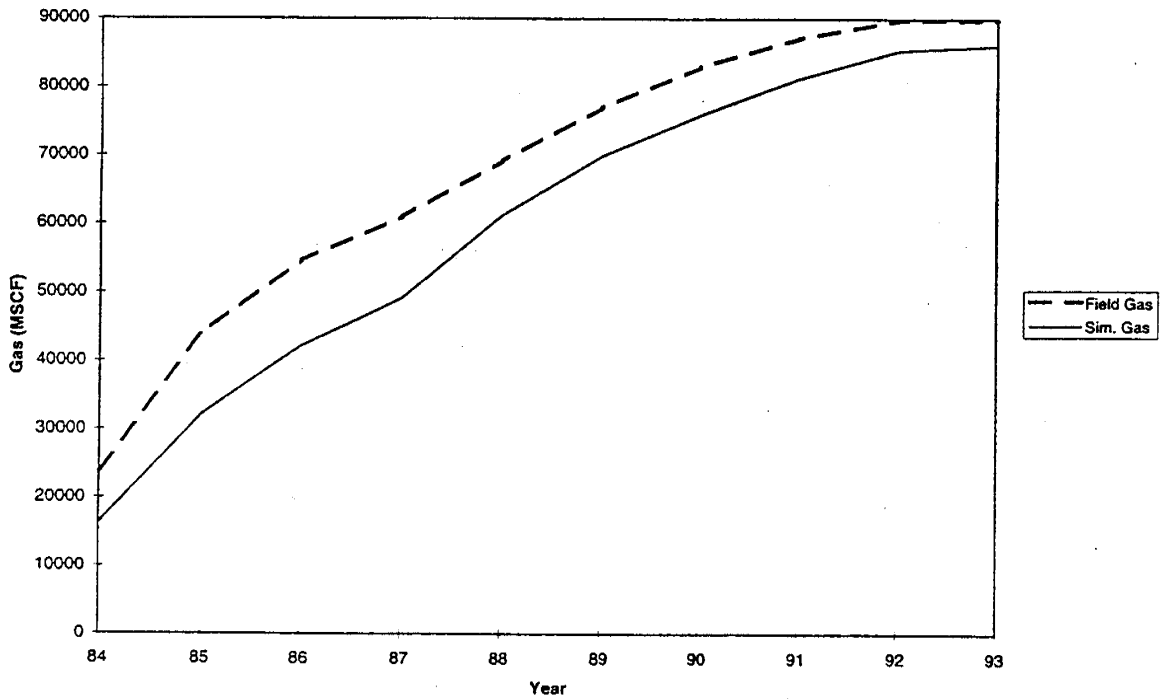


Figure 7.6. Comparison of the field (field gas) to simulated (sim gas) gas production for the Michelle Ute well using the comprehensive, fractured model.

## 7.5 Geostatistics

The concepts of geostatistics were applied to obtain three-dimensional spatial distributions of porosities and water saturations. These distributions were conditioned to the porosity and saturation data at selected wells. The porosity and saturation values were determined from conventional logs and were available at 2-foot (0.6-m) vertical resolution. Such data were available for five wells in the Roosevelt Unit area on the east side and seven wells operated by Pennzoil on the west side. Thus areally, only 12 data sets were available covering two 4-square-mile sections (10.4 km<sup>2</sup>), one on the east side and the other on the west side. In order to apply the geostatistical principles for generating spatial distributions, data would be required at more locations (wells). However, in order to streamline the geostatistical methods and establish formal mathematical procedures, spatial distributions were generated using a hypothetical data set consisting of 12 wells in a 4-square-mile (10.4 km<sup>2</sup>) area. For the purposes of this study, the locations of the 12 wells in the 4-square-mile area were randomly assigned. A maximum thickness of 50 feet (15.2 m) was considered and it was assumed that the wells intersected the same "pay".

The porosity and saturation data sets were studied independently assuming that there is no correlation between them. Each of the data sets was converted into a Gaussian distribution. Spatial correlations were found for each property in terms of semi-variograms. A semi-variogram is calculated as follows:

$$\gamma(h) = \frac{1}{2N(h)} \sum_{i=1}^{N(h)} (x_i - y_i)^2$$

where,  $x_i$  and  $y_i$  are two data values separated by distance  $h$  (also known as lag distance).  $N$  is total number of pairs  $(x_i, y_i)$ .  $\gamma(h)$  is the value of the semi-variogram at  $h$ . A number of semi-variogram values are calculated for various lag distances.

Semi-variograms provide quantitative estimates of spatial correlations between data points and the distances over which these correlations exist. Two separate semi-variograms were calculated; one to find the correlation between data points in the horizontal direction and the other to establish the correlation in the vertical direction. The two-directional semi-variograms were combined to give a three-dimensional semi-variogram for each of the properties (porosity and saturation). These three-dimensional semi-variograms were described by mathematical models.

The semi-variogram model equations are given below:

$$\gamma(\phi) = 0.4 + 1.2 \left[ \text{sph} \left( \frac{h_x}{13000} + \frac{h_y}{13000} + \frac{h_z}{15} \right) \right]$$

$$\gamma(S_w) = 0.7 + 0.85 \left[ \text{sph} \left( \frac{h_x}{13000} + \frac{h_y}{13000} + \frac{h_z}{15} \right) \right]$$

where,

$$\text{sph} \left( \frac{h}{a} \right) = \left[ 1.5 \frac{h}{a} - 0.5 \left( \frac{h}{a} \right)^3 \right] \dots h \leq a$$

$$\text{sph} \left( \frac{h}{a} \right) = 1 \dots h \geq a$$

The above semi-variogram models were employed in performing sequential Gaussian simulations for generating the three-dimensional spatial distributions. These conditional simulations honor the data values at specified locations and also attempt to match the system statistics.

A number of such three-dimensional distributions were generated for porosities and saturations for the hypothetical reservoir. Figures 7.7 and 7.8 show results of one such simulation for porosities and saturations respectively. The figures display two perpendicular planes showing variations of property values in space. The inherent statistical variation in reservoir data can be observed by examining results of several realizations. The reservoir data can be used in flow simulations to generate production estimates for given realizations. The upper and lower production values from a number of simulations will provide the production variability associated with the statistical variation in reservoir properties.

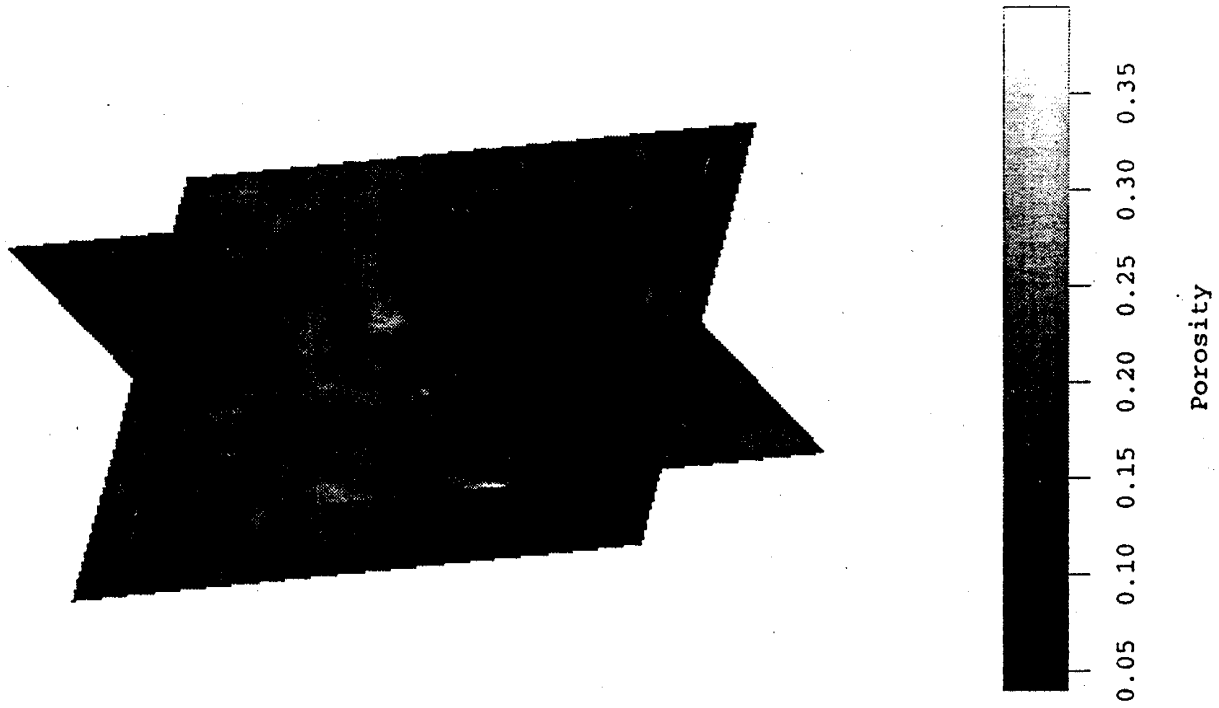


Figure 7.7. Porosity distributions in two cross sections of a hypothetical four-section reservoir. The cross sections are through true, three-dimensional reservoir images generated using sequential, Gaussian simulations.

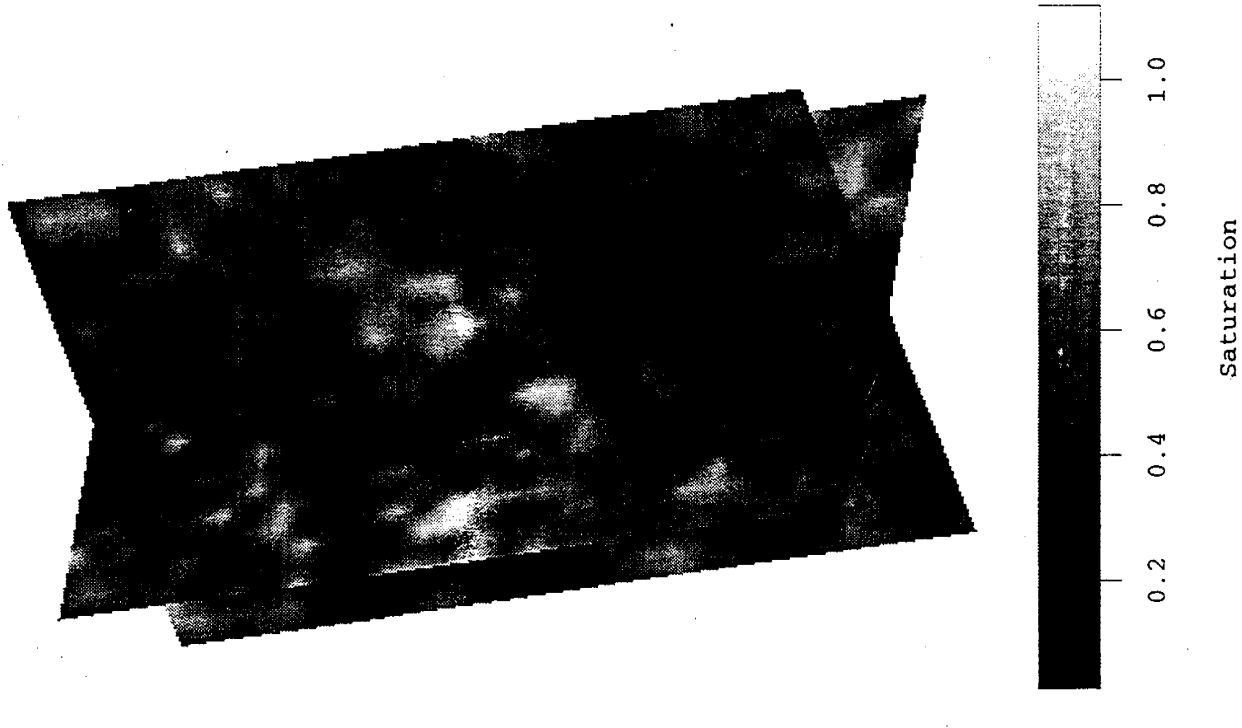


Figure 7.8. Oil saturation distributions in two cross sections of a hypothetical four-section reservoir. The cross sections are through true, three-dimensional reservoir images generated using sequential, Gaussian simulations.

## 7.6 Conclusions

The single-well homogeneous, single-well fractured and 4-square-mile (10.4 km<sup>2</sup>) area reservoir models indicate that a great deal of oil is still in place in several parts of the Bluebell field. The models also indicate that the inherently low reservoir permeability may have been compounded due to extensive near-wellbore damage. The naturally occurring fractures in the Bluebell field typically have low permeabilities due to mineralization. Thus, the oil would be producible only through permeability enhancement and this could be effected only in the near-wellbore region. Based on the original reservoir characteristics and oil produced from individual layers, beds with the best oil production potential could be identified and ten such beds in the Michelle Ute and the Malnar Pike wells have been identified in this report. Due to the extremely heterogeneous nature of the pay beds (oil-bearing layers intermingled with non-oil-bearing layers), targeting thin individual beds may be risky even if the beds contain significant oil-in-place. Targeting a selected series of beds over a reasonable interval may be the best strategy for activating these wells. One or two beds in the Malnar Pike well contain over 250,000 BO (35,000 MT) and are reasonably thick (greater than 12 feet thick [3.7 m]). These beds could be individual targets for stimulation. The feasibility of integrating reservoir information and generating geostatistical reservoir images using available data was demonstrated for a hypothetical data set. These concepts will be extended to map out the fracture networks and flow simulations will be performed using the reservoir data.

## 8. COMPLETION TECHNIQUES

*Richard Curtice*  
Halliburton Energy Services

### 8.1 Introduction

Treatment data was compiled from 246 stimulations (108 different parameters in each treatment) of 67 wells in the study area. The database was analyzed by the Halliburton Energy Services Tech Team in Denver, Colorado. Halliburton determined what types of stimulation treatments have been pumped, which have been the most effective, and what additives have been used and their effectiveness.

Production of hydrocarbons in the Bluebell field is generally from the lower Green River and Wasatch Formations. The gross productive interval in most wells is over 3,000 feet (900 m) thick. During the life of a well, perforations are constantly being added, increasing the net footage being treated. To improve completion techniques in the Bluebell field it is important to identify the productive beds and reduce the number of beds the operator is trying to stimulate.

Hydrochloric (HCl) acid is the most common treatment fluid used in the Bluebell field. Corrosion inhibitors, surfactants, and iron, scale, and clay control additives are commonly used in most, but not all treatments. If acid is the fluid treatment selected, an additive package in the proper concentration should be included which will enhance the production of the well. The tubulars should be pickled prior to acidizing and the treatment fluid recovered as quickly as possible.

Diverters are important when trying to treat large intervals to ensure that the fluids flow into as many of the perforated beds as possible. The most commonly used diverters in the Bluebell field are rubber coated nylon (RCN) ball sealers and benzoic acid flakes. Rock salt, wax beads, and moth balls, have all been used as diverters. It is common practice to use more than one type of diverter in a single treatment. If diverters are to be used, enough diverter should be added to a sufficient amount of fluid to allow the diverter to work.

High-rate hydraulic fracture treatments are a viable option that have been overlooked as a completion technique in this field and should be considered on newer wells. If higher rates are desired, pumping the treating fluid down the casing instead of the tubulars should be considered. Extended hydro-jetting has not been used in the Bluebell field but may be a technique to overcome near-wellbore damage caused by drilling and treatment fluids. Extended hydro-jetting can also be used to provide a small horizontal wellbore into several producing intervals within the same well.

### 8.2 Production and Well Data

The primary producing intervals in the study area can be divided into three primary zones. Zone one consists of the upper Wasatch transition zone that may include part of the lower Green River. Productive beds in zone one are typically interbedded limestone, dolomite, calcareous sandstone, marlstone, and ostracodal limestone. Many of these beds are laterally extensive and highly fractured. Testing of this zone, first drilled in 1948, resulted in the discovery of the Roosevelt field (now part of the Bluebell field). Zone one has a pressure gradient of around 0.43 pounds per

square inch per foot (psi/ft) to 0.52 psi/ft (0.9-1.1 kPa/m). Typically, zone one is found at depths below sea level of 9,000 to 10,000 feet (2,700-3,000 m).

Zones two and three include the Wasatch and the lower Wasatch transition zone, which is sometimes referred to as the Flagstaff Member of the Green River Formation. These zones are typically overpressured with pressure gradients of 0.75 psi/ft (1.6 kPa/m) and higher. Typically, zone two and three are found at an average depth of 11,000 to 14,000 feet (3,300-4,300 m). These zones became primary drilling targets beginning in the early 1970s. The Wasatch Formation typically consists of sandstone, siltstone, and shale. The lower Wasatch transition consists of mudstone, argillaceous limestone, dolomite, and some sandstone. Production from the Wasatch Formation is primarily from sandstone and siltstone while production from the lower Wasatch transition is dominantly from carbonates and a small number of sandstone beds. Production is partially dependent on natural fractures which allow both vertical and horizontal pressure communication.

Individual producing beds are difficult to evaluate because fracturing, clay content, and complex formation water chemistry make conventional geophysical log analysis difficult. Production testing of individual beds in either cased or open hole can be quite costly because of the number of beds, and therefore is typically not done. However, this makes it difficult if not impossible to determine which beds are major producers, limited producers, water producers, or thief zones. Also the liquid hydrocarbons that are produced from these zones are very high in paraffin which makes producing and handling difficult and expensive. Pour points typically will range from 90 to 110 °F (32°-43° C), and in some cases higher, depending on the paraffin content.

A completion history database was developed which includes: (1) the well name, (2) well location, and (3) operator. Total depths (TD) of the wells included in the database vary from 12,314 to 17,419 feet (3,753.3-5,309.3 m). Typically, there are three strings of pipe set. The surface pipe is 9-5/8 inch (24.4 cm) diameter or in some cases 10-3/4 inch (27.3 cm) diameter. The intermediate string of pipe is 7 or 7-5/8 inch (17.8 or 19.4 cm) diameter set from a depth of 9,450 to 13,982 feet (2,880.4-4,261.7 m). The most common liner set is 5 inch (12.7 cm) diameter, 18 pounds per foot (lb/ft [26.8 kg/m]), along with some 5-1/2-inch-(13.9-cm)- and a few 4-1/2-inch-(11.4-cm)-diameter strings. Typically, the depth of the liner is from 12,314 to 17,419 feet (3,753.3-5,309.3 m) and varies in length from 1,859 to 5,314 feet (566.6-1,619.7 m). Not all of the wells have liners; seven wells or 10.4 percent of the wells in the database, have no indication that a liner has been set.

The perforated interval is often quite large. The reported net interval (total footage perforated) varies from 4 to 1,310 feet (1.2-399.3 m), and the reported gross interval (depth of the lowest perforation minus the depth of the top perforation) varies from 4 to 3,009 feet (1.2-917.1 m). The number of perforations range from four shots to a maximum of 5,240 shots. Perforations vary in size from 0.26 to 0.56 inch (0.660-1.422 cm) diameter with the most common being 0.38 inch (0.965 cm) diameter. The density of the perforations varies from one shot per foot (spf) to four spf with the most common being two spf. The depth to the top perforation varies from 8,195 to 15,450 feet (2,497.8-4,709.2 m) and the depth to the bottom perforation varies from 9,656 to 16,417 feet (2,943.1-5,003.9 m). The average perforated interval has the top perforation at 11,350 feet (3,459.5 m) and the bottom perforation at 12,539 feet (3,821.9 m). These represent an overall average gross interval of 1,190 feet (362.7 m) with 284 perforations. Currently, it is common practice to perforate everything that

looks like a potentially productive interval at the same time. Historically, the trend has gone from producing a small interval to a larger interval, a few perforations to many perforations, and from small to large acid treatments. However, improvement in well response over time is questionable.

### 8.3 Stimulation Fluid Treatment Data

The database includes treatments performed during the period from August 1968 to November 1994. The 246 stimulation treatments were performed on the following formations (formation name - number of treatments): (1) Wasatch Formation - 172, (2) Green River Formation - 69, (3) Green River and Wasatch Formation combined - 3, (4) transition zone - 1, and (5) unknown - 1. The reported treatment fluids were: (1) HCl acid - 221, (2) mud acid (acid combination designed to remove drilling mud) - 9, (3) hydrofluoric (HF) acid - 5, (4) MSR (Dowell brand name) acid - 6, (5) diesel - 1, (6) WFC (Western Atlas brand name) acid - 1, and (7) fracture treatments with proppant - 3. Fluid volumes varied from a low of 250 gallons (945 L) to a high of 200,000 gallons (757,000 L). The overall average volume of acid being pumped in four different stages was 20,000 gallons (75,700 L). Acid treatments have been pumped in as few as one stage to as many as 24 acid stages.

Hydrochloric acid is the most common treatment fluid used (90 percent) in the study area. Of the 221 HCl acid treatments, 207 had concentrations of 15 percent, ten were 7-1/2 percent, two were 10 percent, and two combined 15 percent and 7-1/2 percent acid. The other treatments that refer to an acid also included HCl acid in part. Ninety-eight percent of the treatments studied were pumped using some type of acid, while the remaining 2 percent consisted of a proppant frac. The three proppant fracs included the following fluid types: (1) borate crosslinked fluid pumped in the Green River Formation in 1991 with 100,000 lb (45,360.0 kg) of 20/40 mesh sand, (2) gelled oil pumped in the Wasatch Formation in 1979 with only 2,000 lb (907.2 kg) of sand and 2,000 lb (907.2 kg) of glass beads, and (3) Super E (oil and water emulsion) pumped in the Green River Formation in 1978 with 24,000 lb (10,886.4 kg) of 40/60 mesh sand and 76,000 lb (34,473.6 kg) of 20/40 mesh sand. The trend of pumping acid is still the preferred treatment today. However, the response to acid treatments typically has decreased with time. In the late 1960s, for every gallon (3.8 L) of acid pumped, approximately 10 barrels (1.4 MT) of incremental oil was produced while the current trend is now less than one barrel (0.1 MT) of incremental oil for every gallon (3.8 L) of acid pumped (figure 8.1).

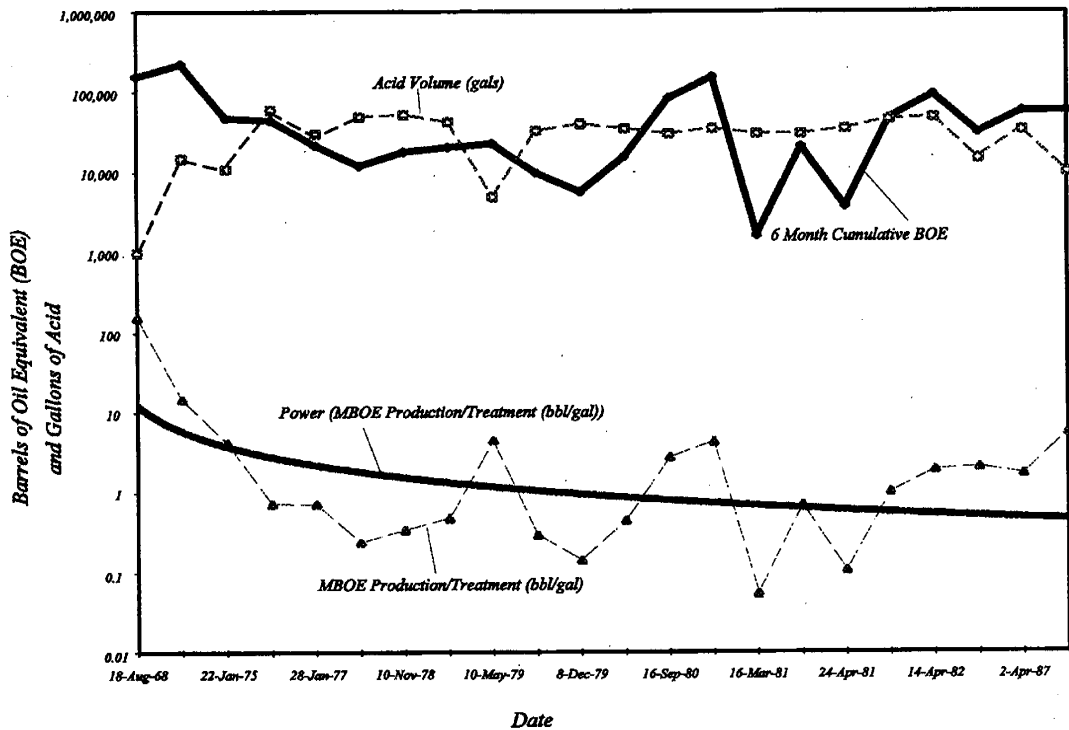


Figure 8.1. Treatment volumes and resulting hydrocarbon production. Production in barrels of oil equivalent (BOE).

### 8.3.1 Acid Additives

When a formation is treated with acid to increase production there is a large arsenal of chemical additives which help to enhance oil production. Typically an acid system will contain, as a minimum, the following types of additives: (1) surfactants, (2) corrosion inhibitor, (3) iron control, and (4) some type of clay control. Other additives are available but have a more specific application depending on the problem. There were ten different additive types used which can be categorized according to their effects. The frequency of use of these additives by category is shown in figure 8.2.

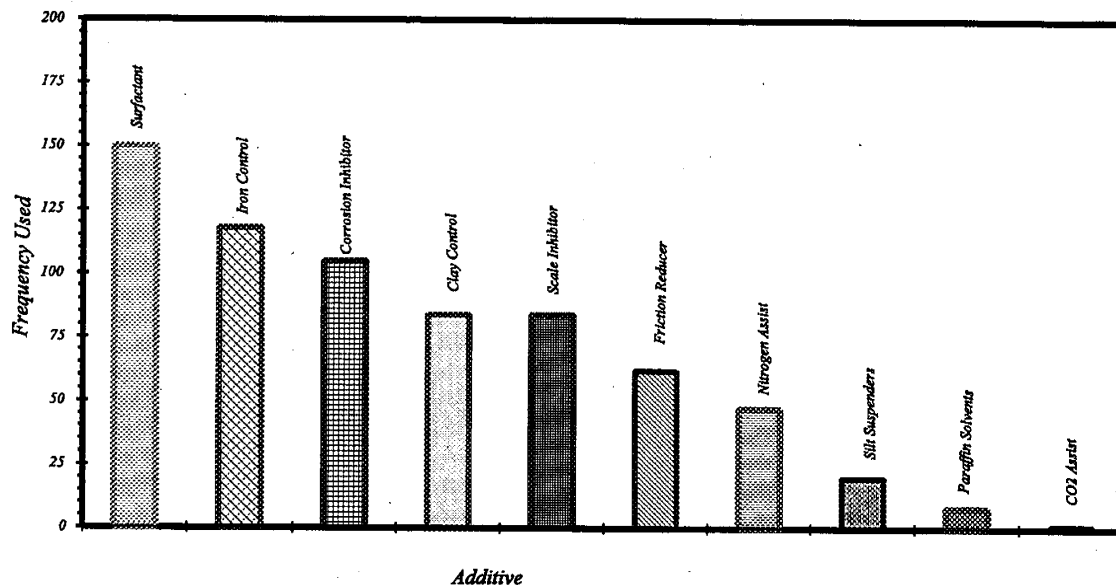


Figure 8.2. Frequency of additives used in treatments.

Not all the additive types were used in all treatments, but it is surprising that certain additives were not used on all of the treatments. For instance, corrosion inhibitor is one chemical additive which one would expect to find in all the acid treatments. The primary purpose of corrosion inhibitor is to protect tubular goods and surface equipment from being damaged by acid. Without this additive it is quite possible to damage some tubing or casing in the wellbore, yet this additive was only used in 105 treatments.

Surfactants are commonly found in most acid systems, but again only 150 of the treatments had any mention of some type of surfactant being used. The primary use of surfactants is to reduce the surface tension of a liquid to allow it to flow easier and prevent emulsions from forming. They also are used to change the wettability of a formation. The type of surfactants available to the industry has increased over the years, but in some cases the same surfactant package that was used in 1968 is still being used today. However, the data shows the surfactant had little to no effect on post-treatment production. Generally this additive should be left out unless other types and concentrations of surfactant prove to perform better in the future.

Iron control is the second most commonly used additive (used in 118 treatments). Formation damage due to iron precipitation has been recognized as a significant problem in wellbores for over 30 years, yet is often ignored. Pyrite, a source of iron in the formation, was identified in several core samples taken from wells in the Bluebell field. However, the most common source of iron is the tubulars in the wellbore.

The wellbore tubulars are a constant source of iron yet operators apparently never take the prudent action of pickling tubulars prior to acidizing. Millscale on new pipe also contains a large amount of iron. One study on millscale which was conducted in new 2-7/8-inch-(7-cm)-diameter, 6.5 lb/ft (9.7 kg/m) tubing indicated that a minimum of 690 gallons (2,610 L) of 15 percent HCl acid could react with millscale in 10,000 feet (3,048.0 m) of tubing. If the iron stayed in solution, the acid would contain 81,360 parts per million (ppm) of total iron. The iron that is present in wellbore tubulars typically is just common rust, but this can severely damage the formation when mobilized during an acid treatment. Ignoring this problem while conducting repeated treatments could damage a formation beyond repair.

The purpose of scale inhibitors is to prevent or slow, the process of mineral scale build up. Scale inhibitors were used in 84 of the treatments studied. Scale inhibitors should be used in any wellbore where scaling is a known problem. There are a large number of scale inhibitors, varying by type and activity level, on the market today. Typically the activity level will vary from 15 to 30 percent depending on the type of scale inhibitor.

Clay control additives were used in 84 of the treatments studied. Clay control additives in proper concentration, can prevent swelling and/or migration of clay particles. The most common clays in the Green River Formation are illite-smectite and chlorite-smectite mixed-layered clays and a minor amount of kaolinite (Wegner and Morris, this volume). Therefore, use of a good clay control additive is recommended when treating the Green River Formation.

Friction reducers are used to reduce the friction pressure loss caused by pumping down small tubulars at high rates. Friction reducers can help maintain the desired pump rate to treat the formation or reduce the number of high pressure pumps needed. Two hundred thirty-four treatments studied pumped down 2-7/8-inch-(7-cm)-diameter tubing; the average depth of the tubing is 10,812 feet (3,295.5 m). Figure 8.3 illustrates friction pressure per 1,000 feet (304.8 m) for various fluid types pumped at various rates. The rates which were pumped down 2-7/8-inch-(7-cm)-diameter tubing varied from 0.3 barrel per minute (BPM) to 19.5 BPM (0.04-2.73 MTM). The overall average pump rate down 2-7/8-inch-(7-cm)-diameter tubing was 9.2 BPM (1.29 MTM). It is quite apparent that to obtain rates much over 8 BPM (1.12 MTM) it is necessary to use some type of friction reducer.

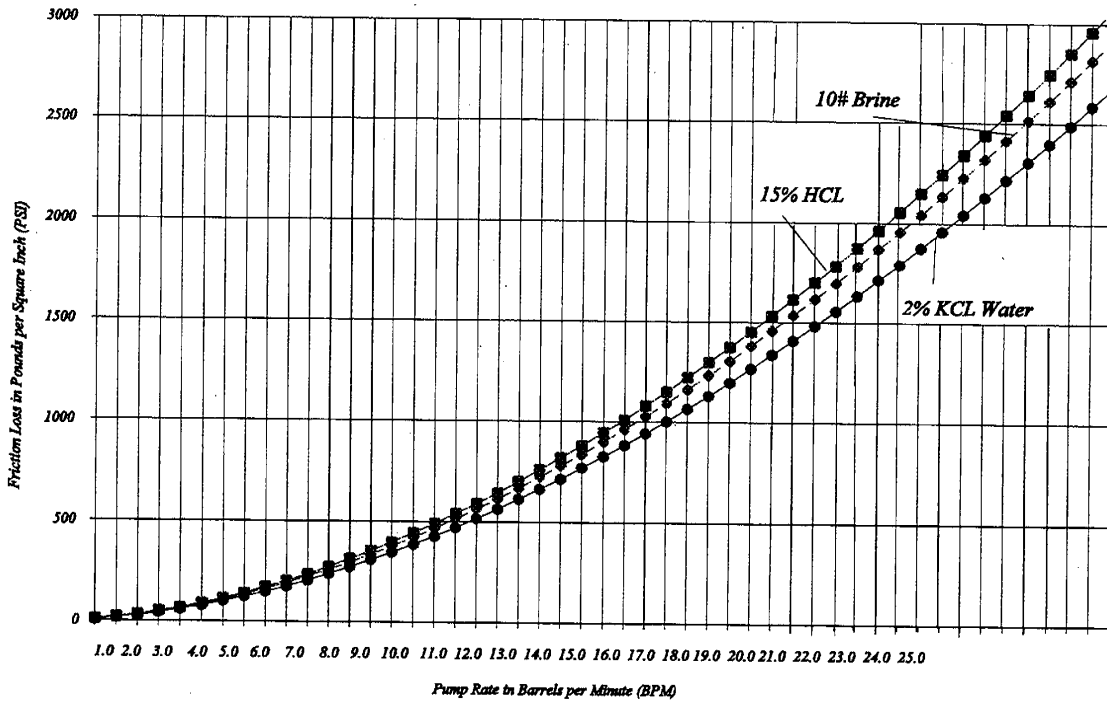


Figure 8.3. Friction pressure loss per 1,000 feet (305 m) of 2-7/8 inch (7 cm) diameter tubing for HCl, brine, and KCl water.

Figure 8.4 illustrates the significant effect in which friction pressure loss can be reduced in the treating fluids to decrease well-head-treating pressure (WHTP). This will lower the hydraulic horse power (HHP) needed for increased pump rates. Although friction reducers do not enhance the acid system, they do affect the placement of the treatment. If acid is pumped at 9 BPM (1.26 MTM) and no friction reducer is used in the acid, the friction pressure loss alone for the average depth of 2-7/8-inch-(7-cm)-diameter tubing would be equal to 5,400 psi (379 kg/cm<sup>2</sup>). If the acid contained a gelling agent friction reducer, the friction pressure loss for the same string of tubing would only be 1,520 psi (107 kg/cm<sup>2</sup>). By using a gelled acid instead of a non-gelled acid the WHTP would be reduced by 3,880 psi (273 kg/cm<sup>2</sup>) at 9 BPM (1.26 MTM) and the HHP requirement would also be reduced by 856.

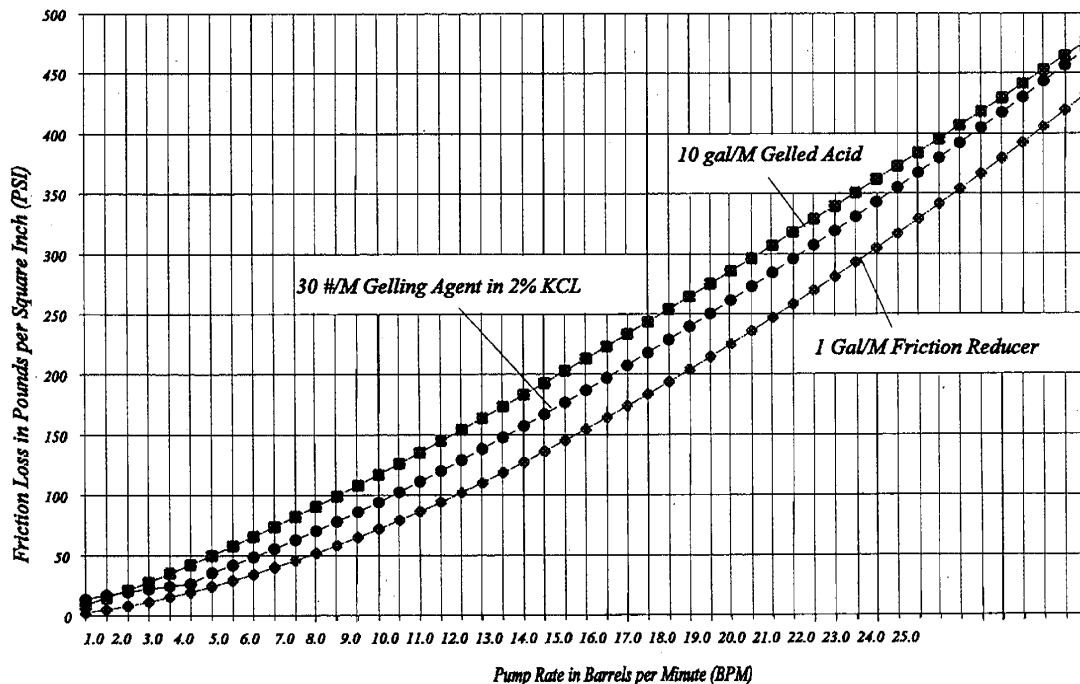


Figure 8.4. Friction pressure loss per 1,000 feet (305 m) of 2-7/8 inch (7 cm) diameter tubing for gelled acid, gelled KCl solution, and acid with friction reducer.

Silt suspenders and foaming agents were used in 20 of the treatments studied. In some cases the foaming agent appeared in the surfactant category because this additive fits both categories. This type of additive is typically used if a foamed fluid is desired or if removal of fines is a problem. For instance, if a sandstone is held together by calcium carbonate cement, then the acid will remove the cement and the rock basically falls apart leaving behind fines that will plug pore throats. If plugging of pore throats by fines is a problem, then either this type of additive should be used or the acid should contain a gelling agent that will maintain a high enough viscosity to carry fines out of the formation during cleanup.

Nitrogen ( $N_2$ ) and carbon dioxide ( $CO_2$ ) are not chemical additives, but are common gases used in the treatments. The use of a gas in a treatment does several things: (1) enhances cleanup, (2) increases the volume of the treatment, and (3) in the case of  $N_2$  decreases the hydrostatic pressure during the treatment. There were 47 treatments reported to have used  $N_2$  and only one treatment used  $CO_2$ . Of the treatments analyzed, the first use of nitrogen was in 1975, the last was in 1992. The only well which had  $CO_2$  in the treatment was pumped in 1989. Gas-assisted treatments took place in 20 percent of the treatments analyzed. One of the advantages of using a gas assist is that well clean up is faster and sometimes more thorough. A foaming agent is often used in gas-assist treatments resulting in a foamed fluid which helps in removing fines generated from the acid treatment. One of the disadvantages of using a gas is that it is compressible, making it difficult to determine what type of

diverter action is taking place. Gas-assist treatments did not result in a significantly better well response compared to the typical acid treatment.

Paraffin buildup is a problem in the Bluebell field and throughout the Uinta Basin. Yet only eight treatments used some type of solvent or paraffin control in the acid system. When solvents were used, the volumes were so small (100 to 1,000 gallons [375-3,785 L]) that they were probably not effective. When a solvent was used it was spear headed in front of all the other fluids and probably only affected one interval, if there was any active ingredients left by the time it reached the perforations.

Acid can only react with a material if it contacts it. Scale is a problem throughout the Bluebell field and is typically layered (scale then paraffin or paraffin then scale similar to rings found in a tree trunk). When an acid, without some type of solvent, comes in contact with layered-scale the chances of reacting with more than one layer of scale is questionable. An acid containing a solvent will remove layers of both scale and paraffin.

Treatment fluids are usually heated prior to being pumped down the hole. This is a good practice and should be continued. Heating the fluids helps prevent paraffin from solidifying and plugging the porosity in the formation. However, only the water phase of the acid is heated and the heat loss when cooler acid is added to the water can be quite substantial. The temperature of the acid solution is typically high enough to prevent solidifying paraffin, but may not be high enough to dissolve paraffin layers in the scaling.

### **8.3.2 Diverters**

Good diversion (diverting the treatment fluid into all of the perforations) is needed when attempting to treat large intervals. There have been several types of diverters used in the treatments studied (figure 8.5). The most often used diverter are 7/8 inch (2 cm) diameter, RCN ball sealers with a specific gravity (SG) of 1.1 or 1.3 except in older treatments where 1.4 SG balls were used. The number of balls pumped ranged from 7 to 3,000 for a single treatment. The amount of excess ((number of holes/number of ball sealers) \* 100 percent) ranged from 13 to 389 percent for an average of 160 percent. Ball sealers provide excellent diversion if given enough fluid and high enough flow rate to allow the balls to seat in the perforations. Typically, the balls are slugged or given such a small fluid volume it is difficult to get a good seal. Balls were run in both the acid system and spacers as the diverter fluid. Perforations must also be in fairly good shape for balls to seal properly; if there is severe corrosion or pipe deterioration the efficiency of the ball sealer will decrease. A minimum of 50 gallons (190 L) of fluid should be used per ball sealer whether the ball sealer is placed in the acid or the spacer fluid. A minimum pump rate of 5 to 8 BPM (795-1,272 LPM) should provide adequate velocity to seat the ball; fluid viscosity can also help with ball action. If at all possible the SG of the balls should be as close to or equal to the fluid density of the fluid in which the ball sealer is placed in. This will increase the seating efficiency of the ball sealer.

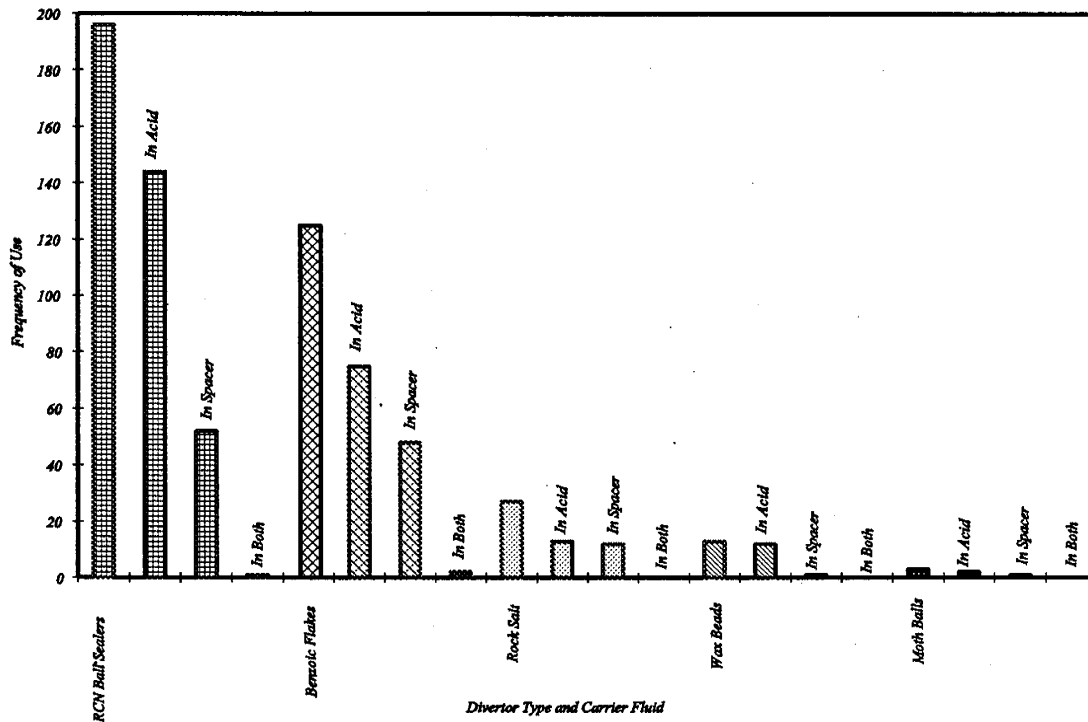


Figure 8.5. Number of times used and type of carrier fluid for each type of diverter.

Benzoic acid flakes are the second most commonly used diverting agent in the treatments studied. The advantages of benzoic acid flakes are: (1) they are soluble in water, acid, and oil, and (2) they will also sublime in gas wells. Some of the disadvantages are: (1) they do not form as strong a bridge as other diverting material, (2) they cost more than other diverting materials, (3) they will not bridge a 3/8 inch (1 cm) diameter perforation or slot having a width greater than 0.13 inches (0.3 cm), (4) the material will not dissolve without adequate fluid flow, and (5) high concentrations of acid flakes can also cause erratic pump rates because they have a tendency to settle out underneath pump valves. Concentrations in the treatments studied range from 0.25 to 10 lb/gal (0.03-1.19 kg/L). There were several reports of this material being pumped at a concentration higher than 2 lb/gal (0.24 kg/L), but those reports are questionable. Most treatments have concentrations from 0.1 to 1 lb/gal (0.01-0.12 kg/L) with the majority of the treatments having a concentration of 0.25 to 0.5 lb/gal (0.03-0.06 kg/L). Total volume of flakes used in a treatment ranged from 200 to 20,000 lb (90.7-9,072.0 kg). The fluids used to carry the benzoic acid flakes were acid or a spacer fluid. Recommended concentrations are from 0.5 to 2 lb/gal (0.06-0.24 kg/L) in the carrier fluid.

Salt is the third most commonly used diverting agent in the treatments studied. Salt used for diversion comes in two forms: (1) rock salt which is very coarse in size from 2/8 to 8/12 mesh, and (2) graded salt which range in size from 0.003 to 0.25 inch (0.01-0.64 cm). Laboratory tests indicate that the graded salt forms a more effective bridging material than the coarser graded salt. However, both are effective in forming

temporary seals. Advantages of salt are: (1) low cost, compared to almost all water-based gelled carrier fluids, (2) readily soluble in aqueous fluids, and (3) can be used in both oil and gas wells that have some water production. The disadvantages of salt are: (1) it is not compatible with HF acid, (2) it must be used in high concentration due to its solubility in water, (3) it will not degrade in oil, and (4) it is not recommended for use at temperatures above 180° F (82.3° C), due to its solubility in water. The range of concentration of salt used was from 1/4 to 10 lb/gal (0.03-1.19 kg/L) with an overall average of 4 lb/gal (0.48 kg/L). Recommended concentrations of salt range from 1 to 5 lb/gal (0.12-0.59 kg/L) depending on brine concentration of the fluid. Laboratory test indicate that graded salt will bridge on a 3/8-inch-(1-cm)-diameter perforation or a slot having a width of 0.32 inches (0.8 cm). The carrier fluid should be a high concentration of brine, preferable saturated brine water, if not the salt will go into solution. Gelling the carrier fluid will help suspend the salt particles and carry them through perforations to bridge on fractures.

Wax beads were used in 14 of the treatments studied. The advantages of wax beads are: (1) they are soluble in oil but not in water, (2) they can be used in temperatures from 80° to 185° F (26.7-84.9° C), (the melting point of wax beads depends on the type of bead used), and (3) wax beads can be used in both oil and gas wells that produce condensate. The disadvantages of wax beads are: (1) their low melting point can lead to agglomeration problems, and (2) they should not be used in wells which produce no liquid hydrocarbons. Concentrations were not reported but total volumes range from 400 to 20,000 lb (181.4-9,072.0 kg). Particle sizes ranged from 0.07 to 0.23 inches (0.2-0.6 cm) depending on the type of wax bead used. The fluids used as carriers in the treatments studied were both acid and spacer, but most were pumped in acid. Recommended concentrations are 0.5 to 2 lb/gal (0.06-0.24 kg/L) in a gelled carrier fluid.

Moth balls are another diverter used in the treatments studied. The advantages of moth balls are: (1) they are soluble in oil and condensate, (2) they will bridge on a 3/8-inch-(1-cm)-diameter perforation or a slot which is up to 0.24 inches (0.6 cm) in width, (3) they can support a differential pressure up to 1,000 psi (6,900 kPa), (4) they can be used in fluids up to 176° F (79.9° C) (their melting point), (5) they are compatible with most water-based fluids, and (6) they help reduce paraffin buildup. The disadvantages of moth balls are: (1) they should be pumped in a viscous gelled fluid due to their high density, and (2) they should not be used in disposal or injection wells. Graded particle sizes ranged from 0.002 to 0.25 inches (0.01-0.6 cm). Recommended concentrations are 1/2 to 2 lb/gal (0.06-0.24 kg/L) in a gelled carrier fluid.

Spacers are another type of fluid that was commonly used to carry diverting agents. The most commonly used fluids for spacing are: (1) water-based fluid, commonly brine when rock salt was used, (2) formation water, and (3) 2 percent potassium-chloride (KCL) water. The advantage of spacers is it is an excellent way to carry a diverting agent when large quantities of diverters are to be run. The disadvantage is that formation water should be avoided as a carrier or a displacement fluid because of its high content of bicarbonates which react with the acid. The reaction generates CO<sub>2</sub> which can gas lock the centrifugal pump that feeds the high pressure pumps. This results in erratic pump rates and in some cases affects the placement of the treatment.

More than one type of diverter was commonly used in the treatments studied. It is common to find at least two and in some treatments, as many as three different types of diverter being used. Diverter action varied from excellent to none (figure 8.6).

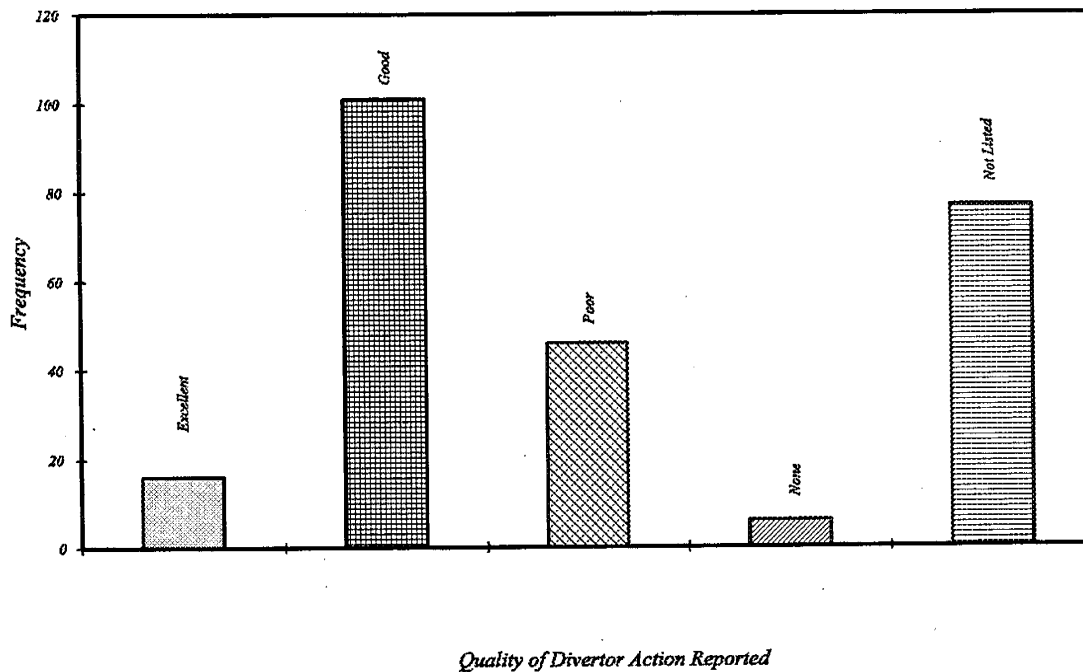


Figure 8.6. Frequency of diverter action by quality of action.

### 8.3.3 Fracture Gradient

Fracture gradients (pressure gradient needed to fracture the rock) are calculated from the instant shut-in pressure (ISIP) which is recorded immediately after pumping has stopped. The ISIP is then used to determine the bottom-hole treating pressure (BHTP). The frac gradients in the treatments studied range from less than 0.44 to 1.24 psi/ft (101-285 g/cm<sup>2</sup>/m) with an average of 0.76 psi/ft (175 g/cm<sup>2</sup>/m) (figure 8.7). The BHTP needed to treat the bottom perforation can range from less than 5,520 to 15,550 psi (388-1,093 kg/cm<sup>2</sup>) with an average of 9,530 psi (670 kg/cm<sup>2</sup>). This is a wide variation in fracture gradients, resulting in a wide range of anticipated well-head treating pressures (WHTP). In order to overcome the average frac gradient it will take an WHTP of 3,940 psi (277 kg/cm<sup>2</sup>), ignoring friction. If the treatment fluid is gelled acid being pumped down a typical string of 2-7/8-inch-(7-cm)-diameter tubing, the WHTP would be approximately 5,460 psi (384 kg/cm<sup>2</sup>) at 9 BPM (1,431 LPM). Without a good friction reducer the WHTP would be approximately 9,260 psi (651 kg/cm<sup>2</sup>) at 9 BPM (1,431 LPM) but the BHTP would be the same in both cases.

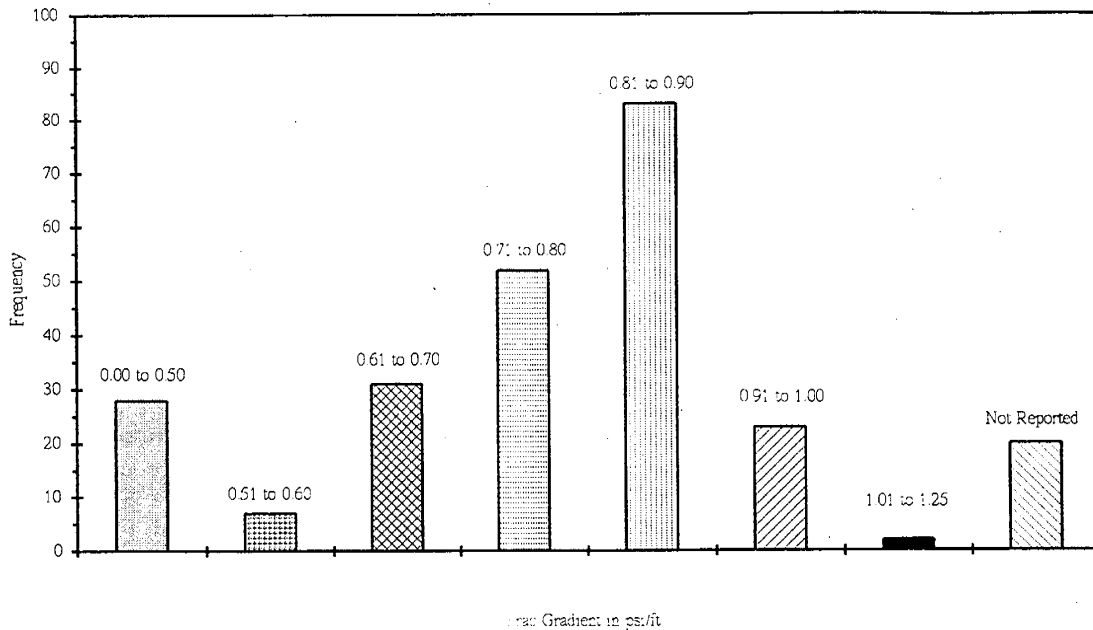


Figure 8.7. Frequency of various fracture gradients.

#### 8.4 Correlations

No clear correlations could be made between hydrocarbon production and type and size of treatment. However, it appears that the acid treatments are under stimulating the wells as shown by the limited amount of time the wells are in linear flow. Surprisingly, no correlation could be made between the amount of acid pumped and the size of the interval being treated. Moderate-sized acid treatments appear to be as economical as large acid treatments. This appears to be independent of the interval being treated. Most wells in the study area have been treated more than once. One well had as many as 11 treatments. Typically, the first and second treatment yielded the best results, the third and fourth treatment did not appear to be as effective, but were also typically smaller in size (see the decline curves in figure 8.8). The first and second treatments appear to be fairly effective for up to four to five months. Why the later treatments in the same interval are not as effective is not known at this time. This could indicate damage to the formation is not being removed, or that the beds are depleted. The volume of the treatment does not appear to be a major factor. Treatments which ranged from 20,000 to 30,000 gallons (75,700-113,600 L) seem to be slightly more effective but apparently, the most critical acid treatment is the first one. If additional acid treatments are to be pumped they should be about the same size as the first treatment.

Higher pump rates and well-head treating pressure appeared to make better wells also. The higher pressures could be an indication of good diversion taking place allowing more of the treatment to go into more of the formation, caused by the higher

pump rates. However, higher pump rates that just increase the WHTP are not necessary. Pump rates from 8 to 12 BPM (1.12-1.68 MTM) are adequate to carry diverters, and maintain a reasonable WHTP.

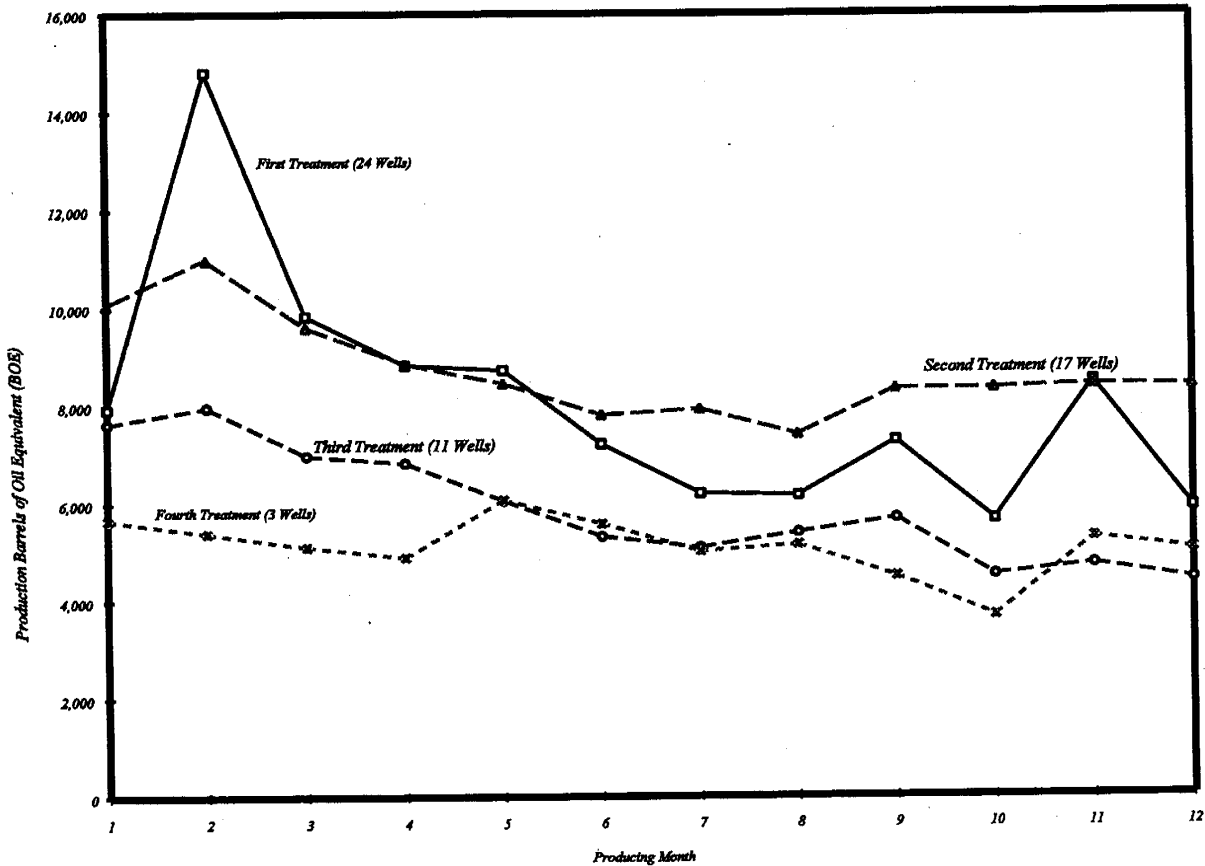


Figure 8.8. Average decline curves by consecutive treatments.

### 8.5 Drilling-Mud Loss

The mud lost during drilling operations can affect how the well produces. An attempt was made to document the amount of drilling mud which was lost while drilling the well. Lost mud is not always well documented and was only reported for eight of the wells studied. The amount that was lost ranged from 50 to 4,040 barrels (7,949-642,239 L). Drilling mud lost into a producing bed can cause severe plugging problems. If the amount of mud lost and where it was lost is known, it could explain why production from some beds declines so rapidly. Wells which were drilled into the deeper Wasatch Formation during the early 1970s needed 15.0 to 15.5 lb/gals (1.79-1.86 kg/L) to drill to total depth. The mud weight which is needed to drill the deeper Wasatch Formation today in some parts of the field has decreased to as low as 10 lb/gal (1.19 kg/L), possibly indicating that parts of the field are pressure depleted. If mud damage is known to be present, a treatment or procedure can be designed to overcome the formation damage caused by the lost mud.

## 8.6 Conclusions and Recommendations

Regardless of what type of stimulation is tried, who tries it, or what it cost, better bed evaluation is critical to increasing production from the Bluebell field. The interval to be treated could be reduced either by isolating smaller intervals: (1) with a bridge plug and packer, (2) use of a Pin Point Injection packer (PPI tool), or (3) use of a packer and the natural pressure gradient which is present within the formation to isolate zones. Large perforated intervals are extremely difficult to treat down 2-7/8-inch-(7-cm)-diameter tubing. Good diversion is critical to treating the entire interval and a high enough pump rate must be maintained to carry the diverting agent. A pump rate between 8 to 12 BPM (1.12-1.68 MTM) with proper gelling agents in the fluid will divert the fluid to the perforated intervals. By holding a constant rate and allowing the diverter to do its job, the WHTP should increase and break back as the diverter works. Maximum pressure should be reached toward the end of the treatment if enough diverter is pumped and pumped properly.

At ultra-high pump rates treating an 800- to 1,000-foot (243.8-304.8 m) interval is realistic. One way to obtain ultra-high pump rates in new wells is to pull the tubing out of the hole and pump down the casing. By pumping down the casing, WHTP pressure would be approximately 5,000 psi (351 kg/cm<sup>2</sup>) at pump rates up to 100 BPM (15,900 LPM). Ultra-high pump rates may not be an option in older wells due to bad casing, inadequate cement, or a combination of both. Increasing pump rates down 2-7/8-inch-(7-cm)-diameter tubing will only increase the WHTP not the BHTP. Changing out the 2-7/8- to 3-1/2-inch-(7-9-cm)-diameter tubing to increase pump rates may not be cost effective. There will be a rate increase with the larger diameter pipe, but friction is still a significant problem. When treating down the tubing, an adequate pump rate must be maintained and the pressure allowed to increase on its own due to the diversion and sealing of perforations. It is critical that there is enough diverter and sufficient fluid pumped to carry it, to treat all of the perforated beds in the interval.

Hydrochloric acid has been and still is, the recommended treating fluid. The following list of additives would be advisable to be run per 1,000 gallons (3,800 L) of 15 percent HCl:

- (1) 5 to 10 gal (19-38 L) corrosion inhibitor (temperature dependent).
- (2) 3 to 10 gal (11-38 L) surfactant (concentration will vary depending on compatibility of surfactant with the produced oil).
- (3) 3 to 7 gal (11-26 L) clay control (concentration will vary depending type of clay control additive that is used).
- (4) 10 gal (28 L) iron control (minimum).
- (5) 10 gal (28 L) acid gelling agent.
- (6) 10 gal (28 L) solvent (minimum).
- (7) 10 gal (28 L) scale inhibitor.

Also, the tubing should be pickled and reversed out just prior to doing the main acid treatment. This may involve more cost but will minimize formation damage from iron dissolved from the tubulars. A rule of thumb for pickling tubulars is 100 gallons (375 L) of HCl for every 1,000 feet (304.8 m) of tubing. The treating fluid should be recovered as quickly as possible, not allowing it to sit in the formation; this will help prevent fines and other solids from dropping out in the formation. The initial acid treatment is generally the largest and appears to be the most effective. If additional acid treatments are pumped it is advisable to pump volumes similar, or smaller, than

the initial acid treatment. The most cost effective acid treatment appears to be between 20,000 and 30,000 gallons (75,700 and 113,600 L) of 15 percent HCl pumped in four acid stages. This would mean pumping three diverter stages with enough volume to divert the fluid from one zone to another. The diverter fluid should be gelled so that the friction characteristics are similar to that of the acid. The diverter fluid should be compatible with the diverter material, and contain the same surfactants and clay control additives that are used in the acid system. If ball sealers are used, a minimum of 50 percent excess will give proper diversion if the fluid volume and pump rate is appropriate, and the perforations are in good shape.

Even successful acid treatments do not maintain adequate linear flow indicating under stimulation of the producing formation. Operators generally believe that past performance shows that proppant fracture treatments don't work in the Bluebell field. There have been over 300 wells drilled in the Bluebell field. The treatment database is comprised of only 67 wells representing 246 stimulation treatments, yet only 2 percent of the treatments were proppant fracture treatments indicating that hydraulic fracturing with proppant has not been adequately tested, mainly because of the cost. The treatments studied which were hydraulically fractured with a proppant, only used a small volume of sand as the propping agent. The ability to do high-rate proppant fracs over large intervals has been proven in other fields and can be done in the Bluebell field. Many older wells may not be suitable for this treatment, but newer wells should be considered as likely candidates for high-rate proppant fracture treatments.

## 9. FACTORS AFFECTING THE FORMATION AND RATE OF CALCIUM CARBONATE SCALING

*J. Wallace Gwynn*  
Utah Geological Survey

### 9.1 Introduction

Calcium carbonate scaling is an oil production related problem within the Bluebell oil field, Uintah and Duchesne Counties, Utah. Excessive scaling results in reduced production rates, equipment failure, costly down time, and increased production costs. Calcium carbonate ( $\text{CaCO}_3$ ) is the most common and abundant scale type; other scale types include iron sulfide (FeS), acid insolubles, and paraffin.

Waters with high percentages of calcium and bicarbonate, high pH, low carbon dioxide ( $\text{CO}_2$ ) partial pressure, high salinity, and high temperatures favor the formation of  $\text{CaCO}_3$  scale. The production of Green River Formation water with Wasatch Formation water increases the amount of scale that forms, over that which is produced from Wasatch Formation water alone. Scale inhibitors such as phosphonates are commonly used. Other potential scale-mitigating measures include the maintenance of high hydrostatic and  $\text{CO}_2$  partial pressures, maintenance of low pH in power-water supplies through the addition of small amounts of hydrochloric or acetic acid, and maintenance of the lowest possible operating temperatures.

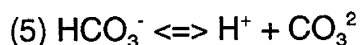
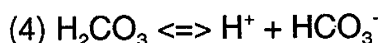
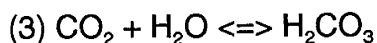
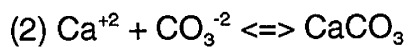
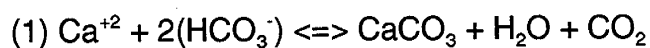
The purpose of this study is to gain a better understanding of the physical and chemical variables which cause and can be used to control  $\text{CaCO}_3$  scaling. This report will review: (1) the types of scale that are found, (2) the basic chemistry of  $\text{CaCO}_3$  scale formation, (3) the water chemistry that is found in the vicinity of the Michelle Ute demonstration well, (4) methods of predicting scale formation, (5) quantity and rate of scale production, (6) factors which affect the tendency for scale formation, and (7) the effect of mixing Wasatch and Green River Formation waters on scaling. Potential scale-mitigating methods, beyond the use of scale inhibitors, will also be discussed.

### 9.2 Scale Types

In the vicinity of the Michelle Ute well (NE1/4SW1/4 section 7, T.1 S., R.1 E., Uinta Base Line),  $\text{CaCO}_3$  is reported as the dominant, inorganic scale type that is precipitated in oil/water/gas-producing wells and related subsurface and surface production equipment. Other types of scale reported by operators and service company personnel include minor FeS, acid insolubles (including sand, silt, or clay), and paraffin. Calcium-, barium-, and strontium-sulfate scale types are not reported.

### 9.3 Basic Chemistry of Calcium Carbonate Scaling

Strickland (1981) states that the precipitation of  $\text{CaCO}_3$  results from the reactions between calcium ions ( $\text{Ca}^{+2}$ ) and bicarbonate ions ( $\text{HCO}_3^-$ ) or carbonate ions ( $\text{CO}_3^{-2}$ ); or indirectly from  $\text{CO}_2$  that dissolves in water and ultimately ionizes to carbonate ions ( $\text{CO}_3^{-2}$ ). The following five chemical equations show the possible reactions:



#### 9.4 Water Chemistry in the Vicinity of the Michelle Ute Well

Forty-four chemical analyses of waters from wells within the vicinity of the Bluebell field were provided for this study by various producers. The well name, location, chemical analyses, and source of the data are shown in table 9.1. Figure 9.1 shows a trilinear plot of the water chemistries. From these data it can be seen that the brines are high in sodium chloride, with lesser but varying amounts of bicarbonate, sulfate, calcium, and magnesium. The circled, tightly clustered group of points marked "M" on the anion triangular plot, represent waters from wells in close proximity to the Michelle Ute well.

In the immediate vicinity of the Michelle Ute well (T.1 S., R. 1 E. and R.1 W.), most of the waters are found to be very similar in their chemical makeup, each containing greater than 85 percent sodium chloride (on a dry-weight basis). A listing of the 18 similar-chemistry waters ("M" grouping on figure 9.1) is given in table 9.2. Figure 9.2 is a trilinear plot of these 18 water chemistries.

Because of the variability in the water chemistries that is found, even within the 18 similar-chemistry samples, it is difficult to select one or even two or three samples which are representative. For the purposes of this report, the average of these 18 samples will be used to represent the oil-field waters in the vicinity of the Michelle Ute well. The average values are shown in table 9.3.

#### 9.5 Methods of Predicting Scale Formation

Tomson and Oddo (unpublished report) state that numerous methods have been developed to predict  $\text{CaCO}_3$  scale formation by calculating a saturation or stability index (SI) for a given water. Most of these methods compare the saturation state of a solution, with respect to  $\text{CaCO}_3$ , to the solubility of  $\text{CaCO}_3$  in that solution under similar conditions. Three such widely accepted methods include: (1) the Langelier Saturation Index (LSI), (2) the Stiff-Davis Stability Index (SSI), and (3) the Ryznar Stability Index (RSI). In addition, many oil-well service companies develop their own service-oriented SI determinant methods. There are also a number of SI-determinant software programs which have been developed by private research organizations, the Illinois State Water Survey, the U. S. Geological Survey, and the U. S. Environmental Protection Agency. The calculation of SI in most of these programs is based on relative saturation, with some using alkalinity-based pH, and bicarbonate-based pH.

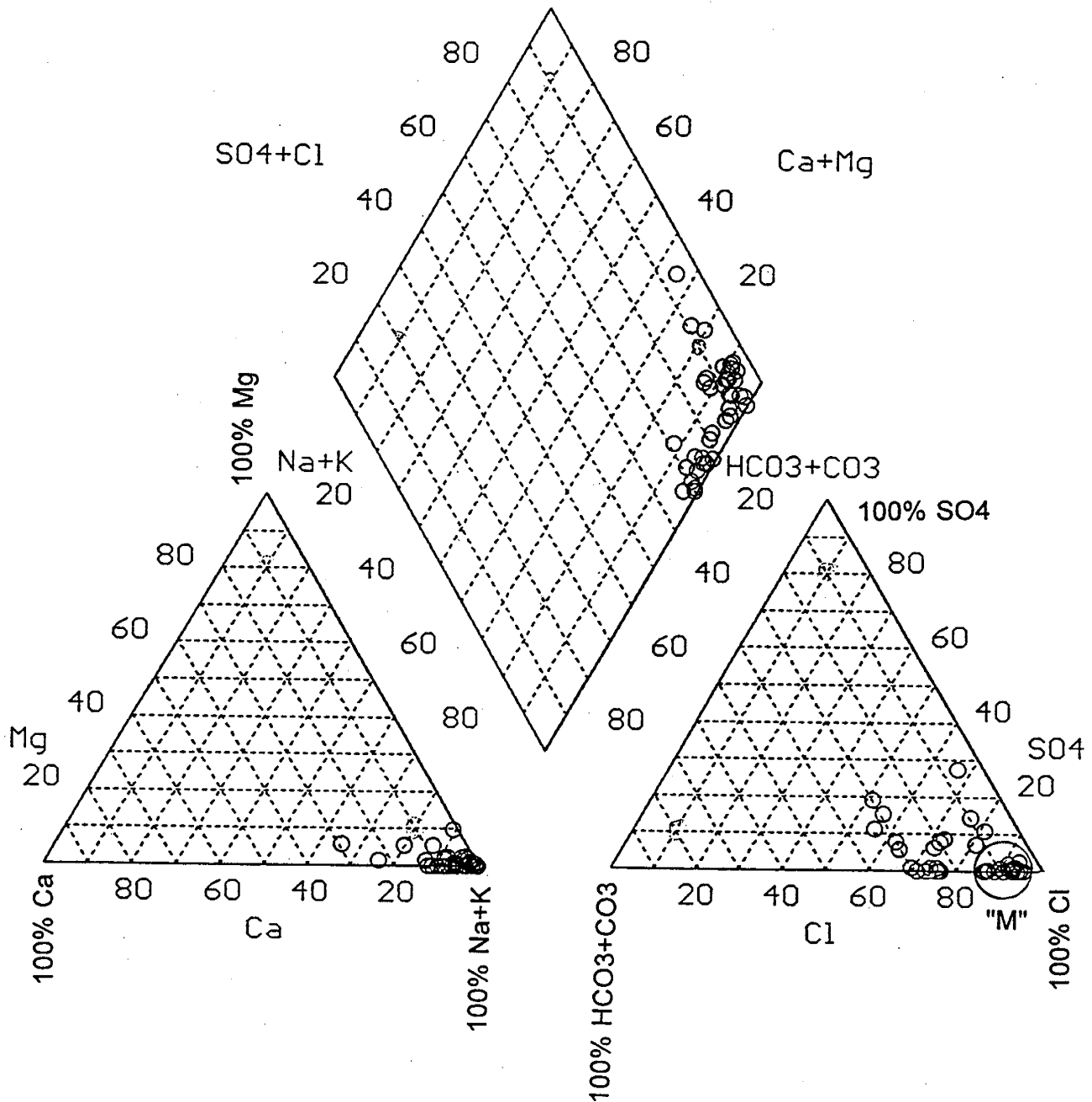


Figure 9.1. Trilinear diagram showing the chemical composition of 44 waters in the general vicinity of the Michelle Ute well. The circular cluster of points labeled "M" represent similar waters in the immediate vicinity of the Michelle Ute well.

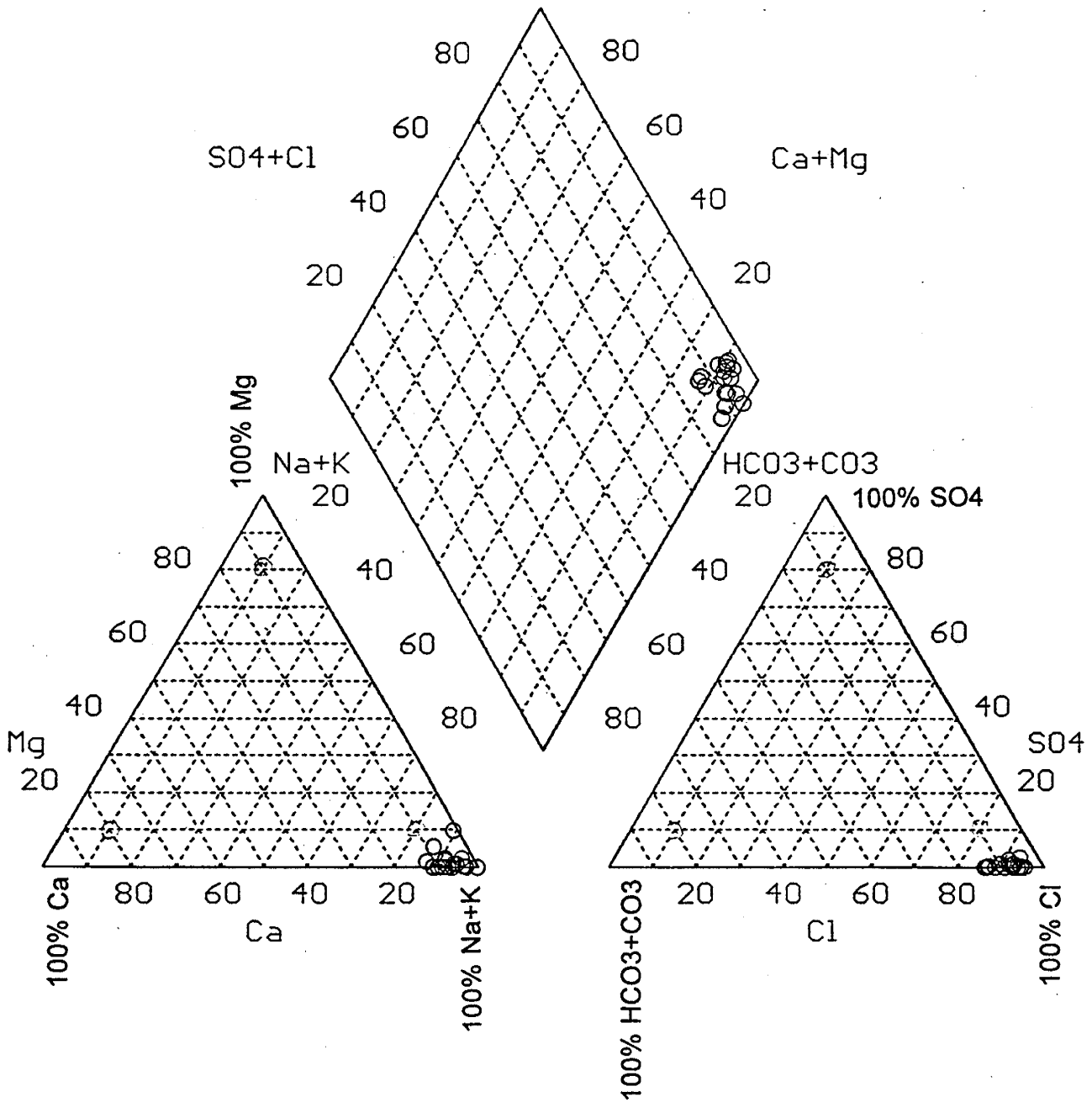


Figure 9.2. Trilinear diagram showing the chemical composition of 18 waters in the immediate vicinity of the Michelle Ute well. These waters represent the similar waters circled and labeled as "M" on figure 9.2.

Table 9.1. Oil-well water chemistry of 44 waters in the general vicinity of the Michelle Ute well.

WELL NAME	WELL ID	SEC	TOWN	RANG.	Na	K	Mg	Ca	Cl	SO <sub>4</sub>	HCO <sub>3</sub>	IDS	pH	ASG	C-SG	H <sub>2</sub> S	Fe	DATA SOURCE
WILKERSON 1-20Z1	30942	20	1N	1W	2489	0	85	200	4000	10	1000	7845	7.8	1.003	1.0056	0	17	COASTAL
WILKERSON 1-20Z1	30942A	20	1N	1W	3292	0	97	1440	7800	0	100	12729	5.5	1.002	1.0105	1.5	200	COASTAL
MOON 1-23Z1	31479	23	1N	1W	18335	0	0	8000	42000	0	900	69235	5.2	1.053	1.049	0	190	COASTAL
OBERSHANSLY 2-31Z1	30970	31	1N	1W	3101	0	31	208	5000	60	610	9010	7.6	1.001	1.0075	0.5	4.2	COASTAL
MICHELLE 7-1	31390	07	1S	1E	5179	0	2	12	7400	100	950	13643	8.6	1.001	1.011	1	0.5	QUINEX
WALKER UTE 1-8A1E	30173	08	1S	1E	5169	0	10	64	5400	3015	839	14498	7.5	1.005	1.0118	0	1	COASTAL
WALKER 1-14A1E	30805	14	1S	1E	5834	0	0	440	8900	80	1260	16514	8.3	1.007	1.0133	1.5	1.1	FLYING J
UTE 1-15A1E	30820	15	1S	1E	4471	0	0	480	7080	200	960	13191	8.0	1.005	1.0108	0	6.2	FLYING J
MALNAR PIKE	31714	17	1S	1E	2003	0	0	240	2500	0	1750	6495	8.1	1.005	1.0056	2	1	QUINEX
UTE 1-17A1E	30829	17	1S	1E	4839	0	0	220	7080	0	900	13036	8.0	1.005	1.0106	1.5	9	FLYING J
D.R. LONG 2-19A1E	31470	19	1S	1E	4812	0	0	400	7790	0	750	13752	7.4	1.001	1.0113	12	0.6	FLYING J
ROOSEVELT A-7	31402	19	1S	1E	4500	64	17	120	5700	11	978	12454	7.9	1.000	1.0102	0	0	STATE LAB
BOLTON 2-29A1E	31112	29	1S	1E	2020	0	0	64	1770	480	1810	6144	8.0	1.001	1.0053	35	1.2	FLYING J
UTE 1-29A1E	30937	29	1S	1E	2185	0	0	128	2800	720	610	6474	8.3	1.002	1.0056	3	1.4	FLYING J
H.D. LANDY 1-30A1E	30790	30	1S	1E	3127	0	0	248	4250	760	720	9125	7.2	1.001	1.0077	5	6	FLYING J
LANDY 2-30A1E	31895	30	1S	1E	2495	0	15	40	2830	0	1800	7180	7.2	1.003	1.0061	1	3.4	FLYING J
NELSON 1-31A1E	30671	31	1S	1E	1937	0	5	96	1770	660	1600	6086	8.2	1.002	1.0053	1.5	1	FLYING J
BASTIAN 1-2A1	31373	2	1S	1W	6459	0	0	600	10500	25	976	18560	8.2	1.015	1.015	0.5	3.5	FLYING J
HORROCKS 2-4A1	30954	4	1S	1W	3747	0	10	16	3000	1500	3000	11273	7.8	1.003	1.0094	0.5	1.6	COASTAL
THE PERFECT 10-1-10A1	30935	10	1S	1W	3290	0	17	173	5106	1	561	9148	7.3	1.005	1.0075	4	0.5	FLYING J
I. BOLTON 1-12A1	31295	12	1S	1W	3724	0	0	218	40	23	1464	11169	7.0	1.005	1.0094	0.5	14	FLYING J
QUINEX-CMS	31711	13	1S	1W	3575	0	0	240	5700	0	450	9965	7.8	1.005	1.008	0.5	3.6	QUINEX
BADGER-SAM H.U. MONGUS	30949	15	1S	1W	2257	0	2	60	3106	2	842	6282	7.9	1.000	1.005	2	0.1	FLYING J
EULA-UTE 1-16A1	30782	16	1S	1W	2897	0	16	130	4255	63	769	8130	7.4	1.000	1.0065	0	0	FLYING J
CHASEL 2-17A1	30732	17	1S	1W	2437	0	24	640	4500	0	800	8401	7.8	1.001	1.0071	0.5	2.3	FLYING J
CHASEL 2-17A1	30732A	17	1S	1W	3708	0	170	1440	8100	120	900	14438	7.8	1.002	1.0118	2	1.1	COASTAL
EJ ASAY FEE 31 (1-20A1)	30102	20	1S	1W	2549	0	19	72	3000	480	1300	7420	8.6	1.001	1.0062	2	1.4	COASTAL
EJ ASAY FEE 31 (1-20A1)	30103A	20	1S	1W	4073	0	36	480	6400	0	1750	12739	8.3	1.002	1.0105	7.5	1	COASTAL
SAM HOUSTON 24-4	31653	24	1S	1W	2597	0	97	420	4950	50	600	8714	8.2	1.002	1.0074	2	1	QUINEX
LILA D. 2-25A1	31797	25	1S	1W	2944	0	14	40	3500	0	1950	8448	8.7	1.008	1.0072	6	1.3	FLYING J
FOWLES 1-27A1	31296	26	1S	1W	2944	0	14	40	3500	0	1950	8448	8.7	1.008	1.0072	2	1.3	FLYING J
BIRCHELL 1-27A1	30758	27	1S	1W	6020	0	0	40	6000	720	4880	17660	8.3	1.005	1.0142	2	0.8	FLYING J
ST LND BRD UTE 1-35A1	30182	35	1S	1W	2650	0	15	40	3400	406	864	7412	7.6	1.005	1.0063	4	37	PENNZOIL
UTE CARSON 2-36A1	31407	36	1S	1W	3882	0	24	56	2500	40	1850	6652	8.9	1.002	1.0057	1.5	1.5	FLYING J
MURRAY 3-2A2	30816	2	1S	2W	1738	0	19	24	2100	0	1150	5131	8.0	1.001	1.0045	0.5	2.2	COASTAL
UTE INDIAN TRIBE 1-14B1	30774	14	2S	1E	4683	0	61	120	7000	0	1200	13125	8.4	1.008	1.0105	1.5	13	COASTAL
UTE TRIBAL 1-18B1E	30969	18	2S	1E	6888	0	0	400	10500	150	1200	19138	8.0	1.009	1.0155	11	1	COASTAL
GALLOWAY 1-18B1	30575	18	2S	1W	2280	0	5	72	3200	0	700	6257	7.9	1.001	1.005	0.5	4.1	COASTAL
UTE 2-6B2	31140	6	2S	2W	2127	0	29	32	2500	360	1180	6228	8.4	1.001	1.0054	0.5	0.3	COASTAL
UTE 2-6B2	31140A	6	2S	2W	2163	0	0	16	2500	300	1300	6279	8.7	1.002	1.0054	2	1.1	COASTAL
UTE 1-06B2	30349	6	2S	2W	1789	0	7	32	1770	300	1450	5348	8.7	1.001	1.0047	1.5	0.9	COASTAL
LINMAR 1-19B2	30600	19	2S	2W	2380	0	0	32	2800	0	1500	6712	8.4	1.001	1.0055	3.5	1	COASTAL
LINMAR 1-19B2	30600A	19	2S	2W	1618	0	0	80	2000	35	1200	5013	8.2	1.002	1.0044	1	1.5	COASTAL
FLY. DIAMOND ROPER 1-14	30217	14	2S	3W	1794	0	7	16	2100	35	1150	5102	8.5	1.001	1.0045	6	0.9	COASTAL

Explanation of column headings (next page)

WELL NAME = name of the well from which water is obtained.  
 WELL ID = the last 5 numerals of the well's API number ("A" designates a second sample from the same well).  
 SEC, TOWN., RANG. = Section, Township, and Range, all are in the Uinta Basse Line Meridian.  
 Na, K, Mg, Ca, Cl, SO<sub>4</sub>, and HCO<sub>3</sub> are major ions reported in mg/l.  
 TDS = sum of the above seven major ions reported in mg/l.  
 pH = pH in standard units.  
 A SG = specific gravity as reported on analytical reports.  
 C SG = specific gravity determined from TDS versus specific gravity graph.  
 H<sub>2</sub>S and Fe = hydrogen sulfide and iron in mg/l.  
 DATA SOURCE = entity supplying the water analysis.

Table 9.2. Oil-well water chemistry of 18 similar waters in the immediate vicinity of the Michelle Ute well.

WELL NAME	WELL ID	SEC	TOWN.	RANG.	N <sub>a</sub>	K	Mg	Ca	Cl	SO <sub>4</sub>	HCO <sub>3</sub>	TDS	ASG	C.SG	I.ALK	pH	H <sub>2</sub> S	Fe	Ba	DATA SOURCE
MICHELLE 7-1	31390	7	1S	1E	5179	0	2	12	7400	100	950	13643	1.001	1.011	950	8.6	1	0.5	0	QUINEX
QUINEX-CMS	31711	13	1S	1W	3575	0	0	240	5700	0	450	9965	1.005	1.008	450	7.8	0.5	3.6	0	QUINEX
THE PERFECT 10 1-10A1	30935	10	1S	1W	3290	0	17	173	5106	1	561	9148	1.005	1.008	561	7.3	4	0.5	0	FLYING J
BADGER-SAM HU MONGUS	30949	15	1S	1W	2257	0	2	60	3106	2	842	6282	1.000	1.005	842	7.9	2	0.1	12	FLYING J
EULA UTE 1-16A1	30782	16	1S	1W	2897	0	16	130	4255	63	769	8130	1.000	1.006	769	7.4	0	0	0	FLYING J
OBERHANSLY 2-31Z1	30970	31	1N	1W	3101	0	31	208	5000	60	610	9010	1.001	1.008	610	7.6	0.5	4.2	0	COASTAL
UTE INDIAN TRIBE 1-14B1	30774	14	2S	1E	4683	0	61	120	7000	10	1000	13125	1.008	1.010	1200	8.4	1.5	13	0	COASTAL
WILKERSON 1-20Z1	30942	20	1N	1W	2489	0	85	200	4000	0	1750	7845	1.003	1.006	1000	7.8	0	17	0	COASTAL
EJ ASAY FEE 31 (1-20A1)	30102A	20	1S	1W	4073	0	36	480	6400	0	1750	12739	1.002	1.010	1750	8.3	7.5	1	0	COASTAL
UTE TRIBAL 1-18B1E	30969	18	2S	1E	6888	0	0	400	10500	150	1200	19138	1.009	1.016	1200	8.0	11	1	0	COASTAL
GALLOWAY 1-18B1	30575	18	2S	1W	2280	0	5	72	3200	0	700	6357	1.001	1.005	700	7.9	0.5	4.1	0	COASTAL
BASTIAN 1-2A1	31373	2	1S	1W	6459	0	0	600	10500	25	976	18560	1.015	1.015	976	8.2	0.5	3.5	0	FLYING J
L BOLTAN 1-12A1	31295	12	1S	1W	3724	0	218	40	5700	23	1464	11169	1.005	1.009	1464	7.0	0.5	14	0	FLYING J
DR LONG 1-19A1E	31470	19	1S	1E	4812	0	0	400	7790	0	750	13752	1.001	1.011	750	7.4	12	0.6	0	FLYING J
WALKER 1-14A1E	30805	14	1S	1E	5834	0	0	440	8900	80	1260	16514	1.007	1.013	1260	8.3	1.5	1.1	0	FLYING J
UTE 1-15A1E	30820	15	1S	1E	4471	0	0	480	7080	200	960	13191	1.005	1.011	960	8.0	0	6.3	0	FLYING J
UTE 1-17A1E	30828	17	1S	1E	4839	0	0	220	7080	0	900	13036	1.005	1.011	900	8.0	1.5	9	0	FLYING J
ROOSEVELT A-7	31402	19	1S	1E	4500	64	17	120	5700	11	978	12454	1.000	1.010	978	7.9	0	0	0	STATE LAB

Explanation of column headings

WELL NAME = name of the well from which water is obtained.  
 WELL ID = the last 5 numerals of the well's API number ("A" designates a duplicate sample from the well).  
 SEC, TOWN., RANG. = Section, Township, and Range, all are in the Uinta Special Meridian.  
 Na, K, Mg, Ca, Cl, SO<sub>4</sub>, and HCO<sub>3</sub> are major ions reported in mg/l.  
 TDS = sum of the above seven major ions reported in mg/l.  
 A SG = specific gravity reported on analytical reports.  
 C SG = specific gravity determined from TDS versus Specific Gravity graph.  
 T.ALK = Total Alkalinity  
 pH = pH in standard units.  
 H<sub>2</sub>S, Fe and Ba = hydrogen sulfide, iron and barium in mg/l.  
 DATA SOURCE = entity supplying the water analysis.

Table 9.3. Average water chemistry in the immediate vicinity of the Michelle Ute well.

Sodium	4,186.00 mg/l	Chloride	6,357.00 mg/l
Potassium	0.00 mg/l	Sulfate	40.28 mg/l
Magnesium	27.20 mg/l	Carbonate	0.00 mg/l
Calcium	244.20 mg/l	Bicarbonate	962.20 mg/l
pH	7.878	Hydrogen sulfide	2.5 ppm
SG	1.01 g/cc	Iron	4.4 ppm
TDS <sup>1</sup>	11,887.00 mg/l	Rw	0.8 ohm-meters

<sup>1</sup>TDS is total dissolved solids

The SI and/or the quantity of scale predicted by different algorithms disagree, and often produce vastly different results. The reasons for these disagreements are many, and beyond the scope of this paper. For this study the PHREEQE program (Parkhurst and others, 1987) will be used in testing the various parameters which affect the solubility or precipitation of CaCO<sub>3</sub>. This program is used because of the historical soundness of its development, versatility, time-proven applications by U. S. Geological Survey geochemists to water/brine-mineral equilibrium studies, and the rigorous technical reviews which these studies and the program itself have undergone.

## 9.6 Quantity and Rate of Scale Production

### 9.6.1 Quantity of Scale

The quantities of CaCO<sub>3</sub> predicted by the PHREEQE program, herein reported in terms of pounds per 1,000 barrels of water (BW [160 kl]), are equilibrium or maximum amounts. Under actual field production conditions, however, a quantity less than this is probably precipitated in the well as scale. This is due to the fact that it takes more time for the water to come to equilibrium, under changing or new conditions, than the water's residence time in the well and associated production equipment. Values in this report should, therefore, be used to identify trends or tendencies to precipitate CaCO<sub>3</sub> under specified conditions, but not to establish absolute values.

### 9.6.2 Rate of Scale Production

It is sometimes useful to determine the rate at which CaCO<sub>3</sub> scale will form, for example, on the inside of a pipe during production. While this subject is not used in the context of this study, the following is given as potentially valuable reference information. Mason and Oddo (unpublished report) discuss the rate of calcite-scale build-up in well tubing. They calculate the rate (flux) at which scale will form within a pipe, in terms of inches per month, dependent upon five variables: (1) brine flow rate, (2) length of tubing, (3) tubing radius, (4) the amount of calcium and carbonate in solution in excess of equilibrium (SI=0.00), and (5) a precipitation rate constant, referred to as a "mass transfer."

Flux is calculated as follows:

$$\text{Flux} = \frac{SQ}{6.28318r} \{1 - \exp(-6.28318r k_m x)\}$$

Flux = mass of CaCO<sub>3</sub> deposited per unit time per unit area of pipe wall.

S = rate of change of the calculated equilibrium concentration of calcium from the bottom of the well to the surface in units of mg-calcium/liter) per foot (typically 160 mg/l/8,000 ft = 0.02 mg/1-ft).

Q = brine flow rate in barrels per day, BPD (typically 1,000 to 5,000 BWPD).

r = inside pipe radius (typically 1.25 in.)

k<sub>m</sub> = mass transport constant, length per time

x = distance from well bottom (typically 0 to 10,000 feet)

## 9.7 Factors Affecting CaCO<sub>3</sub> Scale Formation

The many physical and chemical factors which initiate and control the precipitation of CaCO<sub>3</sub> from saline water, the quantity of material precipitated, the rate of precipitation, and other mineral/water interactions, are interrelated and complex. It is not the intent of this paper to discuss these factors in depth, but to illustrate, with output from the PHREEQE program, how changes in some of these factors can influence the amount of CaCO<sub>3</sub> that is produced. The six factors to be discussed, and their relation to the Michelle Ute well area are: (1) basic water chemistry, (2) pH, (3) the CO<sub>2</sub> content of the water, (4) pressure drops, (5) salinity (TDS), and (6) temperature.

### 9.7.1 Effect of Water Chemistry on the Precipitation of CaCO<sub>3</sub>

The amount of CaCO<sub>3</sub> (calcite) that will precipitate from an oil-well water is due, in part, to the chemical composition of the water. Larger quantities of calcite will precipitate from waters high in both calcium and bicarbonate than from waters low in one or both of these ions.

Table 9.4 illustrates the affect of water composition on the predicted amount of CaCO<sub>3</sub> precipitate. In specifying the PHREEQE-program setup, water is placed in equilibrium with calcite, as calcite is the main inorganic mineral scaling component that has been reported.

The first two brine types in the table represent the average water composition of similar waters in the vicinity of the Michelle Ute well, and the average composition of many waters from throughout the Uinta Basin, respectively. The next six sample analyses represent waters from throughout the Uinta Basin which are high in the following ions, respectively: sodium plus potassium, magnesium, calcium, chloride, sulfate, and bicarbonate plus carbonate. Each analysis is the average of the six samples in the UGS oil-well brine database (Gwynn, 1995) which are highest in the particular ion.

For comparison, and to eliminate the influence of different pH, SG, and temperature values in the PHREEQE calculations, a pH of 7.781 (average of all the samples) is assigned to all samples. Also, the individual ion concentrations are adjusted up or down a given percentage to bring the TDS of each sample to approximately 29,579 mg/l, which equates to a SG of about 1.17 g/cc. The sample temperature is set at 100 °C, or the approximate temperature of the earth at a depth of 12,000 to 14,000 feet (3,600 - 4,300 m).

Table 9.4. Pounds of calcite precipitated from 1,000 BW of varying chemical compositions, Bluebell field.

BRINE TYPE/SOURCE	Na+K	Mg	Ca	Cl	SO <sub>4</sub>	HCO <sub>3</sub>	Cal TDS	pH	SG	Lbs Calcite
VICINITY OF MICHELLE UTE	10416	67.7	607.6	15818	100.2	2394.3	29404	7.781	1.170	405.2
AVG. UINTA BASIN	10335	77.5	421.1	12697	2102.1	3940.1	29572	7.781	1.170	317.5
HIGH Na+K BRINE	11661	5.2	10.6	4647	126.6	12971.8	29422	7.781	1.17	6.4
HIGH Mg BRINE	3307	1444.7	3283.9	1770	9657.8	10412.9	29876	7.781	1.17	2291.5
HIGH Ca BRINE	4475	627.2	6099.8	18034	278.4	64.8	29579	7.781	1.17	11.8
HIGH Cl BRINE	7926	331.4	3757.8	17264	212.2	86.72	29578	7.781	1.17	15.6
HIGH SO <sub>4</sub> BRINE	8747	128.6	668.4	1918	15243.3	2820.14	29525	7.781	1.17	410.8
HIGH HCO <sub>3</sub> BRINE	8339	14.1	84.9	605	58.93	20463.5	29565	7.781	1.17	64.4

Explanation of column headings

BRINE TYPE/SOURCE = indicates the area from which the brine was collected, or a specific ion that the brine contains in large quantity.  
 Na+K, Mg, Ca, Cl, SO<sub>4</sub> and HCO<sub>3</sub> = ions or ion-pairs reported in mg/l.  
 Cal TDS = the sum of the above seven ions.  
 pH = the assigned pH value of 7.781, in standard pH units (same for all samples).  
 SG = the assigned density of 1.17 g/cc (same for all samples).  
 Lbs Calcite = the amount of calcite (in pounds) precipitated from 1,000 barrels of water.

While the chemical composition of the water from a given producing zone may change slightly over time, the effect of such changes on the amount of CaCO<sub>3</sub> scale will probably be minimal. Factors which may change water chemistry to a greater degree, and thus the amount of CaCO<sub>3</sub> that is precipitated, include mixing with dissimilar waters from other water-producing zones, the injection of dissimilar waters during water floods, or the addition of hydropump-makeup water.

The equilibrium amount of CaCO<sub>3</sub> that is predicted by PHREEQE, as the result of using Uinta River water as hydropump makeup water in the Michelle Ute well, is shown as follows in table 9.5. The Michelle Ute water (at 25 °C) is mixed with the Uinta River water (at 11.6 °C) and brought to equilibrium at 104 °C at pump depth. For informational purposes, the chemistry of the major rivers running through the Bluebell field, which may be used in oil-production or water-flood operations, are shown in appendix D.

Table 9.5. Effect of mixing Michelle Ute and Uinta River water on the precipitation of CaCO<sub>3</sub>.

Michelle/Uinta ratio	Lbs CaCO <sub>3</sub> /1,000 BW
90/10	1.164
50/50	3.382
10/90	3.694

### 9.7.2 Effect of pH on the Precipitation of CaCO<sub>3</sub>

The measurement of pH may be the most questionable parameter in a brine analysis and one of the most critical in determining the SI or amount of CaCO<sub>3</sub> that will precipitate from an oil-well water. In most cases, pH is determined on the water sample that is collected in the field and brought into the laboratory for analysis. At best, pH is measured in the field immediately after the sample is collected. In either case, the measured pH is most likely not representative of the water as it emerges from the formation and enters the well bore.

Tomson and Oddo (unpublished report) state the following concerning the collection of samples and the measurement of pH:

"The pH value should be measured in the flowing brine stream, not in a collected sample. As the collected sample degasses, the dissolved carbon dioxide evolves and various brine components react with atmospheric oxygen. Degassing, reaction with oxygen, etc. change the solution pH."

They further suggest that the use of high-temperature and high-pressure pH electrodes is desirable.

Because of the uncertainty about the accuracy of pH measurements, the following data (table 9.6) were generated (courtesy of Richard Curtice, Halliburton Energy Services, Vernal, Utah), to show changes in pH, bicarbonate, and carbonate measurements over time (after a sample reached the laboratory). Successive measurements were made over a three week period after the sample had been taken and maintained in a closed container at laboratory temperatures. It appears that the sample undergoes minimal change in pH, but the bicarbonate content appears to increase slightly. These data do not suggest that the pH of the brine does not change from formation level to the point of collection, however, but that once collected, there is minimal change with time.

Table 9.6. Changes in pH and bicarbonate values over time in one brine sample.

Parameter	Date of Analysis						
	5/15/95	5/16/95	5/17/95	5/20/95	5/24/95	6/06/95	6/08/95
pH	7.3	7.3	7.5	7.5	7.4	7.4	7.4
Temperature (°C)	40	25	23	25	24	25	25
Bicarbonate (mg/l)	1082	1082	1082	1090	1095	1100	1095
Carbonate (mg/l)	nil	nil	nil	nil	nil	nil	nil
Time (hr:min)	14:45	18:45	14:15	15:30	14:00	17:50	17:50

Even slight changes in pH can cause significant changes in the amount of  $\text{CaCO}_3$  that is precipitated, as illustrated in the following example. The average pH of 18 similar samples from within the vicinity of the Michelle Ute well is 7.878, with a standard deviation of 0.453. The amounts of  $\text{CaCO}_3$  precipitated from the average water chemistry at the average pH and one standard deviation above and below the average are determined by the PHREEQE program. The initial or bottom-hole temperature (BHT) is 100 °C, and the water density 1.01. Figure 9.3 shows the amount of  $\text{CaCO}_3$ , in terms of lbs per 1,000 BW, that is precipitated at three pH values through seven increasing equilibrium temperatures.

These data suggest there is a very significant change in the amount of  $\text{CaCO}_3$  that is precipitated with relatively minor changes in pH. A lowering of the pH in the water, through the introduction of small amounts of acid, for example, would decrease the amount of  $\text{CaCO}_3$  that is precipitated. The introduction of some low-pH scale inhibitors may tend to inhibit the formation of  $\text{CaCO}_3$  simply on the basis of pH change.

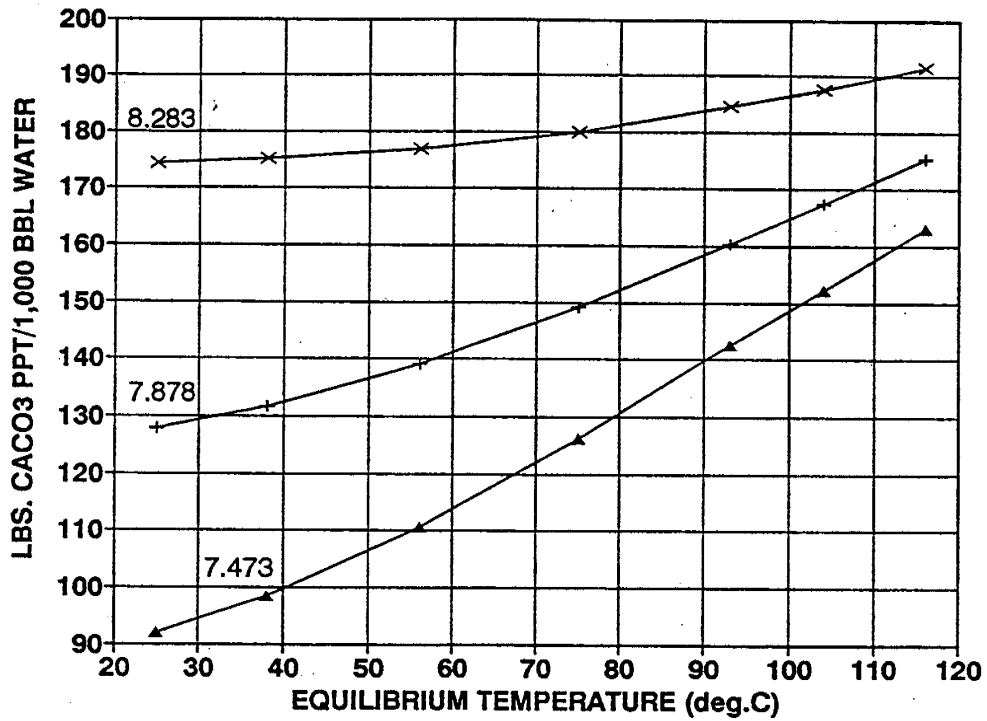


Figure 9.3. Precipitation of calcite at equilibrium temperatures from the same water at three different pH values. Water chemistry is the average of 18 similar waters in the immediate vicinity of the Michelle Ute well.

These data also suggest that errors in pH measurement, due to improper or careless sampling or measurement techniques, may greatly influence the amount of CaCO<sub>3</sub> scale that is predicted by SI programs which incorporate pH input.

### 9.7.3 Effect of CO<sub>2</sub> Content on the Precipitation of CaCO<sub>3</sub>

The total amount of gas that is dissolved in oil-well oils and co-produced waters varies from well to well and from field to field, and is dependent upon oil/gas/water ratios, temperature, and pressure. It is also dependent upon whether the pressure is greater or lesser than the bubble point of the gas in the well fluids (oil and/or water). At pressures above the bubble point, there is no separate gas phase. Below the bubble point, gas escapes from the liquids and both gas and liquid phases are present. The amount of CO<sub>2</sub> dissolved in the water is partially dependent upon the percentage of CO<sub>2</sub> in the produced gas. The following data, table 9.7, provided by Gary Williams Energy, Roosevelt, Utah, shows six typical CO<sub>2</sub> values in gases produced from, and in the vicinity of the Michelle Ute well. As can be seen, the amount of CO<sub>2</sub> contained in these gases is very low.

Table 9.7. Specific gravity and current mole-percent content of gases from wells in the vicinity of the Michelle Ute well.

Sample	Gas SG <sup>1</sup>	Methane <sup>2</sup>	Ethane <sup>2</sup>	Propane <sup>2</sup>	CO <sub>2</sub> <sup>2</sup>
A	.7750	76.76	9.86	7.34	0.58
B	.8227	71.69	13.61	6.99	0.68
C	.8364	69.96	14.48	7.32	0.95
D	.7416	78.92	10.12	4.79	0.69
E	.8253	69.30	15.35	7.57	0.94
F	.8791	67.52	15.16	7.55	0.97
Average	.8134	72.35	13.10	6.93	0.80

<sup>1</sup>Gas SG is in terms of grams per liter

<sup>2</sup>Methane, ethane, propane, and CO<sub>2</sub> are in terms of the current mole percent.

While the amount of CO<sub>2</sub> actually present in the oil-well water at depth is not known, the PHREEQE-predicted effect of increasing amounts of CO<sub>2</sub> (in moles) in the produced water is shown on figure 9.4. Positive values (above zero) are precipitated CaCO<sub>3</sub> in lbs per 1,000 BW, while the negative values (below zero) represent the amounts (same units) that would be dissolved into the water to maintain equilibrium.

### 9.7.4 Effects of Pressure Drops and Turbulence on the Precipitation of CaCO<sub>3</sub>

The effects of pressure drops as the brine emerges from the formation and moves into the well, and as pressure-drop conditions are encountered within the well and the production system, (summarized by Tomson and Oddo unpublished report) as follows:

"As hydrocarbons are produced, the pressure drops and calcite precipitates for two reasons. First, the theoretical solubility of calcite decreases as the pressure decreases; this is true for most deposits, including all of the sulfates. The second effect is generally more important and is related to the partial pressure of carbon dioxide. As the overall pressure drops, so does the

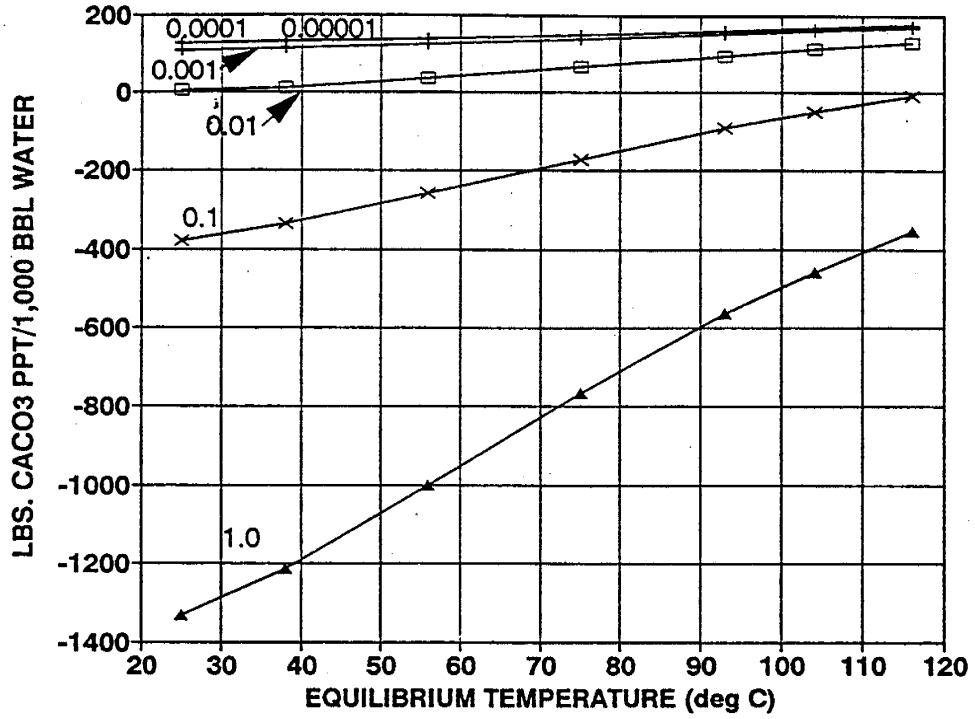


Figure 9.4. Precipitation of calcite at equilibrium temperatures from the same water but containing different amounts of CO<sub>2</sub> (moles). Water chemistry is the average of the 18 waters in the immediate vicinity of the Michelle Ute well.

partial pressure of carbon dioxide. As the partial pressure of carbon dioxide drops, carbon dioxide which was previously dissolved in the water goes into the gas phase....Therefore, as the partial pressure decreases, so does the concentration of carbonic acid in solution and this raises the pH....The higher pH causes  $\text{CaCO}_3$  to precipitate."

$\text{CaCO}_3$  precipitation may occur as water emerges from the formation and moves through the perforations into the well. Operators report that  $\text{CaCO}_3$  scale is present within, and in the immediate vicinity of pumps, where the hydrostatic pressure is decreased. Other pressure-drop conditions exist where water flows from a small- to a larger-diameter pipe, or under conditions where there is cavitation of the water.

#### **9.7.5 Effects of Water Salinity on the Precipitation of $\text{CaCO}_3$**

Salinity, defined as the total amount of dissolved salts in a given quantity of water, has a direct influence on the amount of  $\text{CaCO}_3$  that will precipitate from the water. If water of a given chemical composition is diluted such that its salinity is decreased, the amount of  $\text{CaCO}_3$  that will precipitate, under specified equilibrium conditions, will be less than from the original water. Likewise, if water of a given composition is concentrated to a higher salinity, without mineral precipitation occurring, the amount of  $\text{CaCO}_3$  that will precipitate under specified equilibrium conditions, will be greater than from the original water. Figure 9.5 illustrates the effect of reducing the salinity of the water (while maintaining the same chemical composition) found in the vicinity of the Michelle Ute well to 80, 60, and 40 percent of its original salinity.

#### **9.7.6 Effects of Temperature Changes on the Precipitation of $\text{CaCO}_3$**

The amount of  $\text{CaCO}_3$  that is precipitated from produced waters is influenced by two temperatures. The first is the water temperature as it emerges from the formation, through the perforations, and into the well. This is referred to herein as its initial temperature, and is dependent upon its depth below the surface of the ground, as represented in figure 9.6. The data are taken mainly from production test temperatures measured in the Wasatch Formation.

The second water temperature is the final equilibrium temperature. This may represent the cooler temperatures that the water reaches while ascending to different elevations within the well, or it may represent the cooler temperatures it reaches in different parts of the surface production facilities (heaters, pipes, separators, power-water tanks, disposal pits, and so forth).

Figure 9.7 is a plot of the amount of  $\text{CaCO}_3$  that is precipitated versus its equilibrium temperature for seven initial temperatures. These data show that the higher the initial or the final equilibrium temperatures are, the greater the amount of  $\text{CaCO}_3$  precipitated.

### **9.8 Effect of Mixing Wasatch and Green River Formation Waters**

In some oil wells in the vicinity of the Michelle Ute well, co-produced water comes from zones within both the Wasatch and Green River Formations and is mixed as it ascends the well. The average chemical composition of these two waters is different, as shown in table 9.8. Due to these differences, the amount of  $\text{CaCO}_3$  that

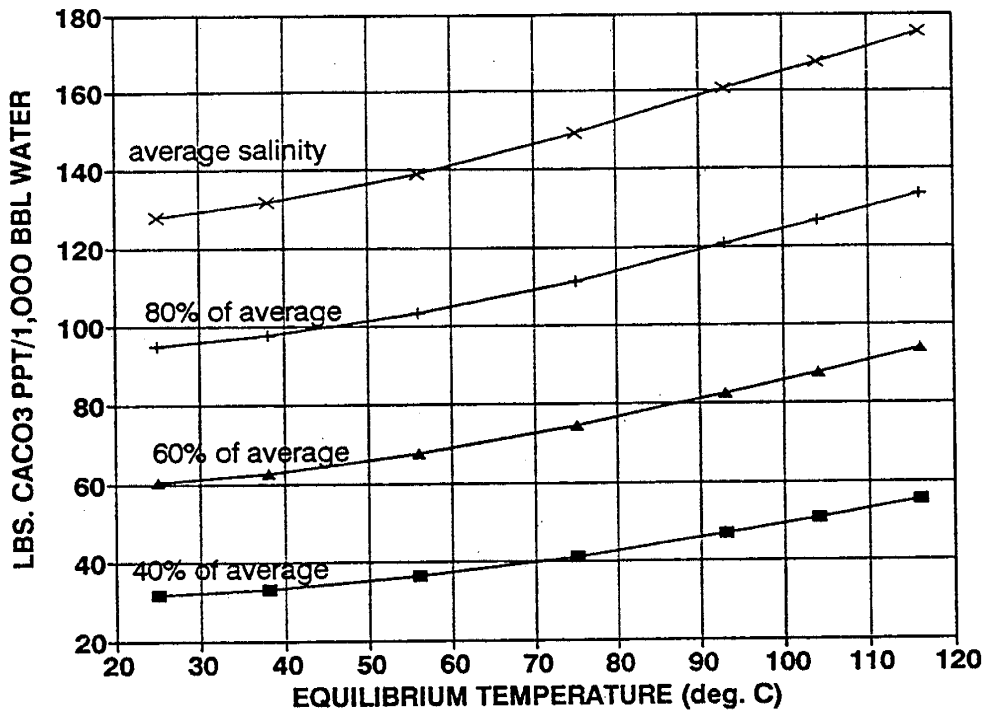


Figure 9.5. Precipitation of calcite at equilibrium temperatures from waters of the same chemical composition, but varying degrees of dilution or salinity. Water chemistry is the average of the 18 waters in the immediate vicinity of the Michelle Ute well.

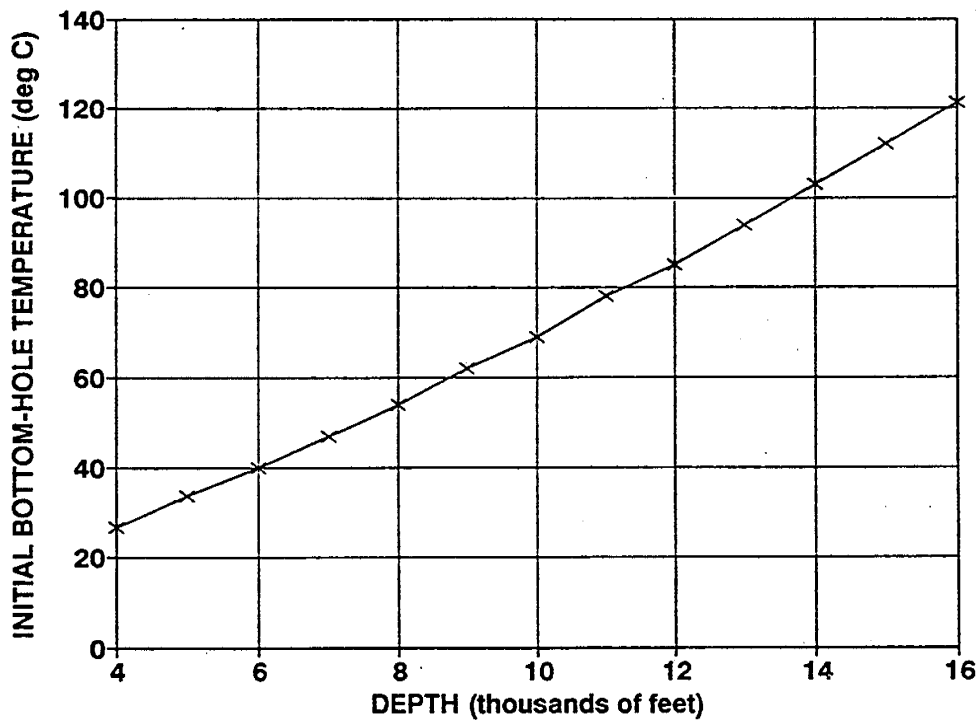


Figure 9.6. Plot of initial BHT versus depth from the land surface in the Wasatch Formation.

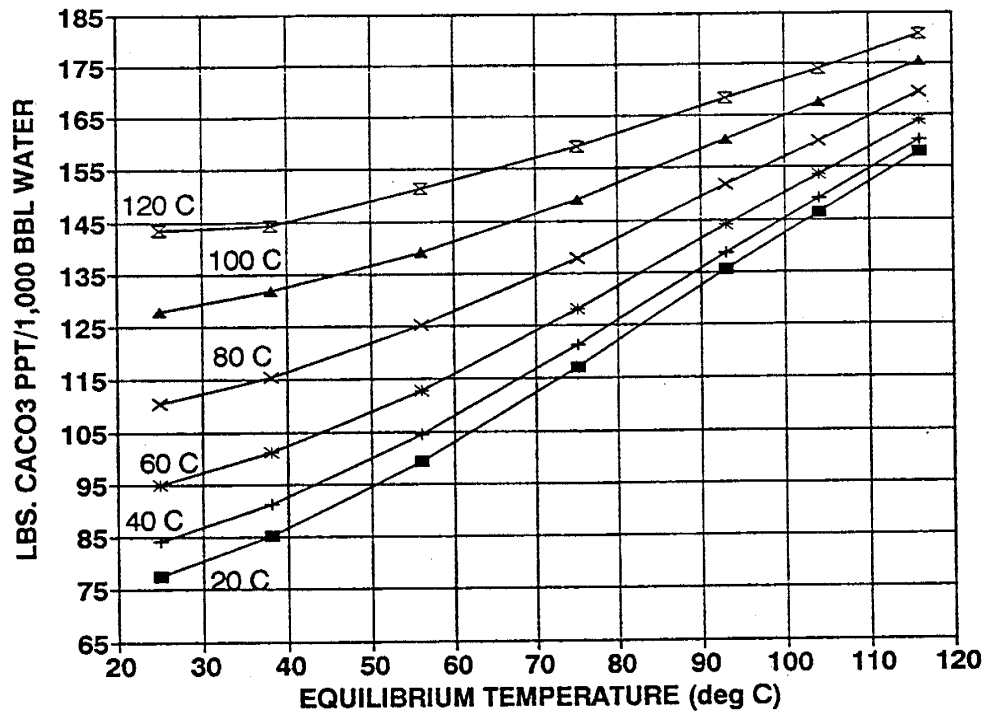


Figure 9.7. Precipitation of calcite at equilibrium temperatures from the same water but at increasing initial BHT (20°C to 120°C). Water chemistry is the average of the 18 waters in the immediate vicinity of the Michelle Ute well.

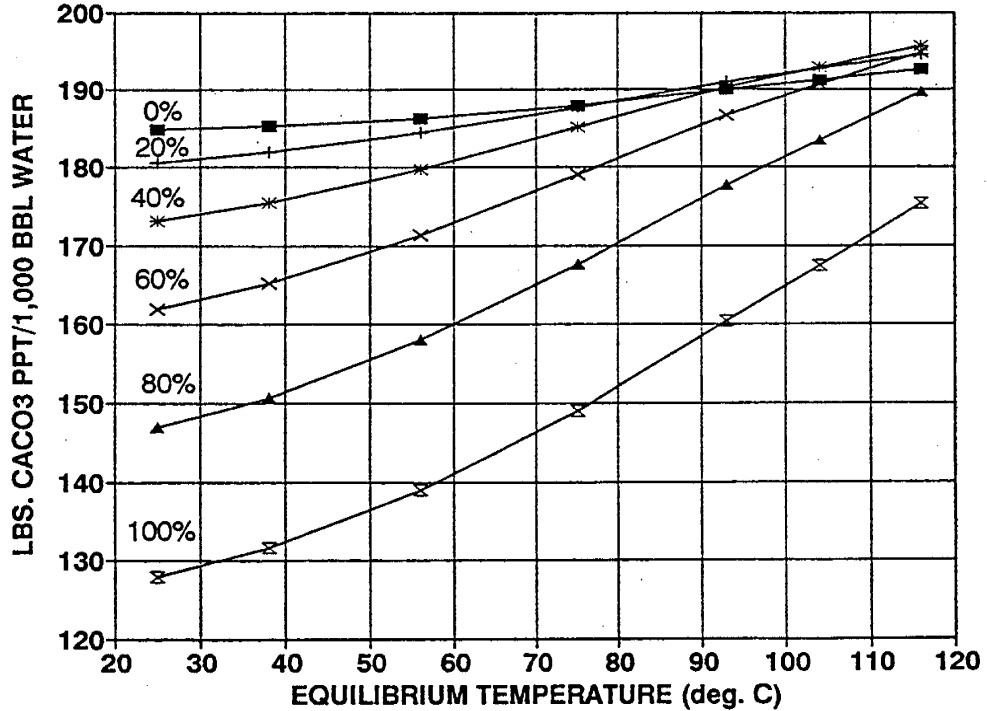


Figure 9.8. Precipitation of calcite at equilibrium temperatures from varying-ratio mixtures of average Wasatch Formation and average Green River Formation waters (in percent of Wasatch water), in the immediate vicinity of the Michelle Ute well.

Table 9.8. Comparison of average Wasatch and Green River Formation waters in the vicinity of the Michelle Ute well.

<u>Chemical parameter</u>	<u>Wasatch Fm.</u>	<u>Green River Fm.</u>
Sodium	4186.00	4826.95
Potassium	3.60	92.57
Magnesium	27.20	30.76
Calcium	244.20	225.66
Chloride	6357.00	5198.57
Sulfate	40.28	2095.19
Bicarbonate	962.20	2117.45
pH	7.87	8.009
SG	1.01	1.012

will precipitate from the mixed waters, at equilibrium temperatures, is different than that which would precipitate from either water alone. Figure 9.8 shows these differences. The amount of precipitate from the mixed waters is less than that which comes from the Green River Formation alone, and more than that which comes from the Wasatch Formation alone.

There are not sufficient producing-zone specific chemical data to determine the precipitation-tendency effects due to the mixing of waters from two or more individual producing zones within either the Wasatch Formation or the Green River Formation. If the waters from two different zones within a formation are different in chemical composition, the tendency for, and amount of precipitation from the mixed waters, will be somewhat different than for the waters from the individual zones.

### 9.9 Possible Scale-Mitigating Actions (Excluding Inhibitors)

While little can be done with the basic chemistry of the brine that is produced by a given well, some actions can be taken to minimize  $\text{CaCO}_3$  scaling during production. The use of scale inhibitors such as phosphonates is not discussed. Discussions on the use of these agents are found in Oddo and others (1993). Three ways to reduce scale are:

- (1) By the addition of small amounts of an acid to the hydro-pump power-water supply, the pH of the water moving through the pump and up the well can be lowered, thus reducing the amount of scale that is formed. Weak acids like acetic or citric are less corrosive than a strong acid like hydrochloric.
- (2) By maintaining a high hydrostatic pressure at the level of the pump and the perforations, the partial pressure of  $\text{CO}_2$  (a minor component of the mostly-methane gas in this area) might be maintained and help to prevent scaling. Devising a method of increasing the  $\text{CO}_2$  content of the hydro-pump power water, or installing a low-level  $\text{CO}_2$  injection system, might have a scale-reducing effect as well.
- (3) As increased equilibrium temperatures favor the precipitation of greater amounts of  $\text{CaCO}_3$ , maintaining the production system at as low a temperature

as possible may help to minimize scaling. Temperatures must, of course, be maintained high enough to prevent hydrocarbon solidification.

### 9.10 Conclusions

Variations in six parameters were explored, one at a time, to determine the effects of these variations on the precipitation of  $\text{CaCO}_3$  from produced oil-well waters in the vicinity of the Michelle Ute well, Bluebell field. The six parameters are: (1) basic water chemistry, (2) pH, (3)  $\text{CO}_2$  content, (4) pressure changes, (5) salinity changes, and (6) temperature changes.

Waters with high percentages of both calcium and bicarbonate favor greater precipitation. Low pH (more acidic) waters precipitate less  $\text{CaCO}_3$  than high pH (more basic) waters. High  $\text{CO}_2$  content favors less precipitation than low  $\text{CO}_2$ -content waters. Decreases in pressure and/or increased turbulence favor the precipitation of  $\text{CaCO}_3$ . Reductions in salinity favor less precipitation. Increased temperatures, both initial and equilibrium, favor increased precipitation. The co-production of Green River Formation and Wasatch Formation waters increases the amount of  $\text{CaCO}_3$  scale that is produced over that which is produced from Wasatch Formation water alone.

## 10. TECHNOLOGY TRANSFER

*Roger L. Bon*  
Utah Geological Survey

Technology transfer activities for the year include information exhibits at two regional and one national petroleum industry meeting, seven oral presentations and one poster presentation at regional and national industry meetings and one technical seminar, one presentation made to a local professional organization, and a progress summary which was included in the July 1995 issue of *UGS Petroleum News*.

### 10.1 Information Exhibits

Society of Petroleum Engineers, Rocky Mountain Section Meeting, March 1995, Denver, CO.  
American Association of Petroleum Geologists, Annual Meeting and Exhibition, March 1995, Houston, TX.  
American Association of Petroleum Geologists, Rocky Mountain Section Meeting, July 1995, Reno, NV.

### 10.2 Oral and Poster Presentations

#### 10.2.1 Geological Society of America, Annual Meeting, October 1994, Seattle, WA.

Garner, Ann, and Morris, T.H.: *Reservoir characterization through facies analysis of the lower Green River Formation for hydrocarbon production enhancement in the Altamont-Bluebell field, Uinta Basin, Utah.*

#### 10.2.2 American Association of Petroleum Geologists Annual Meeting and Exhibition, March 1995, Houston, TX.

Garner, Ann: *Reservoir characterization through facies analysis of the lower Green River Formation for hydrocarbon production enhancement in the Altamont-Bluebell field, Uinta Basin, Utah.*

Wegner, MaryBeth, Garner, Ann, and Morris, T.H.: *Reservoir Characterization through facies analysis of core and outcrop of the lower Green River Formation: hydrocarbon production enhancement in the Altamont-Bluebell field, Uinta Basin, Utah.*

#### 10.2.3 American Association of Petroleum Geologists Rocky Mountain Section Meeting, July 1995, Reno, NV.

Tripp, C.N.: *Reservoir characterization of potential targets for horizontal drilling in the Tertiary Green River and Wasatch Formations, Bluebell field, Uintah County, Utah.*

Morgan, C.D.: *A multi-disciplinary team approach to reservoir characterization of the Bluebell field, Uintah Basin, Utah.*

Wegner, MaryBeth, Garner, Ann, and Morris, T.H.: *Reservoir characterization through facies analysis of core and outcrop of the lower Green River Formation: hydrocarbon production enhancement in the Altamont-Bluebell field, Uinta Basin, Utah.*

**10.2.4 Ninth Annual Spring Research Conference, Brigham Young University, March 1995, Provo, UT**

Wegner, MaryBeth, Garner, Ann, and Morris, T.H.: *Reservoir characterization through facies analysis of core and outcrop of the lower Green River Formation: hydrocarbon production enhancement in the Altamont-Bluebell field, Uinta Basin, Utah.*

Garner, Ann: *Reservoir characterization through facies analysis of the lower Green River Formation for hydrocarbon production enhancement in the Altamont-Bluebell field, Uinta Basin, Utah.*

**10.2.5 Utah Geological Association Meeting, August 1995, Salt Lake City, UT**

Morgan, C.D.: *Bluebell field: Increasing production in a fluvial-deltaic reservoir.*

**10.3 Petroleum News**

*UGS Petroleum News* is a newsletter published by the Utah Geological Survey. The newsletter keeps petroleum companies, researchers, and other parties involved in exploring and developing Utah energy resources, informed of the progress on various energy-related projects of the Utah Geological Survey. The newsletter is free to anyone interested and is currently sent to roughly 300 organizations and individuals. Three issues have been published since inception, the first in January 1994, the second in June 1994, and the third in July 1995.

## 11. PROPOSED DEMONSTRATION

*Craig D. Morgan<sup>1</sup>, DeForrest Smouse<sup>2</sup>, and Lewis Wells<sup>2</sup>*  
Utah Geological Survey<sup>1</sup>,  
Quinex Energy Corporation<sup>2</sup>

### 11.1 Introduction

The characterization study included evaluations of outcrop, well core, geophysical well logs, reservoir and fluid properties, production and past completion techniques, and stimulation fluids. Based on criteria determined during the study, individual beds were analyzed in the Michelle Ute, Malnar Pike, and neighboring wells. A three-part demonstration is recommended to show how oil recovery can be improved from old and new wells in the Bluebell field: (1) recomplate the Michelle Ute well, (2) recomplate the Malnar Pike well, and (3) drill and complete a new well. Each part of the demonstration is designed to allow detailed documentation of success or failure of each aspect of the characterization and stimulation techniques.

The recommendations will be demonstrated over the next three years. The first part of the demonstration will be a low-friction, high-rate, and high-diversion, acid stimulation of several zones in the Michelle Ute well. The zones were identified by the characterization study and each zone will be stimulated separately. The second part of the demonstration will involve drilling mini-laterals into a few selective beds and stimulating each bed separately in the Malnar Pike well. Cased-hole geophysical logs and radioactive tracers will be used to determine the diversion of the stimulation fluids, quantify fracturing and its role in production before and after the treatment on a bed basis, and quantify the production from each bed treated. The actual results will be compared to the predicted characterization which will be modified as needed after each part of the demonstration. The third part of the demonstration will be to drill and complete a new well. The well will be located based on the characterization study. The completion technique used in the new well will be based on the results from the two recompletions.

### 11.2 Michelle Ute Well

The first part of the demonstration will be to recomplate the Michelle Ute well by stimulating individual pressure zones (each about 500 feet [150 m] thick) using a high-diversion, low-friction treatment.

Volumetric calculations and reservoir simulations show the Michelle Ute well has much less oil-in-place per individual bed than the Malnar Pike well. Therefore, we believe more beds will need to be stimulated in the Michelle Ute well than in the Malnar Pike well, for the treatment to be economical.

Using the drilling mud data, several pressure zones were identified in the Michelle Ute well. The top of a pressure zone is defined by a drilling "kick", requiring an increase in mud weight. Pulsed neutron decay and dipole sonic logs will be run before treatment to further evaluate remaining oil and determine which beds currently have open fractures. Each pressure zone will be stimulated separately, and each will contain a different radioactive tracer. After all zones have been stimulated and the well is cleaned up, tracer, temperature, spinner, and dipole sonic logs will be run. The logs will quantify how well the treatment fluids were dispersed, which beds are producing,

their volume, and how many beds had fractures opened or induced by the treatment. The results will be compared to the original formation evaluations and the beds in the Malnar Pike well will be re-evaluated.

### **11.3 Malnar Pike Well**

The second part of the demonstration will be to horizontally drill 10 feet (3 m) directionally into three or more key beds. Pulsed neutron decay and dipole sonic logs will be run in the Malnar Pike well if they are effective in the Michelle Ute well. The cased-hole logs will be used with the revised formation evaluations to help select individual beds for stimulation. Three or more beds will be drilled horizontally for a distance of up to 10 feet (3 m) using an extended-reach hydro-jet lance tool. The beds will be isolated and individually stimulated using a pinpoint injection tool. After the well has been stimulated and cleaned up, temperature and spinner logs will be run to determine the contribution each bed is making to the production of the well. The results will be compared to the formation evaluations made before treatment. The formation evaluation parameters proven to be the most reliable in identifying hydrocarbons in the Michelle Ute and Malnar Pike wells will be determined.

### **11.4 New Well**

The third part of the demonstration will be to select a location, drill, evaluate, perforate, and stimulate a new well based on the knowledge gained from the characterization study and results of the first two parts of the demonstration. The oil-producing beds identified in Michelle Ute and Malnar Pike wells will be correlated and mapped. These data will be used to help select a location for a new well. Formation evaluation, selection of perforated intervals, and type of stimulation, in the new well will be based on the experience gained from the Michelle Ute and Malnar Pike demonstrations.

### **11.5 Benefits and Value**

Michelle Ute and Malnar Pike wells are at or near their economic limit. Recompletions have been attempted in both of these wells before with limited success. Improved recompletion techniques will increase the total recovery and prevent premature abandonment of Michelle Ute, Malnar Pike, and many other wells in the Uinta Basin. The Bluebell field encompasses 249 sections (a section is 640 acres [one square mile]). There are 33 sections within the field boundary that have never been drilled, and 123 sections that have only one well per section. Demonstration of an improved completion technique that increases the primary recovery of a well, will make additional development drilling much more economically appealing.

The low recovery in many older wells and the possibility for hundreds of additional development wells gives Bluebell field and the Uinta Basin a potential that could be in the hundreds of millions barrels of oil. But even a more conservative 5 to 10 percent incremental increase in recovery could result in additional tens of millions of barrels from the Bluebell field. After the demonstrations have been completed and evaluated, the financial benefit resulting from the project will be more accurately determined.

## REFERENCES

- Allison, M.L., 1995, Increased oil production and reserves from improved completion techniques in the Bluebell field, Uinta Basin, Utah-Annual Report for the Period September 30, 1993 to September 30, 1994: U.S. Department of Energy Report DOE/BC/14953-10, (DE95000171), 123 p.
- Bruhn, R.L., Picard, M.D., and Beck, S.L., 1983, Mesozoic and early Tertiary structure and sedimentology of the central Wasatch Mountains, Uinta Mountains and Uinta Basin: Utah Geological and Mineral Survey Special Studies 59, p. 63-105.
- Carozzi, A.V., 1993, Sedimentary Petrography: Englewood Cliffs, N.J., Prentice Hall, 263 p.
- Cashion, W.B., 1967, Geology and fuel resources of the Green River Formation, southeastern Uinta Basin, Utah and Colorado: U.S. Geological Survey Professional Paper 168, 58 p.
- Castle, J.W., 1991, Sedimentation in Eocene lake Uinta (lower Green River Formation), northeastern Uinta Basin, Utah, *in* Katz, B.J., editor, Lacustrine basin exploration-case studies and modern analogs: American Association of Petroleum Geologists Memoir 50, p. 243-263.
- Chidsey, T.C., Jr., 1993, Wasatch Formation, *in* Robertson, J.M., and Broadhead, R.F., project directors, Atlas of Major Rocky Mountain gas reservoirs: New Mexico Bureau of Mines and Mineral Resources, p. 87-88.
- Dott, R.H., Jr., 1964, Wacke, graywacke, and matrix - what approach to immature sandstone classification?: Journal of Sedimentary Petrology, v. 34, p. 625-632.
- Dunham, R.J., 1962, Classification of carbonate rocks according to depositional texture, *in* Ham, W.E., editor, Classification of Carbonate Rocks: American Association of Petroleum Geologists Memoir 1, p. 108-121.
- Fouch, T.D., 1975, Lithofacies and related hydrocarbon accumulation in Tertiary strata of the western and central Uinta Basin, Utah, *in* Bolyard, D.W., editor, Symposium on deep drilling frontiers of the central Rocky Mountains: Rocky Mountain Association of Geologists, p. 163-173.
- 1976, Revision of the lower part of the Tertiary system in the central and western Uinta Basin, Utah: U.S. Geological Survey Bulletin 1405-c, 7 p.
- 1981, Distribution of rock types, lithologic groups, and interpreted depositional environments for some lower Tertiary and Upper Cretaceous rocks from outcrops at Willow Creek - Indian Canyon through the subsurface of Duchesne and Altamont oil fields, southeast to north-central parts of the Uinta Basin, Utah: U.S. Geological Survey Oil and Gas Investigations Map, Chart OC-81, 2 sheets.

- Fouch, T.D., Nuccio, V.F., and Chidsey, T.C., Jr., editors, 1992, Hydrocarbon and mineral resources of the Uinta Basin, Utah and Colorado: Utah Geological Association Guidebook 20, 366 p.
- Fouch, T.D., and Pitman, J.K., 1991, Tectonic and climate changes expressed as sedimentary cycles and stratigraphic sequences in the Paleogene Lake Uinta system, central Rocky Mountains, Utah and Colorado (abstract): American Association of Petroleum Geologists Bulletin, v. 75, no. 3, p. 575.
- 1992, Tectonic and climate changes expressed as sedimentary and geochemical cycles - Paleogene Lake systems, Utah and Colorado - implications for petroleum source and reservoir rocks, *in* Carter, L.J., editor, U.S. Geological Survey research on energy resources, 1992 McKelvey forum program and abstracts (abstract): U.S. Geological Survey Circular 1074, p. 29-30.
- Fouch, T.D., Pitman, J.K., Wesley, J.B., Szantay, Adam, and Ethridge, F.G., 1990, Sedimentology, diagenesis, and reservoir character of Paleogene fluvial and lacustrine rocks, Uinta Basin, Utah - evidence from the Altamont and Red Wash fields, *in* Carter, L.M., editor, Sixth V. E. McKelvey forum on mineral and energy resources, U.S. Geological Survey research on energy resources - 1990 - program and abstracts: U.S. Geological Survey Circular 1060, p. 31-32.
- Franczyk, K.J., Fouch, T.D., Johnson, R.C., Molenaar, C.M., and Cobban, W.A., 1992, Cretaceous and Tertiary paleogeographic reconstructions for the Uinta-Piceance Basin study area, Colorado and Utah: U. S. Geological Survey Bulletin 1787-Q, 37 p.
- Gwynn, J.W., 1995, Resistivities and chemical analyses of selected oil and gas field, water well, and spring waters, Utah: Utah Geological Survey Circular 87, 142 p.
- Hosterman, J.W., and Dyni, J.R., 1972, Clay mineralogy of the Green River Formation, Piceance Creek basin, Colorado--A preliminary study: U.S. Geological Survey Professional Paper 800-D, p. D159-D163.
- Lucas, P.T., and Drexler, J.M., 1975, Altamont-Bluebell-a major fractured and overpressured stratigraphic trap, Uinta Basin, Utah, *in* Bolyard, D.W., editor, Symposium on deep drilling frontiers of the central Rocky Mountains: Rocky Mountain Association of Geologists, p. 265-273.
- Moore, D.M., and Reynolds, R.C., Jr., 1989, X-ray diffraction and the identification and analysis of clay minerals, 332 p.
- Morris, T.H., and Richmond, D.R., 1992, A predictive model of reservoir continuity in fluvial sandstone bodies of a lacustrine deltaic system, Colton Formation, Utah, *in* Fouch, T.D., Nuccio, V.F., and Chidsey, T.C., Jr., editors, Hydrocarbon and mineral resources of the Uinta Basin, Utah and Colorado: Utah Geological Association Guidebook 20, p. 227-236.

- Morris, T.H., Richmond, D.R., and Marino, J.E., 1991, The Paleocene/Eocene Colton Formation-A fluvial-dominated lacustrine deltaic system, Roan Cliffs, Utah, in Chidsey, T.C., editor, *Geology of east-central Utah: Utah Geological Association Field Symposium and Guidebook*, p. 129-139.
- Narr, W.N., 1977, The origin of fractures in Tertiary strata of the Altamont field, Uinta Basin, Utah: Toronto, Masters thesis University of Toronto, 132 p.
- Narr, W.N., and Currie, J.B., 1982, Origin of fracture porosity--example from Altamont field, Utah: *American Association of Petroleum Geologists Bulletin*, v. 66 no. 9, p. 231-247.
- Oddo, J.E., Kan, A.T., Al-Borno, A., Hunter, M., and Tomson, M.B., 1993, Brine chemistry and control of adverse chemical reactions with natural gas production: Gas Research Institute Contract No. 5088-212-1717. (Authors are associated with Rice Engineering Design and Development Institute, Rice University, P.O. Box 1892, Houston, Texas, 77251)
- Parkhurst, D.L., Thorstenson, D.C., and Plummer, L.N., 1987, PHREEQE - A computer program for geochemical calculations: U.S. Geological Survey Water-Resources Investigation 80-96, 192 p.
- Pitman, J.K., Anders, D.E., Fouch, T.D., and Nichols, D.J., 1986, Hydrocarbon potential of nonmarine Upper Cretaceous and Lower Tertiary rocks, eastern Uinta Basin, Utah, in Spencer, C.W., and Mast, R.F., editors, *Geology of tight gas reservoirs: American Association of Petroleum Geologists Studies in Geology* 24, p. 235-252.
- Pitman, J.K., Fouch, T.D., and Goldaber, M.B., 1982, Depositional setting and diagenetic evolution of some Tertiary unconventional reservoir rocks, Uinta Basin, Utah: *American Association of Petroleum Geologists Bulletin*, v. 66, no. 10, p. 1581-1596.
- Remy, R.R., 1991, Analysis of lacustrine deltaic sedimentation in the Green River Formation, southern Uinta Basin, Utah (volumes 1 and 2): Baton Rouge, Ph.D. Dissertation, Louisiana State University and Agricultural and Mechanical College, 393 p.
- Ryder, R.T., Fouch, T.D., and Elison, J.H., 1976, Early Tertiary sedimentation in the western Uinta Basin, Utah: *Geological Society of America Bulletin*, v. 87, p. 496-512.
- Smith, J.D., 1986, Depositional environments of the Tertiary Colton and basal Green River Formations in Emma Park, Utah: Provo, Brigham Young University *Geology Studies*, v. 33, p. 135-174.
- Stokes, W.L., 1986, *Geology of Utah: Utah Geological Survey Miscellaneous Publication S*, 317 p.

Strickland, L.N., 1981, Various methods used in evaluating the quality of oil-field waters for subsurface injection, *in* Johnson, J.L., Stanford, J.R., Wright, C.C., and Ostroff, A.G., editors, *Water for subsurface injection*: American Society for Testing Materials Special Technical Publication 735, p.68-88.

Tomson, M.B., and Oddo, J.E., (unpublished), Handbook of calcite scale measurement, prediction and control: (manuscript has been accepted for publication (as of 1995) by Pennwell Press, Tulsa, OK, contingent upon GRI approval for release. Mason Tomson is professor of Environmental Science and Engineering, Rice University, Houston, Texas).

Velde, B., 1992, *Introduction to Clay Minerals*: 2-6 Boundary Row, London, Chapman and Hall, 198 p.

**APPENDIX A**  
**Description of Bluebell Cores**

# Pennzoil 3-17A2 Lamicq Urruty 17-T1S-R2W NWSE

Date logged:  
 Logged by: MaryBeth Wegner  
 Ground: 0.00 ft      KB: 5992.00 ft  
 Remarks: Core diameter is 6.5 cm (2.5"). Flagstaff Formation.

## LEGEND

### LITHOLOGY

 Sand/Sandstone	 Shale	 Limestone	 Sandy Limestone
 Silt/Siltstone	 Mud/Mudstone	 Limey Mudstone	

### CONTACTS

 Sharp	 Scoured	 Bioturbated	 Uncertain
 Undulating			

### PHYSICAL STRUCTURES

 - Ripple Lamination	 - Planar Lamination	 - Flaser Bedding
 - Wavy Parallel Bedding	 - Microfault	 - Horizontal fracture(s)
 - Haphazard fractures	 - Vertical fracture(s)	 - Horizontal and vertical fractures

### LITHOLOGIC ACCESSORIES

Py - Pyrite	 - Rip Up Clasts
-------------	---

### ICHNOFOSSILS

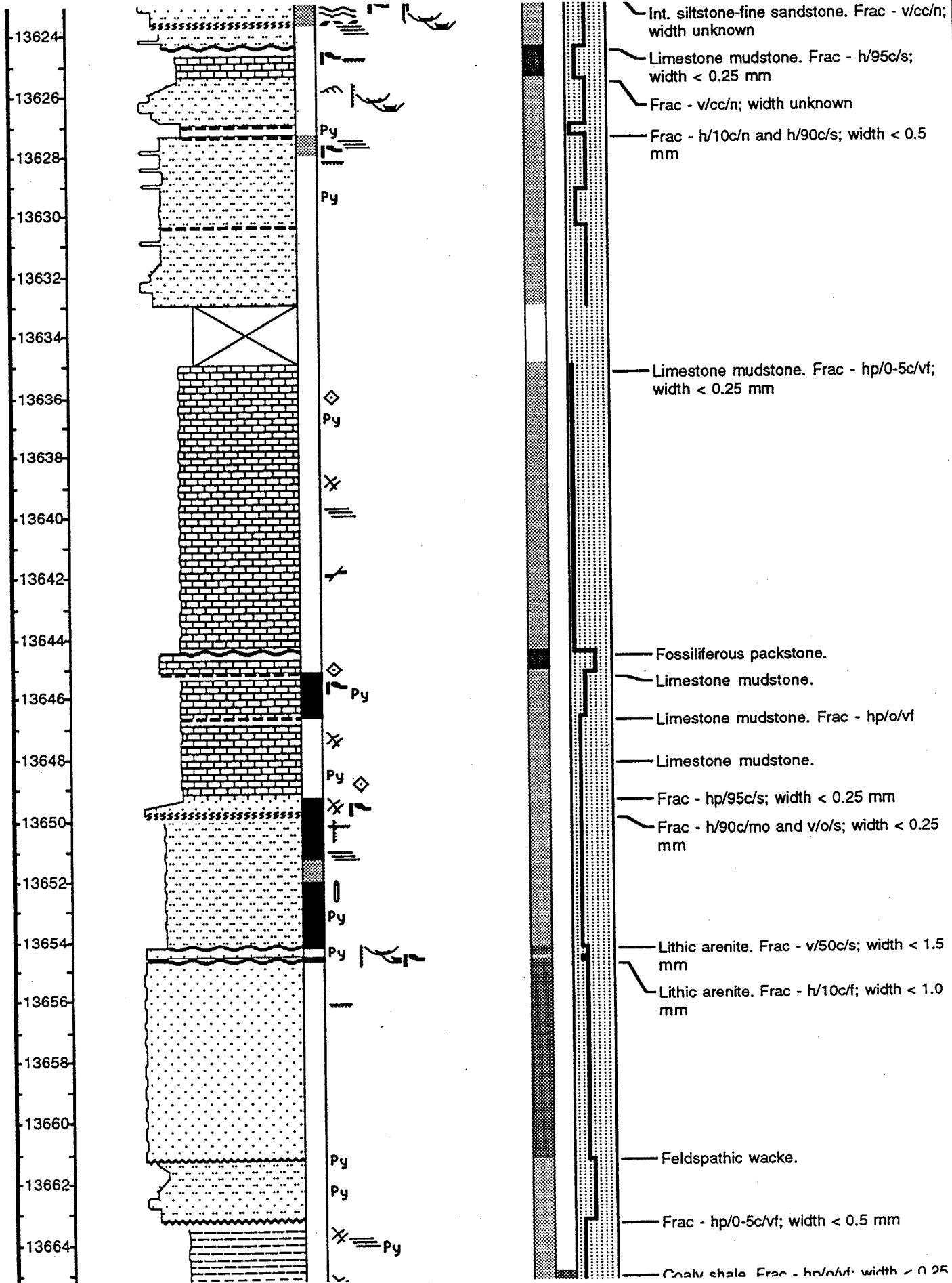
 - Vertical Burrows	 - Undifferentiated Bioturbation
--	---

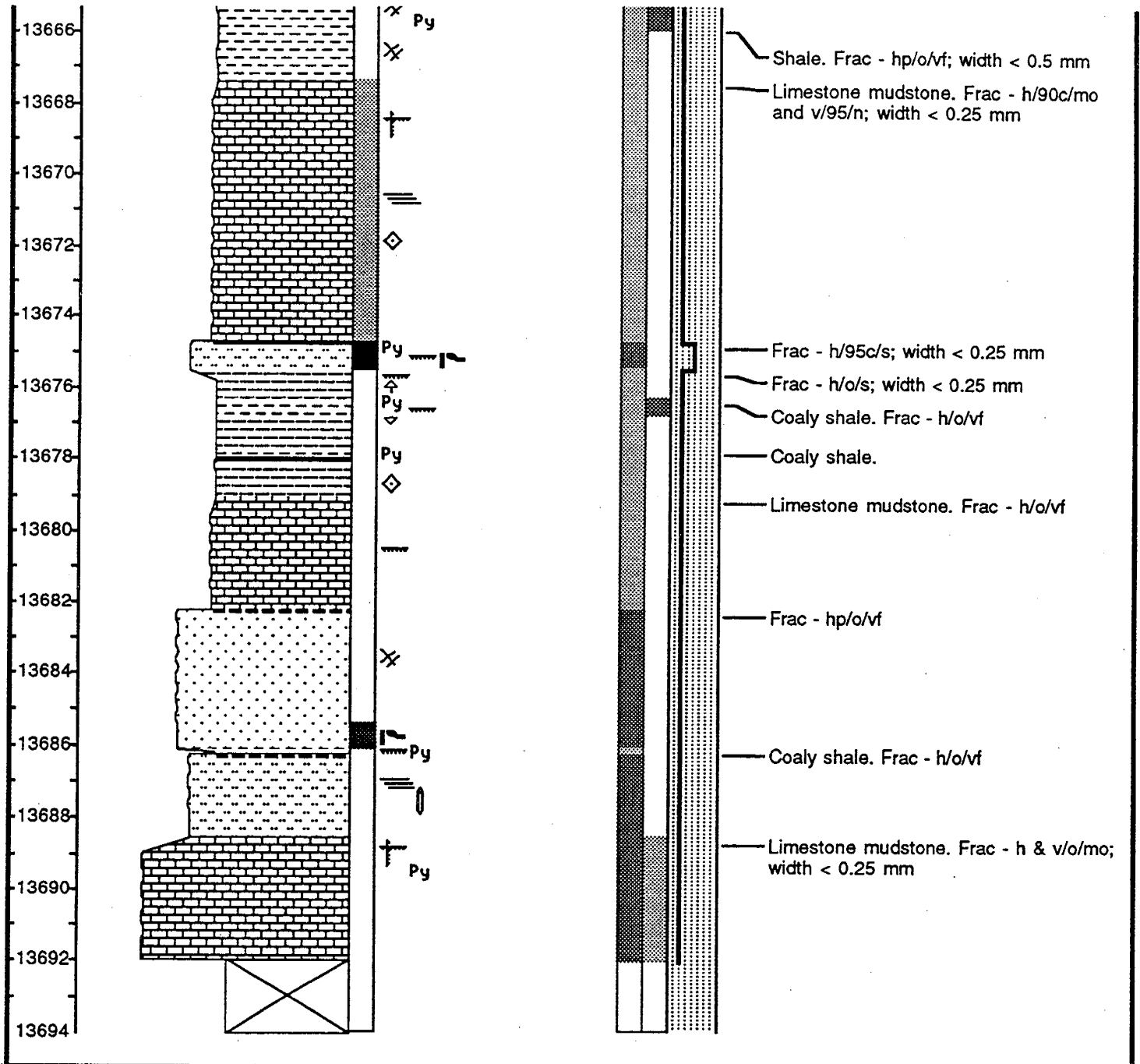
### FOSSILS

 - Molluscs (undifferentiated)	 - Gastropods	 - Fossils (undifferentiated)
---	--	--

FEET	GRAIN SIZE	BIOTURBATION INTENSITY	PHYSICAL STRUCTURES	ACCESSORIES	ICHNOFOSSILS	FOSSILS	POROSITY	STAIN	SORTING	REMARKS
	cobble pebble granule sand silt clay vc mfv									POROSITY: visual ranking; poor (light) to good (dark).  STAIN: no visible oil or bitumen staining (light) to heavy staining (dark)
										Frac - v, h, hp/10c/vf; width < 0.5 mm







# Chevron Springfield Marine 2-10C

## 10-T1S-R2W SWSW

Date logged:

Logged by: MaryBeth Wegner

Ground: 0.00 ft      KB: 5873.00 ft

Remarks: Core diameter is 9 cm (3.5 in.). Base of core is 11,158' 3". Green River Formation.

### LEGEND

#### LITHOLOGY

 Sand/Sandstone	 Organic Shale with inter	 Oolitic Lst	 Sandy Limestone
 Silt/Siltstone	 Limestone		

#### CONTACTS

 Sharp	 Scoured	 Bioturbated	 Uncertain
 Undulating			

#### PHYSICAL STRUCTURES

 - Ripple Lamination	 - Convolute Bedding	 - Graded Bedding
 - Reverse Graded Bedding	 - Load Casts	 - Stylolites
 - Horizontal fracture(s)	 - Vertical fracture(s)	

#### LITHOLOGIC ACCESSORIES

 - Shale Lamina	Py - Pyrite	 - Rip Up Clasts
--	-------------	---

#### ICHTNOFOSSILS

 - Undifferentiated Bioturbation		
---	--	--

#### FOSSILS

 - Gastropods	O - Ostracods	 - Fossils (undifferentiated)
--	---------------	--

	GRAIN SIZE		BIOTURBATION INTENSITY	PHYSICAL STRUCTURES	ACCESSORIES	ICHTNOFOSSILS	FOSSILS	POROSITY	STAIN	SORTING	
FEET	<div style="display: flex; justify-content: space-between;"> <div style="text-align: right;"> <p>vc mf v</p> </div> <div style="text-align: left;"> <p>cobble</p> <p>pebble</p> <p>granule</p> <p>sand</p> <p>silt</p> <p>clay</p> </div> </div>										<p>POROSITY: visual ranking; poor (light) to good (dark).</p> <p>STAIN: no visible oil or bitumen staining (light) to heavy staining (dark)</p> <p style="text-align: center;">REMARKS</p>
11106											Sublithic arenite;Frac- v and h/50c/s.



# Chevron Hiko Bell 1-12A2

## 12-T1S-R2W NESWSW

Date logged:

Logged by: MaryBeth Wegner

Ground: 0.00 ft      KB: 5843.00 ft

Remarks: Some of the core is in poor shape. Core diameter is 10 cm (4"). Green River Formation.

### LEGEND

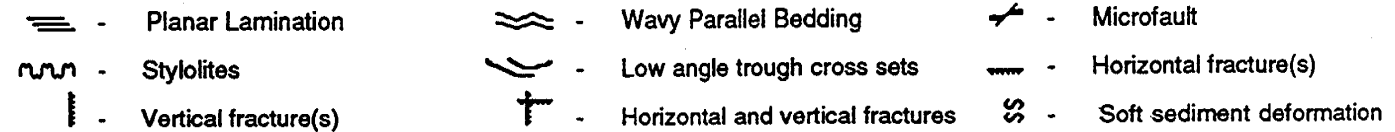
#### LITHOLOGY



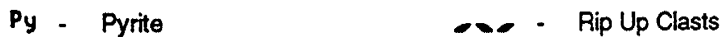
#### CONTACTS



#### PHYSICAL STRUCTURES



#### LITHOLOGIC ACCESSORIES



#### ICHTNOFOSSILS

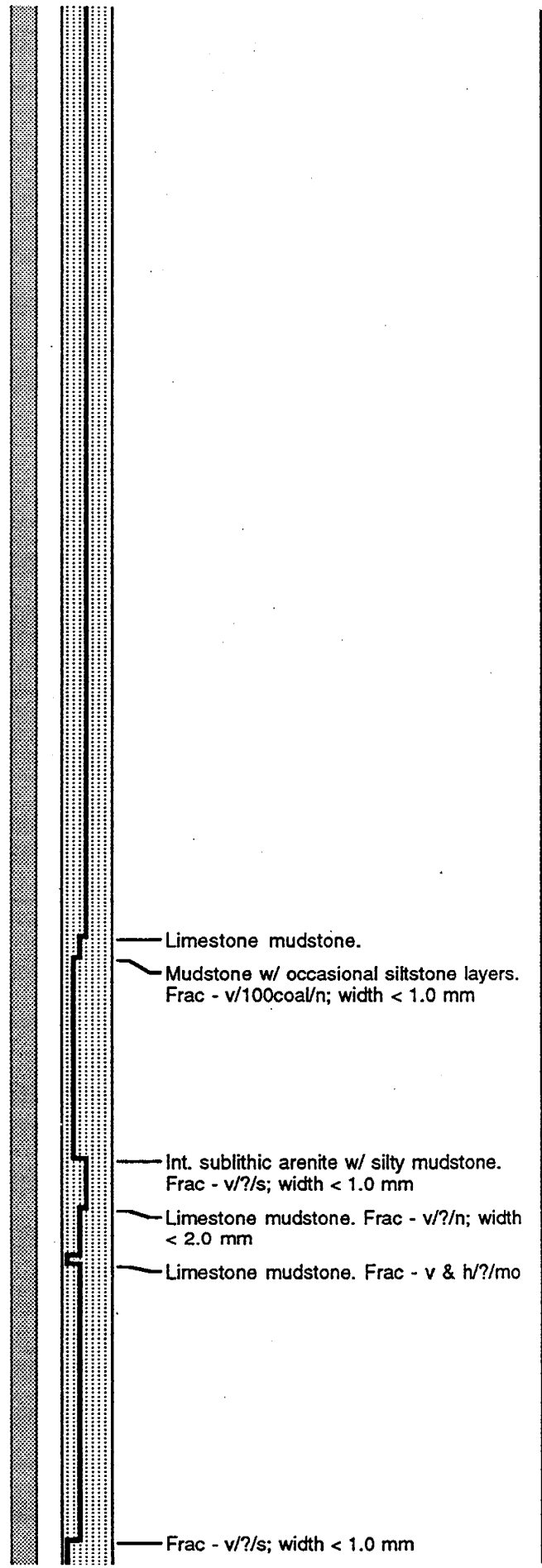
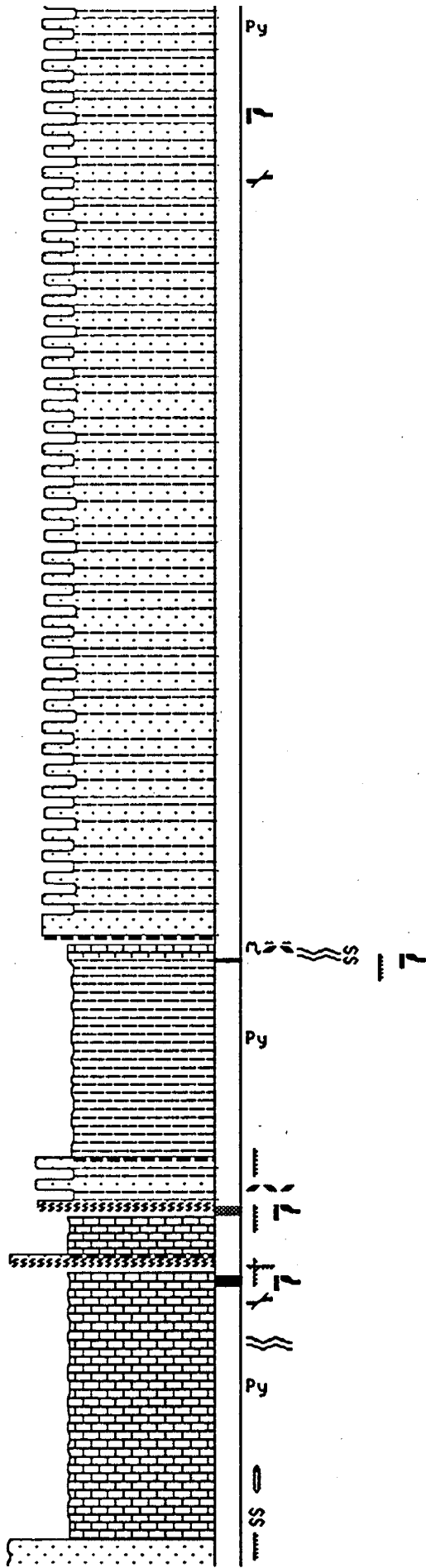


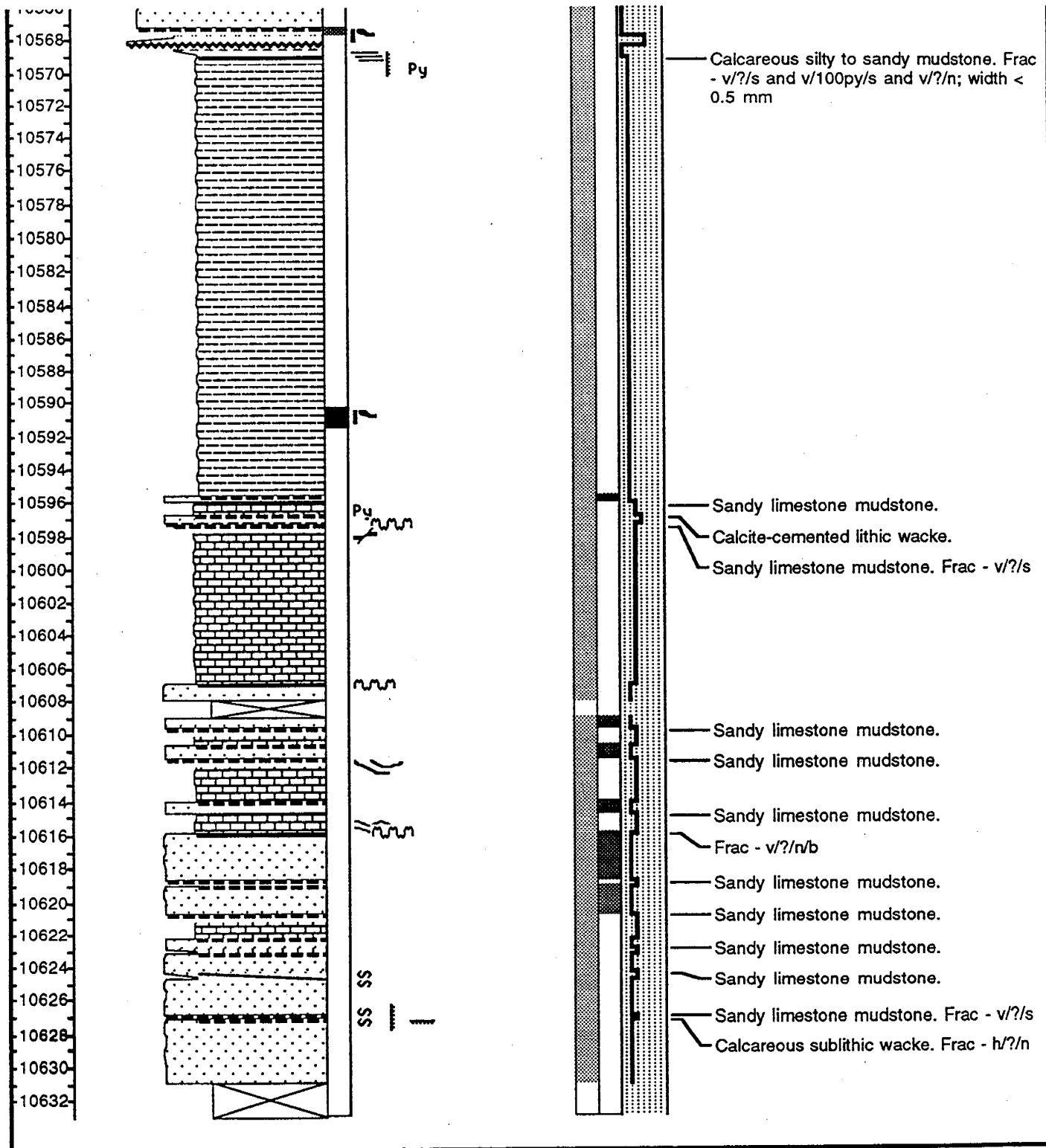
#### FOSSILS



FEET	GRAIN SIZE	BIOTURBATION INTENSITY	PHYSICAL STRUCTURES	ACCESSORIES	ICHTNOFOSSILS	FOSSILS	POROSITY	STAIN	SORTING	REMARKS
	cobble pebble granule sand silt clay vc   mf   v									POROSITY: visual ranking; poor (light) to good (dark).  STAIN: no visible oil or bitumen staining (light) to heavy staining (dark)
										Int. subfeldspathic, sublithic arenite w/ silty mudstone. Frac - h/2/mo and v/2/c

10482  
10484  
10486  
10488  
10490  
10492  
10494  
10496  
10498  
10500  
10502  
10504  
10506  
10508  
10510  
10512  
10514  
10516  
10518  
10520  
10522  
10524  
10526  
10528  
10530  
10532  
10534  
10536  
10538  
10540  
10542  
10544  
10546  
10548  
10550  
10552  
10554  
10556  
10558  
10560  
10562  
10564  
10566





# Chevron 1-7A1 J. Yack Unit 2-70

## 7-T1S-R1W NESW

Date logged:

Logged by: MaryBeth Wegner

Ground: 0.00 ft      KB: 5858.00 ft

Remarks: Core 1 of 2. Core diameter is 6.5 cm (2.5"). Wasatch Formation.

### LEGEND

#### LITHOLOGY



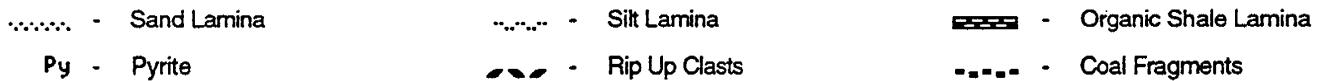
#### CONTACTS



#### PHYSICAL STRUCTURES



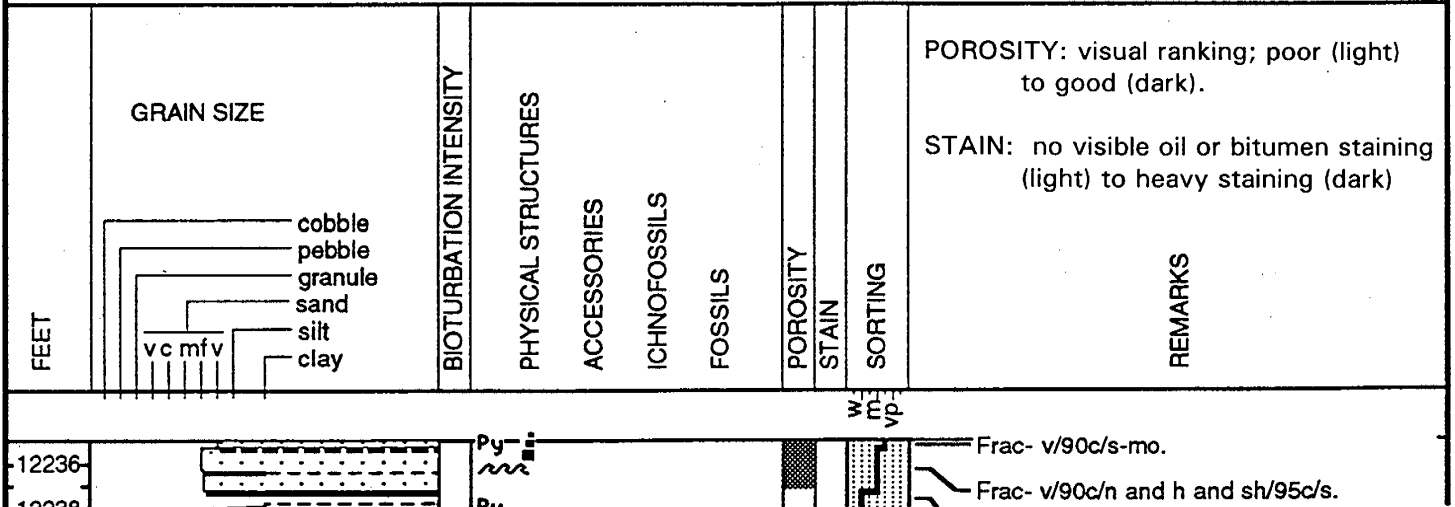
#### LITHOLOGIC ACCESSORIES



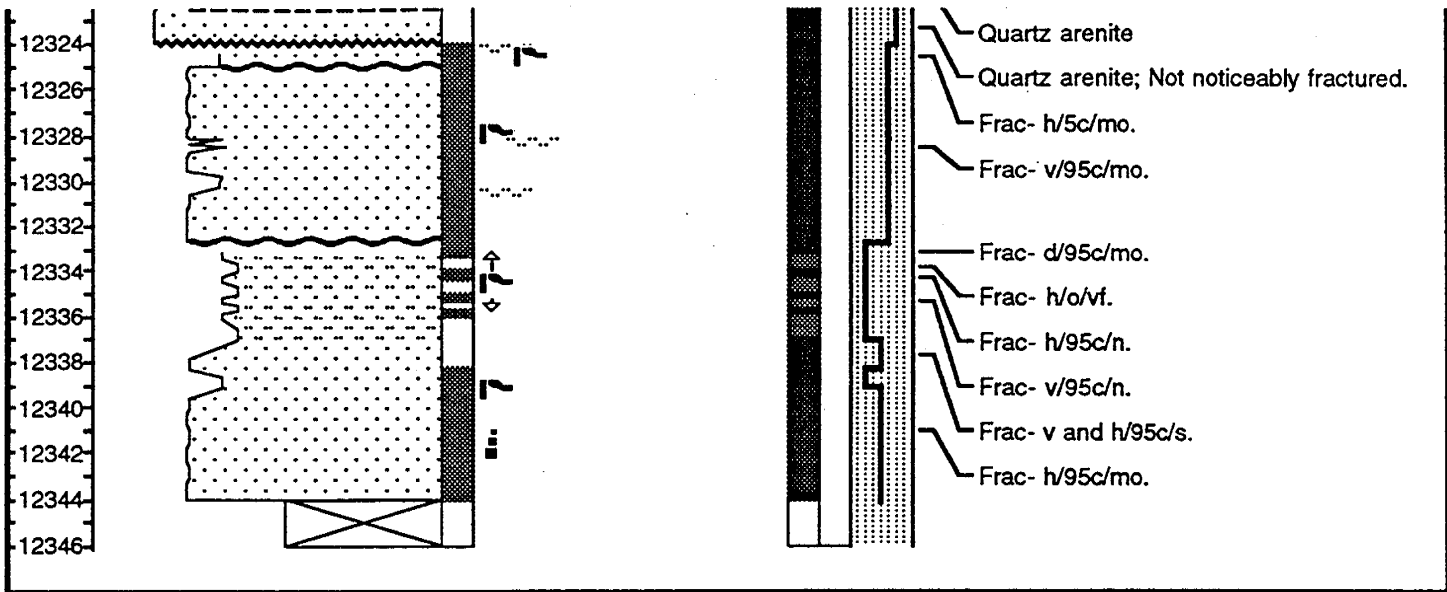
#### ICHTNOFOSSILS



#### FOSSILS







# Chevron 1-7A1 J. Yack Unit 2-70

## 7-T1S-R1W NESW

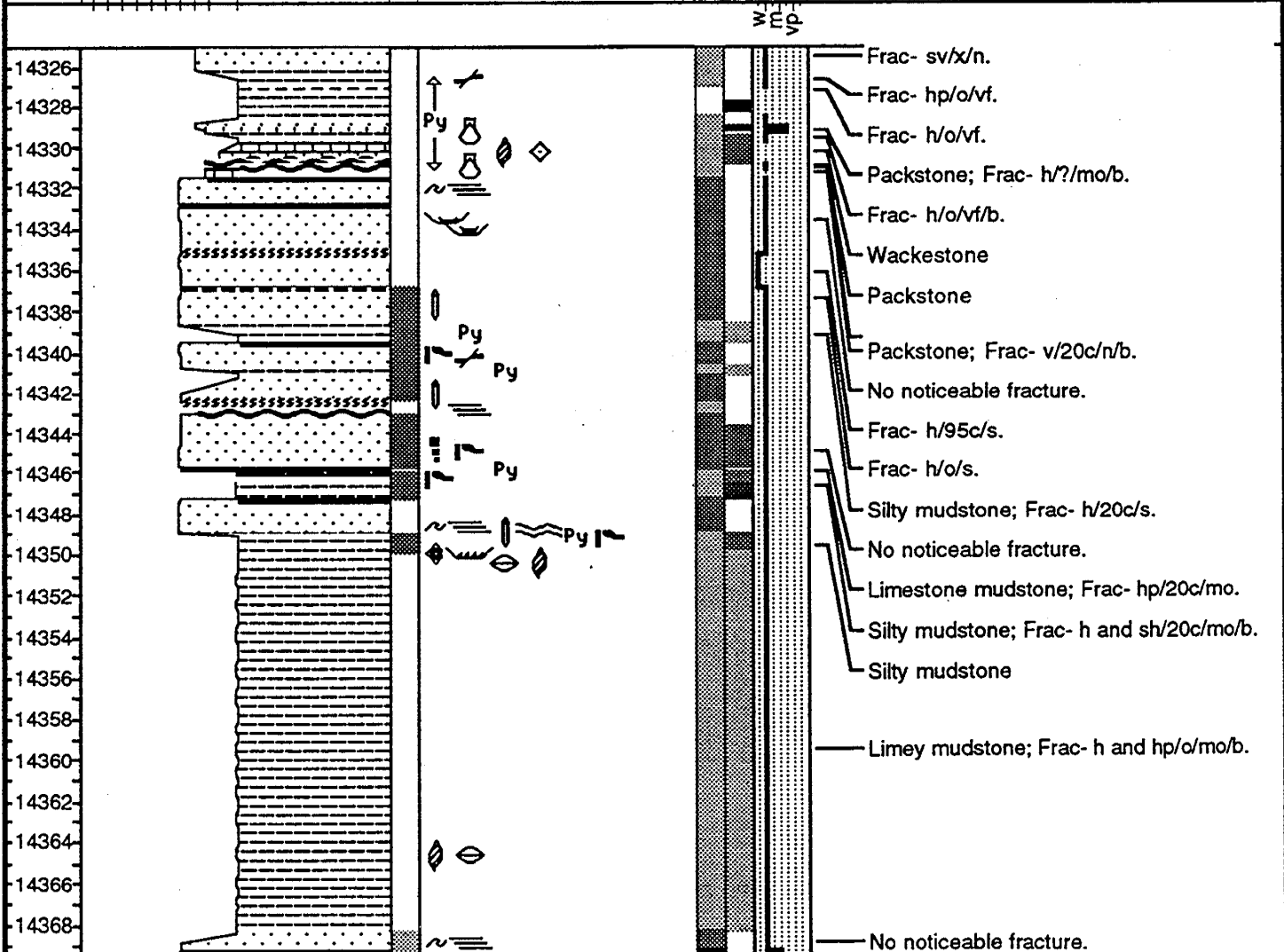
Date logged:

Logged by: MaryBeth Wegner

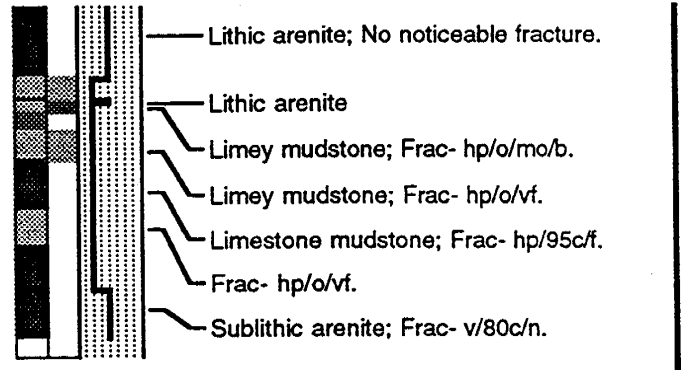
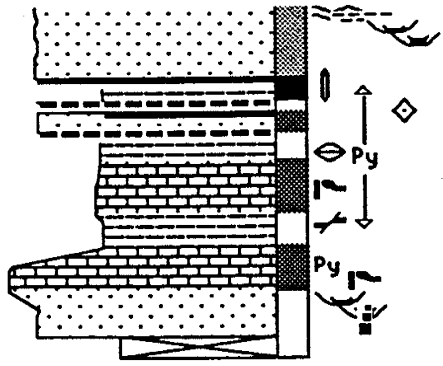
Ground: 0.00 ft      KB: 5858.00 ft

Remarks: Core 2 of 2. Core diameter is 6.5 cm (2.5"). Flagstaff Formation.

FEET	GRAIN SIZE	BIOTURBATION INTENSITY	PHYSICAL STRUCTURES	ACCESSORIES	ICHTHOFOSSILS	FOSSILS	POROSITY	STAIN	SORTING	REMARKS
	<div style="display: flex; align-items: center;"> <div style="width: 10px; height: 10px; border: 1px solid black; margin-right: 5px;"></div> <div style="font-size: 8px;">cobble</div> </div> <div style="display: flex; align-items: center;"> <div style="width: 10px; height: 10px; border: 1px solid black; margin-right: 5px;"></div> <div style="font-size: 8px;">pebble</div> </div> <div style="display: flex; align-items: center;"> <div style="width: 10px; height: 10px; border: 1px solid black; margin-right: 5px;"></div> <div style="font-size: 8px;">granule</div> </div> <div style="display: flex; align-items: center;"> <div style="width: 10px; height: 10px; border: 1px solid black; margin-right: 5px;"></div> <div style="font-size: 8px;">sand</div> </div> <div style="display: flex; align-items: center;"> <div style="width: 10px; height: 10px; border: 1px solid black; margin-right: 5px;"></div> <div style="font-size: 8px;">silt</div> </div> <div style="display: flex; align-items: center;"> <div style="width: 10px; height: 10px; border: 1px solid black; margin-right: 5px;"></div> <div style="font-size: 8px;">clay</div> </div>									POROSITY: visual ranking; poor (light) to good (dark).  STAIN: no visible oil or bitumen staining (light) to heavy staining (dark)



14370  
 14372  
 14374  
 14376  
 14378  
 14380  
 14382  
 14384



# Chevron Chasel Unit 1-18A1

## 18-T1S-R1W CNE

Date logged:

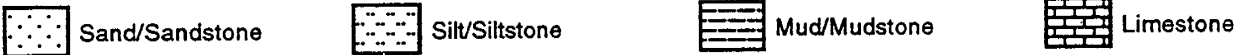
Logged by: MaryBeth Wegner

Ground: 0.00 ft      KB: 5686.00 ft

Remarks: Core 1 of 2. Core diameter is 10 cm (4"). Wasatch Formation.

### LEGEND

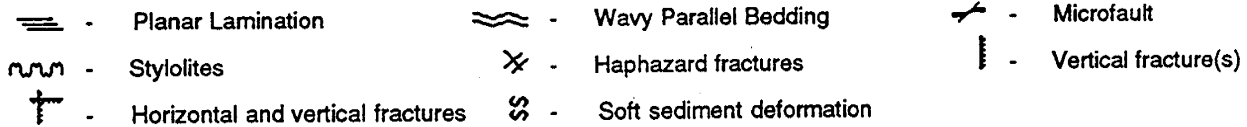
#### LITHOLOGY



#### CONTACTS



#### PHYSICAL STRUCTURES



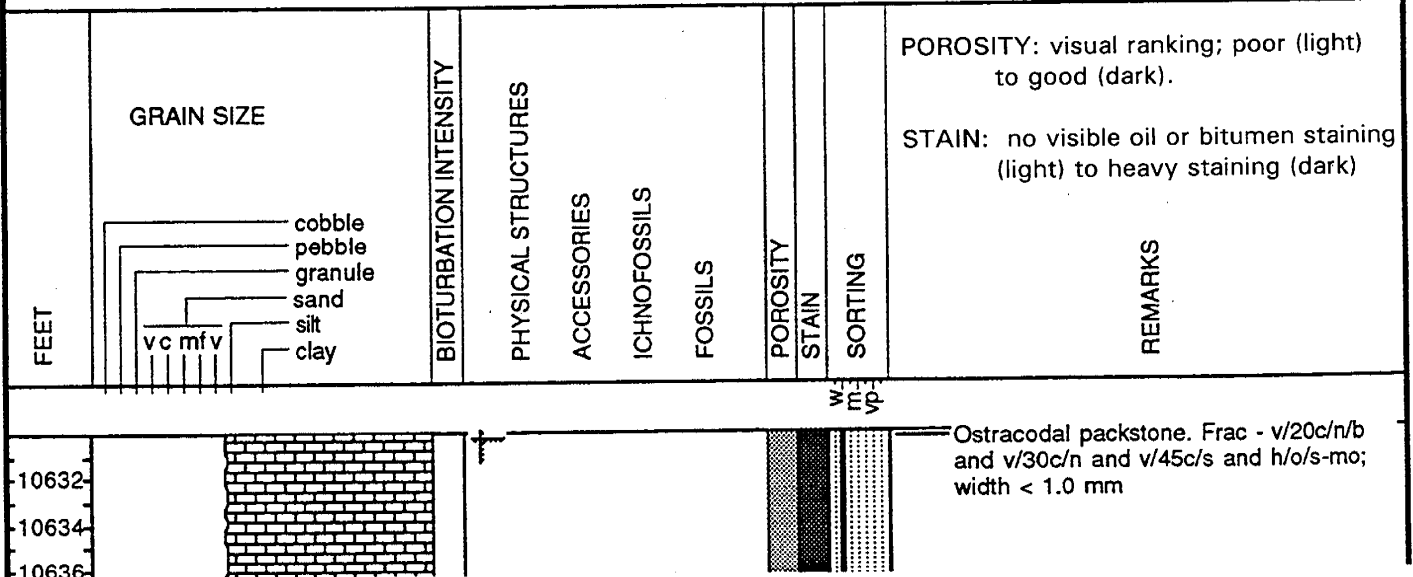
#### LITHOLOGIC ACCESSORIES

Py - Pyrite

#### ICHTNOFOSSILS

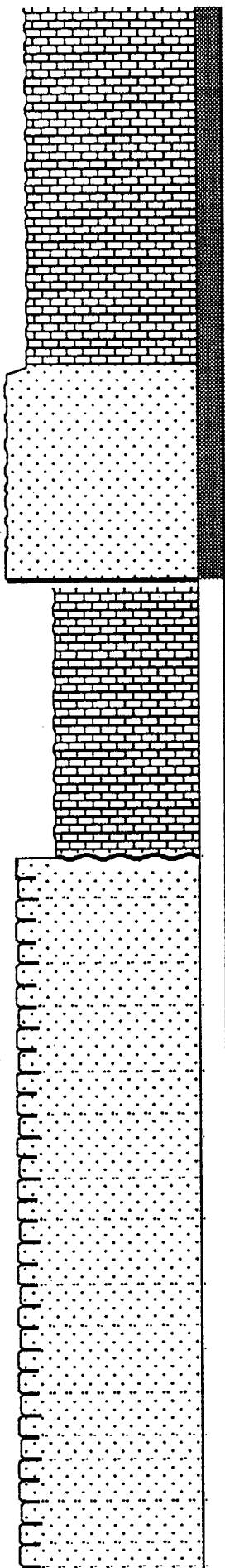


#### FOSSILS



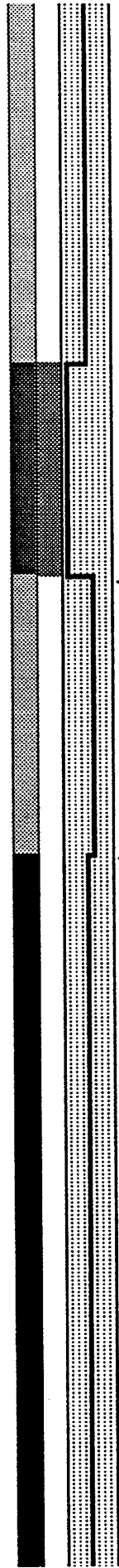


10722  
10724  
10726  
10728  
10730  
10732  
10734  
10736  
10738  
10740  
10742  
10744  
10746  
10748  
10750  
10752  
10754  
10756  
10758  
10760  
10762  
10764  
10766  
10768  
10770  
10772  
10774  
10776  
10778  
10780  
10782  
10784  
10786  
10788  
10790  
10792  
10794  
10796  
10798  
10800  
10802  
10804



ss

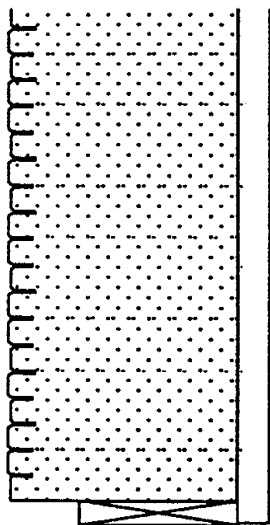
Py



Fossiliferous mudstone. Frac - v and h/o/s

Sublithic wacke. Frac - v & h/90c/f (in ss) and hp/o/very frequent; width < 0.5 mm

10806  
10808  
10810  
10812  
10814  
10816  
10818  
10820  
10822  
10824  
10826  
10828



# Chevron Chasel Unit 1-18A1

## 18-T1S-R1W CNE

Date logged:

Logged by: MaryBeth Wegner

Ground: 0.00 ft      KB: 5686.00 ft

Remarks: Core 2 of 2. Core diameter is 10 cm (4"). Wasatch Formation.

### LEGEND

#### LITHOLOGY

 Sand/Sandstone

#### CONTACTS

 Bioturbated       Undulating

#### PHYSICAL STRUCTURES

 - Haphazard fractures

 - Vertical fracture(s)

 - Horizontal and vertical fractures

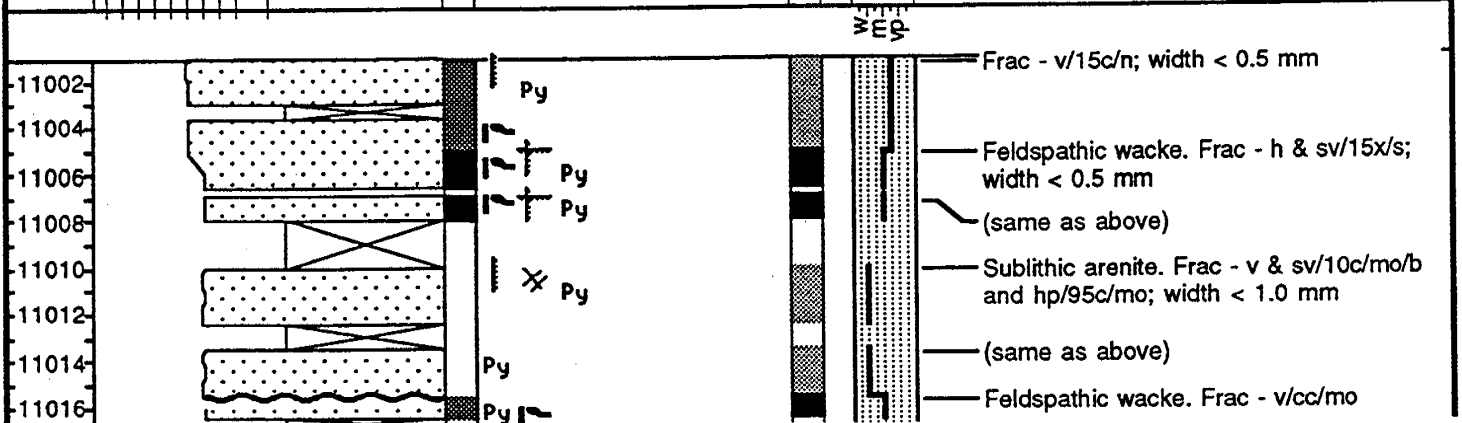
#### LITHOLOGIC ACCESSORIES

Py - Pyrite

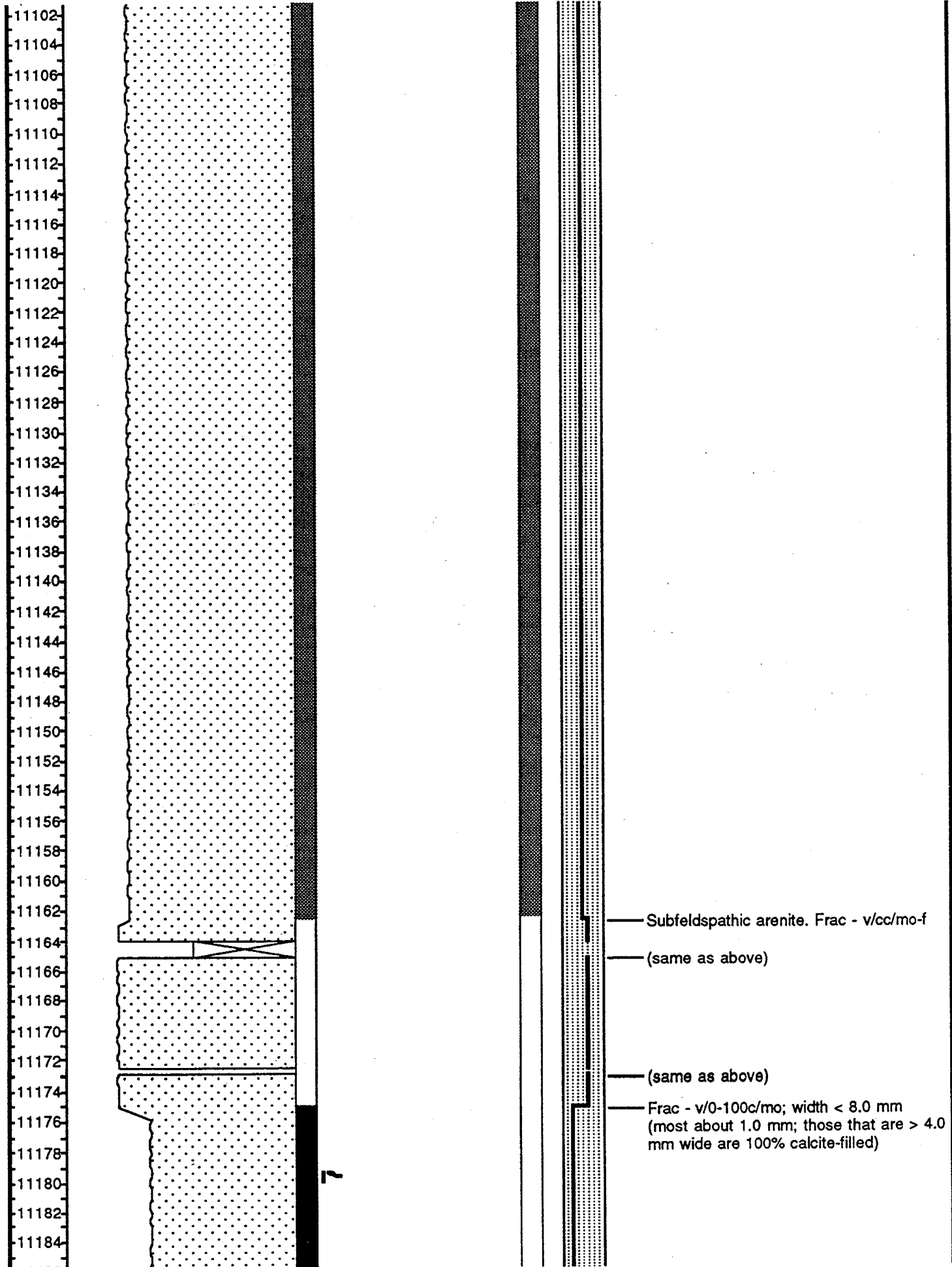
#### ICHTNOFOSSILS

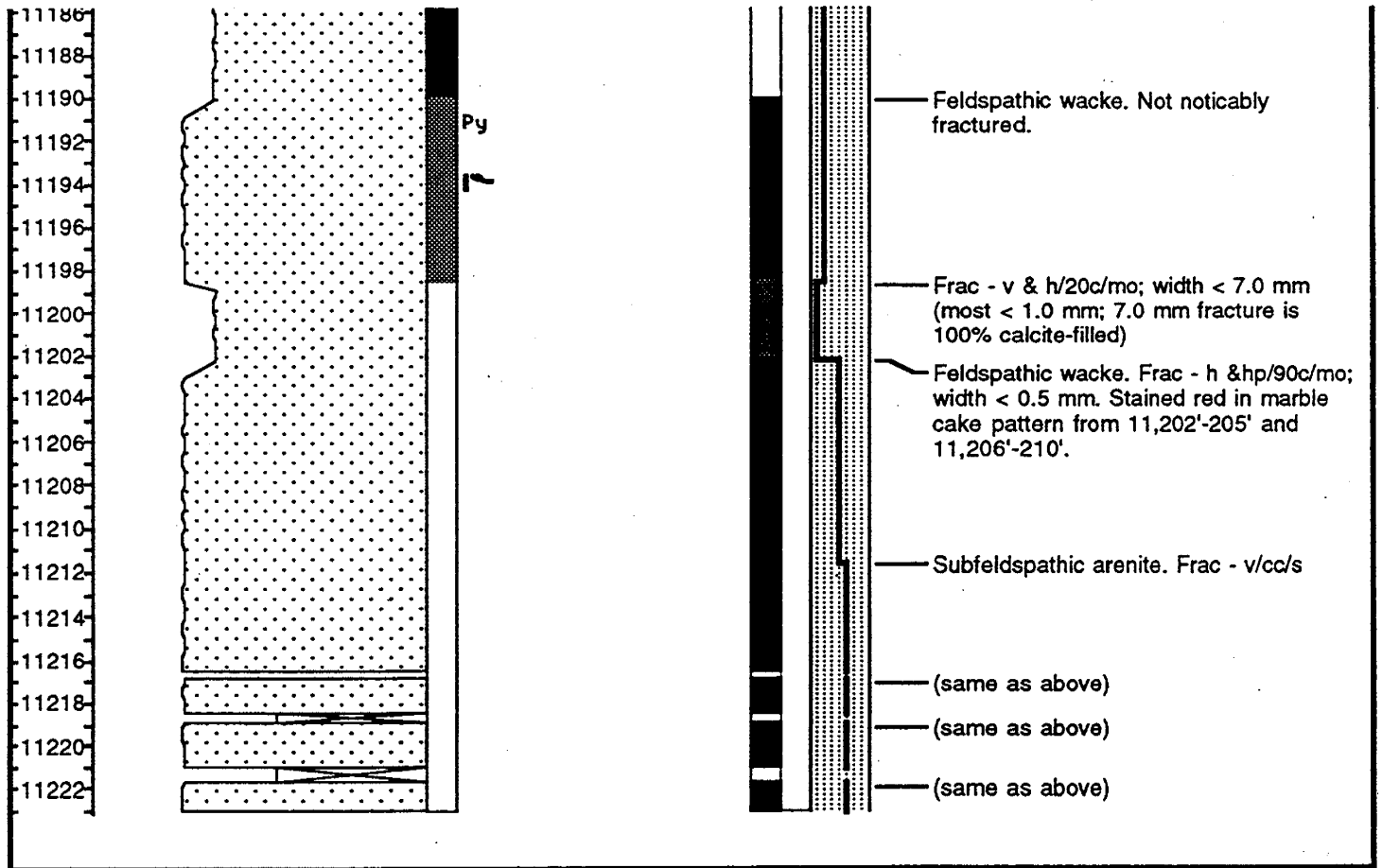
 - Undifferentiated Bioturbation

FEET	GRAIN SIZE	BIOTURBATION INTENSITY	PHYSICAL STRUCTURES	ACCESSORIES	ICHTNOFOSSILS	FOSSILS	POROSITY	STAIN	SORTING	REMARKS
	<ul style="list-style-type: none"> <li>_____ cobble</li> <li>_____ pebble</li> <li>_____ granule</li> <li>_____ sand</li> <li>_____ silt</li> <li>_____ clay</li> </ul>									POROSITY: visual ranking; poor (light) to good (dark).  STAIN: no visible oil or bitumen staining (light) to heavy staining (dark)









# Chevron 1-24 L. Boren Unit

## 24-T1S-R2W SENW

Date logged:

Logged by: MaryBeth Wegner

Ground: 0.00 ft      KB: 5577.00 ft

Remarks: Core diameter is 6.5 cm (2.5").

### LEGEND

#### LITHOLOGY



Sand/Sandstone



Silty Sand



Limestone

#### CONTACTS

— Sharp

#### PHYSICAL STRUCTURES

— Horizontal fracture(s)

✕ - Haphazard fractures

⋮ - Vertical fracture(s)

#### LITHOLOGIC ACCESSORIES

Py - Pyrite

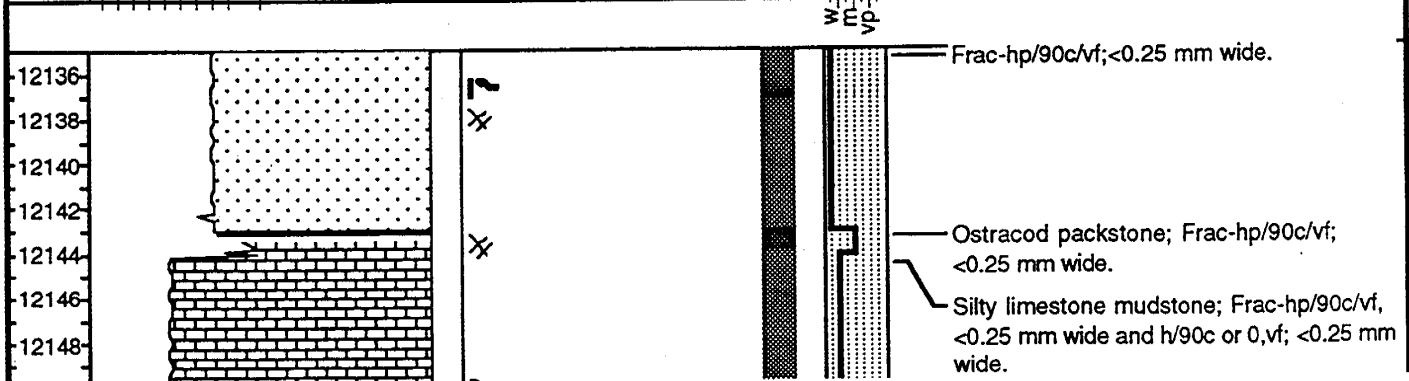
#### ICHTNOFOSSILS

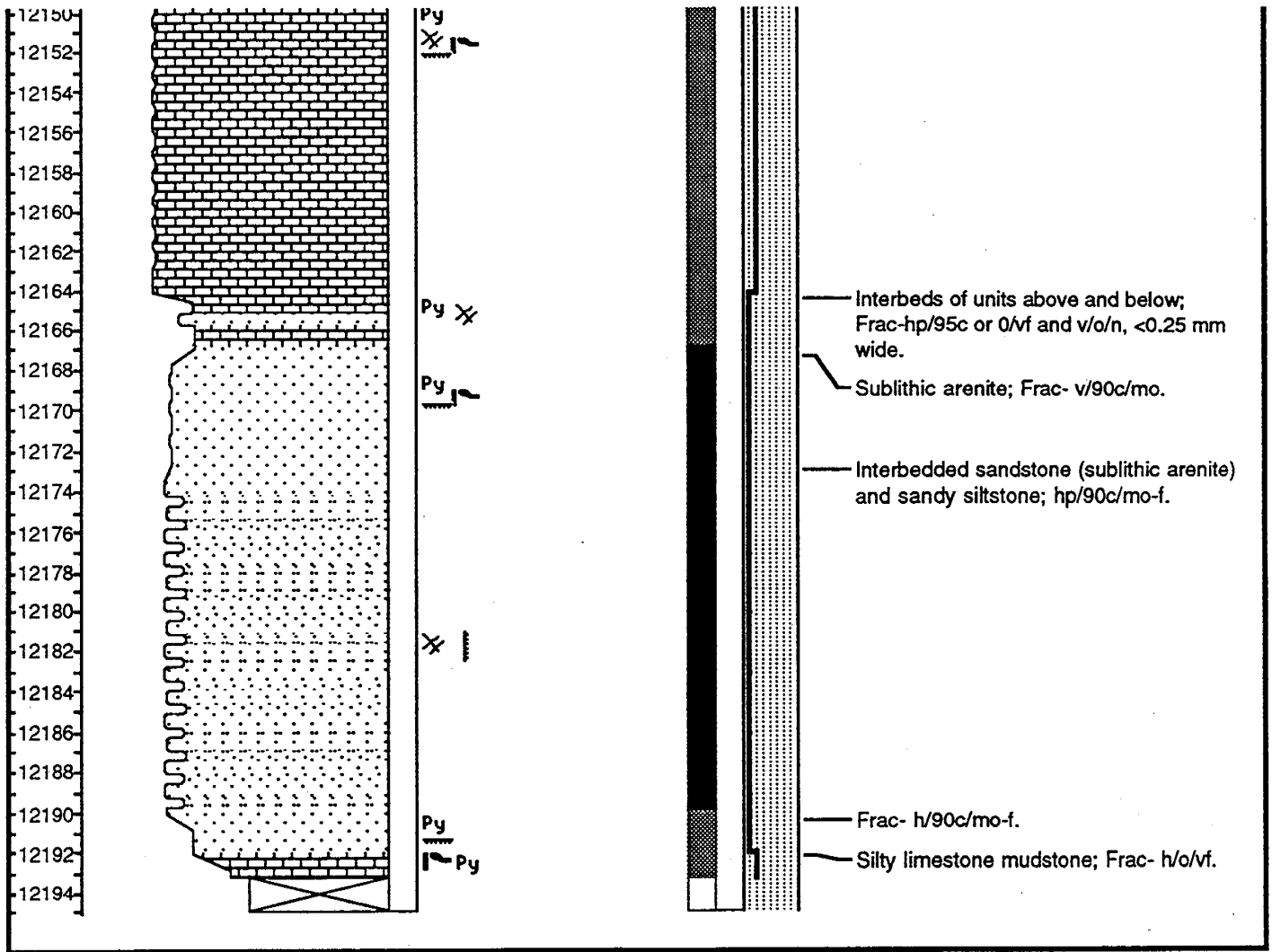
— Undifferentiated Bioturbation

POROSITY: visual ranking; poor (light) to good (dark).

STAIN: no visible oil or bitumen staining (light) to heavy staining (dark)

FEET	GRAIN SIZE	BIOTURBATION INTENSITY	PHYSICAL STRUCTURES	ACCESSORIES	ICHTNOFOSSILS	FOSSILS	POROSITY	STAIN	SORTING	REMARKS
	<ul style="list-style-type: none"> <li>— cobble</li> <li>— pebble</li> <li>— granule</li> <li>— sand</li> <li>— silt</li> <li>— clay</li> </ul>									





## Chevron 9-4B1 Ute Tribal 4-T2S-R1W SENW

Date logged:

Logged by: MaryBeth Wegner

Ground: 0.00 ft      KB: 5284.00 ft

Remarks: Core 1 of 3: 11,006' - 11,143'. Core diameter is 6.5 cm (2.5"). Wasatch Formation.

### LEGEND

#### LITHOLOGY



Sand/Sandstone



Mud/Mudstone



Limestone

#### CONTACTS

Sharp

Bioturbated

Uncertain

Undulating

Inclined

#### PHYSICAL STRUCTURES

- Ripple Lamination

- Planar Lamination

- Microfault

- Horizontal fracture(s)

- Haphazard fractures

- Vertical fracture(s)

- Horizontal and vertical fractures

- Soft sediment deformation

#### LITHOLOGIC ACCESSORIES

- Calcareous

**Py** - Pyrite

- Rip Up Clasts

#### ICHTNOFOSSILS

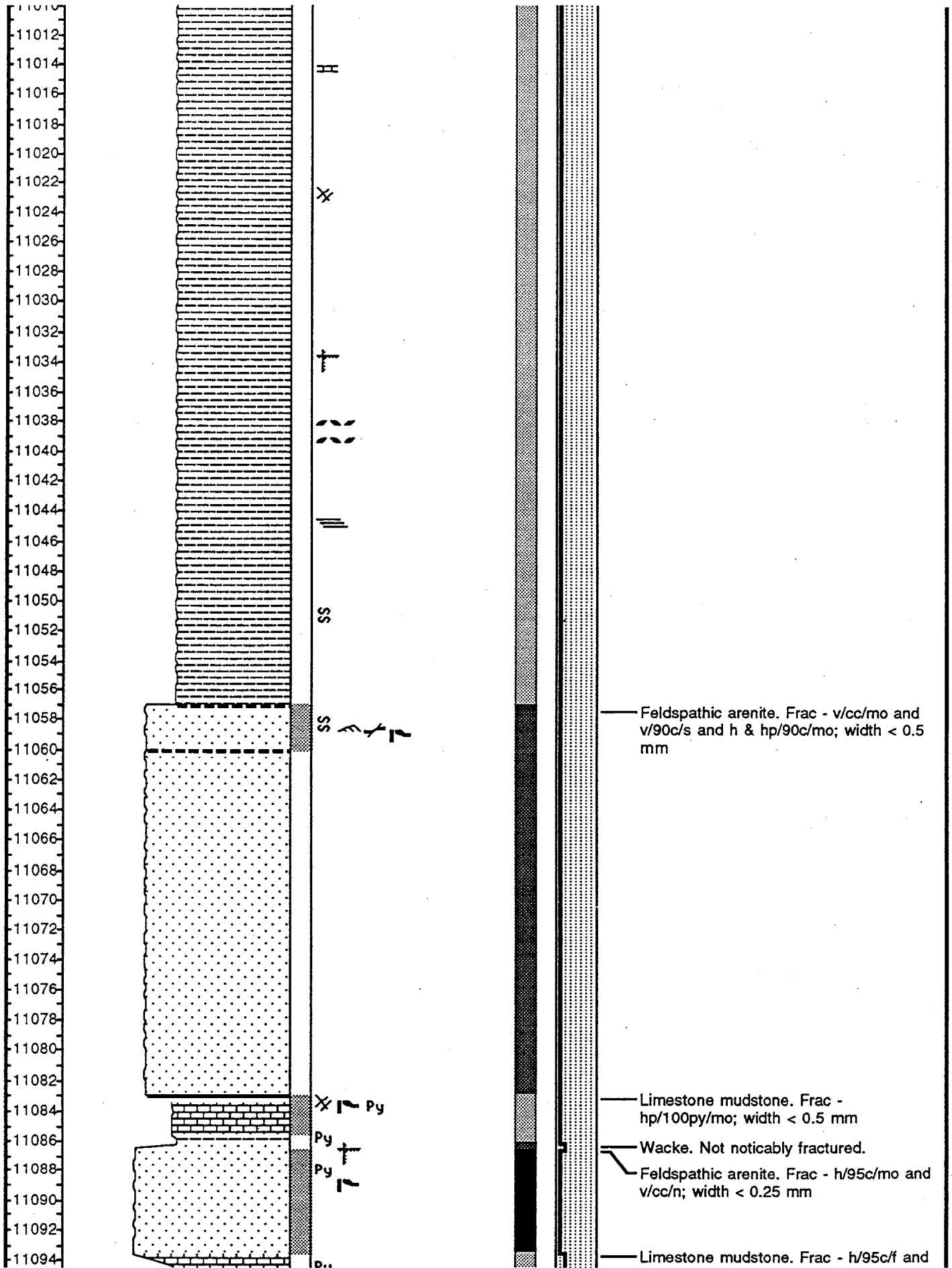
- Undifferentiated Bioturbation

#### FOSSILS

- Molluscs (undifferentiated)

- Fossils (undifferentiated)

FEET	GRAIN SIZE	BIOTURBATION INTENSITY	PHYSICAL STRUCTURES	ACCESSORIES	ICHTNOFOSSILS	FOSSILS	POROSITY	STAIN	SORTING	REMARKS
11008 11010	<div style="display: flex; justify-content: space-between;"> <div style="width: 40%;"> <p>vc mfv</p> <p>cobble</p> <p>pebble</p> <p>granule</p> <p>sand</p> <p>silt</p> <p>clay</p> </div> <div style="width: 60%;"> <p>POROSITY: visual ranking; poor (light) to good (dark).</p> <p>STAIN: no visible oil or bitumen staining (light) to heavy staining (dark)</p> </div> </div>									<p>Silty mudstone. Frac - h/o/vf and v/o/s and hp/o/f; width &lt; 0.25 mm.</p>





## Chevron C9-4B1 Ute Tribal 4-T2S-R1W SENW

Date logged:

Logged by: MaryBeth Wegner

Ground: 0.00 ft      KB: 5284.00 ft

Remarks: Core 2 of 3: 11,500'- 11,595'. Core diameter is 6.5 cm (2.5"). Wasatch Formation.

### LEGEND

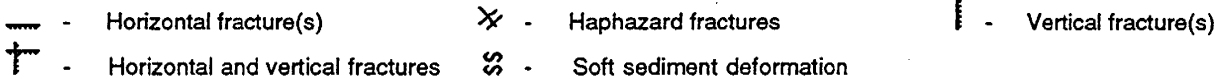
#### LITHOLOGY



#### CONTACTS



#### PHYSICAL STRUCTURES



#### LITHOLOGIC ACCESSORIES

Py - Pyrite

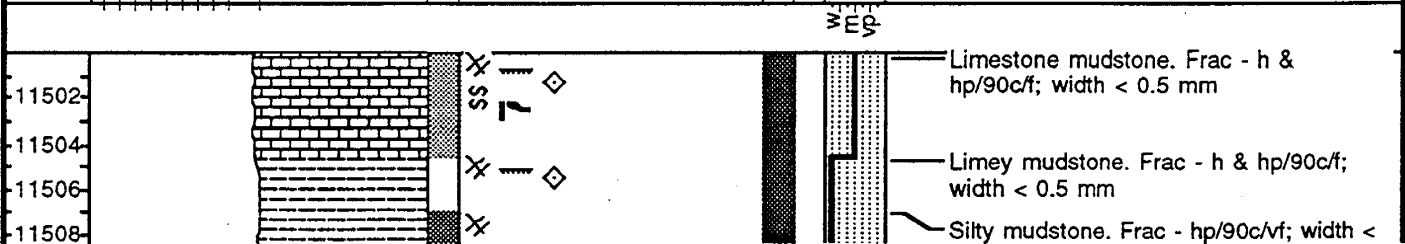
#### ICHTNOFOSSILS

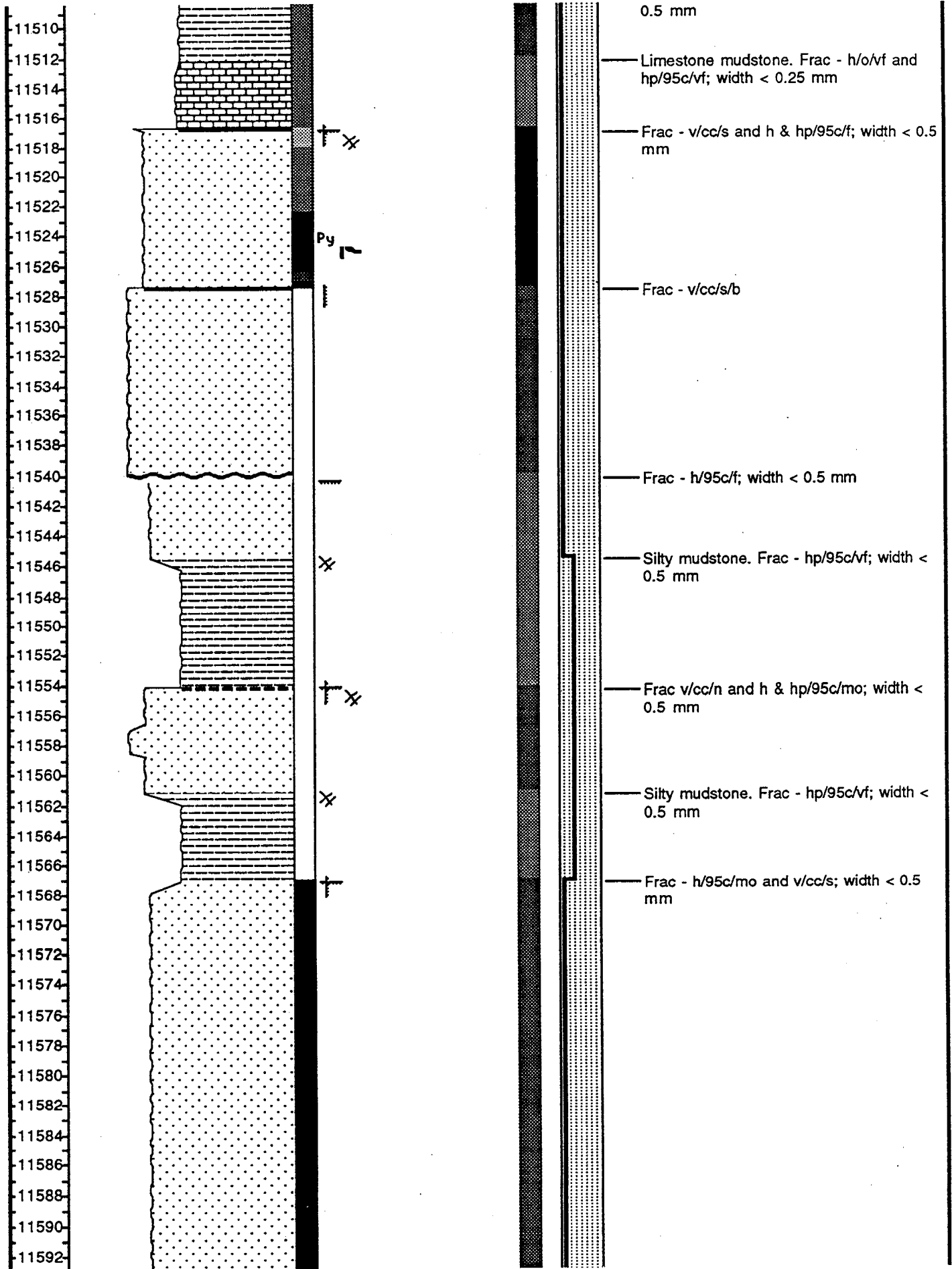
U - Undifferentiated Bioturbation

#### FOSSILS

F - Fossils (undifferentiated)

FEET	GRAIN SIZE	BIOTURBATION INTENSITY	PHYSICAL STRUCTURES	ACCESSORIES	ICHTNOFOSSILS	FOSSILS	POROSITY	STAIN	SORTING	REMARKS
	cobble pebble granule sand silt clay vc mf v									POROSITY: visual ranking; poor (light) to good (dark).  STAIN: no visible oil or bitumen staining (light) to heavy staining (dark)





11594  
11596



# Chevron 9-4B1 Ute Tribal 4-T2S-R1W SENW

Date logged:

Logged by: MaryBeth Wegner

Ground: 0.00 ft      KB: 5284.00 ft

Remarks: Core 3 of 3: 12,651' - 12,769'. Core diameter is 6.5 cm (2.5"). Wasatch Formation.

## LEGEND

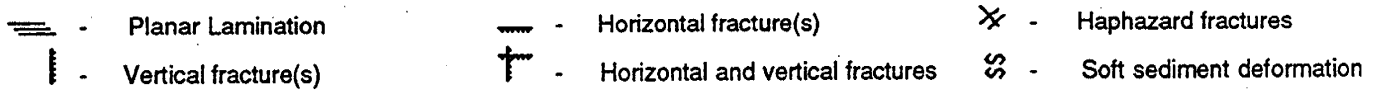
### LITHOLOGY



### CONTACTS



### PHYSICAL STRUCTURES



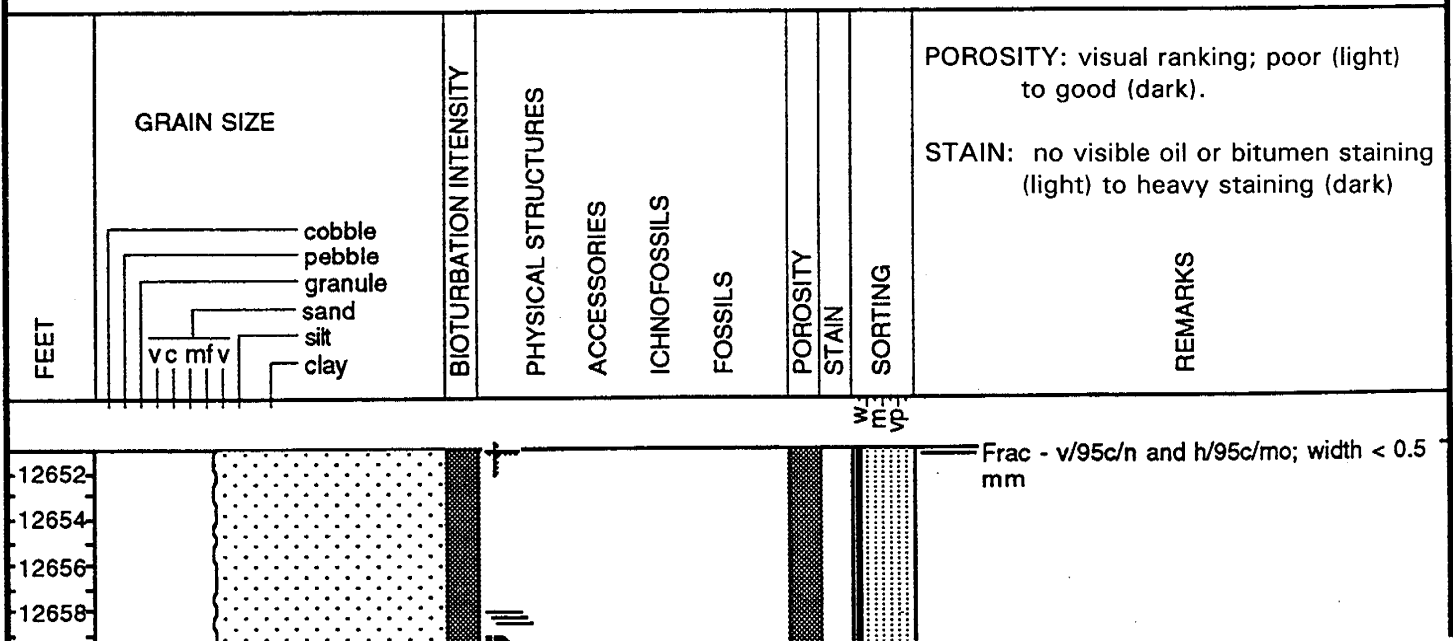
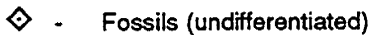
### LITHOLOGIC ACCESSORIES

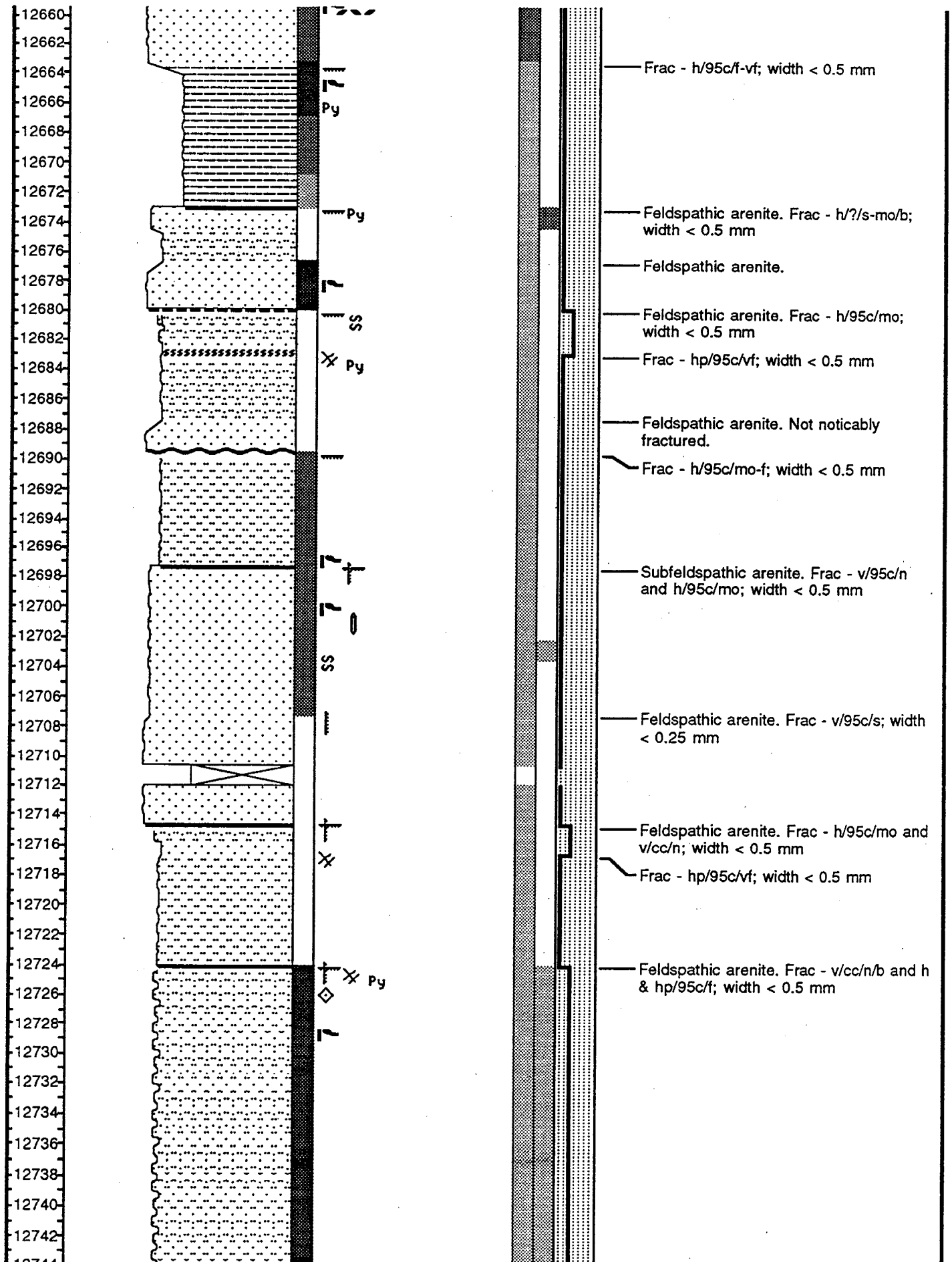


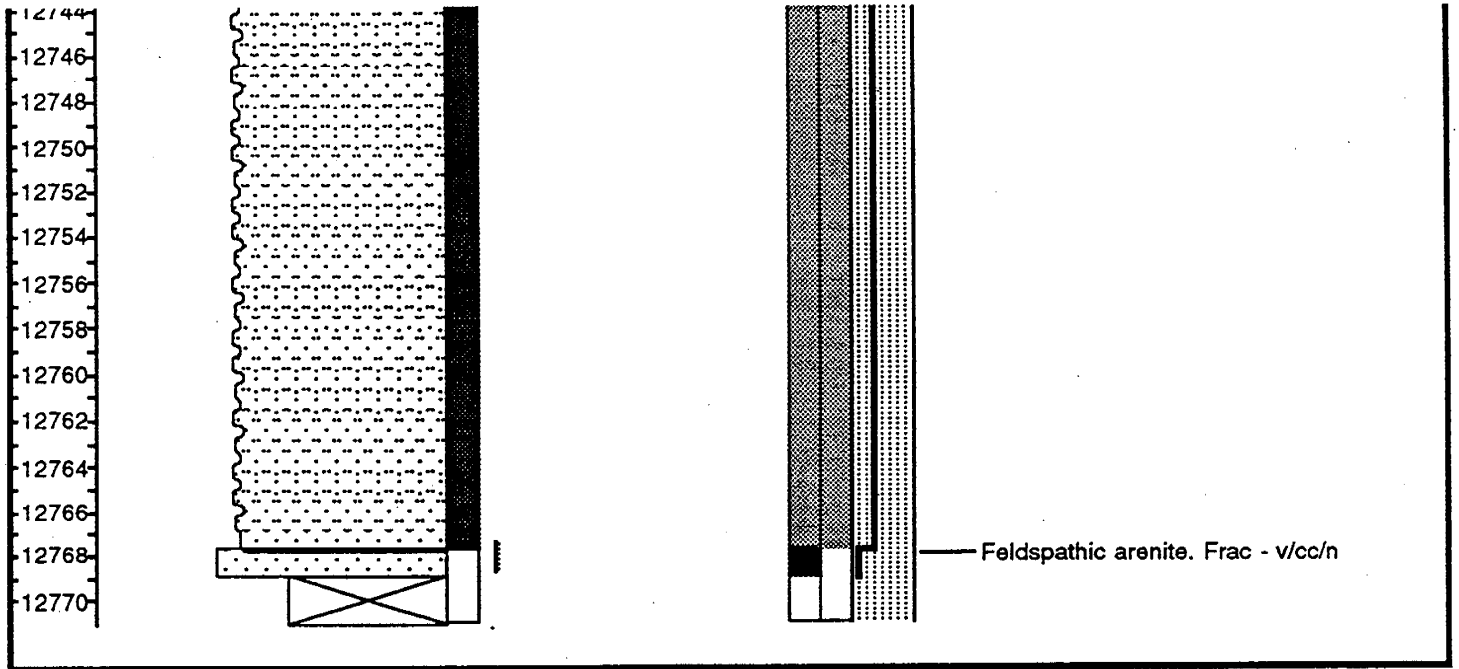
### ICHTNOFOSSILS



### FOSSILS







# Quinex Leslie Taylor 24-T1S-R1W SENW

Date logged:

Logged by: MaryBeth Wegner

Ground: 0.00 ft      KB: 5518.00 ft

Remarks: This core is a full, cylindrical core. Therefore the drill marks on the outside make features unclear. Contacts and sedimentary structures were difficult to impossible to determine. Wasatch Formation.

## LEGEND

### LITHOLOGY



### CONTACTS



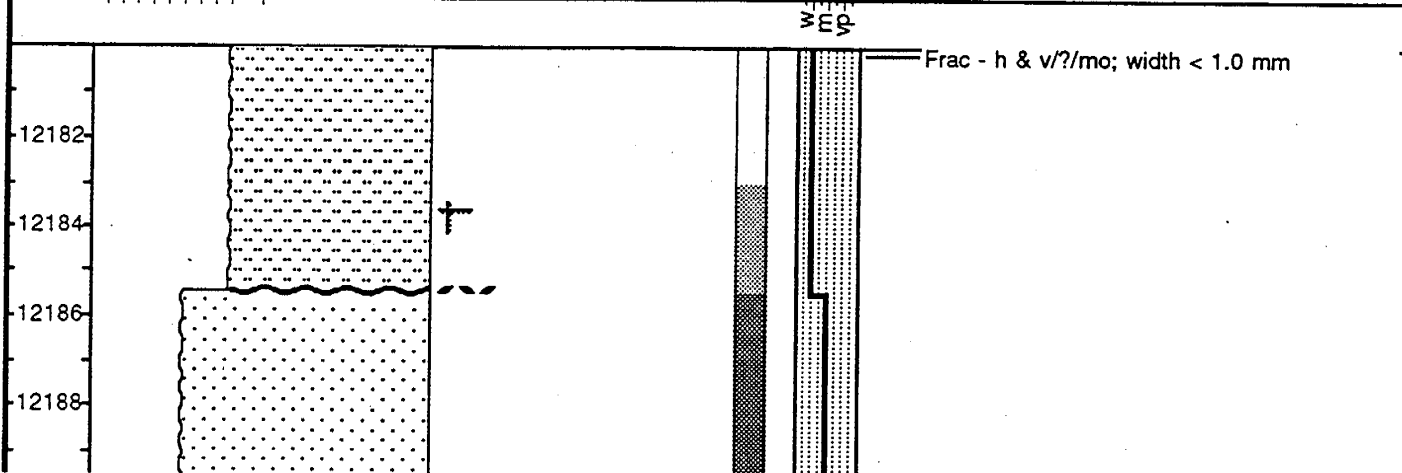
### PHYSICAL STRUCTURES

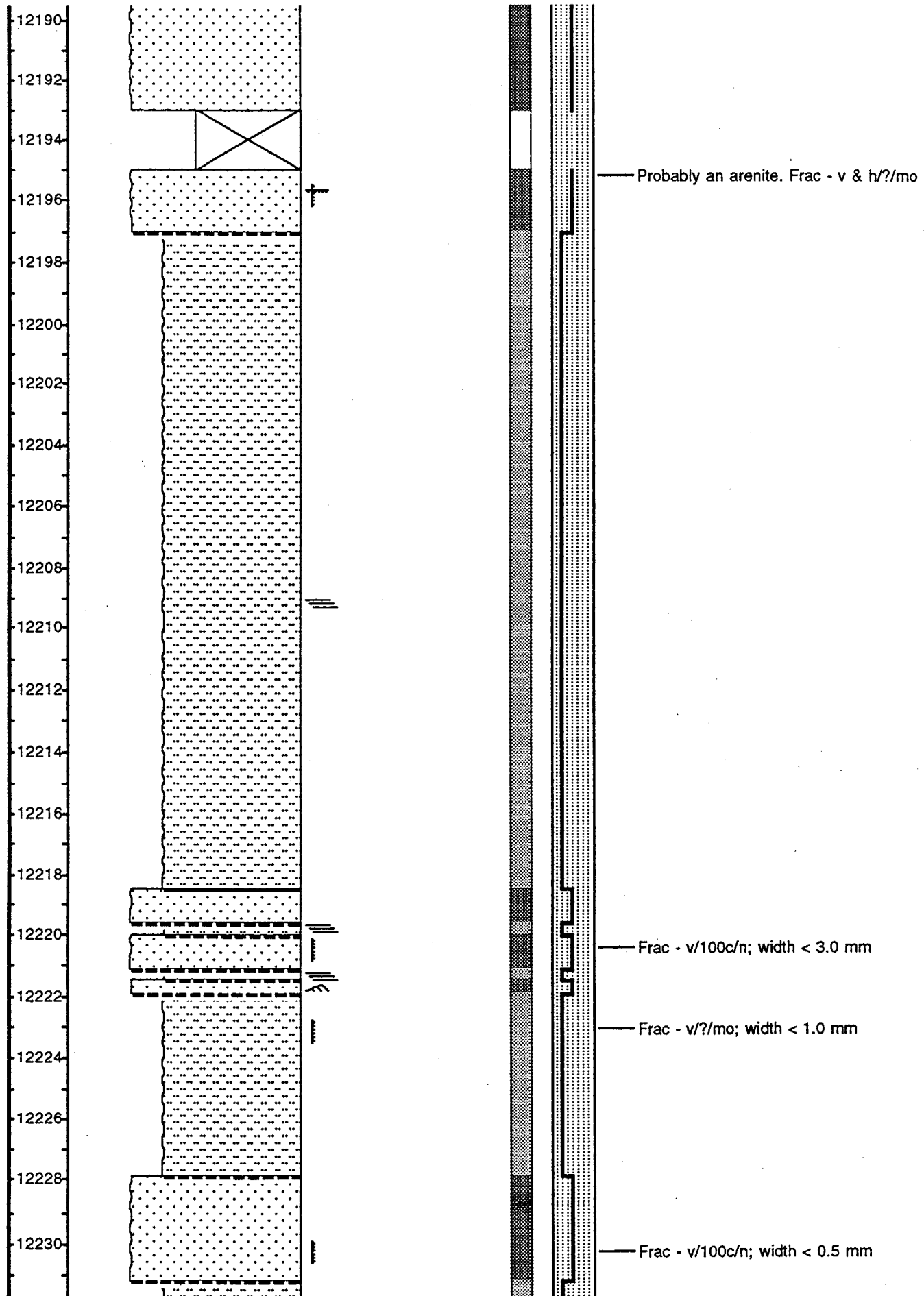


### LITHOLOGIC ACCESSORIES

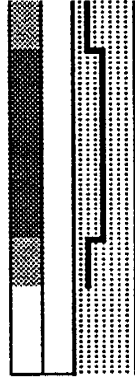
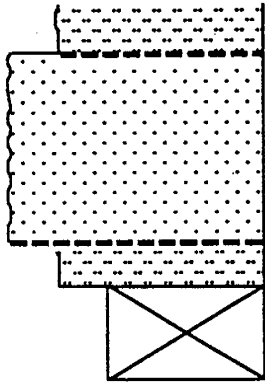


FEET	GRAIN SIZE	PHYSICAL STRUCTURES	ACCESSORIES	ICHNOFOSSILS	FOSSILS	POROSITY	STAIN	SORTING	REMARKS
	<ul style="list-style-type: none"> <li>— cobble</li> <li>— pebble</li> <li>— granule</li> <li>— sand</li> <li>— silt</li> <li>— clay</li> </ul>								POROSITY: visual ranking; poor (light) to good (dark). STAIN: no visible oil or bitumen staining (light) to heavy staining (dark)





12232  
12234  
12236  
12238  
12240



# Bow Valley Petroleum 2-19A1E D.R. Long 19-T1S-R1E SWSE

Date logged:

Logged by: MaryBeth Wegner

Ground: 0.00 ft      KB: 5450.00 ft

Remarks: Core 1 of 2. Core diameter is 8.75 cm (3.5"). Green River Formation.

## LEGEND

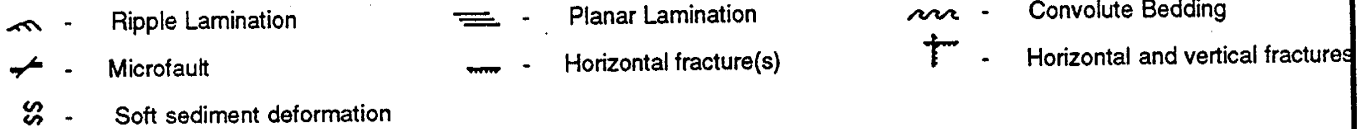
### LITHOLOGY



### CONTACTS



### PHYSICAL STRUCTURES



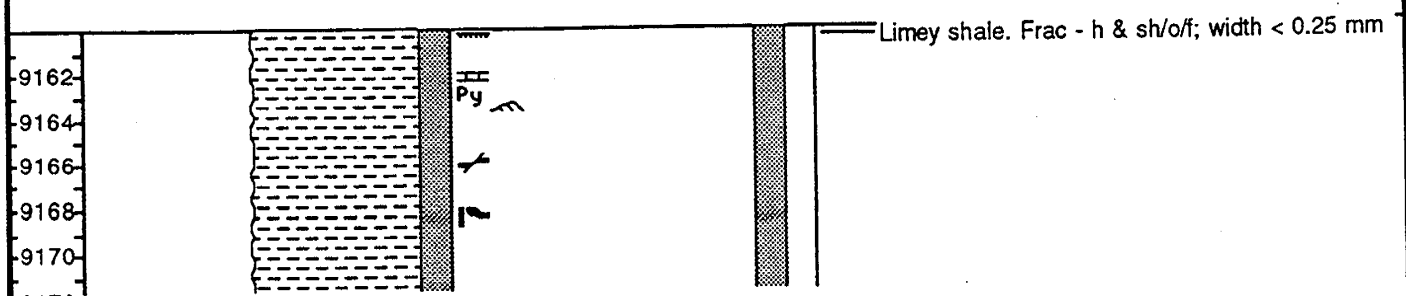
### LITHOLOGIC ACCESSORIES



### ICHTNOFOSSILS



FEET	GRAIN SIZE	BIOTURBATION INTENSITY	PHYSICAL STRUCTURES	ACCESSORIES	ICHTNOFOSSILS	FOSSILS	POROSITY	STAIN	REMARKS
	<ul style="list-style-type: none"> <li>— cobble</li> <li>— pebble</li> <li>— granule</li> <li>— sand</li> <li>— silt</li> <li>— clay</li> </ul>								POROSITY: visual ranking; poor (light) to good (dark).  STAIN: no visible oil or bitumen staining (light) to heavy staining (dark)





# Bow Valley Petroleum 2-19A1E D.R. Long 19-T1S-R1E SWSE

Date logged:

Logged by: MaryBeth Wegner

Ground: 0.00 ft      KB: 5450.00 ft

Remarks: Core 2 of 2. Core diameter is 8.75 cm (3.5"). Green River Formation.

## LEGEND

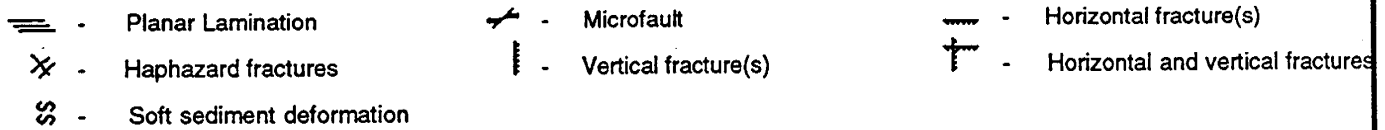
### LITHOLOGY



### CONTACTS



### PHYSICAL STRUCTURES



### LITHOLOGIC ACCESSORIES

Py - Pyrite

### ICHTNOFOSSILS

U - Undifferentiated Bioturbation

### FOSSILS

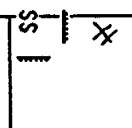
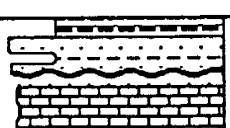
◆ - Carbonized fossils (undifferentiated)

POROSITY: visual ranking; poor (light) to good (dark).

STAIN: no visible oil or bitumen staining (light) to heavy staining (dark)

FEET	GRAIN SIZE	BIOTURBATION INTENSITY	PHYSICAL STRUCTURES	ACCESSORIES	ICHTNOFOSSILS	FOSSILS	POROSITY	STAIN	REMARKS
	<ul style="list-style-type: none"> <li>— cobble</li> <li>— pebble</li> <li>— granule</li> <li>— sand</li> <li>— silt</li> <li>— clay</li> </ul>								

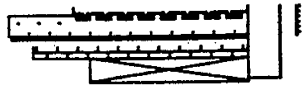
9630  
9632



Frac - v/100c/s; width < 0.25 mm  
Frac - h/o/vf  
Quartz arenite. Frac - h/o/mo; width < 0.5 mm



9718  
9720



— Frac - v/cc/n  
— Ostracodal packstone.

# Bow Valley Petroleum Ute 2-22A1E

## 22-T1S-R1E SWNE

Date logged:

Logged by: MaryBeth Wegner

Ground: 0.00 ft      KB: 5375.00 ft

Remarks: The core is in poor condition, especially in the shaley units, therefore it is difficult to measure accurately. Core diameter is 6.5 cm (2.5"). Wasatch Formation.

### LEGEND

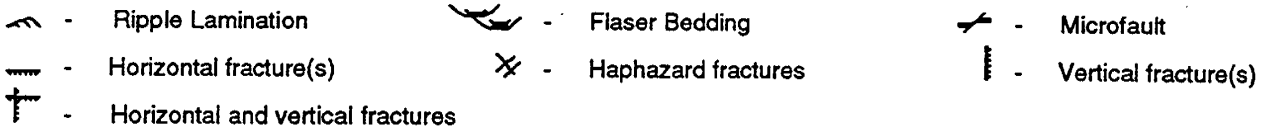
#### LITHOLOGY



#### CONTACTS

----- Uncertain

#### PHYSICAL STRUCTURES



#### LITHOLOGIC ACCESSORIES

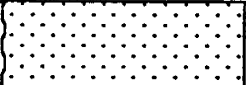


#### ICHTNOFOSSILS

 - Undifferentiated Bioturbation

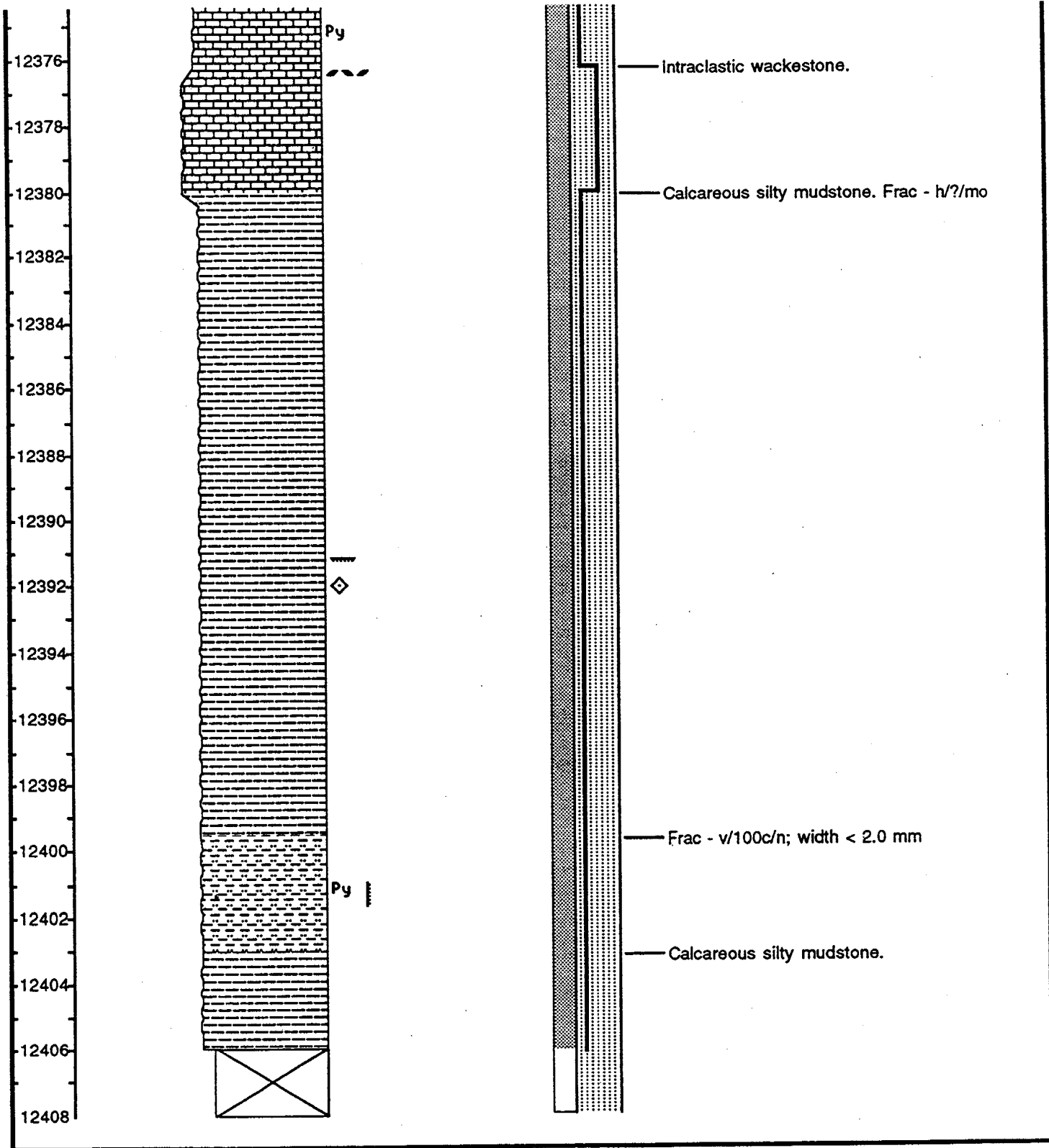
#### FOSSILS



	GRAIN SIZE	PHYSICAL STRUCTURES	ACCESSORIES	ICHTNOFOSSILS	FOSSILS	POROSITY	SORTING	REMARKS
FEET	<div style="display: flex; justify-content: space-between;"> <div style="writing-mode: vertical-rl; transform: rotate(180deg);">vc</div> <div style="writing-mode: vertical-rl; transform: rotate(180deg);">mf</div> <div style="writing-mode: vertical-rl; transform: rotate(180deg);">v</div> </div> <div style="margin-top: 10px;"> <p>cobble</p> <p>pebble</p> <p>granule</p> <p>sand</p> <p>silt</p> <p>clay</p> </div>							<p>POROSITY: visual ranking; poor (light) to good (dark).</p> <p>STAIN: no visible oil or bitumen staining (light) to heavy staining (dark)</p>
								<p>Sublithic wacke.</p>







**APPENDIX B**  
**Petrographic Descriptions of Samples from Nine Cores**  
**(tenth core not available for sampling).**

**Petrographic Descriptions of Lower Green River, Wasatch,  
and Flagstaff Formation Samples Taken from Nine  
Cores in Bluebell Field, Uinta Basin, Utah**

Descriptions are listed from cores west to east (see cross-section, Figure 4.4).

**Chevron (Pennzoil) 3-17A2 Lamicq Urruty; Flagstaff Formation**

P17 13,584--Fossiliferous wackestone to packstone with fragments of ostracods, gastropods, and bivalves. Most less than 3.0 mm, but a few larger. One up to 8.0 mm long. Estimated: 50% fossils, 1% quartz, 1% opaques (probably pyrite), 48% matrix.

P17 13,587-- Limestone mudstone with pyrite less than 3.0 mm long. Estimated: 5% pyrite, 1% fossils, 94% matrix (very finely crystalline calcite).

P17 13,589 -- 300 point count.

Constituent	Number = Percent	Constituent	Number = Percent
Quartz (mono)	50 = 16.6	Cement	12 = 4
Quartz (poly)	3 = 1.0	Pyrite	7 = 2.3
Chert	11 = 3.6	Mica	1 = 0.3
Feldspar	17 = 5.6	Opagues	10 = 3.3
Lithics	12 = 4.0	Fossils	22 = 7.3
Matrix	155 = 51.6	Porosity	0 = 0.0

Moderately sorted, angular to rounded (most subrounded), fine- to medium-grained, calcareous lithic wacke with significant feldspar. Porosity < 1%. Calcite cement is microcrystalline. A few open microfractures. Oil staining on some quartz grains (dead oil in some pores?). Some fossils have been replaced by silica. Texturally and compositionally submature.

P17 13,590 -- 300 point count.

Constituent	Number = Percent	Constituent	Number = Percent
Quartz (mono)	7 = 2.3	Cement	6 = 2.0
Quartz (poly)	0 = 0.0	Pyrite	10 = 3.3
Chert	3 = 1.0	Mica	2 = 0.6
Feldspar	5 = 1.6	Opagues	5 = 1.6
Lithics	3 = 1.0	Fossils	0 = 0.0
Matrix	258 = 86.0	Heavy	1 = 0.3

Sand is well sorted, but overall, lithology is very poorly sorted, angular to subrounded, fine-grained, sandy limestone mudstone. Bioturbated. Pyrite up to 2.0 mm diameter. Dead oil (?) in pores.

P17 13,592 -- 300 point count.

Constituent	Number = Percent	Constituent	Number = Percent
Quartz (mono)	56 = 18.6	Cement	22 = 7.3
Quartz (poly)	1 = 0.3	Pyrite	26 = 8.6
Chert	7 = 2.3	Mica	8 = 2.6
Feldspar	41 = 13.6	Opaques	1 = 0.3
Lithics	13 = 4.3	Fossils	0 = 0.0
Matrix	124 = 41.3	Heavy	1 = 0.3

Poorly sorted, angular to rounded, fine-grained, calcareous lithic wacke with significant feldspar. Bioturbated, with a burrow less than 1.0 cm wide filled with medium-grained sand. Grain contacts are long or concavo-convex. Texturally and compositionally submature.

P17 13,603 -- Fossiliferous wackestone. Very finely crystalline calcite matrix. One microfracture. Fossils up to 13 mm long, broken up and oriented with long dimension horizontal. Pyrite in microfracture and starting to replace some fossils. Estimated: 15% fossils, <1% quartz, 3% pyrite, 81% matrix.

P17 13,605 -- Limestone mudstone with minor pyrite and quartz. Matrix appears to be neomorphosed to pseudospar. Organics present and perhaps some dead oil. Some patches are more finely crystalline and a bit lighter in color. Pyrite is filling a vertical fracture less than 1 mm wide. Bedding is horizontal. Estimated: 2% pyrite, <1% quartz, 97% matrix.

P17 13,606 -- Fossiliferous packstone to wackestone in alternating layers with ostracods and bivalves, mostly crushed to form a "fossil hash." Estimated: 60% fossils, 40% matrix.

P17 13,607 -- Fossiliferous wackestone with dark and light layers less than about 15 mm thick. Highly bioturbated. Probable root casts, most of which are calcite, but some are siliceous. Could also be collapsed molds. Organics present. Estimated: 3% quartz, 22% calcite (root casts), 75% matrix.

P17 13,608 -- Fossiliferous wackestone, highly bioturbated. Three different shades of brown. Nearly vertical microfractures are calcite-filled. The quartz has the appearance of being somewhat fibrous, possibly has replaced some fossils. Estimated: 3% quartz, 20% fossils, 77% matrix.

P17 13,609 -- Limestone mudstone with some fossil and calcite crystal hash. Color varies between 6 shades of brown. Soft sediment deformation (and/or scour and/or rip-ups) at color boundaries. One horizontal microfracture filled with silica. Occasional undulating very thin laminae are dark and resemble stylolites, but are too smooth to be stylolites. Perhaps they are dead oil. One microfault, possibly with dead oil in it. Estimated: 1% pyrite, 10% calcite grains, 15% fossils, 1% quartz, 73% matrix.

P17 13,624 -- Muddy limestone mudstone with minor bioturbation, pyrite less than 3 mm long, and minor spots of dead oil (?). Estimated: 7% pyrite, 5% quartz, and 88% matrix.

P17 13,644 -- Fossiliferous packstone to wackestone. Fossils include bivalves, gastropods, ostracods, and a few miscellaneous and are poorly sorted, but less than 3 mm long. Some fossils are apatite; perhaps fish remains. One larger grain is light brown with clear inclusions in PPL, but becomes a patchwork of multiple-colored grains grown together in XN (biotite?). Estimated: 1%

biotite, 55% fossils, 44% matrix.

P17 13,656 -- 300 point count.

Constituent	Number = Percent	Constituent	Number = Percent
Quartz (mono)	133 = 44.3	Cement	22 = 7.3
Quartz (poly)	2 = 0.6	Pyrite	2 = 0.6
Chert	18 = 6.0	Mica	5 = 1.6
Feldspar	37 = 12.3	Opaques	37 = 12.3
Lithics	42 = 14.0	Fossils	0 = 0.0
Matrix	0 = 0.0	Heavy	2 = 0.6

Very well sorted, subangular to subrounded, medium-grained, calcite-cemented, lithic arenite with significant feldspar. Contacts are long. Structureless. About 3 green grains. Feldspars highly altered. Porosity filled with dead oil(?). Texturally mature, compositionally immature to submature.

P17 13,661 -- 300 point count.

Constituent	Number = Percent	Constituent	Number = Percent
Quartz (mono)	108 = 36.0	Cement	36 = 12.0
Quartz (poly)	5 = 1.6	Pyrite	3 = 1.0
Chert	8 = 2.6	Mica	4 = 1.3
Feldspar	57 = 19.0	Opaques	0 = 0.0
Lithics	21 = 7.0	Fossils	0 = 0.0
Matrix	56 = 18.6	Heavy	2 = 0.6

Very well sorted, subangular, medium-grained, calcite-cemented, feldspathic wacke with significant lithics. Contacts long or sutured. Structureless. Possibly dead oil filling pores. Most feldspar significantly altered to calcite. Some quartz overgrowths. Microfracturing can be seen in at least one quartz grain. Texturally mature, compositionally immature.

### **Chevron Springfield Marine 2-10C; Green River Formation**

CSM 11,109 -- 300 point count.

Constituent	Number = Percent	Constituent	Number = Percent
Quartz (mono)	183 = 61.0	Cement	54 = 18.0
Quartz (poly)	3 = 1.0	Pyrite	0 = 0.0
Chert	3 = 1.0	Mica	6 = 2.0
Feldspar	8 = 2.6	Fe-oxide	3 = 1.0
Lithics	4 = 1.3	Fossils	0 = 0.0
Matrix	34 = 11.3	Heavy	2 = 0.6

Poorly sorted, subangular to rounded, fine- to medium-grained, calcareous to calcite-cemented, sublithic arenite. When present, contacts are long or concavo-convex. Fines upward. Bioturbated. One vertical fracture  $\leq 0.5$  mm wide, calcite-filled. Possible oil staining. Matrix decreases upward as calcite increases. Matrix is silica, clay and calcite. Texturally and compositionally immature.

CSM 11,115.5 -- Oolitic packstone with irregular lighter layers containing better preserved ooids, and darker layers containing more hash, perhaps peloids. Stylolite between upper light and dark layers. Combination of calcite and silica cement in top layer. Some whole ostracods as nuclei. Estimated: 50% ooids, 6% quartz, 24% cement, 20% matrix.

CSM 11,121.5 -- 300 point count.

Constituent	Number = Percent	Constituent	Number = Percent
Quartz (mono)	158 = 52.6	Cement	108 = 36.0
Quartz (poly)	3 = 1.0	Pyrite	0 = 0.0
Chert	0 = 0.0	Mica	1 = 0.3
Feldspar	16 = 5.3	Fe-oxide	2 = 0.6
Lithics	4 = 1.3	Porosity	7 = 2.3
Matrix	0 = 0.0	Heavy	1 = 0.3

Poorly sorted, subangular to subrounded, fine-to medium-grained, calcite-cemented, subfeldspathic arenite. Where present, contacts are sutured, concavo-convex or long. Seemingly structureless. Possible oil staining. Texturally and compositionally immature.

CSM 11,124.5 -- 300 point count.

Constituent	Number = Percent	Constituent	Number = Percent
Quartz (mono)	28 = 9.3	Cement	193 = 64.3
Quartz (poly)	0 = 0.0	Pyrite	15 = 5.0
Chert	0 = 0.0	Mica	5 = 1.6
Feldspar	9 = 3.0	Opales	0 = 0.0
Lithics	3 = 1.0	Fossils	46 = 15.3
Matrix	0 = 0.0	Heavy	1 = 0.3

Overall, very poorly sorted, subangular to rounded, mud and fine- to medium-grained. Really there are three lithology present: top 1/3 is a poorly washed, ostracodal grainstone; middle 1/3 is an impure argillaceous limestone; bottom 1/3 is a calcareous to calcite-cemented, sublithic arenite. There is possible oil staining along the bedding of the arenite. In the upper grainstone, there is a burrow filled with very finely crystalline calcite. Texturally and compositionally immature.

CSM 1,128 -- Fossiliferous wackestone with fossils  $\leq 8$  mm. Filled moldic porosity. Gastropod(s) and bivalves. Estimated: 65% fossils, 3% pyrite, 32% cement.

**CSM 11,134** -- Contact between two lithology; 300 point count each lithology.

Constituent	Number = Percent	Constituent	Number = Percent
Quartz (mono)	31 = 10.3	Cement	0 = 0.0
Quartz (poly)	0 = 0.0	Pyrite	3 = 1.0
Chert	0 = 0.0	Mica	2 = 0.6
Feldspar	8 = 2.6	Porosity	2 = 0.6
Lithics	0 = 0.0	Fossils	4 = 1.3
Matrix (Ca-mud)	249 = 83.0	Heavy	1 = 0.3

Upper lithology is a sandy to silty limestone mudstone (same as CSM 11,128, except fossils decrease and sand increases). Some wavy, light layers. The contact between units is gradational but distinct (get more clay instead of calcite between grains), and there is a stylolite at the border. Fossils present are ostracods and bivalves.

Constituent	Number = Percent	Constituent	Number = Percent
Quartz (mono)	134 = 44.6	Cement	0 = 0.0
Quartz (poly)	0 = 0.0	Pyrite	2 = 0.6
Chert	3 = 1.0	Mica	1 = 0.3
Feldspar	7 = 2.3	Opagues	1 = 0.3
Lithics	6 = 2.0	Fossils	14 = 4.6
Matrix	132 = 44.0	Heavy	0 = 0.0

Lower unit is an extremely poorly sorted, subangular to rounded, fine- to very coarse-grained, calcite-cemented, sublithic arenite with significant feldspar. Contacts are long when present. Virtually structureless. Texturally and compositionally submature.

**CSM 11,146.5** -- 300 point count.

Constituent	Number = Percent	Constituent	Number = Percent
Quartz (mono)	82 = 27.3	Cement	0 = 0.0
Quartz (poly)	0 = 0.0	Pyrite	0 = 0.0
Chert	0 = 0.0	Mica	13 = 4.3
Feldspar	31 = 10.3	Fe-oxides	trace
Lithics	0 = 0.0	Fossils	0 = 0.0
Matrix	174 = 58.0	Heavy	0 = 0.0

Very poorly sorted, subangular to rounded, very fine- to fine-grained, calcareous, subfeldspathic wacke. Very few grain-to-grain contacts, but long when present. A burrow < 7 mm wide is filled with medium-grained sand and is at an angle of about 45°. Some grains ≤ 3 mm long are a bit lighter in color, with even more finely crystalline calcite cement. Texturally and compositionally submature.

CSM 11,151.5 -- 300 point count.

Constituent	Number = Percent	Constituent	Number = Percent
Quartz (mono)	81 = 27.0	Cement	162 = 54.0
Quartz (poly)	0 = 0.0	Pyrite	0 = 0.0
Chert	0 = 0.0	Mica	5 = 1.6
Feldspar	27 = 9.0	Fe-oxide	trace
Lithics	0 = 0.0	Porosity	2 = 0.6
Matrix	22 = 7.3	Heavy	1 = 0.3

Very poorly sorted, subangular to rounded, fine-grained, calcareous to calcite-cemented, subfeldspathic wacke. No grain-to-grain contacts. Extremely finely crystalline calcite cement. A couple open microfractures. Slightly bioturbated. Dirty. Texturally immature to submature; compositionally immature.

CSM 11,154.5 -- 300 point count.

Constituent	Number = Percent	Constituent	Number = Percent
Quartz (mono)	58 = 19.3	Cement	0 = 0.0
Quartz (poly)	0 = 0.0	Pyrite	0 = 0.0
Chert	1 = 0.3	Mica	4 = 1.3
Feldspar	28 = 9.3	Fe-oxide	1 = 0.3
Lithics	0 = 0.0	Porosity	10 = 3.3
Matrix	197 = 65.6	Heavy	1 = 0.3

Extremely poorly sorted, subangular to rounded, very fine- to medium-grained, sandy, limestone mudstone. Highly haphazardly fractured,  $\leq 0.5$  mm wide, open, some connected. Sand is texturally immature to submature and compositionally immature. Porosity is fracture porosity and may be due to slide preparation.

CSM 11,156 -- 300 point count.

Constituent	Number = Percent	Constituent	Number = Percent
Quartz (mono)	135 = 45.0	Cement	0 = 0.0
Quartz (poly)	5 = 1.6	Pyrite	0 = 0.0
Chert	7 = 2.3	Mica	9 = 3.0
Feldspar	24 = 8.0	Fe-oxide	trace
Lithics	0 = 0.0	Porosity	7 = 2.3
Matrix	113 = 37.6	Heavy	trace

Extremely poorly sorted, subangular to rounded, fine- to very coarse-grained, calcareous, subfeldspathic wacke. No grain-to-grain contacts. Structureless and dirty. Texturally submature and compositionally immature.

**CSM 11,157.5 -- 300 point count.**

Constituent	Number = Percent	Constituent	Number = Percent
Quartz (mono)	123 = 41.0	Cement	150 = 50.0
Quartz (poly)	2 = 0.6	Pyrite	0 = 0.0
Chert	7 = 2.3	Mica	1 = 0.3
Feldspar	10 = 3.3	Fe-oxide	1 = 0.3
Lithics	5 = 1.6	Fossils	0 = 0.0
Matrix	0 = 0.0	Heavy	1 = 0.3

Extremely poorly sorted, angular to rounded, fine- to very coarse-grained, calcite-cemented, subfeldspathic arenite with an approximately equal amount of lithics. Very few grain-to-grain contacts, but a couple sutured. Structureless. A few stylolites between and around grains. Appears that calcite cement is altering either from micrite to spar or vice versa. Texturally submature and compositionally immature.

**Chevron Hiko Bell 1-12A2; Green River Formation**

**CHIKO 10,482 -- 300 point count.**

Constituent	Number = Percent	Constituent	Number = Percent
Quartz (mono)	42 = 14.0	Cement	34 = 11.3
Quartz (poly)	0 = 0.0	Pyrite	3 = 1.0
Chert	0 = 0.0	Mica	1 = 0.3
Feldspar	11 = 3.6	Opagues	0 = 0.0
Lithics	6 = 2.0	Fossils	0 = 0.0
Matrix	202 = 67.3	Heavy	1 = 0.3

Bottom 1/3 is a calcareous, silty mudstone. Upper 2/3 is very poorly sorted, subangular to rounded, fine-grained, calcite-cemented, subfeldspathic, sublithic arenite. No grain-to-grain contacts. One large fossil, bivalve, about 25 mm long, cup side-down. Fossil itself is dark brown (apatite?) and looks like material has "flowed." Sparry calcite fills intraparticle porosity. Texturally and compositionally immature.

**CHIKO 10,547 -- 300 point count.**

Constituent	Number = Percent	Constituent	Number = Percent
Quartz (mono)	16 = 5.3	Cement	60 = 20.0
Quartz (poly)	0 = 0.0	Pyrite	5 = 1.6
Chert	0 = 0.0	Mica	2 = 0.6
Feldspar	4 = 1.3	Opagues	0 = 0.0
Lithics	0 = 0.0	Fossils	0 = 0.0
Matrix	211 = 70.3	Heavy	2 = 0.6

Poorly sorted, subangular to rounded, fine-grained, calcite-cemented, sublithic arenite alternating with darker bands of calcareous, silty mudstone. No grain-to-grain contacts. Matrix found in the dark bands, is extremely finely crystalline calcite and clays. Cement, found in the lighter layers, is finely crystalline calcite. Texturally and compositionally immature.

CHIKO 10,595.5 -- 300 point count.

Constituent	Number = Percent	Constituent	Number = Percent
Quartz (mono)	56 = 18.6	Cement	0 = 0.0
Quartz (poly)	0 = 0.0	Pyrite	4 = 1.3
Chert	0 = 0.0	Mica	6 = 2.0
Feldspar	13 = 4.3	Opaques	0 = 0.0
Lithics	0 = 0.0	Fossils	0 = 0.0
Matrix	220 = 73.3	Heavy	1 = 0.3

Poorly sorted, subangular to subrounded, very fine- to fine-grained, calcareous, silty to sandy mudstone. No grain-to-grain contacts. Bottom 1/3 is slightly less muddy. Upper 2/3 is finely laminated. Possible dead oil around grains and filling some microfractures. Texturally and compositionally immature.

CHIKO 10,596 -- Sandy limestone mudstone. Light and dark brown laminae, some feathery, some inclined. Vertical fracture < 0.5 mm wide is partially calcite-filled (90-100%) and bitumen-stained. Neomorphosed cement. Sand is very fine-grained, moderately well sorted, angular to subrounded. Estimated: 10% quartz, 2% mica, 6% pyrite, 82% cement.

CHIKO 10,597.5 -- 300 point count.

Constituent	Number = Percent	Constituent	Number = Percent
Quartz (mono)	40 = 13.3	Cement	90 = 30.0
Quartz (poly)	0 = 0.0	Pyrite	5 = 1.6
Chert	0 = 0.0	Mica	3 = 1.0
Feldspar	10 = 3.3	Opaques	0 = 0.0
Lithics	26 = 8.6	Fossils	0 = 0.0
Matrix	124 = 41.3	Heavy	2 = 0.6

Lower 1/2 is extremely poorly sorted, subangular to rounded, very fine- to very coarse-grained, calcite-cemented to calcareous, lithic wacke with significant feldspar and a few pyrite lenses. Upper 1/2 contains more mud, is laminated with some lighter, coarser layers, and displays some possible soft sediment deformation. Texturally and compositionally immature.

**CHIKO 10,629.5 -- 300 point count.**

Constituent	Number = Percent	Constituent	Number = Percent
Quartz (mono)	129 = 43.0	Cement	126 = 42.0
Quartz (poly)	2 = 0.6	Pyrite	0 = 0.0
Chert	0 = 0.0	Mica	6 = 2.0
Feldspar	25 = 8.3	Opaques	0 = 0.0
Lithics	trace	Fossils	0 = 0.0
Matrix	12 = 4.0	Heavy	0 = 0.0

Moderately sorted, subangular to subrounded, very fine- to fine-grained. Upper 1/2 is more of a calcareous, subfeldspathic wacke, is slightly finer-grained and is bioturbated, while lower 1/2 is more of a calcareous to calcite-cemented, subfeldspathic arenite, is faintly laminate and contains a stylolite. Possible dead oil around grains. Texturally and compositionally immature.

**Chevron 1-7A1 J. Yack; Wasatch (12,235-12,345) and Flagstaff (14,325-14,384) Formations**

**C17A1 12,248 -- 300 point count.**

Constituent	Number = Percent	Constituent	Number = Percent
Quartz (mono)	181 = 60.3	Cement	46 = 15.3
Quartz (poly)	0 = 0.0	Pyrite	5 = 1.6
Chert	0 = 0.0	Mica	1 = 0.3
Feldspar	56 = 18.6	Opaques	0 = 0.0
Lithics	6 = 2.0	Porosity	1 = 0.3
Matrix	0 = 0.0	Heavy	4 = 1.3

Moderately sorted, subrounded to rounded, fine- to coarse-grained, calcite-cemented, subfeldspathic arenite. Fines slightly upwards, otherwise structureless. Feldspars highly altered; many to calcite. Texturally submature and compositionally immature.

**C17A1 12,248.5 -- 300 point count.**

Constituent	Number = Percent	Constituent	Number = Percent
Quartz (mono)	204 = 68.0	Cement	51 = 17.0
Quartz (poly)	0 = 0.0	Pyrite	11 = 3.6
Chert	0 = 0.0	Mica	0 = 0.0
Feldspar	24 = 8.0	Opaques	0 = 0.0
Lithics	9 = 3.0	Fossils	0 = 0.0
Matrix	0 = 0.0	Heavy	1 = 0.3

Well sorted, subangular to rounded, calcite-cemented, subfeldspathic arenite with approximately equal lithics. Layers of coarse and of medium sand with somewhat scoured contacts; otherwise structureless. Grain-to-grain contacts are long where present, with some sutured in the

coarse-grained layer. One horizontal, pyrite-filled fracture. Some quartz grains highly fractured, especially near the top of the slide. Texturally mature and compositionally submature.

C17A1 12,252 -- 300 point count.

Constituent	Number = Percent	Constituent	Number = Percent
Quartz (mono)	174 = 58.0	Cement	56 = 18.6
Quartz (poly)	0 = 0.0	Pyrite	13 = 4.3
Chert	0 = 0.0	Mica	2 = 0.6
Feldspar	48 = 16.0	Opaques	0 = 0.0
Lithics	5 = 1.6	Porosity	1 = 0.3
Matrix	0 = 0.0	Heavy	1 = 0.3

Upper 3/4: Well sorted, subangular to rounded, medium- to coarse-grained, calcite-cemented, subfeldspathic arenite, with some sutured contacts and long, where present. Texturally mature and compositionally submature (same unit as C17A1 12,248.5). Lower 1/4: Moderately sorted, subangular to rounded, very fine-grained, calcite-cemented, subfeldspathic arenite, with long contacts where present. Texturally and compositionally submature. Sharp, undulating contact. One vertical fracture cuts through both layers and is sparry calcite-filled. One 8 mm long black lens (?).

C17A1 12,259 -- 300 point count.

Constituent	Number = Percent	Constituent	Number = Percent
Quartz (mono)	157 = 52.3	Cement	108 = 36.0
Quartz (poly)	0 = 0.0	Pyrite	1 = 0.3
Chert	0 = 0.0	Mica	2 = 0.6
Feldspar	21 = 7.0	Opaques	0 = 0.0
Lithics	9 = 3.0	Fossils	0 = 0.0
Matrix	0 = 0.0	Heavy	2 = 0.6

Very poorly sorted, subangular to well-rounded, fine- to coarse-grained, calcite-cemented, subfeldspathic arenite. Very few grain-to-grain contacts, but long where present. A subvertical burrow about 11 mm wide is filled with very slightly finer sand, otherwise structureless. Texturally and compositionally submature.

C17A1 12,264 -- 300 point count.

Constituent	Number = Percent	Constituent	Number = Percent
Quartz (mono)	175 = 58.3	Cement	84 = 28.0
Quartz (poly)	0 = 0.0	Pyrite	trace
Chert	0 = 0.0	Mica	1 = 0.3
Feldspar	30 = 10.0	Opaques	0 = 0.0
Lithics	9 = 3.0	Fossils	0 = 0.0
Matrix	0 = 0.0	Heavy	1 = 0.3

Moderately well sorted, subangular to well-rounded, fine- to medium-grained, calcareous, subfeldspathic arenite (from same unit as C17A1 12,259). Grain-to-grain contacts are long where present. One coarse grain noticed. Structureless. Texturally and compositionally submature.

C17A1 12,269.5 -- 300 point count.

Constituent	Number = Percent	Constituent	Number = Percent
Quartz (mono)	243 = 81.0	Cement	34 = 11.3
Quartz (poly)	0 = 0.0	Pyrite	trace
Chert	0 = 0.0	Mica	0 = 0.0
Feldspar	11 = 3.6	Opaques	0 = 0.0
Lithics	10 = 3.3	Porosity	trace
Matrix	0 = 0.0	Heavy	2 = 0.6

Moderately well sorted, subangular to subrounded, fine- to coarse-grained, calcite-cemented, quartz arenite. Grain-to-grain contacts are long, concavo-convex and some sutured. Cement is calcite, but some quartz grains show overgrowth and some show pressure solution. Calcite also replaces some feldspar. Texturally and compositionally submature.

C17A1 12,275 -- 300 point count.

Constituent	Number = Percent	Constituent	Number = Percent
Quartz (mono)	107 = 35.6	Cement	0 = 0.0
Quartz (poly)	0 = 0.0	Pyrite	0 = 0.0
Chert	0 = 0.0	Mica	1 = 0.3
Feldspar	14 = 4.6	Opaques	0 = 0.0
Lithics	7 = 2.3	Porosity	17 = 5.6
Matrix	152 = 50.6	Heavy	2 = 0.6

Very poorly sorted, subangular to subrounded, fine- to medium-grained, calcareous, subfeldspathic wacke. No grain-to-grain contacts. Open diagonal microfractures. Texturally and compositionally immature,

C17A1 12,283 -- 300 point count.

Constituent	Number = Percent	Constituent	Number = Percent
Quartz (mono)	53 = 17.6	Cement	3 = 1.0
Quartz (poly)	0 = 0.0	Pyrite	trace
Chert	0 = 0.0	Mica	0 = 0.0
Feldspar	4 = 1.3	Opaques	0 = 0.0
Lithics	4 = 1.3	Porosity	6 = 2.0
Matrix	229 = 76.3	Heavy	1 = 0.3

Very poorly sorted, subrounded to rounded, fine- to medium-grained, calcareous, silty to

sandy mudstone. No grain-to-grain contacts. Red and green mud matrix, swirled in a marble-cake effect. Texturally and compositionally immature.

C17A1 12,286 -- 300 point count.

Constituent	Number = Percent	Constituent	Number = Percent
Quartz (mono)	109 = 36.3	Cement	0 = 0.0
Quartz (poly)	0 = 0.0	Pyrite	0 = 0.0
Chert	0 = 0.0	Mica	0 = 0.0
Feldspar	3 = 1.0	Opagues	0 = 0.0
Lithics	4 = 1.3	Porosity	6 = 2.0
Matrix	176 = 58.6	Heavy	2 = 0.6

Very poorly sorted, subrounded to rounded, medium-grained, calcareous, (very) sublithic wacke. Very few sutured contacts, otherwise none. Calcite replacing some feldspar. Texturally and compositionally immature.

C17A1 12,292 -- 300 point count.

Constituent	Number = Percent	Constituent	Number = Percent
Quartz (mono)	151 = 50.3	Cement	11 = 3.6
Quartz (poly)	0 = 0.0	Pyrite	trace
Chert	0 = 0.0	Mica	0 = 0.0
Feldspar	20 = 6.6	Opagues	0 = 0.0
Lithics	5 = 1.6	Porosity	5 = 1.6
Matrix	107 = 35.6	Heavy	1 = 0.3

Extremely poorly sorted, subangular to subrounded, fine- to coarse-grained, calcareous, subfeldspathic wacke. No grain-to-grain contacts. Structureless. Texturally and compositionally immature.

C17A1 12,299 -- 300 point count.

Constituent	Number = Percent	Constituent	Number = Percent
Quartz (mono)	269 = 89.6	Cement	20 = 6.6
Quartz (poly)	0 = 0.0	Pyrite	0 = 0.0
Chert	0 = 0.0	Mica	trace
Feldspar	6 = 2.0	Opagues	0 = 0.0
Lithics	5 = 1.6	Porosity	trace
Matrix	0 = 0.0	Heavy	trace

Well sorted, angular to subrounded, fine- to coarse-grained, calcite-cemented, quartz arenite. Grain-to-grain contacts are sutured, concavo-convex and long. Structureless. Some triple junctions and quartz overgrowths. Calcite replacing some feldspar. Texturally mature and

compositionally submature.

C17A1 12,303 -- 300 point count.

Constituent	Number = Percent	Constituent	Number = Percent
Quartz (mono)	274 = 91.3	Cement	17 = 5.6
Quartz (poly)	0 = 0.0	Pyrite	0 = 0.0
Chert	0 = 0.0	Mica	0 = 0.0
Feldspar	1 = 0.3	Opagues	0 = 0.0
Lithics	4 = 1.3	Porosity	4 = 1.3
Matrix	0 = 0.0	Heavy	0 = 0.0

Well sorted, subangular to subrounded, medium-grained, minor calcite-cemented, quartz arenite. Grain-to-grain contacts are sutured, concavo-convex and long. Structureless. Possible oil staining around most grains. Texturally and compositionally mature.

C17A1 14,372 (Flagstaff) -- 300 point count.

Constituent	Number = Percent	Constituent	Number = Percent
Quartz (mono)	152 = 50.6	Cement	51 = 17.0
Quartz (poly)	0 = 0.0	Pyrite	0 = 0.0
Chert	0 = 0.0	Mica	0 = 0.0
Feldspar	24 = 8.0	Opagues (oil?)	16 = 5.3
Lithics	51 = 17.0	Porosity	5 = 1.6
Matrix	0 = 0.0	Heavy	1 = 0.3

Very well sorted, subangular to subrounded, fine-to medium-grained, calcite-cemented, lithic arenite. Grain-to-grain contacts are concavo-convex and long. Many feldspars altering to calcite. Some bioturbation. Texturally mature and compositionally submature.

C17A1 14,377.5 (Flagstaff) -- Bulk rock is limestone mudstone, bioturbated, pyrite up to 3 mm long. A couple open microfractures. Estimated: 10% pyrite, 1% quartz, 89% matrix. The left 1/3 of the slide is a burrow filled with sandstone as described below by a 300 point count.

Constituent	Number = Percent	Constituent	Number = Percent
Quartz (mono)	46 = 15.3	Cement	24 = 8.0
Quartz (poly)	0 = 0.0	Pyrite	23 = 7.6
Chert	3 = 1.0	Mica	1 = 0.3
Feldspar	16 = 5.3	Opagues	0 = 0.0
Lithics	0 = 0.0	Fossils	0 = 0.0
Matrix	187 = 62.3	Heavy	0 = 0.0

Poorly sorted, subangular to subrounded, very fine- to fine-grained, calcareous, sublithic wacke. Texturally and compositionally immature.

C17A1 14,384 (Flagstaff) -- 300 point count.

Constituent	Number = Percent	Constituent	Number = Percent
Quartz (mono)	99 = 33.0	Cement	151 = 50.3
Quartz (poly)	0 = 0.0	Pyrite	0 = 0.0
Chert	0 = 0.0	Mica	1 = 0.3
Feldspar	19 = 6.3	Opaques	0 = 0.0
Lithics	29 = 9.6	Porosity	1 = 0.3
Matrix	0 = 0.0	Heavy	trace

Very well sorted, angular to subrounded, fine-grained, calcite-cemented, sublithic arenite. Grain-to-grain contacts are primarily concavo-convex and long, but a few are sutured. Some sedimentary structure, but hard to determine what kind. Texturally mature and compositionally submature.

**Chevron Chasel 1-18A1; Wasatch Formation**

CCHAS 10,632 -- Overly densely packed, ostracodal packstone to poorly washed grainstone. Faintly laminated. Possible oil staining. Mud in the shells has been neomorphosed to microspar. Fuzzy boundaries between the microspar and the spar. Estimate: 3% quartz, 10% matrix, 87% fossils and coated grains. Some evidence of compaction. Cement probably meteoric or burial.

CCHAS 10,661.5 -- 300 point count.

Constituent	Number = Percent	Constituent	Number = Percent
Quartz (mono)	137 = 45.6	Cement	94 = 31.3
Quartz (poly)	1 = 0.3	Pyrite	6 = 2.0
Chert	0 = 0.0	Mica	0 = 0.0
Feldspar	3 = 1.0	Porosity	5 = 1.6
Lithics	5 = 1.6	Fossils	48 = 16.0
Matrix	0 = 0.0	Heavy	1 = 0.3

Poorly sorted, subangular to rounded, fine- to coarse-grained, calcite-cemented, lithic arenite. Structureless. Some ostracods, some micritic lithics; some quartz grains are micrite-coated. Some quartz overgrowths. Texturally submature and compositionally immature.

CCHAS 10,795 -- 300 point count.

Constituent	Number = Percent	Constituent	Number = Percent
Quartz (mono)	107 = 35.6	Cement	0 = 0.0
Quartz (poly)	0 = 0.0	Pyrite	14 = 4.6
Chert	0 = 0.0	Mica	13 = 4.3
Feldspar	19 = 6.3	Opaques	0 = 0.0
Lithics	7 = 2.3	Porosity	20 = 6.6
Matrix	116 = 38.6	Heavy	4 = 1.3

Very poorly sorted, subangular to subrounded, very fine- to very coarse-grained (predominantly medium-), calcareous, sublithic wacke with significant feldspar. No grain-to-grain contacts. Pyrite-rich band (about 3 mm thick) near the base with euhedral pyrite crystals. Texturally submature and compositionally immature.

CCHAS 11,010.5 -- 300 point count.

Constituent	Number = Percent	Constituent	Number = Percent
Quartz (mono)	230 = 76.6	Cement	25 = 8.3
Quartz (poly)	0 = 0.0	Pyrite	1 = 0.3
Chert	0 = 0.0	Mica	1 = 0.3
Feldspar	6 = 2.0	Opagues (Oil?)	20 = 6.6
Lithics	8 = 2.6	Porosity	8 = 2.6
Matrix	0 = 0.0	Heavy	1 = 0.3

Extremely poorly sorted, subangular to rounded, fine- to coarse-grained, calcite-cemented, sublithic arenite. Grain-to-grain contacts are sutured, concavo-convex and long. Structureless. Possible dead oil in pore spaces. Texturally submature and compositionally immature.

CCHAS 11,192 -- 300 point count.

Constituent	Number = Percent	Constituent	Number = Percent
Quartz (mono)	110 = 36.6	Cement	3 = 1.0
Quartz (poly)	0 = 0.0	Pyrite	0 = 0.0
Chert	0 = 0.0	Mica	3 = 1.0
Feldspar	44 = 14.6	Opagues	0 = 0.0
Lithics	7 = 2.3	Porosity	6 = 2.0
Matrix	127 = 42.3	Heavy	trace

Poorly sorted, subangular to rounded, very fine- to medium-grained, calcareous, feldspathic wacke. No grain-to-grain contacts. Structureless. Cement may be altered feldspars and/or micas. Possible dead oil. Possible stylolite, and or oil staining along irregular lamina. Texturally and compositionally submature.

CCHAS 11,220.5 -- 300 point count.

Constituent	Number = Percent	Constituent	Number = Percent
Quartz (mono)	194 = 64.6	Cement	71 = 23.6
Quartz (poly)	0 = 0.0	Pyrite	0 = 0.0
Chert	0 = 0.0	Mica	1 = 0.3
Feldspar	17 = 5.6	Opagues	0 = 0.0
Lithics	7 = 2.3	Porosity	9 = 3.0
Matrix	0 = 0.0	Heavy	1 = 0.3

Very poorly sorted, subangular to rounded, fine- to very coarse-grained, calcite-cemented, (very) subfeldspathic arenite. Grain-to-grain contacts are concavo-convex where present. Structureless. Texturally and compositionally submature.

**Chevron L. Boren 1-24A2; Wasatch Formation**

CBOR 12,168.5 -- 300 point count.

Constituent	Number = Percent	Constituent	Number = Percent
Quartz (mono)	215 = 71.6	Cement	41 = 13.6
Quartz (poly)	0 = 0.0	Pyrite	0 = 0.0
Chert	0 = 0.0	Mica	5 = 1.6
Feldspar	18 = 6.0	Opagues	5 = 1.6
Lithics	12 = 4.0	Porosity	3 = 1.0
Matrix	0 = 0.0	Heavy	1 = 0.3

Very poorly sorted, subangular to rounded, very fine- to medium-grained, calcite-cemented, sublithic arenite with significant feldspar. Grain-to-grain contacts are long and concavo-convex when present.. Structureless. Texturally and compositionally submature.

CBOR 12,181.5 -- 300 point count.

Constituent	Number = Percent	Constituent	Number = Percent
Quartz (mono)	147 = 49.0	Cement	127 = 42.3
Quartz (poly)	0 = 0.0	Pyrite	2 = 0.6
Chert	0 = 0.0	Mica	3 = 1.0
Feldspar	5 = 1.6	Opagues	2 = 0.6
Lithics	5 = 1.6	Porosity	7 = 2.3
Matrix	0 = 0.0	Heavy	2 = 0.6

Well sorted, angular to rounded, fine-grained, calcite-cemented, sublithic arenite. Contacts long where present. Some quartz overgrowths. Pyrite < 3 mm. One thin layer of Very fine-grained sand, otherwise similar to the fine sand. Texturally and compositionally submature.

**Chevron Ute Tribal 9-4B1; Wasatch Formation**

C94B1 11,062 -- 300 point count.

Constituent	Number = Percent	Constituent	Number = Percent
Quartz (mono)	82 = 27.3	Cement	106 = 35.3
Quartz (poly)	0 = 0.0	Pyrite	1 = 0.3
Chert	10 = 3.3	Mica	11 = 3.6
Feldspar	62 = 20.6	Opagues (oil?)	1 = 0.3
Lithics	25 = 8.3	Fossils	0 = 0.0
Matrix	0 = 0.0	Heavy	2 = 0.6

Well sorted, subangular to subrounded, fine-grained, calcareous feldspathic arenite with significant lithics. Few grain-to-grain contacts, but long where present. Feldspar highly altered, primarily to calcite. Some thin laminae near the base of the slide. Texturally submature and compositionally immature.

C94B1 11,091.5 -- 300 point count.

Constituent	Number = Percent	Constituent	Number = Percent
Quartz (mono)	45 = 15.0	Cement	162 = 54.0
Quartz (poly)	0 = 0.0	Pyrite	7 = 2.3
Chert	0 = 0.0	Mica	6 = 2.0
Feldspar	63 = 21.0	Opagues	0 = 0.0
Lithics	10 = 3.3	Fossils	0 = 0.0
Matrix	5 = 1.6	Heavy	2 = 0.6

Very poorly sorted, subangular to rounded, very fine-grained, calcite-cemented, feldspathic arenite with significant lithics. Few grain-to-grain contacts, but long where present. Possible dead oil. Some irregular laminae. Texturally submature and compositionally immature.

C94B1 11,110.5 -- 300 point count.

Constituent	Number = Percent	Constituent	Number = Percent
Quartz (mono)	97 = 32.3	Cement	64 = 21.3
Quartz (poly)	1 = 0.3	Pyrite	2 = 0.6
Chert	0 = 0.0	Mica	1 = 0.3
Feldspar	51 = 17.0	Opagues (oil?)	32 = 10.6
Lithics	51 = 17.0	Fossils	0 = 0.0
Matrix	0 = 0.0	Heavy	1 = 0.3

Very well sorted, angular to subrounded, medium-grained, calcite-cemented, lithic arenite with significant feldspar. Grain-to-grain contacts are long where present. Structureless. Occasional euhedral calcite. Calcite replacing feldspar. Texturally submature and compositionally immature.

C94B1 12,678 -- 300 point count.

Constituent	Number = Percent	Constituent	Number = Percent
Quartz (mono)	64 = 21.3	Cement	63 = 21.0
Quartz (poly)	0 = 0.0	Pyrite	9 = 3.0
Chert	0 = 0.0	Mica	10 = 3.3
Feldspar	112 = 37.3	Opagues (oil?)	5 = 1.6
Lithics	35 = 11.6	Fossils	0 = 0.0
Matrix	0 = 0.0	Heavy	2 = 0.6

Well sorted, subangular to subrounded, fine-grained, calcite-cemented, feldspathic arenite with significant lithics. Grain-to-grain contacts long where present. Irregular laminae and/or bioturbation (very difficult to see). Highly altered feldspars (to calcite or clay). Texturally submature and compositionally immature.

**Quinex Leslie Taylor 24-5; Wasatch Formation**

Full diameter core. No samples taken.

**Bow Valley Petroleum D.R. Long 2-19A1E; Green River Formation**

BVP19 9173.5 -- 300 point count.

Constituent	Number = Percent	Constituent	Number = Percent
Quartz (mono)	55 = 18.3	Cement	176 = 58.6
Quartz (poly)	0 = 0.0	Pyrite	3 = 1.0
Chert	0 = 0.0	Mica	1 = 0.3
Feldspar	28 = 9.3	Opagues (oil?)	36 = 12.0
Lithics	0 = 0.0	Fossils	0 = 0.0
Matrix	0 = 0.0	Heavy	1 = 0.3

Extremely poorly sorted, subangular to rounded, fine- to coarse-grained, calcareous, lithic wacke with significant feldspar. One microfracture is silica-filled, one is oil stained. Possible dead oil in pore spaces. One very dark clast is at least 17 mm long and up to 4 mm wide, angled at about 45°, with a folded interior. Texturally immature and compositionally submature.

BVP19 9177 -- Limey shale to mudstone, very finely laminated at the top. Calcite laminae increase in number and thickness downward. Microfractures generally on one or both sides of the calcite laminae. Calcite in laminae is sparry. Possible dead oil. Estimated: 15% pyrite, 30% calcite, 55% matrix.

BVP19 9632 -- Contact between two lithology is sharp and deformed. Upper 1/3 is a very well sorted, fine- to medium-grained, calcareous to calcite-cemented, (sublithic) quartz arenite, lighter in color than the lower unit. Estimated: 2% pyrite, 3% mica, 50% quartz, 45% calcite cement. Lower 2/3 is a darker, fossiliferous (ostracodal) grainstone. Possible dead oil in both lithology. Anomalous clear grain (PPL) is amber in XN, and is euhedral (square). Estimated: 1% quartz, 9% cement, 90% fossils.

**BVP19 9638** -- Contact between a very fine-grained sandstone and a silty mudstone is sharp with some bioturbation. Cement grain size is the main difference between the two; also lower half has more organics, making it darker. Possible dead oil. Neomorphosed cement. Estimated (upper half): 45% quartz, 50% calcite (cement), 1% mica, 1% feldspar, 3% Fe-oxide. Estimated (lower half): 45% quartz, 40% calcite (cement), 1% Fe-oxide, 1% fossils, 13% matrix.

**BVP19 9648** -- 300 point count.

Constituent	Number = Percent	Constituent	Number = Percent
Quartz (mono)	137 = 45.6	Cement	124 = 41.3
Quartz (poly)	0 = 0.0	Pyrite	0 = 0.0
Chert	0 = 0.0	Mica	2 = 0.6
Feldspar	30 = 10.0	Opaques	0 = 0.0
Lithics	6 = 2.0	Fossils	0 = 0.0
Matrix	0 = 0.0	Heavy	1 = 0.3

Poorly sorted, subangular to subrounded, fine- to medium-grained, calcareous to calcite-cemented, subfeldspathic arenite. No grain-to-grain contacts. Structureless. Calcite replacing feldspar. Calcite is mostly euhedral, but some is radial. One lithic consists of about eight peloids glued together. Texturally and compositionally submature.

**Bow Valley Petroleum Ute 2-22A1E; Wasatch Formation**

**BVP22 12,289** -- 300 point count.

Constituent	Number = Percent	Constituent	Number = Percent
Quartz (mono)	120 = 40.0	Cement	30 = 10.0
Quartz (poly)	5 = 1.6	Pyrite	2 = 0.6
Chert	18 = 6.0	Mica	0 = 0.0
Feldspar	23 = 7.6	Porosity	7 = 2.3
Lithics	31 = 10.3	Fossils	0 = 0.0
Matrix	62 = 20.6	Heavy	2 = 0.6

Very well sorted, angular to rounded, fine- to medium-grained, slightly calcite-cemented, sublithic wacke with significant feldspar. Grain-to-grain contacts are sutured and long. Structureless. Most feldspar is at least partially altered to calcite. Lithics include metamorphic clasts. Texturally and compositionally immature.

BVP22 12,299 -- 300 point count.

Constituent	Number = Percent	Constituent	Number = Percent
Quartz (mono)	62 = 20.6	Cement	66 = 22.0
Quartz (poly)	1 = 0.3	Pyrite	2 = 0.6
Chert	7 = 2.3	Mica	9 = 3.0
Feldspar	39 = 13.0	Opagues	31 = 10.3
Lithics	10 = 3.3	Fossils	0 = 0.0
Matrix	71 = 23.6	Heavy	2 = 0.6

Moderately sorted, subangular to subrounded, very fine-grained, calcareous, feldspathic wacke with significant lithics. No grain-to-grain contacts. Bedding slightly bowed down in the middle. One black stringer about 6 mm long, contains "floating" grains of quartz and calcite. Altered feldspar. Possible dead oil in microfractures and pore spaces. Texturally and compositionally immature.

BVP22 12,300 -- 300 point count.

Constituent	Number = Percent	Constituent	Number = Percent
Quartz (mono)	91 = 30.3	Cement	77 = 25.6
Quartz (poly)	1 = 0.3	Pyrite	7 = 2.3
Chert	11 = 3.6	Mica	19 = 6.3
Feldspar	20 = 6.6	Porosity	10 = 3.3
Lithics	14 = 4.6	Fossils	0 = 0.0
Matrix	46 = 15.3	Heavy	4 = 1.3

Poorly to moderately sorted, subangular to subrounded, very fine- to fine-grained, calcareous to calcite-cemented, lithic wacke with significant feldspar. Grain-to-grain contacts are sutured and concavo-convex. Undulatory bedding. A few grains of embayed quartz. Texturally and compositionally immature.

BVP22 12,305 -- Fossiliferous wackestone with assorted fossils (bivalves and gastropods) up to 6 mm long. Dark and light rip-ups and bioturbation. Porosity is partially-filled moldic and fracture. Estimated: 3% quartz, 30% fossils, 10% rip-ups, 57% matrix.

BVP22 12,307 -- Interclastic packstone with some altered fossils (bivalves, ostracods). Matrix between some clasts is sparse wackestone. Clasts are poorly sorted and vary in shade of brown. Estimated: 10% fossils, 20% matrix, 70% (rip-up) clasts.

BVP22 12,310 -- Fossiliferous mudstone. Fossils are very fine hash, but a couple up to 7 mm long. Bioturbated. Estimated: 2% quartz, 1% dead oil (?), 40% fossils, 57% matrix.

BVP22 12,314 -- Calcareous silty mudstone with four haphazard fractures < 0.5 mm wide, open. A few lighter areas are finer-grained with little to no included silt. One of the lighter areas contains a gastropod (?) that is filled with fibrous quartz (like spun glass). Estimated: 5% quartz, 1% dead oil (?), 94% matrix.

BVP22 12,365 -- 300 point count.

Constituent	Number = Percent	Constituent	Number = Percent
Quartz (mono)	76 = 25.3	Cement	101 = 33.6
Quartz (poly)	8 = 2.6	Pyrite	0 = 0.0
Chert	9 = 3.0	Mica	9 = 3.0
Feldspar	29 = 9.6	Opagues	15 = 5.0
Lithics	9 = 3.0	Fossils	0 = 0.0
Matrix	41 = 13.6	Heavy	3 = 1.0

Moderately well sorted, subangular to subrounded, fine-grained, calcite-cemented to calcareous, sublithic wacke with significant feldspar. No grain-to-grain contacts. Bedding dips. Possible dead oil. Texturally and compositionally submature.

**APPENDIX C**  
**Tables of Raw Fracture Data.**

Pennzoil 3-17A2 (sec. 17, T1S, R2W)

Core	Top (ft)	Base (ft)	Thickness (ft)	Lithology	Orientation	% Filling	Frequency	Bitumen	Width (mm)	Length (cm)	Elev. Top	Elev. Base
P17	13580.00	13580.7	0.67	shale	v, h, hp	10 c	very freq.	na	< 0.5	~ 8.0	-7588.00	-7588.67
P17	13580.7	13583.7	3.00	mudstone	na	na	na	na	na	na	-7588.67	-7591.67
P17	13583.7	13586.3	2.66	packstone	hp	tight	moderate	na	< 0.25	< 7	-7591.67	-7594.33
P17	13586.3	13588.7	2.34	ls mudstone	na	na	na	na	na	na	-7594.33	-7596.67
P17	13588.7	13589.3	0.66	sandstone	na	na	na	na	na	na	-7596.67	-7597.33
P17	13589.3	13591.3	2.00	ls mudstone	h	85 c	one	na	< 0.5	> 7	-7597.33	-7599.33
P17	13591.3	13597.00	5.67	sandstone	sv, h	85c, 90 c	one, occ.	na	< 1.0, < 0.5	> 14, > 7	-7599.33	-7605.00
P17	13600.00	13601.50	1.50	int. ss-ls md.	h (mudst)	80 c	moderate	na	< 0.25	> 7	-7608.00	-7609.50
P17	13601.50	13602.67	1.17	ls mudstone	h	80 c	moderate	na	< 0.25	> 7	-7609.50	-7610.67
P17	13602.67	13604.00	1.33	wackestone	h	open	occasional	yes	< 0.5	> 7	-7610.67	-7612.00
P17	13604.00	13604.33	0.33	packstone	sv, h	95 c	occasional	na	< 0.25	< 8	-7612.00	-7612.33
P17	13604.33	13604.67	0.34	ls mudstone	na	na	na	na	na	na	-7612.33	-7612.67
P17	13604.67	13605.08	0.41	packstone	na	na	na	na	na	na	-7612.67	-7613.08
P17	13605.08	13605.50	0.42	ls mudstone	na	na	na	na	na	na	-7613.08	-7613.50
P17	13605.50	13605.92	0.42	ls mudstone	h	tight	one	yes	< 0.25	> 7	-7613.50	-7613.92
P17	13605.92	13607.46	1.54	packstone	v, h	95 c	occasional	na	< 0.25, < 0.5	< 18, > 5	-7613.92	-7615.46
P17	13607.46	13607.67	0.21	wackestone	v	95 c	one	na	< 0.25	cont. from 17	-7615.46	-7615.67
P17	13607.67	13608.21	0.54	wackestone	na	na	na	na	na	na	-7615.67	-7616.21

Core	Top (ft)	Base (ft)	Thickness (ft)	Lithology	Orientation	% Filling	Frequency	Bitumen	Width (mm)	Length (cm)	Elev. Top	Elev. Base
P17	13608.21	13610.33	2.12	ls mudstone	v & h, h	100 c, black	occasional	na	< 0.5, < 0.5	< 8	-7616.21	-7618.33
P17	13610.33	13610.83	0.50	shale	hp	open	very freq.	na	crumbled	crumbled	-7618.33	-7618.83
P17	13610.83	13615.50	4.67	ls mudstone	na	na	na	na	na	na	-7618.83	-7623.50
P17	13615.50	13615.92	0.42	ls mudstone	h	100 mud	moderate	yes	< 0.5	> 7	-7623.50	-7623.92
P17	13615.92	13617.50	1.58	ls mudstone	hp	0-5 c	moderate	na	< 0.5	> 7	-7623.92	-7625.50
P17	13617.50	13618.33	0.83	siltstone	hp	5 c	very freq.	na	< 0.5	< 7 <	-7625.50	-7626.33
P17	13618.33	13618.71	0.38	ls mudstone	h	95 c	one	na	< 0.25	> 2	-7626.33	-7626.71
P17	13618.71	13619.25	0.54	sandstone	na	na	na	na	na	na	-7626.71	-7627.25
P17	13619.25	13620.00	0.75	mudstone	d, h	95 c, tight	one	na	< 0.5, 0.0	> 9, < 5	-7627.25	-7628.00
P17	13620.00	13622.67	2.67	siltstone	v	cc	one	na	(see below)	(see below)	-7628.00	-7630.67
P17	13622.67	13623.67	1.00	int. silt-ss	v	cc	one (cont)	na	unknown	65.8	-7630.67	-7631.67
P17	13623.67	13624.42	0.75	int. silt-ss	v	cc	one (cont)	na	(see above)	(see above)	-7631.67	-7632.42
P17	13624.42	13625.50	1.08	ls mudstone	h	95 c	occasional	na	< 0.25	~ 8	-7632.42	-7633.50
P17	13625.50	13626.67	1.17	int. silt-ss	v	cc	one	na	unknown	25.4	-7633.50	-7634.67
P17	13626.67	13627.00	0.33	int. silt-ss	na	na	na	na	na	na	-7634.67	-7635.00
P17	13627.00	13627.33	0.33	shale	na	na	na	na	na	na	-7635.00	-7635.33
P17	13627.33	13629.17	1.84	int. silt-ss	h, h	5 c, 90 c	one, occ.	na	< 0.5, < 0.25	> 7	-7635.33	-7637.17
P17	13629.17	13630.42	1.25	siltstone	na	na	na	na	na	na	-7637.17	-7638.42

Core	Top (ft)	Base (ft)	Thickness (ft)	Lithology	Orientation	% Filling	Frequency	Bitumen	Width (mm)	Length (cm)	Elev. Top	Elev. Base
P17	13630.42	13631.50	1.08	int. silt-ss	na	na	na	na	na	na	-7638.42	-7639.50
P17	13631.50	13633.00	1.50	int. silt-ss	na	na	na	na	na	na	-7639.50	-7641.00
P17	13635.00	13644.46	9.46	ls mudstone	hp	0-5 c	very freq.	na	< 0.25	> 5	-7643.00	-7652.46
P17	13644.46	13645.17	0.71	packstone	na	na	na	na	na	na	-7652.46	-7653.17
P17	13645.17	13646.67	1.50	ls mudstone	na	na	na	na	na	na	-7653.17	-7654.67
P17	13646.67	13648.17	1.50	ls mudstone	hp	open	very freq.	na	crumbled	crumbled	-7654.67	-7656.17
P17	13648.17	13649.33	1.16	ls mudstone	na	na	na	na	na	na	-7656.17	-7657.33
P17	13649.33	13649.83	0.50	sandstone	hp	95 c	occasional	na	< 0.25	~ 5	-7657.33	-7657.83
P17	13649.83	13654.25	4.42	siltstone	h, v	90 c, open	mod., occ.	na	< 0.25, < 0.5	> 7, < 6	-7657.83	-7662.25
P17	13654.25	13654.58	0.33	sandstone	v	50 c	occasional	na	< 1.5	> 13	-7662.25	-7662.58
P17	13654.58	13654.71	0.13	siltstone	na	na	na	na	na	na	-7662.58	-7662.71
P17	13654.71	13661.25	6.54	sandstone	h	10 c	frequent	na	< 1	> 7	-7662.71	-7669.25
P17	13661.25	13663.25	2.00	int. silt-ss	na	na	na	na	na	na	-7669.25	-7671.25
P17	13663.25	13665.00	1.75	mudstone	hp	0-5 c	very freq.	na	< 0.5	up to > 7	-7671.25	-7673.00
P17	13665.00	13665.92	0.92	carb. shale	hp	open	very freq.	coaly	< 0.25	up to > 7	-7673.00	-7673.92
P17	13665.92	13667.42	1.50	shale	hp	open	very freq.	na	< 0.5	up to > 7	-7673.92	-7675.42
P17	13667.42	13674.75	7.33	ls mudstone	h, v	90 c, 95 c	mod., one	na	< 0.25, < 1.0	> 7, < 5	-7675.42	-7682.75
P17	13674.75	13675.50	0.75	siltstone	h	95 c	occasional	na	< 0.25	~ 7	-7682.75	-7683.5
P17	13675.50	13676.33	0.83	mudstone	h	open	occasional	na	< 0.25	~ 7	-7683.50	-7684.33
P17	13676.33	13676.75	0.42	carb. shale	h	open	very freq.	possible	< 0.25	up to > 7	-7684.33	-7684.75

Core	Top (ft)	Base (ft)	Thickness (ft)	Lithology	Orientation	% Filling	Frequency	Bitumen	Width (mm)	Length (cm)	Elev. Top	Elev. Base
P17	13676.75	13677.75	1.00	mudstone	na	na	na	na	na	na	-7684.75	-7685.75
P17	13677.75	13678.00	0.25	carb. shale	na	na	na	na	na	na	-7685.75	-7686.00
P17	13678.00	13679.00	1.00	mudstone	na	na	na	na	na	na	-7686.00	-7687.00
P17	13679.00	13682.25	3.25	ls mudstone	h	open	very freq.	na	< 0.25	> 7	-7687.00	-7690.25
P17	13682.25	13686.08	3.83	sandstone	hp	open	very freq.	na	unknown	> 7	-7690.25	-7694.08
P17	13686.08	13686.25	0.17	carb. shale	h	open	very freq.	na	< 0.25	> 7	-7694.08	-7694.25
P17	13686.25	13688.50	2.25	siltstone	na	na	na	na	na	na	-7694.25	-7696.50
P17	13688.50	13692.00	3.50	ls mudstone	h, v	open	moderate	na	< 0.25, same	> 7	-7696.50	-7700.00

## Chevron Hiko Bell 1-12A2 (sec. 12, T1S, R2W)

Core	Top (ft)	Base (ft)	Thickness (ft)	Lithology	Orientation	% Filling	Frequency	Bitumen	Width (mm)	Length (cm)	Elev. Top	Elev. Base
CHIKO	10480.00	10532.13	52.13	int. mud-ss	h, v	na	mod., occ.	na	na	na	-4637.00	-4689.13
CHIKO	10532.13	10533.25	1.12	ls mudstone	na	na	na	na	na	na	-4689.13	-4690.25
CHIKO	10533.25	10543.96	10.71	mudstone	v	100 coal	one	(coal)	< 1	< 13	-4690.25	-4700.96
CHIKO	10543.96	10546.71	2.75	int. ss-mud.	v	na	occasional	na	< 1	< 20	-4700.96	-4703.71
CHIKO	10546.71	10549.33	2.62	ls mudstone	v	na	one	na	< 2	< 10	-4703.71	-4706.33
CHIKO	10549.33	10549.79	0.46	sandstone	na	na	na	na	na	na	-4706.33	-4706.79
CHIKO	10549.79	10564.58	14.79	ls mudstone	v, h	n	moderate	na	na	na	-4706.79	-4721.58
CHIKO	10564.58	10567.33	2.75	sandstone	v	na	occasional	na	< 1	na	-4721.58	-4724.33
CHIKO	10567.33	10567.71	0.38	siltstone	na	na	na	na	na	na	-4724.33	-4724.71
CHIKO	10567.71	10568.33	0.62	sandstone	na	na	na	na	na	n	-4724.71	-4725.33
CHIKO	10568.33	10568.58	0.25	siltstone	na	na	na	na	na	na	-4725.33	-4725.58
CHIKO	10568.58	10569.04	0.46	shale	h	na	frequent	na	na	na	-4725.58	-4726.04
CHIKO	10569.04	10595.67	26.63	mudstone	v, v	100 py., na	occ., one	na	< 0.5, < 1.5	< 25, < 35.5	-4726.04	-4752.67
CHIKO	10595.67	10596.00	0.33	sandstone	na	na	na	yes	na	na	-4752.67	-4753.00
CHIKO	10596.00	10596.83	0.83	ls mudstone	na	na	na	na	na	na	-4753.00	-4753.83
CHIKO	10596.83	10597.21	0.38	sandstone	na	na	na	na	na	na	-4753.83	-4754.21

Core	Top (ft)	Base (ft)	Thickness (ft)	Lithology	Orientation	% Filling	Frequency	Bitumen	Width (mm)	Length (cm)	Elev. Top	Elev. Base
CHIKO	10597.21	10597.38	0.17	packstone	na	na	na	na	na	na	-4754.21	-4754.38
CHIKO	10597.38	10607.00	9.62	ls mudstone	v	na	occasional	na	na	na	-4754.38	-4764.00
CHIKO	10607.00	10608.00	1.00	sandstone	na	na	na	yes	na	na	-4764.00	-4765.00
CHIKO	10609.00	10609.67	0.67	sandstone	na	na	na	yes	na	na	-4766.00	-4766.67
CHIKO	10609.67	10610.67	1.00	ls mudstone	na	na	na	yes	na	na	-4766.67	-4767.67
CHIKO	10610.67	10611.50	0.83	sandstone	na	na	na	na	na	na	-4767.67	-4768.50
CHIKO	10611.50	10614.00	2.50	ls mudstone	na	na	na	na	na	na	-4768.50	-4771.00
CHIKO	10614.00	10614.71	0.71	sandstone	na	na	na	yes	na	na	-4771.00	-4771.71
CHIKO	10614.71	10615.83	1.12	ls mudstone	na	na	na	na	na	na	-4771.71	-4772.83
CHIKO	10615.83	10618.67	2.84	sandstone	v	na	one	yes	na	na	-4772.83	-4775.67
CHIKO	10618.67	10619.00	0.33	ls mudstone	na	na	na	na	na	na	-4775.67	-4776.00
CHIKO	10619.00	10620.75	1.75	sandstone	na	na	na	yes	na	na	-4776.00	-4777.75
CHIKO	10620.75	10622.21	1.46	ls mudstone	na	na	na	na	na	na	-4777.75	-4779.21
CHIKO	10622.21	10622.79	0.58	sandstone	na	na	na	na	na	na	-4779.21	-4779.79
CHIKO	10622.79	10623.17	0.38	ls mudstone	na	na	na	na	na	na	-4779.79	-4780.17

Core	Top (ft)	Base (ft)	Thickness (ft)	Lithology	Orientation	% Filling	Frequency	Bitumen	Width (mm)	Length (cm)	Elev. Top	Elev. Base
CHIKO	10623.17	10624.27	1.10	sandstone	na	na	na	na	na	na	-4780.17	-4781.27
CHIKO	10624.27	10624.73	0.46	ls mudstone	na	na	na	na	na	na	-4781.27	-4781.73
CHIKO	10624.73	10626.85	2.12	sandstone	na	na	na	yes	na	na	-4781.73	-4783.85
CHIKO	10626.85	10627.08	0.23	ls mudstone	v	na	occasional	na	< 0.5	< 30.5	-4783.85	-4784.08
CHIKO	10627.08	10630.92	3.84	sandstone	h	na	one	yes	na	na	-4784.08	-4787.92

## Chevron 1-7A1 (sec. 7, T1S, R2W)

Core	Top (ft)	Base (ft)	Thickness (ft)	Lithology	Orientation	% Filling	Frequency	Bitumen	Width (mm)	Length (cm)	Elev. Top	Elev. Base
C17A1	12235.00	12235.33	0.33	sandstone	v	90 c	moderate	na	< 1	> 10	-6377.00	-6377.33
C17A1	12235.33	12237.17	1.84	sandstone	v, h & sh	90 c, 95 c	one, occ.	na	< 0.5, < 0.5	10, na	-6377.33	-6379.17
C17A1	12237.17	12237.75	0.58	shale	hp	open	very freq.	na	na	na	-6379.17	-6379.75
C17A1	12237.75	12238.69	0.94	int. ss-shale	na	na	na	na	na	na	-6379.75	-6380.69
C17A1	12238.69	12247.81	9.12	shale	na	na	na	na	na	na	-6380.69	-6389.81
C17A1	12247.81	12248.00	0.19	sandstone	na	na	na	na	na	na	-6389.81	-6390.00
C17A1	12248.00	12252.38	4.38	sandstone	v & sv	90 c	occasional	na	< 1	up to > 90	-6390.00	-6394.38
C17A1	12252.38	12252.46	0.08	sandstone	v	90 c	one (cont)	na	< 1	~ 1	-6394.38	-6394.46
C17A1	12252.46	12255.50	3.04	shale	hp	open	very freq.	na	na	na	-6394.46	-6397.50
C17A1	12255.50	12257.17	1.67	sandstone	h	90 c	occasional	na	< 0.5	> 10	-6397.50	-6399.17
C17A1	12257.17	12258.75	1.58	sandy mud.	hp	open	very freq.	na	< 0.25	na	-6399.17	-6400.75
C17A1	12258.75	12264.92	6.17	sandstone	h	90 c	occasional	na	< 0.5	> 10	-6400.75	-6406.92
C17A1	12264.92	12267.00	2.08	sandstone	h	60 c	occasional	na	< 0.5	> 10	-6406.92	-6409.00
C17A1	12267.00	12268.71	1.71	sandstone	v	95 c	frequent	na	< 2	< 8	-6409.00	-6410.71
C17A1	12268.71	12270.42	1.71	sandstone	na	na	na	na	na	na	-6410.71	-6412.42
C17A1	12270.42	12271.92	1.50	sandy mud.	na	na	na	na	na	na	-6412.42	-6413.92
C17A1	12271.92	12272.50	0.58	sandstone	na	na	na	na	na	na	-6413.92	-6414.50
C17A1	12272.50	12274.33	1.83	sandy mud.	na	na	na	na	na	na	-6414.50	-6416.33
C17A1	12274.33	12275.25	0.92	sandstone	h	10 c	occasional	na	< 0.25	< 5	-6416.33	-6417.25
C17A1	12275.25	12281.42	6.17	sandstone	h	95 c	occasional	na	< 0.25	> 10	-6417.25	-6423.42
C17A1	12281.42	12283.50	2.08	sandy mud.	na	na	na	na	na	na	-6423.42	-6425.50
C17A1	12283.50	12285.50	2.00	sandstone	h	95 c	occasional	na	< 0.5	< 25.5	-6425.50	-6427.50

Core	Top (ft)	Base (ft)	Thickness (ft)	Lithology	Orientation	% Filling	Frequency	Bitumen	Width (mm)	Length (cm)	Elev. Top	Elev. Base
C17A1	12285.50	12288.58	3.08	sandstone	h	95 c	occasional	na	< 0.25	< 8	-6427.50	-6430.58
C17A1	12288.58	12290.08	1.50	sandstone	v	95 c	occasional	na	< 0.5	< 23	-6430.58	-6432.08
C17A1	12290.08	12294.42	4.34	sandstone	hp	open	very freq.	na	na	na	-6432.08	-6436.42
C17A1	12294.42	12298.08	3.66	sandstone	na	na	na	na	na	na	-6436.42	-6440.08
C17A1	12298.08	12299.42	1.34	sandstone	none	na	na	na	na	na	-6440.08	-6441.42
C17A1	12299.42	12300.42	1.00	sandstone	na	na	na	na	na	na	-6441.42	-6442.42
C17A1	12300.42	12305.50	5.08	sandstone	v	90 c	two	na	< 1	< 46	-6442.42	-6447.50
C17A1	12305.50	12305.92	0.42	sandstone	v (cont.)	95 c	one	na	< 1	~ 10	-6447.50	-6447.92
C17A1	12305.92	12306.50	0.58	sandstone	na	na	na	na	na	na	-6447.92	-6448.50
C17A1	12306.50	12307.00	0.50	sandstone	na	na	na	na	na	na	-6448.50	-6449.00
C17A1	12307.00	12310.67	3.67	sandstone	v	95 c	occasional	na	< 1	< 33	-6449.00	-6452.67
C17A1	12310.67	12311.25	0.58	sandstone	na	na	na	na	na	na	-6452.67	-6453.25
C17A1	12311.25	12312.50	1.25	sandstone	na	na	na	na	na	na	-6453.25	-6454.50
C17A1	12312.50	12314.33	1.83	sandstone	na	na	na	na	na	na	-6454.50	-6456.33
C17A1	12314.33	12315.67	1.34	sandstone	h	95 c	one	na	< 0.25	> 10	-6456.33	-6457.67
C17A1	12315.67	12319.00	3.33	sandstone	h	95 c	occasional	na	< 0.25	< 8	-6457.67	-6461.00
C17A1	12319.00	12319.83	0.83	sandstone	sv	95 c	one	na	< 0.25	~ 10	-6461.00	-6461.83
C17A1	12319.83	12320.83	1.00	sandstone	na	na	na	na	na	na	-6461.83	-6462.83
C17A1	12320.83	12322.42	1.59	sandstone	na	na	na	na	na	na	-6462.83	-6464.42
C17A1	12322.42	12324.00	1.58	sandstone	na	na	na	na	na	na	-6464.42	-6466.00
C17A1	12324.00	12325.00	1.00	sandstone	h	5 c	moderate	na	< 0.25	> 10	-6466.00	-6467.00
C17A1	12325.00	12332.67	7.67	sandstone	v	95 c	moderate	na	< 1	< 54	-6467.00	-6474.67
C17A1	12332.67	12333.42	0.75	sandstone	d	95 c	moderate	na	< 0.5	< 8	-6474.67	-6475.42

Core	Top (ft)	Base (ft)	Thickness (ft)	Lithology	Orientation	% Filling	Frequency	Bitumen	Width (mm)	Length (cm)	Elev. Top	Elev. Base
C17A1	12333.42	12334.00	0.58	siltstone	h	open	very freq.	na	broken up	broken up	-6475.42	-6476.00
C17A1	12334.00	12334.42	0.42	sandstone	h	95 c	one	na	< 0.5	> 10	-6476.00	-6476.42
C17A1	12334.42	12335.00	0.58	siltstone	na	na	na	na	na	na	-6476.42	-6477.00
C17A1	12335.00	12335.33	0.33	sandstone	v	95 c	one	na	na	na	-6477.00	-6477.33
C17A1	12335.33	12335.67	0.34	siltstone	na	na	na	na	na	na	-6477.33	-6477.67
C17A1	12335.67	12336.00	0.33	sandstone	na	na	na	na	na	na	-6477.67	-6478.00
C17A1	12336.00	12337.00	1.00	siltstone	na	na	na	na	na	na	-6478.00	-6479.00
C17A1	12337.00	12338.25	1.25	sandstone	v, h	95 c	occasional	na	< 1, < 0.5	< 13, > 10	-6479.00	-6480.25
C17A1	12338.25	12339.08	0.83	sandstone	na	na	na	na	na	na	-6480.25	-6481.08
C17A1	12339.08	12344.08	5.00	sandstone	h	95 c	moderate	na	< 0.25	> 10	-6481.08	-6486.08
C17A1	14325.00	14326.00	1.00	sandstone	sv	x	one	na	< 0.25	< 10	-8467.00	-8468.00
C17A1	14326.00	14326.92	0.92	mudstone	hp	open	very freq.	na	na	na	-8468.00	-8468.92
C17A1	14326.92	14327.25	0.33	shale	h	open	very freq.	na	< 0.5	up to > 10	-8468.92	-8469.25
C17A1	14327.25	14328.54	1.29	mudstone	na	na	na	yes	na	na	-8469.25	-8470.54
C17A1	14328.54	14328.96	0.42	int. ss-mud.	na	na	na	na	na	na	-8470.54	-8470.96
C17A1	14328.96	14329.17	0.21	packstone	h	na	moderate	yes	na	na	-8470.96	-8471.17
C17A1	14329.17	14329.58	0.41	mudstone	h	na	very freq.	yes	na	na	-8471.17	-8471.58
C17A1	14329.58	14330.67	1.09	wackestone	na	na	na	yes	na	na	-8471.58	-8472.67
C17A1	14330.67	14330.83	0.16	packstone	na	na	na	yes	na	na	-8472.67	-8472.83
C17A1	14330.83	14331.00	0.17	mudstone	na	na	na	na	na	na	-8472.83	-8473.00
C17A1	14331.00	14331.50	0.50	packstone	v	20 c	one	yes	< 1	< 5	-8473.00	-8473.50
C17A1	14331.50	14332.71	1.21	sandstone	na	na	na	na	na	na	-8473.50	-8474.71

Core	Top (ft)	Base (ft)	Thickness (ft)	Lithology	Orientation	% Filling	Frequency	Bitumen	Width (mm)	Length (cm)	Elev. Top	Elev. Base
C17A1	14332.71	14335.17	2.46	sandstone	none	na	na	na	na	na	-8474.71	-8477.17
C17A1	14335.17	14336.83	1.66	sandstone	h	95 c	occasional	na	< 0.5	> 10	-8477.17	-8478.83
C17A1	14336.83	14338.50	1.67	sandstone	h	open	occasional	na	< 0.25	up to > 10	-8478.83	-8480.50
C17A1	14338.50	14339.50	1.00	silty mud.	h	open	occasional	na	< 0.25	up to > 10	-8480.50	-8481.50
C17A1	14339.50	14340.58	1.08	sandstone	na	na	na	na	na	na	-8481.50	-8482.58
C17A1	14340.58	14341.08	0.50	silty mud.	na	na	na	na	na	na	-8482.58	-8483.08
C17A1	14341.08	14342.50	1.42	sandstone	na	na	na	na	na	na	-8483.08	-8484.50
C17A1	14342.50	14343.00	0.50	sandstone	na	na	na	na	na	na	-8484.50	-8485.00
C17A1	14343.00	14343.67	0.67	sandstone	na	na	na	na	na	na	-8485.00	-8485.67
C17A1	14343.67	14345.71	2.04	sandstone	none	na	na	na	na	na	-8485.67	-8487.71
C17A1	14345.71	14346.00	0.29	ls mudstone	hp	20 c, 100 py	moderate	na	< 0.25	up to > 10	-8487.71	-8488.00
C17A1	14346.00	14347.17	1.17	silty mud.	h, sh	20 c	moderate	yes	< 0.25	up to > 10	-8488.00	-8489.17
C17A1	14347.17	14348.83	1.66	sandstone	na	na	na	na	na	na	-8489.17	-8490.83
C17A1	14348.83	14349.83	1.00	silty mud.	na	na	na	yes	na	na	-8490.83	-8491.83
C17A1	14349.83	14368.33	18.50	mudstone	h, hp	open	moderate	yes	< 0.25	up to > 10	-8491.83	-8510.33
C17A1	14368.33	14369.17	0.84	sandstone	none	na	na	na	na	na	-8510.33	-8511.17
C17A1	14369.17	14372.67	3.50	sandstone	none	na	na	na	na	na	-8511.17	-8514.67
C17A1	14372.67	14373.67	1.00	silty mud.	na	na	na	na	na	na	-8514.67	-8515.67
C17A1	14373.67	14373.75	0.08	sandstone	na	na	na	na	na	na	-8515.67	-8515.75
C17A1	14373.75	14374.17	0.42	mudstone	hp	open	moderate	yes	< 0.5	up to > 10	-8515.75	-8516.17

Core	Top (ft)	Base (ft)	Thickness (ft)	Lithology	Orientation	% Filling	Frequency	Bitumen	Width (mm)	Length (cm)	Elev. Top	Elev. Base
C17A1	14374.17	14375.00	0.83	sandstone	na	na	na	na	na	na	-8516.17	-8517.00
C17A1	14375.00	14376.33	1.33	mudstone	hp	open	very freq.	na	< 0.25	up to > 10	-8517.00	-8518.33
C17A1	14376.33	14378.50	2.17	ls mudstone	hp	95 c	frequent	na	< 0.25	up to > 10	-8518.33	-8520.50
C17A1	14378.50	14380.00	1.50	mudstone	hp	open	very freq.	na	crumbled	crumbled	-8520.50	-8522.00
C17A1	14380.00	14382.00	2.00	siltstone	na	na	na	na	na	na	-8522.00	-8524.00
C17A1	14382.00	14384.00	2.00	sandstone	v	80 c	one	na	unknown	< 18	-8524.00	-8526.00

## Chevron Chasel 1-18A1 (sec. 18, T1S, R1W)

Core	Top (ft)	Base (ft)	Thickness (ft)	Lithology	Orientation	% Filling	Frequency	Bitumen	Width (mm)	Length (cm)	Elev. Top	Elev. Base
CCHAS	10630.00	10637.00	7.00	packstone	v, h	20-45c, open	occasional	yes	< 1.5	up to > 10	-4944.00	-4951.00
CCHAS	10637.00	10643.00	6.00	mudstone	na	na	na	na	na	na	-4951.00	-4957.00
CCHAS	10651.00	10661.00	10.00	wackestone	v, v & h	95 c, open	one, frequent	yes	< 2, < 0.25	> 61, ~ > 10	-4965.00	-4975.00
CCHAS	10661.00	10663.25	2.25	sandstone	v	cc	one	na	unkno wn	> 31	-4975.00	-4977.25
CCHAS	10663.25	10670.25	7.00	packstone	v & h	100 c	moderate	na	< 0.25	na	-4977.25	-4984.25
CCHAS	10670.25	10676.75	6.50	sandstone	v	10 c	occasional	yes	< 1	> 20	-4984.25	-4990.75
CCHAS	10676.75	10712.50	35.75	wackestone	v, hp	cc, tight	occ., mod.	yes	unkn., < 0.25	> 46, ~ > 10	-4990.75	-5026.50
CCHAS	10712.50	10715.00	2.50	sandstone	v	cc	one	yes	unkno wn	> 31	-5026.50	-5029.00
CCHAS	10715.00	10740.25	25.25	packstone	v, v & sh	cc, 90 c	three, mod.	na	unkn., < 1	> 31, ~ > 10	-5029.00	-5054.25
CCHAS	10740.25	10751.92	11.67	sandstone	v	cc	occasional	yes	unkno wn	> 31	-5054.25	-5065.92
CCHAS	10751.92	10767.00	15.08	ls mudstone	v & h	open	occasional	na	na	na	-5065.92	-5081.00
CCHAS	10767.00	10827.00	60.00	int. ss-silt.	v & h, hp	90 c, open	freq., v.freq.	na	< 0.5	na	-5081.00	-5141.00
CCHAS	11001.00	11005.00	4.00	sandstone	v	15 c	one	na.	< 0.5	< 31	-5315.00	-5319.00
CCHAS	11005.00	11008.00	3.00	sandstone	h & sv	15 x	occasional	na	< 0.5	< 10	-5319.00	-5322.00
CCHAS	11010.00	11015.58	5.58	sandstone	v & sv, hp	10 c, 95 c	moderate	yes	< 1, < 0.25	> 31, ~ < 10	-5324.00	-5329.58

Core	Top (ft)	Base (ft)	Thickness (ft)	Lithology	Orientation	% Filling	Frequency	Bitumen	Width (mm)	Length (cm)	Elev. Top	Elev. Base
CCHAS	11015.58	11022.08	6.50	sandstone	v	cc	moderate	na	unkno wn	up to > 31	-5329.58	-5336.08
CCHAS	11022.67	11026.00	3.33	sandstone	v	90 c	occasional	na	< 2	> 8	-5336.67	-5340.00
CCHAS	11026.00	11162.50	136.50	sandstone	h, v, hp	10-100 c	occ., mod.	na	< 0.5, < 1.5	up to > 62	-5340.00	-5476.50
CCHAS	11162.50	11175.00	12.50	sandstone	v	cc	moderate	na	unkno wn	> 183	-5476.50	-5489.00
CCHAS	11175.00	11190.00	15.00	sandstone	v, v	mc, 100 c	moderate	na	< 4, < 8	> 45	-5489.00	-5504.00
CCHAS	11190.00	11198.50	8.50	sandstone	none	na	na	na	na	na	-5504.00	-5512.50
CCHAS	11198.50	11202.17	3.67	sandstone	v, v & h	100 c, 20 c	one, mod.	na	< 7, < 1	unkn., > 7	-5512.50	-5516.17
CCHAS	11202.17	11211.50	9.33	sandstone	h & hp	90 c	moderate	na	< 0.5	> 10	-5516.17	-5525.50
CCHAS	11211.50	11222.00	10.50	sandstone	v	cc	occasional	na	unkno wn	> 25	-5525.50	-5536.00

## Chevron 9-4B1 (sec. 4, T2S, R1W)

Core	Top (ft)	Base (ft)	Thickness (ft)	Lithology	Orientation	% Filling	Frequency	Bitumen	Width (mm)	Length (cm)	Elev. Top	Elev. Base
C94B1	11006.00	11057.00	51.00	silty mud.	h, v, hp	open	v. fr., occ., fr.	na	< 0.25	> 7	-5722.00	-5773.00
C94B1	11057.00	11083.00	26.00	sandstone	v, v, h & hp	cc, 90c, 90c	mo., o., mo.	na	unkn., < 0.5	> 20, < 23	-5773.00	-5799.00
C94B1	11083.00	11085.50	2.50	ls mudstone	hp	100 pyrite	moderate	na	< 0.5	> 5	-5799.00	-5801.50
C94B1	11085.50	11086.08	0.58	silty mud.	na	na	na	na	na	na	-5801.50	-5802.08
C94B1	11086.08	11086.50	0.42	sandstone	none	na	na	na	na	na	-5802.08	-5802.50
C94B1	11086.50	11093.50	7.00	sandstone	h, v	95 c, cc	mod., one	na	< 0.25, unkn.	> 7, > 4	-5802.50	-5809.50
C94B1	11093.50	11097.67	4.17	ls mudstone	h, v	95 c	freq., occ.	na	< 0.25	> 7, > 15	-5809.50	-5813.67
C94B1	11097.67	11104.17	6.50	sandstone	sv	cc	one	na	unkno wn	> 35	-5813.67	-5820.17
C94B1	11104.17	11108.67	4.50	sandstone	h	95 c	moderate	na	< 0.25	> 7	-5820.17	-5824.67
C94B1	11108.67	11113.67	5.00	sandstone	none	na	na	na	na	na	-5824.67	-5829.67
C94B1	11113.67	11143.00	29.33	silty mud.	v, hp	cc, 90 c	occ., v. freq.	na	unkn., < 0.25	u.t., > 122, > 7	-5829.67	-5859.00
C94B1	11500.00	11504.50	4.50	ls mudstone	h	90 c	frequent	na	< 0.5	2 to > 7	-6216.00	-6220.50
C94B1	11504.50	11507.00	2.50	mudstone	h	90 c	frequent	na	< 0.5	2 to > 7	-6220.50	-6223.00
C94B1	11507.00	11512.00	5.00	silty mud.	hp	90 c	very freq.	na	< 0.5	> 7	-6223.00	-6228.00
C94B1	11512.00	11516.83	4.83	ls mudstone	hp, h	95 c, open	very freq.	na	< 0.25	> 7	-6228.00	-6232.83

Core	Top (ft)	Base (ft)	Thickness (ft)	Lithology	Orientation	% Filling	Frequency	Bitumen	Width (mm)	Length (cm)	Elev. Top	Elev. Base
C94B1	11516.83	11527.50	10.67	sandstone	v, h & hp	cc, 95 c	occ., freq.	na	unkn., < 0.5	< 21, > 7	-6232.83	-6243.50
C94B1	11527.50	11540.08	12.58	sandstone	v	cc	occasional	yes	unkno wn	up to > 61	-6243.50	-6256.08
C94B1	11540.08	11545.33	5.25	sandstone	h	95 c	frequent	na	< 0.5	> 7	-6256.08	-6261.33
C94B1	11545.33	11554.17	8.84	silty mud.	hp	95 c	very freq.	na	< 0.5	> 7	-6261.33	-6270.17
C94B1	11554.17	11561.17	7.00	sandstone	v, h & hp	cc, 95 c	one, mod.	na	unkn., < 0.5	, 45, > 7	-6270.17	-6277.17
C94B1	11561.17	11567.00	5.83	silty mud.	hp	95 c	very freq.	na	< 0.5	> 7	-6277.17	-6283.00
C94B1	11567.00	11595.00	28.00	sandstone	h, v	95 c, cc	mod., occ.	na	< 0.5, unkn.	> 7, < 122	-6283.00	-6311.00
C94B1	12651.00	12663.33	12.33	sandstone	v, h	95 c	one, mod.	na	< 0.5	~25, > 7	-7367.00	-7379.33
C94B1	12663.33	12673.00	9.67	mudstone	h	95 c	frequent	na	< 0.5	> 7	-7379.33	-7389.00
C94B1	12673.00	12674.33	1.33	sandstone	h	na	occasional	yes	< 0.5	> 7	-7389.00	-7390.33
C94B1	12674.33	12676.58	2.25	siltstone	na	na	na	na	na	na	-7390.33	-7392.58
C94B1	12676.58	12679.92	3.34	sandstone	na	na	na	na	na	na	-7392.58	-7395.92
C94B1	12679.92	12683.00	3.08	int. silt-ss	h	95 c	moderate	na	< 0.5	> 7	-7395.92	-7399.00
C94B1	12683.00	12687.33	4.33	siltstone	hp	95 c	very freq.	na	< 0.5	> 7	-7399.00	-7403.33
C94B1	12687.33	12689.50	2.17	sandstone	none	na	na	na	na	na	-7403.33	-7405.50
C94B1	12689.50	12697.33	7.83	siltstone	h	95 c	moderate	na	< 0.5	> 7	-7405.50	-7413.33
C94B1	12697.33	12707.25	9.92	sandstone	v, h	95 c	one, mod.	na	< 0.5	~20, > 7	-7413.33	-7423.25
C94B1	12707.25	12714.67	7.42	sandstone	v	95 c	occasional	na	< 0.25	< 4	-7423.25	-7430.67

Core	Top (ft)	Base (ft)	Thickness (ft)	Lithology	Orientation	% Filling	Frequency	Bitumen	Width (mm)	Length (cm)	Elev. Top	Elev. Base
C94B1	12714.67	12716.67	2.00	int. silt-ss	h, v	95 c, cc	mod., one	na	< 0.5, unkn.	> 7, ~ 20	-7430.67	-7432.67
C94B1	12716.67	12724.00	7.33	siltstone	hp	95 c	very freq.	na	< 0.5	> 7	-7432.67	-7440.00
C94B1	12724.00	12767.67	43.67	int. silt-ss	v, h & hp	cc, 95 c	one, freq.	yes	unkn., < 0.5	> 25, > 7	-7440.00	-7483.67
C94B1	12767.67	12769.00	1.33	sandstone	v	cc	one	na	unkno wn	> 31	-7483.67	-7485.00

Chevron 1-24 Boren (sec. 24, T1S, R2W)  
 Quinex Leslie Taylor (sec. 24, T1S, R1W)

Core	Top (ft)	Base (ft)	Thickness (ft)	Lithology	Orientation	% Filling	Frequency	Bitumen	Width (mm)	Length (cm)	Elev. Top	Elev. Base
CBOR	12135.00	12143.00	8.00	sandstone	hp	90 c	very freq.	na	< 0.25	up to > 7	-6558.00	-6566.00
CBOR	12143.00	12144.00	1.00	wackestone	hp	90 c	very freq.	na	< 0.25	up to > 7	-6566.00	-6567.00
CBOR	12144.00	12164.17	20.17	ls mudstone	hp, h	90c, 0 or 90c	very freq.	na	< 0.25	up to > 7	-6567.00	-6587.17
CBOR	12164.17	12166.83	2.66	int. ls md-ss	hp, v	95 c, open	v. freq., one	na	< 0.25	up to > 7, 15	-6587.17	-6589.83
CBOR	12166.83	12172.58	5.75	sandstone	v	90 c	moderate	na	< 1.5	< 30	-6589.83	-6595.58
CBOR	12172.58	12190.00	17.42	int. ss-silt	hp	90 c	moderate	na	< 0.5	up to > 7	-6595.58	-6613.00
CBOR	12190.00	12192.00	2.00	sandstone	h	90 c	moderate	na	< 0.25	up to > 7	-6613.00	-6615.00
CBOR	12192.00	12193.25	1.25	ls mudstone	h	open	very freq.	na	na	na	-6615.00	-6616.25

Core	Top (ft)	Base (ft)	Thickness (ft)	Lithology	Orientation	% Filling	Frequency	Bitumen	Width (mm)	Length (cm)	Elev. Top	Elev. Base
QLT	12180.00	12185.21	5.21	siltstone	h, v	na	moderate	na	< 1	up to > 9	-6662.00	-6667.21
QLT	12185.21	12185.29	0.08	siltstone	na	na	na	na	na	na	-6667.21	-6667.29
QLT	12185.29	12185.33	0.04	siltstone	na	na	na	na	na	na	-6667.29	-6667.33
QLT	12185.33	12185.42	0.09	siltstone	na	na	na	na	na	na	-6667.33	-6667.42
QLT	12185.42	12193.00	7.58	sandstone	na	na	na	na	na	na	-6667.42	-6675.00
QLT	12195.00	12197.00	2.00	sandstone	v, h	na	moderate	na	na	na	-6677.00	-6679.00
QLT	12197.00	12218.50	21.50	siltstone	na	na	na	na	na	na	-6679.00	-6700.50
QLT	12218.50	12219.58	1.08	sandstone	na	na	na	na	na	na	-6700.50	-6701.58
QLT	12219.58	12220.00	0.42	siltstone	na	na	na	na	na	na	-6701.58	-6702.00
QLT	12220.00	12221.08	1.08	sandstone	v	100 c	one	na	< 3	< 33	-6702.00	-6703.08
QLT	12221.08	12221.44	0.36	siltstone	na	na	na	na	na	na	-6703.08	-6703.44
QLT	12221.44	12221.92	0.48	sandstone	na	na	na	na	na	na	-6703.44	-6703.92
QLT	12221.92	12227.83	5.91	siltstone	v	na	moderate	na	< 1	> 9	-6703.92	-6709.83
QLT	12227.83	12231.17	3.34	sandstone	v	100c	one	na	< 5	na	-6709.83	-6713.17
QLT	12231.17	12232.83	1.66	siltstone	na	na	na	na	na	na	-6713.17	-6714.83
QLT	12232.83	12237.00	4.17	sandstone	na	na	na	na	na	na	-6714.83	-6719.00
QLT	12237.00	12238.00	1.00	siltstone	na	na	na	na	na	na	-6719.00	-6720.00

## Bow Valley Petroleum 2-19A1E (sec. 19, T1S, R1E)

Core	Top (ft)	Base (ft)	Thickness (ft)	Lithology	Orientation	% Filling	Frequency	Bitumen	Width (mm)	Length (cm)	Elev. Top	Elev. Base
BVP19	9160.00	9173.21	13.21	shale	h & sh	open	frequent	na	< 1	> 9	-3710.00	-3723.21
BVP19	9173.21	9173.92	0.71	sandstone	h	open	moderate	na	< 1	> 9	-3723.21	-3723.92
BVP19	9173.92	9196.50	22.58	shale	h	open	very freq.	na	< 1	> 9	-3723.92	-3746.50
BVP19	9196.50	9197.08	0.58	shale	h, v	open	moderate	yes	< 1	> 9	-3746.50	-3747.08
BVP19	9197.08	9199.00	1.92	shale	na	na	na	na	na	na	-3747.08	-3749.00
BVP19	9199.00	9199.33	0.33	shale	na	na	na	yes	na	na	-3749.00	-3749.33
BVP19	9199.33	9215.83	16.50	shale	sh, h & v	100 c, open	occ., one	yes	< 0.6	na	-3749.33	-3765.83
BVP19	9215.83	9216.33	0.50	sandstone	na	na	na	na	na	na	-3765.83	-3766.33
BVP19	9216.33	9217.00	0.67	shale	na	na	na	na	na	na	-3766.33	-3767.00
BVP19	9628.00	9628.50	0.50	mudstone	v	100 c	occasional	na	< 0.25	na	-4178.00	-4178.50
BVP19	9628.50	9628.96	0.46	mudstone	h	open	very freq.	na	crumbled	crumbled	-4178.50	-4178.96
BVP19	9628.96	9630.58	1.62	int. shale-ss	h	open	moderate	na	< 0.5	na	-4178.96	-4180.58
BVP19	9630.58	9633.92	3.34	grainstone	v	cc	one	yes	unknwn	unknwn	-4180.58	-4183.92
BVP19	9633.92	9634.33	0.41	mudstone	na	na	na	na	na	na	-4183.92	-4184.33
BVP19	9634.33	9635.25	0.92	wackestone	h	open	moderate	na	< 0.5	na	-4184.33	-4185.25
BVP19	9635.25	9640.50	5.25	mudstone	h	open	moderate	na	< 0.5	na	-4185.25	-4190.50
BVP19	9640.50	9640.92	0.42	shale	h	open	very freq.	na	< 0.5	na	-4190.50	-4190.92
BVP19	9640.92	9642.92	2.00	mudstone	h	open	moderate	na	< 0.025	> 9	-4190.92	-4192.92
BVP19	9642.92	9643.08	0.16	shale	na	na	na	na	na	na	-4192.92	-4193.08
BVP19	9643.08	9643.92	0.84	mudstone	na	na	na	na	na	na	-4193.08	-4193.92

Core	Top (ft)	Base (ft)	Thickness (ft)	Lithology	Orientation	% Filling	Frequency	Bitumen	Width (mm)	Length (cm)	Elev. Top	Elev. Base
BVP19	9643.92	9644.83	0.91	shale	na	na	na	na	na	na	-4193.92	-4194.83
BVP19	9644.83	9645.17	0.34	mudstone	na	na	na	na	na	na	-4194.83	-4195.17
BVP19	9645.17	9646.17	1.00	int. ls md-ss	na	na	na	na	na	na	-4195.17	-4196.17
BVP19	9646.17	9647.17	1.00	mudstone	na	na	na	na	na	na	-4196.17	-4197.17
BVP19	9647.17	9647.50	0.33	int. ls md-ss	na	na	na	na	na	na	-4197.17	-4197.50
BVP19	9647.50	9648.50	1.00	sandstone	na	na	na	na	na	na	-4197.50	-4198.50
BVP19	9648.50	9648.67	0.17	int. ls md-ss	na	na	na	na	na	na	-4198.50	-4198.67
BVP19	9648.67	9649.50	0.83	sandstone	h	90-95 mud	occasional	na	< 2.5	< 6	-4198.67	-4199.50
BVP19	9649.50	9649.92	0.42	int. ls md-ss	v	50 c	occasional	na	< 1	~ 8	-4199.50	-4199.92
BVP19	9649.92	9650.21	0.29	packstone	v	cc	one	na	unkno wn	> 4	-4199.92	-4200.21
BVP19	9650.21	9650.58	0.37	packstone	na	na	na	na	na	na	-4200.21	-4200.58
BVP19	9650.58	9653.42	2.84	int. ls md-ss	hp	na	very freq.	na	na	na	-4200.58	-4203.42
BVP19	9653.42	9655.00	1.58	packstone	h	open	one	na	< 0.5	> 9	-4203.42	-4205.00
BVP19	9671.00	9674.83	3.83	packstone	h, v	90 c	mod., two	na	< 0.5	> 9, > 45	-4221.00	-4224.83
BVP19	9674.83	9676.42	1.59	ls mudstone	h	10 c	moderate	na	< 0.5	> 9	-4224.83	-4226.42
BVP19	9676.42	9686.58	10.16	mudstone	hp	open	very freq.	na	crumbl ed	crumbl ed	-4226.42	-4236.58
BVP19	9686.58	9687.33	0.75	ls mudstone	h	10 c	moderate	na	< 0.25	> 9	-4236.58	-4237.33
BVP19	9687.33	9687.75	0.42	mudstone	na	na	na	na	na	na	-4237.33	-4237.75
BVP19	9687.75	9688.50	0.75	int. ls md-ss	na	na	na	na	na	na	-4237.75	-4238.50
BVP19	9691.00	9691.58	0.58	ls mudstone	na	na	na	na	na	na	-4241.00	-4241.58

Core	Top (ft)	Base (ft)	Thickness (ft)	Lithology	Orientation	% Filling	Frequency	Bitumen	Width (mm)	Length (cm)	Elev. Top	Elev. Base
BVP19	9691.58	9692.25	0.67	packstone	v	cc	one	na	unkno wn	na	-4241.58	-4242.25
BVP19	9692.25	9698.33	6.08	mudstone	na	na	na	na	na	na	-4242.25	-4248.33
BVP19	9698.33	9701.00	2.67	packstone	h	10 c	moderate	yes	< 0.25	< 9	-4248.33	-4251.00
BVP19	9701.00	9703.50	2.50	packstone	na	na	na	na	na	na	-4251.00	-4253.50
BVP19	9707.00	9710.08	3.08	packstone	v	80 c	moderate	na	< 0.5	~ 8	-4257.00	-4260.08
BVP19	9710.08	9718.00	7.92	mudstone	na	na	na	na	na	na	-4260.08	-4268.00
BVP19	9718.00	9719.00	1.00	sandstone	v	cc	one	na	unkno wn	na	-4268.00	-4269.00
BVP19	9719.00	9719.33	0.33	packstone	na	na	na	na	na	na	-4269.00	-4269.33
BVP19	9719.33	9720.00	0.67	packstone	na	na	na	na	na	na	-4269.33	-4270.00

## Bow Valley Petroleum 2-22A1E (sec. 22, T1S, R1E)

Core	Top (ft)	Base (ft)	Thickness (ft)	Lithology	Orientation	% Filling	Frequency	Bitumen	Width (mm)	Length (cm)	Elev. Top	Elev. Base
BVP22	12288.00	12298.00	10.00	sandstone	na	na	na	na	na	na	-6913.00	-6923.00
BVP22	12298.00	12299.00	1.00	shale	h	na	na	na	na	na	-6923.00	-6924.00
BVP22	12299.00	12299.67	0.67	sandstone	na	na	na	na	na	na	-6924.00	-6924.67
BVP22	12299.67	12299.83	0.16	shale	na	na	na	na	na	na	-6924.67	-6924.83
BVP22	12299.83	12300.00	0.17	sandstone	na	na	na	na	na	na	-6924.83	-6925.00
BVP22	12300.00	12300.67	0.67	shale	na	na	na	na	na	na	-6925.00	-6925.67
BVP22	12300.67	12301.17	0.50	sandstone	na	na	na	na	na	na	-6925.67	-6926.17
BVP22	12301.17	12306.17	5.00	wackestone	na	na	na	na	na	na	-6926.17	-6931.17
BVP22	12306.17	12310.67	4.50	packstone	na	na	na	na	na	na	-6931.17	-6935.67
BVP22	12310.67	12314.00	3.33	ls mudstone	h, v	na, tight	moderate	na	na	na	-6935.67	-6939.00
BVP22	12314.00	12316.42	2.42	silty mud.	h & v	na	moderate	na	na	na	-6939.00	-6941.42
BVP22	12316.42	12318.00	1.58	shale	na	na	na	na	na	na	-6941.42	-6943.00
BVP22	12318.00	12319.00	1.00	silty mud.	na	na	na	na	na	na	-6943.00	-6944.00
BVP22	12319.00	12327.00	8.00	shale	na	na	na	na	na	na	-6944.00	-6952.00
BVP22	12327.00	12327.67	0.67	ls mudstone	na	na	na	na	na	na	-6952.00	-6952.67
BVP22	12327.67	12329.67	2.00	shale	na	na	na	na	na	na	-6952.67	-6954.67
BVP22	12329.67	12333.67	4.00	int. ss-silt	h	na	moderate	na	na	na	-6954.67	-6958.67
BVP22	12333.67	12338.67	5.00	shale	h & d	na	moderate	na	na	na	-6958.67	-6963.67
BVP22	12338.67	12340.50	1.83	ls mudstone	v	5c	one	na	< 3	< 31	-6963.67	-6965.50
BVP22	12340.50	12348.00	7.50	silty mud.	na	na	na	na	na	na	-6965.50	-6973.00
BVP22	12348.00	12356.92	8.92	siltstone	v	100 c	one	na	< 1	< 58	-6973.00	-6981.92
BVP22	12356.92	12357.50	0.58	sandstone	na	na	na	na	na	na	-6981.92	-6982.50
BVP22	12357.50	12362.00	4.50	silty shale	na	na	na	na	na	na	-6982.50	-6987.00

Core	Top (ft)	Base (ft)	Thickness (ft)	Lithology	Orientation	% Filling	Frequency	Bitumen	Width (mm)	Length (cm)	Elev. Top	Elev. Base
BVP22	12362.00	12369.33	7.33	sandstone	na	na	na	na	na	na	-6987.00	-6994.33
BVP22	12369.33	12374.00	4.67	shale	hp	na	very freq.	na	na	na	-6994.33	-6999.00
BVP22	12374.00	12376.25	2.25	ls mudstone	na	na	na	na	na	na	-6999.00	-7001.25
BVP22	12376.25	12380.00	3.75	wackestone	na	na	na	na	na	na	-7001.25	-7005.00
BVP22	12380.00	12399.50	19.50	silty mud.	h	na	moderate	na	na	na	-7005.00	-7024.50
BVP22	12399.50	12403.00	3.50	silty shale	v	100 c	one	na	< 2	< 122	-7024.50	-7028.00
BVP22	12403.00	12406.00	3.00	silty mud.	v (cont)	100 c	one	na	< 2	< 122	-7028.00	-7031.00



APPENDIX D  
Water Chemistry of the Major Rivers  
Running Through the Altamont and Bluebell fields

APPENDIX D - WATER CHEMISTRY OF THE MAJOR RIVERS RUNNING THROUGH  
THE ALTAMONT AND BLUEBELL FIELDS, UINTA BASIN, UTAH

SAMPLE SITE	NA	K	MG	CA	CL	SO4	HCO3	TDS	pH	COND.	BA	FE	TEMP C
DUCHESNE R. - AT TABIONA	13.00	1.63	21.50	55.70	6.39	60.38	230.91	389.51	7.87	469.23	70.65	64.80	8.05
DUCHESNE R. - BL ROCK CR.	12.68	1.50	18.98	48.86	6.35	58.69	190.38	337.44	8.09	402.88	73.13	45.00	8.26
DUCHESNE R. - AB STRAWBERRY R.	26.66	2.13	26.15	56.45	9.81	97.28	230.54	499.02	8.47	542.86	93.13	40.13	10.10
DUCHESNE R. - AT MYTON	97.53	2.97	40.48	71.98	31.15	284.07	272.37	800.55	8.10	983.94	73.82	40.65	10.45
DUCHESNE R. - AT RANDELETT	167.88	3.60	55.55	89.30	70.01	450.23	287.83	1124.40	8.21	1402.29	71.40	31.53	11.37
UINTA R. - AT RANDELETT	189.59	3.75	61.68	101.24	108.79	500.07	299.63	1264.75	8.12	1594.43	73.16	44.98	11.56
STRAWBERRY R. - AB DUCHESNE R.	71.03	2.30	34.81	47.80	19.61	133.71	308.13	617.39	8.32	750.18	75.10	35.20	8.91
WHITEROCKS R. - NEAR WHITEROCKS	1.00	1.00	1.00	3.67	1.00	4.67	14.20	26.54	7.33	36.3	0.00	0.00	10.17
YELLOWSTONE R. - NEAR ALTONA	1.17	1.00	2.33	6.67	1.08	8.17	28.08	48.50	7.05	67.60	0.00	0.00	8.40
ROCK CREEK - AB DUCHESNE R.	4.88	1.04	9.53	29.63	4.18	41.50	92.10	182.86	8.12	235.88	67.89	50.89	8.26
LAKE FORK R. - AB MOON LAKE	1.00	1.00	1.00	2.00	1.00	10.00	11.75	27.75	7.34	39.43	50.00	20.00	9.29

Data from Utah Department of Environmental Quality-  
Division of Water Quality.

